

Measurement of J/ψ production in $p\text{Pb}$ and $\text{Pb}p$ collisions at $\sqrt{s_{NN}} = 8.16 \text{ TeV}$

Vladik Balagura^{1,a}, Francesco Bossù¹, Frédéric Fleuret^{1,a}, Emilie Maurice^{1,a}, Patrick Robbe¹, Michael Winn¹, Yanxi Zhang¹

¹*LAL, Université Paris-Sud, CNRS/IN2P3, Orsay, France*

^a*Laboratoire Leprince-Ringuet, Palaiseau, France*

Abstract

The measurement of J/ψ production in $p\text{Pb}$ and $\text{Pb}p$ collisions at $\sqrt{s_{NN}} = 8.16 \text{ TeV}$ by LHCb is presented. The measurement comprises the production cross-sections, forward to backward ratios and the nuclear modification factors. The measurements are performed as function of the transverse momentum and rapidity of the charmonium states.

VERSION	DATE	COMMENTS
1	1.3.2017	First version Still missing: tracking efficiencies from data, Pbp simulation, most of the result plots and tables, final luminosities and most of the $\psi(2S)$.
2	3.3.2017	Add results for J/ψ , except Forward-Backward ratio Still missing: tracking efficiencies from data, Pbp simulation, final luminosities and most of the $\psi(2S)$.
3	16.3.2017	Add comparisons with theory and tracking efficiencies from data Still missing: Pbp simulation, final luminosities and most of the $\psi(2S)$.
4	23.3.2017	Add final luminosities and all uncertainties Still missing: final simulation and $\psi(2S)$.
5	18.4.2017	Add numbers from Pbp simulation Implement answers to reviewer's questions (Daria and Wenbin)
6	3.5.2017	Documenting the answer to the last question from the reviews: effect of the mass resolution on the selection efficiency.

Contents

1	Introduction	1
2	Definition of observables	2
2.1	Cross-sections	2
2.2	Nuclear modification factor	3
2.3	Forward-Backward ratios	3
3	Data sets	3
3.1	Data samples	3
3.2	Monte Carlo samples	3
3.3	Trigger	5
3.3.1	L0	5
3.3.2	HLT1	5
3.3.3	HLT2	6
4	Selections	7
4.1	Global Event Selection	7
4.2	Candidate Selection	7
5	Signal extraction	8
5.1	Mass fit function	9
5.2	Pseudo-proper time fit function	9
5.3	Fit results	11
6	Acceptance and efficiency	14
6.1	Acceptance	14
6.2	Reconstruction efficiency	14
6.3	Selection efficiency	18
6.4	PID efficiency	20
6.5	Trigger efficiency	23
6.6	Total efficiencies	23
7	Systematic uncertainties	23
7.1	Monte Carlo statistics	24
7.2	Signal extraction	24
7.3	Bin to bin migration	24
7.4	Tracking efficiency	26
7.5	Selection efficiency	27
7.5.1	Global event cut	27
7.5.2	Primary vertex reconstruction efficiency	27
7.5.3	Mass resolution effect	27
7.5.4	Other selection requirements	28
7.6	PID efficiency	28
7.7	Trigger efficiency	29
7.8	Luminosity	30
7.9	Summary	32

8	Reference pp cross-sections	32
8.1	J/ψ cross-section in pp collisions at 8.16 TeV	32
9	Results	38
9.1	Absolute J/ψ production cross-sections	38
9.2	Fraction of J/ψ from b decays	38
9.3	J/ψ nuclear modification factors	47
9.4	J/ψ forward to backward ratio	50
10	Conclusions	50
A	Mass and t_z fit results	53
A.1	Event yields for J/ψ in $p\text{Pb}$	53
A.2	Event yields for J/ψ in $\text{Pb}p$	55
B	Efficiencies numerical results	57
B.1	Acceptance efficiencies	57
B.1.1	Acceptance efficiencies for J/ψ in $p\text{Pb}$	57
B.1.2	Acceptance efficiencies for J/ψ in $\text{Pb}p$	59
B.2	Reconstruction efficiencies	61
B.2.1	Reconstruction efficiencies for J/ψ in $p\text{Pb}$	61
B.2.2	Reconstruction efficiencies for J/ψ in $\text{Pb}p$	63
B.3	Selection efficiencies	65
B.3.1	Selection efficiencies for J/ψ in $p\text{Pb}$	65
B.3.2	Selection efficiencies for J/ψ in $\text{Pb}p$	67
B.4	PID efficiencies	69
B.4.1	PID efficiencies for J/ψ in $p\text{Pb}$	69
B.4.2	PID efficiencies for J/ψ in $\text{Pb}p$	71
B.5	Trigger efficiencies	73
B.5.1	Trigger efficiencies for J/ψ in $p\text{Pb}$	73
B.5.2	Trigger efficiencies for J/ψ in $\text{Pb}p$	75
B.5.3	Total efficiencies for J/ψ in $p\text{Pb}$	77
B.5.4	Total efficiencies for J/ψ in $\text{Pb}p$	79
C	pp cross-section extrapolation numerical results	81
C.1	$\frac{d^2\sigma}{dp_T dy}$ for prompt J/ψ in pp at 8.2 TeV	81
C.2	$\frac{d^2\sigma}{dp_T dy}$ for J/ψ from b in pp at 8.2 TeV	82
D	Cross-section numerical results	83
D.1	$\frac{d^2\sigma}{dp_T dy}$ for prompt J/ψ in $p\text{Pb}$	83
D.2	$\frac{d^2\sigma}{dp_T dy}$ for J/ψ from b in $p\text{Pb}$	85
D.3	$\frac{d^2\sigma}{dp_T dy}$ for prompt J/ψ in $\text{Pb}p$	87
D.4	$\frac{d^2\sigma}{dp_T dy}$ for J/ψ from b in $\text{Pb}p$	89
D.5	J/ψ b fraction	91

E	Nuclear modification factor numerical results	95
E.1	$R_{p\text{Pb}}$ for prompt J/ψ in $p\text{Pb}$	95
E.2	$R_{p\text{Pb}}$ for J/ψ from b in $p\text{Pb}$	98
E.3	$R_{p\text{Pb}}$ for prompt J/ψ in $\text{Pb}p$	100
E.4	$R_{p\text{Pb}}$ for J/ψ from b in $\text{Pb}p$	102
F	Forward to backward ratios numerical results	104
F.1	R_{FB} for prompt J/ψ	104
F.2	R_{FB} for J/ψ from b	106
F.3	Simulation data comparisons of kinematic distribution in phase space . .	108
	References	109

1 Introduction

The production of J/ψ mesons, and more generally, of quarkonium states has been discussed as a probe sensitive to de-confinement since the proposal of J/ψ suppression in heavy-ion collisions as sign of deconfinement by Matsui and Satz in 1986 [1]. The theory understanding of the bound state dynamics of quarkonium by means of lattice QCD and effective field theory has progressed substantially in the last 30 years. A picture is emerging, which indicates strong modifications of the bound state characteristics as their binding energy as well as the appearance of an imaginary part of the $q\bar{q}$ potential [2]. Experimentally, measurements at the SPS, RHIC and LHC revealed interesting patterns [3]. In particular, at the LHC, a low- p_T component contributes to the J/ψ production [4–8]. This phenomenon has been predicted as sign of charmonium originating from unbound charm quarks generated either during the life-time of the de-confined medium [9] or at the phase boundary [10] in 2000.

One of the largest uncertainties of the phenomenological models to describe the PbPb J/ψ data are nuclear phenomena, which are not related to deconfinement, commonly called Cold Nuclear Matter (CNM) effects. They prevent more precise conclusions based on the the available Pb–Pb data. The effects mostly discussed are modifications of the gluon flux coupling to the charm quark line either treated within a collinear parton distribution framework yielding to nuclear Parton Distribution Functions (nPDFs) [11–15] or, for the low- x part, treated within a Color Glass Condensate (CGC) approach used to describe the saturation regime of QCD [16, 17]. Several calculations were persued in the collinear framework to quantify nuclear modifications of J/ψ production [18–21] and in the CGC one [22–24]. It has to be noted that the low- x gluon content of the nucleus is largely unconstrained by any experimental data at perturbative scales. In addition, small angle gluon radiation taking into account interference between initial and final state radiation, called coherent energy loss, was proposed as the dominant nuclear modification of quarkonium production in pA collisions [25]. The discrimination between these phenomena and hence their observation constitute themselves a strong motivation for the study of quarkonium as a hard-scale probe of dense QCD.

The first experimental data on J/ψ production based on the 2013 data taking by ALICE [26–28], LHCb [29] at forward rapidity and at low p_T disfavored the first CGC calculation [22]. Later CGC calculations were however able to describe well the data at forward rapidity [23, 24]. Based on the experimental data by all 4 LHC collaborations [26–31] from the 2013 data taking, no conclusion on the dominant mechanism for nuclear modification of J/ψ production could be drawn.

In addition to these fields of interest for pPb physics at the LHC, the observation of long range correlations in high-multiplicity pp and pPb events were discussed and described in the context of hydrodynamical evolution [32, 33] as well as correlations arising from the gluon dense initial state also described within various ansaetze related to saturation [34]. The measurement of an additional suppression of the excited state $\psi(2S)$ by ALICE [35, 36] and LHCb [37] in pPb collisions at $\sqrt{s_{NN}} = 5$ TeV during LHC Run 1 triggered calculations invoking hadronic or partonic interactions influencing the fate of the $c\bar{c}$ pair after their first interaction [19, 38], since this behaviour cannot be explained neither by the modification of the gluon flux and the coherent energy loss affecting the ground and the excited vector state in a very similar way.

Furthermore, the measurement of prompt and non-prompt J/ψ is laying the ground

for the analysis of J/ψ to Drell-Yan production ratio which can discriminate between nuclear effects due to the coherent energy loss and nuclear parton density functions [39]. In addition, it provides a natural reference for the measurement of χ_c -states, which will further clarify the modification of quarkonium in p -nucleus collisions at the TeV scale. Both measurements down to low p_T or masses are unique capabilities of the LHCb experiment at the LHC. LHCb recorded in 2016 a large data sample at $\sqrt{s_{NN}} = 8.16$ TeV¹ enabling to study with better precision the qualitative Run 1 findings.

2 Definition of observables

All observables are cross-sections or ratios of cross-sections which require efficiency corrections to event yields obtained from data. These raw event yields are extracted from a combined fit of the di-muon invariant mass and of the pseudo-proper decay time to separate the **prompt** and the **non-prompt** signal contributions. **Prompt** here means produced directly at the nucleon-nucleon interaction, or via a decay of a charmonium produced directly at the interaction (such as a $\chi_c \rightarrow J/\psi \gamma$ decay). **Non-prompt** means a charmonium coming from a B decay (either directly, or also via a charmonium decay where the charmonium state is produced in a B decay). The observables of the analysis are measured separately for the prompt and non-prompt charmonium states.

Given the large statistics available, the observables are also computed in bins of p_T , the transverse momentum with respect to the beam axis and of y^* , the rapidity with respect to the beam axis in the center-of-mass frame, taking as axis direction the direction of the proton beam. The rapidity y^* is related to the rapidity in the lab frame, y_{lab} , with $y^* = y_{\text{lab}} - 0.465$ for the $p\text{Pb}$ configuration and with $y^* = -(y_{\text{lab}} + 0.465)$ for the $\text{Pb}p$ configuration. For pp collisions (used as reference in the various ratios given below), $y_{\text{lab}} = y^*$.

2.1 Cross-sections

The absolute double differential cross-sections are defined as,

$$\frac{d^2\sigma}{dp_T dy^*} = \frac{N}{\Delta y^* \Delta p_T \epsilon^{\text{tot}} \mathcal{B}_{\mu\mu} L_{\text{int}}}, \quad (1)$$

where N represents the raw yield of the J/ψ reconstructed in the given rapidity and transverse momentum bin, ϵ^{tot} the total efficiency, including acceptance, $\mathcal{B}_{\mu\mu}$ the branching ratio of the J/ψ decay in two muons and L_{int} the integrated luminosity of the given data sample. The values of the branching fraction used in this measurement is $\mathcal{B}(J/\psi \rightarrow \mu^+ \mu^-) = 5.961 \pm 0.033\%$ [41].

For the J/ψ meson, the observable is extracted in the rapidity range $1.5 < y^* < 4.0$ for $p\text{Pb}$ and $-5.0 < y^* < -2.5$ for $\text{Pb}p$, in bins of 0.5 units, and in the transverse momentum range $0 < p_T < 14$ GeV/ c in bins of 1 GeV/ c . In the $\text{Pb}p$ case, the statistics are too low for the highest rapidity bins, so the measurement is limited to $p_T < 11$ GeV/ c for the bins $-5.0 < y^* < -4.5$ and $-4.5 < y^* < -4.0$.

¹The uncertainty on the center-of-mass energy is less than 0.2% [40], this is why the energy is quoted with two digit precision.

2.2 Nuclear modification factor

The nuclear modification factor is defined as follows,

$$R_{p\text{Pb}}(p_{\text{T}}, y^*) = \frac{\left[\frac{d^2\sigma}{dp_{\text{T}}dy^*} \right]_{p\text{Pb}}}{208 \left[\frac{d^2\sigma}{dp_{\text{T}}dy^*} \right]_{pp}}, \quad (2)$$

where 208 is the atomic number of the Pb ion. The pp -reference cross-section has to be taken at the same energy, *i.e.* 8.16 TeV, as described in Sect. 8. In absence of nuclear effects, the modification factor is expected to be unity.

2.3 Forward-Backward ratios

To investigate nuclear modification in the asymmetric collision system $p\text{Pb}$, it is interesting to compare the production in the forward region with the production in the backward region with respect to the direction of the proton beam, *i.e.* compare production measured with the $p\text{Pb}$ configuration with the measurement in the $\text{Pb}p$ configuration, in a common range of absolute values of y^* . This is obtained with the forward-to-backward ratio,

$$R_{\text{FB}}(p_{\text{T}}, |y^*|) = \frac{\frac{d^2\sigma}{dp_{\text{T}}dy^*}(p_{\text{T}}, y^*)}{\frac{d^2\sigma}{dp_{\text{T}}dy^*}(p_{\text{T}}, -y^*)}. \quad (3)$$

The forward-to-backward ratio is evaluated in the rapidity range $2.5 < |y^*| < 4.0$, which is common to $p\text{Pb}$ and $\text{Pb}p$.

3 Data sets

3.1 Data samples

The data used in this analysis was recorded during the Heavy Ion run of 2016, between Nov. 18th and Nov. 25th for the $p\text{Pb}$ configuration (p in beam 1, coming from upstream of the VELO) and between Nov. 26th and Dec. 4th for the $\text{Pb}p$ configuration (p in beam 2), both at a center of mass collision energy of 8.16 TeV. The total recorded luminosity is of $13.6 \pm 0.3 \text{ nb}^{-1}$ for $p\text{Pb}$ and $20.8 \pm 0.5 \text{ nb}^{-1}$ for $\text{Pb}p$. The magnet polarity was always DOWN (positive polarity) throughout the whole period. The list of selected good runs used in this analysis is given in Table 1 together with the fill number. During the $p\text{Pb}$ run, one run was flagged bad (186560) because of a misconfiguration in the VELO.

3.2 Monte Carlo samples

The efficiency of the various steps in the analysis chain (acceptance, reconstruction, selection and trigger) is estimated using samples of fully simulated events using the standard LHCb simulation software, GAUSS. The simulated events are then reconstructed and analyzed using the same software tools as the ones used for the data. The simulation is done in two successive steps, first a generation phase based on several external tools such as event generators, and second a simulation phase based on the GEANT4 package [42, 43].

Table 1: Fill numbers and list of good runs.

Fill	Good run numbers
<i>pPb</i>	
5519	186555, 186557, 186558, 186564, 186565
5520	186583, 186584, 186585, 186587, 186588, 186590
5521	186601, 186602, 186603, 186604, 186608, 186609, 186610, 186611, 186612, 186613,
5522	186614, 186615, 186616, 186626, 186628, 186629, 186631, 186632, 186633, 186634, 186635, 186636, 186637, 186638, 186639
5523	186647, 186650, 186651, 186652, 186653, 186654, 186655, 186656
5524	186670, 186673
5526	186718, 186721, 186722, 186723, 186724, 186725, 186726, 186727
5527	186735, 186737, 186739, 186740, 186741, 186744, 186745, 186746
5533	186782, 186783, 186785, 186798, 186799, 186802, 186806, 186807
5534	186818, 186819, 186823, 186824
5538	186920, 186915, 186914, 186907, 186903, 186896, 186890, 186884, 186879, 186876
<i>Pbp</i>	
5545	186989, 186990, 186991, 186992, 186993
5546	187002, 187005, 187007
5547	187015, 187018, 187019, 187020, 187021, 187023, 187025, 187026
5549	187038, 187040, 187042, 187043, 187044, 187045, 187047, 187048, 187049, 187050, 187051
5550	187058, 187061, 187062, 187063, 187064, 187065
5552	187074, 187078, 187080, 187082, 187083, 187083, 187084, 187085, 187086
5553	187106, 187109, 187110, 187111, 187112, 187113, 187115
5554	187123, 187124, 187127, 187128, 187129
5558	187178, 187182, 187183, 187184
5559	187198, 187199, 187202, 187203, 187204
5562	187229, 187230, 187232, 187233, 187234
5563	187244, 187247, 187248, 187249, 187250, 187251, 187252, 187253, 187254, 187255
5564	187266
5565	187282, 187283, 187289, 187290, 187291, 187292
5568	187325, 187328, 187329, 187330, 187331, 187332, 187333, 187334, 187335, 187336, 187337, 187339, 187340
5569	187348, 187349, 187350, 187351, 187355, 187357, 187358
5570	187372, 187375, 187376, 187377, 187378, 187380, 187381
5571	187389, 187392, 187393, 187394, 187395
5573	187406, 187409, 187410

113 The simulation phase is the same as the one used for the simulation of *pp* events within
 114 LHCb and is described in Ref. [44] while the generation phase is specific to the heavy ion
 115 analyses. The versions of the software for the simulation is known as **Sim09b**.

116 Minimum bias samples are generated using the EPOS event generator, using the LHC

model [45]. This generator is interfaced with the GAUSS simulation software via the CRMC (Cosmic Ray Monte Carlo) interface library. All short lived particles are decayed with the EVTGEN decay package [46], similarly to what is done for pp simulation in LHCb. Radiative QED corrections to the decays containing charged particles in the final state are applied with the PHOTOS package [47] and is particularly important for $J/\psi \rightarrow \mu^+\mu^-$ decays. Since the instantaneous luminosity of the collisions recorded by the experiment in the various heavy ion configuration is low, no pile-up is generated, and events contain only one interaction.

Signal samples of $J/\psi \rightarrow \mu^+\mu^-$ are generated using an embedding technique: minimum bias events are generated using the PYTHIA (version 8) generator [48], with colliding proton beams having momenta equal to the momenta per nucleon of the heavy ion beams or targets. The J/ψ mesons are then extracted from these minimum bias events, discarding all other particles in the events. Their decays are forced to the signal decay modes using the EVTGEN package, and the resulting decay chain is added to a single minimum bias EPOS event generated with beam parameters identical to those seen in data. All the samples are listed in Table 2.

Table 2: Event type, decay and statistics of the simulation samples.

EventType	Decay chain	Number of events
24142001	$p\text{Pb } J/\psi \rightarrow \mu^+\mu^-$	1.5×10^6
24142001	$\text{Pbp } J/\psi \rightarrow \mu^+\mu^-$	1.0×10^6

3.3 Trigger

The trigger selections applied during the $p\text{Pb}$ and Pbp runs were close but looser than the selections used during the first month of data taking for Run 2, where the measurement of the J/ψ cross-section at 13 TeV was performed.

3.3.1 L0

A single L0 TCK was used throughout this run, 0x1621. The corresponding configuration is given in Table 3. For this analysis, only reconstructed J/ψ with one of their muons fulfills the Muon line criteria are considered (*i.e.* L0Muon TOS candidates). For the lines used in the analysis, no SPD multiplicity cut was applied at L0. The threshold for the muon trigger is also looser than the one used in pp collisions, which is equal to 800 MeV.

3.3.2 HLT1

Two different HLT1 configurations were used: TCK 0x11431621 for runs between 186555 and 187204, and TCK 0x11441621 for the other runs. As far as the analysis presented here is concerned, these two configurations are identical (they differ only for pre-scales of the NoBias line and of dedicated high multiplicity lines). The trigger lines used in the analysis are given in Table 4. All candidates kept for the analysis must be TOS of the DiMuonHighMass line.

Table 3: Definition of L0 TCK 0x1621.

Line name	Condition
SPD	Spd multiplicity > 0
PU	Pile-Up multiplicity > 3
Muon	$p_T > 500$ MeV
DiHadron,lowMult	$E_T(\text{hadron}) > 408$ MeV, SPD multiplicity < 20 and Pile-Up multiplicity < 2
Muon,lowMult	SPD multiplicity < 20 and $p_T > 400$ MeV
DiMuon,lowMult	SPD multiplicity < 20 , $p_{T1} > 100$ MeV and $p_{T2} > 100$ MeV
Electron,lowMult	SPD multiplicity < 20 and $E_T(\text{electron}) > 1.2$ GeV
Photon,lowMult	SPD multiplicity < 20 and $E_T(\text{photon}) > 1.2$ GeV
DiEM,lowMult	SPD multiplicity < 20 , $E_T(\text{electron}) > 480$ MeV and $E_T(\text{photon}) > 480$ MeV
B1gas	SumEt > 4992 MeV on beam-empty crossings
B2gas	Pile-up multiplicity > 9 on empty-beam crossings

Table 4: HLT1 trigger line.

Line name	Conditions
DiMuonHighMass	L0: L0Muon decision Global event cut: number of VELO hits < 8000 μ^\pm : $p_T > 300$ MeV, $p > 4$ GeV, track $\chi^2 < 4$, ghost probability < 999 , lsMuon $\mu^+\mu^-$ combination: $M > 2.5$ GeV

3.3.3 HLT2

Three HLT2 configurations were used: TCK 0x21421621, 0x21451621 and 0x21461621. Here also all these TCKs are identical as far as this analysis is concerned. The selections applied in HLT2 are described in Table 5. The lines used in the analysis are saved in the TURBO format and the triggers candidates saved in the data RAW files are taken directly for the final analysis. The offline processing relevant for this analysis was performed using processing pass Turbo03pLead with DaVinci version v41r3.

The analysis makes use of a large NoBias sample recorded at the same time, for cross-checks or computation of trigger efficiency for example. This sample is acquired with a random trigger on bunch crossings, based only on the LHC filling scheme, without any requirement on detector quantities at L0, HLT1 or HLT2, which are pass-through. The NoBias events are stored in a NoBias stream, reconstructed with the same configuration than the triggered events.

Table 5: HLT2 trigger lines.

Line name	Conditions
DiMuonJPsiTurbo	μ^\pm : $p_T > 500$ MeV $\mu^+\mu^-$ combination: $ M - M(J/\psi) < 150$ MeV and vertex $\chi^2 < 25$
DiMuonPsi2STurbo	μ^\pm : $p_T > 500$ MeV $\mu^+\mu^-$ combination: $ M - M(\psi(2S)) < 150$ MeV and vertex $\chi^2 < 25$

4 Selections

4.1 Global Event Selection

Only events with less than 8000 VELO hits are considered in this analysis, as imposed by the trigger requirements (the standard cut for pp running is 6000 VELO hits). All events are also required to have at least one reconstructed primary vertex since this information is mandatory to separate the prompt from from- b contributions.

4.2 Candidate Selection

The J/ψ and $\psi(2S)$ candidates are formed from two oppositely charged muons coming from a common vertex. Both decay modes are using very close selection criteria. They are required to be TOS (*Trigger On Signal*) for the L0Muon and Hlt1DiMuonHighMass trigger lines, *i.e.* that the reconstructed candidate or its decay products are associated with a trigger object fulfilling the trigger requirements. Then the candidates used are directly the ones selected by the line Hlt2DiMuonJPsiTurbo and Hlt2DiMuonPsi2STurbo lines respectively, in the TURBO stream, without offline reconstruction. The comparison of reconstructions in TURBO stream and offline has been studied using J/ψ candidates in the 13 TeV early measurement analysis, described in section I in the appendix of the analysis note [49]. The conclusion is that concerning signal yields, the difference is well below 0.1%, and other distributions including invariant mass and t_z are also almost identical. After the early measurement period, more tuning have been applied to the turbo stream further reducing online offline differences.

Finally, additional cuts are applied at the analysis level. Muon tracks have to be in the geometrical acceptance of the spectrometer ($2 < \eta < 5$) and to have $p_T > 750$ MeV/ c . Muon tracks are required to have a good fit quality, $\chi^2/ndof < 3$ and a ghost probability less than 0.4. The tracks are identified as muons by requiring $\text{ProbNN}(\mu) > 0.5$ for the J/ψ selection. For the J/ψ , the $\text{ProbNN}(\mu)$ threshold value is chosen to reject a large fraction of background but to be very efficient on signal candidates, as can be seen in Fig. 1. The two muons are required to form a good vertex asking the vertex fit probability $\text{Prob}(\chi^2) > 0.5\%$. The J/ψ candidates are required to have a mass within 120 MeV/ c^2 of the PDG value. All selection criteria are specified in Table 6.

Table 6: Offline selection for J/ψ candidates.

Condition	
μ^\pm	$2 < \eta < 5$ $p_T > 750 \text{ MeV}/c$ $\text{ProbNN}(\mu) > 0.5 [J/\psi]$ Track ghost probability < 0.4 χ^2 per degree of freedom of the track fit < 3
J/ψ	$ M(\mu^+\mu^-) - M(J/\psi) < 120 \text{ MeV}/c^2$ Vertex χ^2 probability $> 0.5\%$

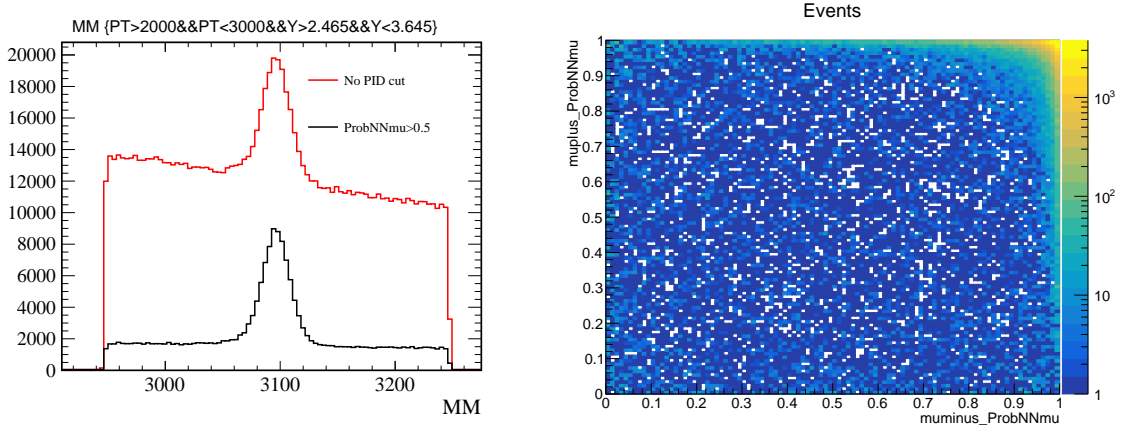


Figure 1: Muon identification cut. Left plot: example of the effect of the $\text{ProbNN}(\mu) > 0.5$ cut on J/ψ candidates in $p\text{Pb}$ for $2 < p_T < 3 \text{ GeV}/c$ and $2 < y^* < 3$ bin. Right plot: two dimensional distribution of $\text{ProbNN}(\mu)$ for the μ^+ (y-axis) and the μ^- (x-axis) for signal only candidates extracted with the *sPlot* technique.

5 Signal extraction

The numbers of prompt and non-prompt J/ψ signal candidates are extracted from a simultaneous fit to the invariant mass and pseudo-proper-time t_z distributions. The pseudo-proper-time is defined as

$$t_z = \frac{(z_{J/\psi} - z_{\text{PV}}) \times M_{J/\psi}}{p_z}, \quad (4)$$

where $z_{J/\psi}$ is the z -coordinate of the J/ψ decay vertex, z_{PV} the z -coordinate of the primary vertex, $M_{J/\psi}$ the nominal J/ψ mass and p_z the longitudinal J/ψ momentum. For prompt production, t_z is equal to 0 while for charmonium coming from the decay of a B hadron, t_z is a good approximation of the B hadron proper-time and should follow an exponential distribution.

5.1 Mass fit function

The function describing the invariant mass of the signal candidates is a Crystal Ball function defined as

$$f_{\text{CB}}(x; M, \sigma, \alpha, n) = \begin{cases} \frac{\left(\frac{n}{|\alpha|}\right)^n e^{-\frac{1}{2}\alpha^2}}{\left(\frac{n}{|\alpha|} - |\alpha| - \frac{x-M}{\sigma}\right)^n}, & \text{if } \frac{x-M}{\sigma} < -|\alpha| \\ \exp\left(-\frac{1}{2}\left(\frac{x-M}{\sigma}\right)^2\right), & \text{if } \frac{x-M}{\sigma} \geq -|\alpha|. \end{cases} \quad (5)$$

The value of the parameter n is fixed to 1 following the physics arguments described in [50], while the value of the parameter α is constrained from the values of the resolution parameter σ following

$$\alpha = 2.066 + 0.0085\sigma - 0.00011\sigma^2, \quad (6)$$

extracted from toy Monte Carlo studies and where σ is expressed in MeV. The background, which is only combinatorics, is described by an exponential function,

$$f_{\text{bkg}}(x; p) = e^{-px}. \quad (7)$$

Figure 2 shows the results of the mass fits for all reconstructed J/ψ and $\psi(2S)$ candidates, for $p\text{Pb}$ and $\text{Pb}p$ in the full analysis range.

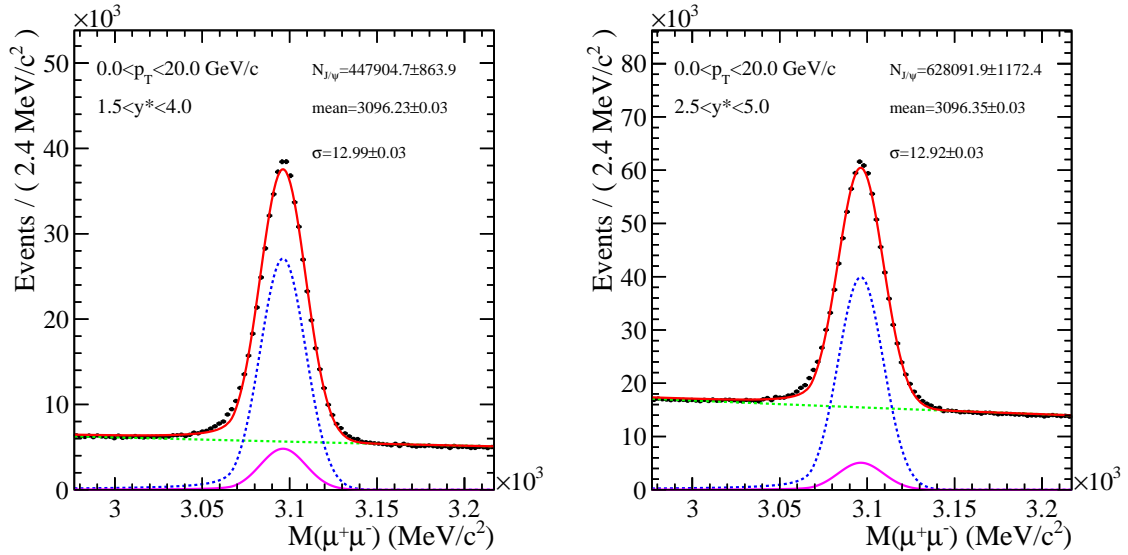


Figure 2: Mass distributions and fits for the left: J/ψ in $p\text{Pb}$, right: J/ψ in $\text{Pb}p$. The black dots are the data points, the red line is the result of the fit described in the text. The blue line is the prompt contribution, the magenta line the contribution from b decays, and the green line the background contribution.

5.2 Pseudo-properlifetime fit function

The function used to fit the t_z distribution describes three components: the prompt J/ψ , the J/ψ from B and the combinatorics background. The prompt component is described by a Dirac function,

$$f_{\text{prompt}}(x) = \delta(x) \quad (8)$$

and the non-prompt component by an exponential,

$$f_{\text{from B}}(x; \tau) = e^{-\frac{x}{\tau}}. \quad (9)$$

The signal J/ψ distributions are then fitted by the sum of these two functions, convoluted with a resolution function which is the sum of three Gaussian functions with a common mean and resolution parameters σ , 2σ and 4σ respectively:

$$f_{\text{resolution}}(x; \sigma, \beta_1, \beta_2, \mu) = \frac{\beta_1}{\sqrt{2\pi}\sigma} e^{-\frac{(x-\mu)^2}{2\sigma^2}} + \frac{\beta_2}{2\sqrt{2\pi}\sigma} e^{-\frac{(x-\mu)^2}{8\sigma^2}} + \frac{1-\beta_1-\beta_2}{4\sqrt{2\pi}\sigma} e^{-\frac{(x-\mu)^2}{32\sigma^2}} \quad (10)$$

The background is described by a function which is the sum of a delta function and five exponentials (three for positive t_z and two for negative t_z , the negative and positive exponentials with the largest lifetimes have their lifetimes fixed to the same value τ_4),

$$f_{\text{background}}(x; \tau_1, \tau_2, \tau_3, \tau_4, f_1, f_2, f_3, f_4) = (1-f_1-f_2-f_3-f_4)\delta(t_z) + \theta(t_z) \left(f_1 \frac{e^{-t_z/\tau_1}}{\tau_1} + f_2 \frac{e^{-t_z/\tau_2}}{\tau_2} \right) + \theta(-t_z) \left(f_3 \frac{e^{t_z/\tau_3}}{\tau_3} \right) + f_4 \frac{e^{-|t_z|/\tau_4}}{2\tau_4}, \quad (11)$$

convoluted with the sum of two Gaussian functions. The shape of the background is chosen empirically based on the shape seen in the t_z distribution of the J/ψ mass side-bands. Figure 3 shows the results of the t_z fits for all reconstructed J/ψ and $\psi(2S)$ candidates.

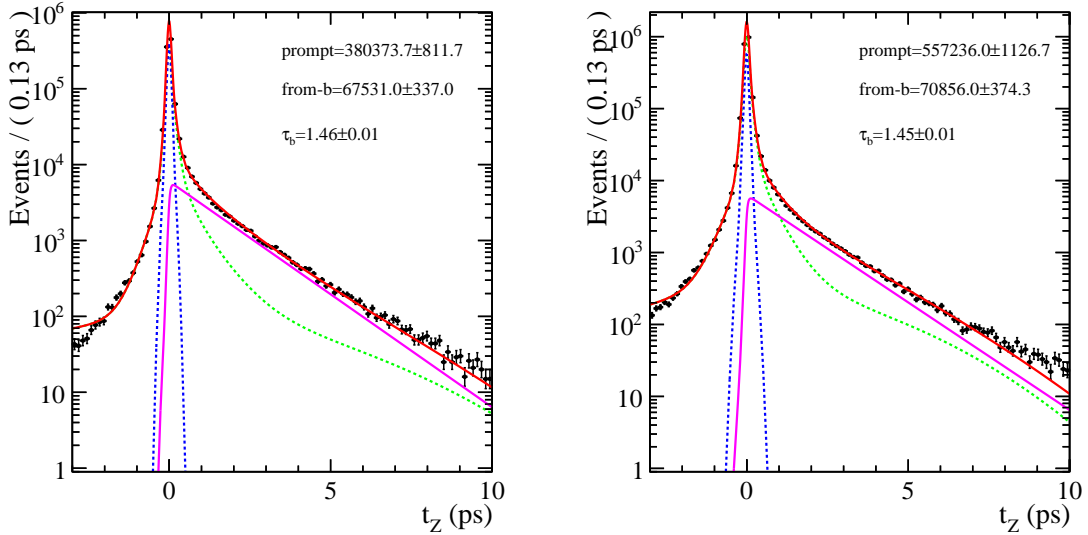


Figure 3: t_z distributions and fits for the left: J/ψ in $p\text{Pb}$, right: J/ψ in Pbp . The black dots are the data points, the red line is the result of the fit described in the text. The blue line is the prompt contribution, the magenta line the contribution from b decays, and the green line the background contribution.

5.3 Fit results

The measurements shown in this analysis use the number of events for each categories (prompt and non-prompt) fitted in each of the analysis bin, with a simultaneous fit to the mass and the pseudo-proper decay time distributions as described in the section above. Tables 10 and 11 give the number of prompt J/ψ , the number of J/ψ from b and the fraction of J/ψ from b (ratio of number of J/ψ from b to the total number of J/ψ) in all analysis bins for $p\text{Pb}$. Tables 12 and 13 give the results for J/ψ in $\text{Pb}p$. As examples, the J/ψ mass and t_z distributions together with the fit results are shown for bin $6 < p_{\text{T}} < 7 \text{ GeV}/c$ and $3.5 < y^* < 4$ in Fig. 4. All other mass and t_z fitted distributions can be found online at <https://twiki.cern.ch/twiki/pub/LHCbPhysics/JpsiInpPb/pPbFits.tar.gz> for $p\text{Pb}$ and at <https://twiki.cern.ch/twiki/pub/LHCbPhysics/JpsiInpPb/PbpFits.tar.gz> for $\text{Pb}p$. The parameters of the fit function are also given in Fig. 5 for all bins of the analysis.

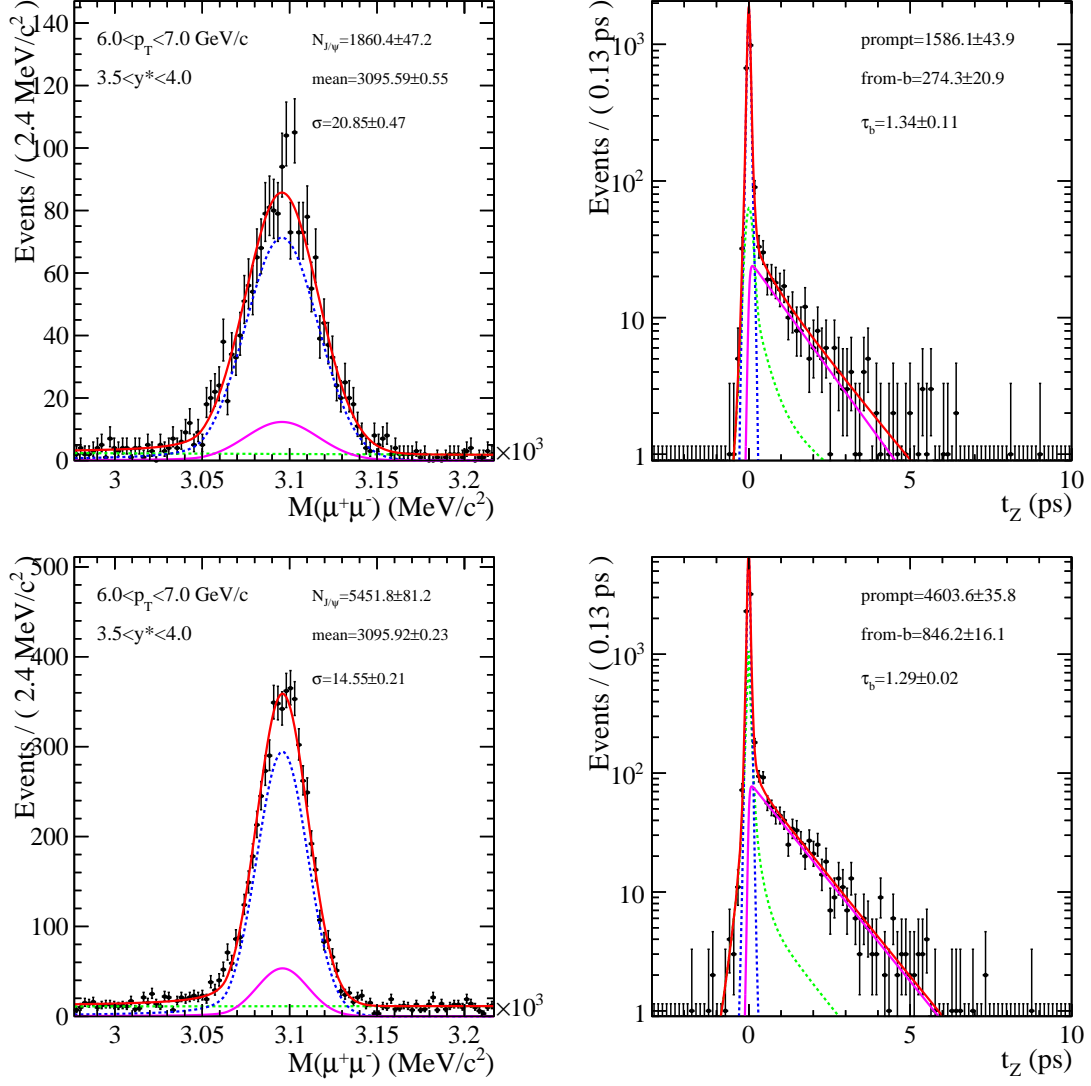


Figure 4: J/ψ left: mass and right: t_z distributions for the bin $6 < p_T < 7 \text{ GeV}/c$ and $3.5 < y^* < 4.0$ for top: $p\text{Pb}$ and bottom: PbPb . The black dots with error bars are the data and the red line is the total fit function described in the text. The blue line is the prompt contribution, the magenta line the contribution from b decays, and the green line the background contribution.

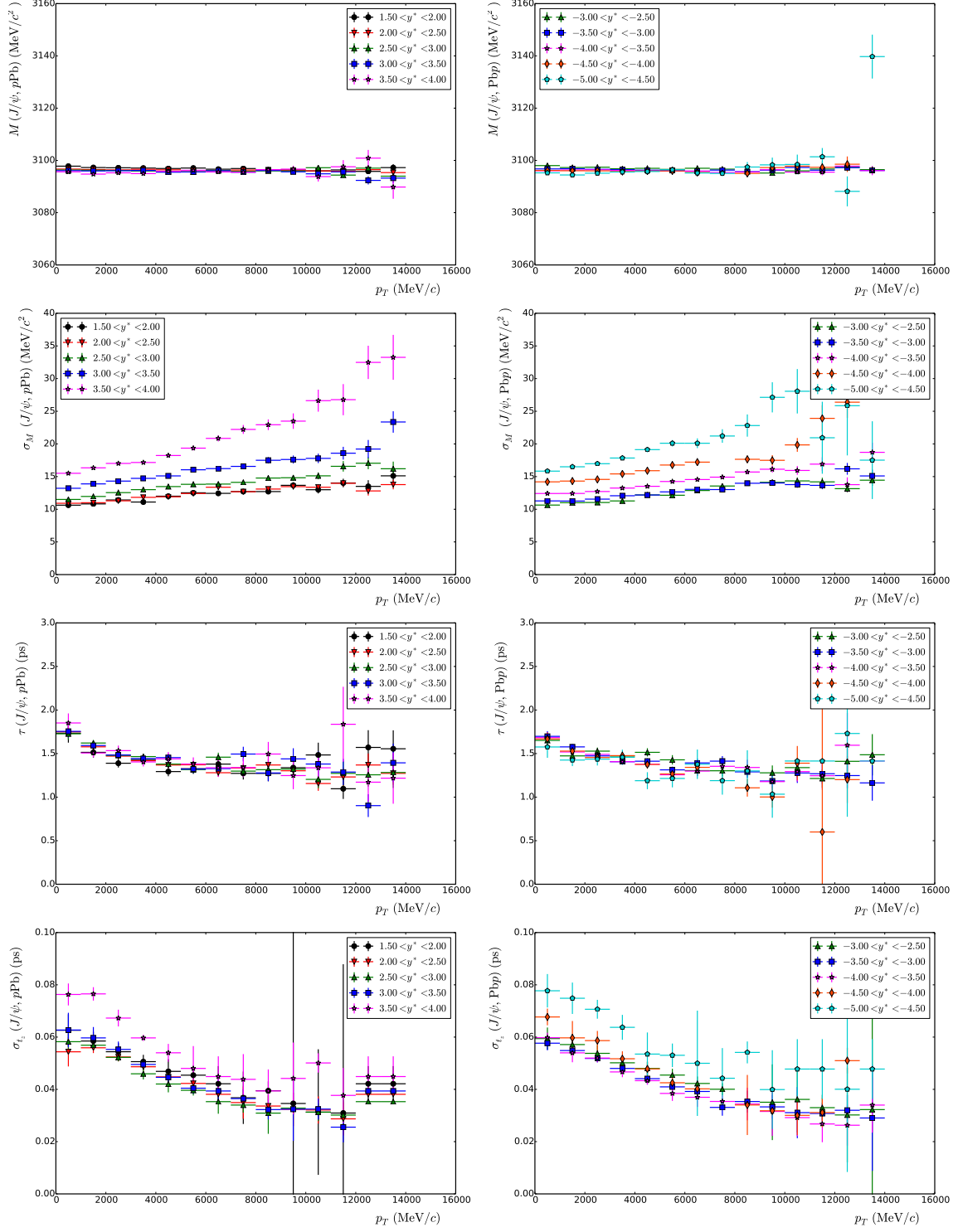


Figure 5: Fit parameters for J/ψ in left: $p\text{Pb}$ and right: PbPb . From top to bottom: M , σ_M , τ and σ_{t_z} .

6 Acceptance and efficiency

The number of signal candidates are corrected, bin by bin, by the total efficiency, $\epsilon(p_T, y^*)$ to obtain the cross-section measurements. The efficiencies are assumed to be equal for prompt J/ψ and J/ψ from b . The total efficiency is the product of the acceptance efficiency (ϵ_{acc}), the reconstruction efficiency (ϵ_{rec}), the selection efficiency (ϵ_{sel}), the particle identification efficiency (ϵ_{PID}) and the trigger efficiency (ϵ_{tri}), defined in the following.

$$\epsilon_{\text{tot}}(p_T, y^*) = \epsilon_{\text{acc}}(p_T, y^*) \times \epsilon_{\text{rec}}(p_T, y^*) \times \epsilon_{\text{sel}}(p_T, y^*) \times \epsilon_{\text{PID}}(p_T, y^*) \times \epsilon_{\text{tri}}(p_T, y^*). \quad (12)$$

All steps are determined from simulation, with truth matched signal decays, except for the tracking efficiency and the particle identification, where data driven methods are used to correct the efficiencies obtained from the simulation. In the simulation, J/ψ mesons are assumed produced without polarization. This assumption affects the efficiencies depending on geometric criteria, mainly the acceptance efficiency and the selection efficiency through transverse momentum selections. For the simulation samples used for this analysis, the truth matching efficiency is equal to $\epsilon_{\text{truth}} = 99.5 \pm 0.1\%$ for both $p\text{Pb}$ and $\text{Pb}p$ samples. A global correction factor of $1/\epsilon_{\text{truth}}$ is applied to take it into account, and is assumed to be independent of p_T and y^* .

6.1 Acceptance

The acceptance efficiency is defined as

$$\epsilon_{\text{acc}}(p_T, y^*) = \frac{J/\psi \text{ in bin } (p_T, y^*) \text{ with both } \mu \text{ in LHCb}}{J/\psi \text{ generated in bin } (p_T, y^*)}. \quad (13)$$

It is estimated from generator-level only simulations, using the settings described in Sect. 3.2. Both μ in LHCb means that the polar angle of the muon momentum with respect to the z axis is between 10 mrad and 400 mrad and that they have a pseudo-rapidity η between 2 and 5, before the magnet. Figures 6 give the values of ϵ_{acc} as a function of p_T for the different y^* bins of the analysis, for all configurations. The errors are the statistical errors from the generator-level simulations. Tables 14, 15, 16 and 17 give the corresponding numerical values.

6.2 Reconstruction efficiency

The reconstruction or tracking efficiency is defined as the fraction of J/ψ in the acceptance, where both muons are reconstructed as long tracks,

$$\epsilon_{\text{rec}}(p_T, y^*) = \frac{J/\psi \text{ in bin } (p_T, y^*) \text{ with both } \mu \text{ reconstructed as long tracks}}{J/\psi \text{ with both } \mu \text{ in LHCb}}. \quad (14)$$

The **long** method (more details in twiki [51]) is implemented to calibrate the tracking efficiency on data [52] and to correct the efficiencies obtained from the simulation. In this method, a **probe** track is reconstructed only with hits in the **TT** and **MUON** stations. This probe muon track is combined with a standard long muon track to form a J/ψ candidate,

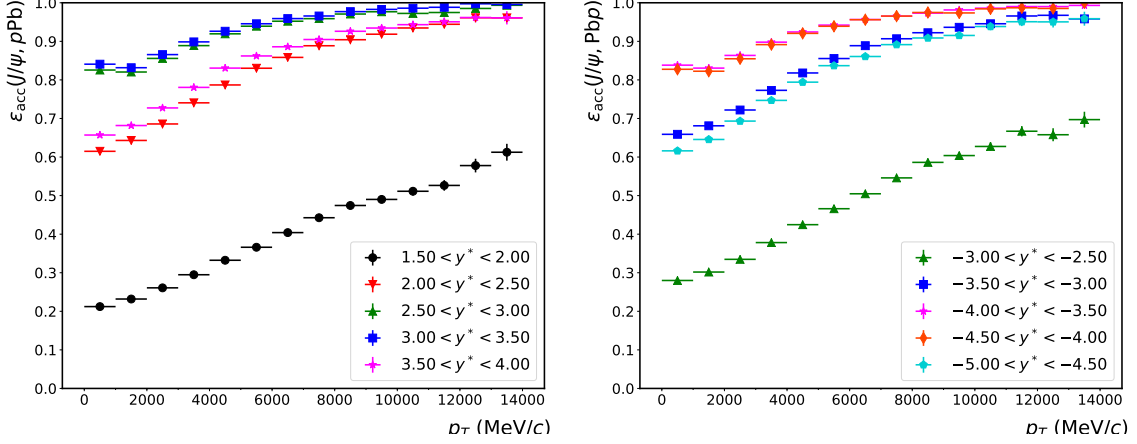


Figure 6: Acceptance efficiency ϵ_{acc} as a function of p_T in different y^* bins for left: J/ψ in pPb, right: J/ψ in PbPb.

and these candidates build a "pre-matched" sample. An additional standard long track, identified as a muon and with the same charge as the **probe** track, is combined with the J/ψ in the "pre-matched" sample to form a good vertex. If this third track shares with the **probe** track more than 40% of the hits in both the TT and MUON station, the probe track is referred to as "matched". The J/ψ candidates in the "pre-match" sample that have the probe track matched, form the "matched" sample. The tracking efficiency is computed as the matching efficiency, which is the fraction of probe tracks that match standard long tracks. The number of signal probe tracks and those matched to long tracks are estimated from the number of J/ψ signals, measured by fitting to the $\mu^+\mu^-$ invariant mass distribution in the "pre-matched" sample and the "matched" sample, respectively. The reconstruction of the probe tracks, of the J/ψ candidates and the implementation of the matching are done at the trigger (HLT) level, available in both pp and proton-lead data. For the **long** method, the relevant trigger lines are called Hlt2TrackEffDiMuonMuonTT(Minus|Plus)*.

Come to the particular case of calibration of proton-lead data, as used in this analysis, the calibration events are taken from TurboCal stream for both proton-lead and lead-proton respectively, where candidates are required to have fired the Hlt2TrackEffDiMuonMuonTT(Minus|Plus)* triggers. The proton-lead simulation used for tracking efficiency calibration is not available yet, however based on the study described in the following, it can be concluded that pp simulation for tracking efficiency could be used as a reference of tracking efficiency in proton-lead sample, after proper detector occupancy reweighting. The tracking calibration sample in pp simulation is produced with sim09b simulation tag, which has the same simulation/reconstruction packages as the proton-lead simulation, the only essential difference is the particles produced at generator level. In the simulation calibration sample, Turbo reconstruction is also enabled, and further offline processing is the same as for real data calibration sample (namely selections, signal extraction and so on).

Due to higher multiplicity in proton-lead data, especially in the backward configuration, further offline selections are applied to the events out of TurboCal stream (which are not applied for pp tracking calibration). The tag track of the J/ψ candidate is required to

have a good muon-pion separation with $\text{PID}(\mu) > 3$, and the probe track is required to have a better fit quality with $\text{Prob}(\chi_{\text{trk}}^2) > 0.2$. The effect of these further selections are studied with the proton-lead forward data sample ($p\text{Pb}$), in which a better signal purity is obtained.

The signal extraction fits are implemented in bins of η and p of the probe tracks, allowing to determine the track reconstruction efficiency in the same bins. The bin boundaries are 1.9, 3.2 and 5.0 for η and 6, 10, 20, 40, 100 and 500 GeV/ c for p . No binning in detector occupancy is implemented due to limited statistics. On the other hand, the multiplicity distribution in the tracking calibration sample is supposed to be reweighted to match the one in the user analysis sample if a strong dependence on occupancy is found. This reweighting can be done using the **sWeights** calibration sample. In this case, the tracking efficiency reweighted with detector occupancy is calculated as $\epsilon = \frac{\sum_i sw_i \times wo_i}{\sum_j sw_j \times wo_j}$, where $sw_{i,j}$ are the **sWeights** and wo_j are weights of occupancy. The indices in the denominator and numerator run over the "pre-matched" sample and "matched" sample, respectively. The occupancy in the detector is measured with the number of SPD hits, and the occupancy weights wo_j are determined as the ratio of detector occupancy between data and simulation in each bin of occupancy distribution for background subtracted signals.

The μ^+ and μ^- probe tracks are fitted separately, so for each kinematic bins, there are eight fits to be performed: μ^+ or μ^- as the probe track, "pre-matched" or "matched" sample, $p\text{Pb}$ or $\text{Pb}p$. For the fits, the same signal shape is used for identical bins, a Gaussian function plus a Crystal Ball function, while the signal yield is an independent parameter. The background is described by an exponential function. An example of the fit is shown in Fig. 7.

The same procedure is applied to a large pp collision simulation sample dedicated for tracking efficiency determination, allowing to get the efficiency ratio between data and simulation. The efficiency ratio determined this way is used to correct the simulation used for the analysis. To make this approach correct, the detector occupancy distribution in the tracking simulation sample should be reweighted to match the analysis simulation sample, in addition to the reweighting of the occupancy in data as mentioned above.

The tracking efficiency for μ^+ and μ^- are averaged, since for the cross-section measurements charge conjugated states are added together. The efficiency measured in data, in bins of the η and p , for $p\text{Pb}$ and $\text{Pb}p$, and the efficiency measured in pp simulation reweighted to match the $p\text{Pb}$ simulation occupancy, are given in Fig. 8. It should be noted that the reweighting with the detector occupancy for pp simulation increases the tracking efficiency per track by about 0.1%, *i.e.* the effect is very small.

Finally, we calculate the ratio of tracking efficiencies between $p\text{Pb}$ data and occupancy weighted MC, and $\text{Pb}p$ data and occupancy weighted MC respectively, in each p and η bin of the track at study. The results are given in Fig. 9. The corresponding uncertainty for each number is also shown, while the details of the studies for the uncertainty is provided in Sect. 7.4.

The reconstruction efficiency ϵ_{rec} is then computed from the full simulation using J/ψ candidates matched to true signal decays, and correcting this efficiency using the per-track efficiency ratios detailed above. The result is shown on Fig. 10, where the errors are the statistical errors from the simulation and the errors on the correction factors for the efficiency, adding quadratically. Tables 18, 19, 20 and 21 give the corresponding numerical

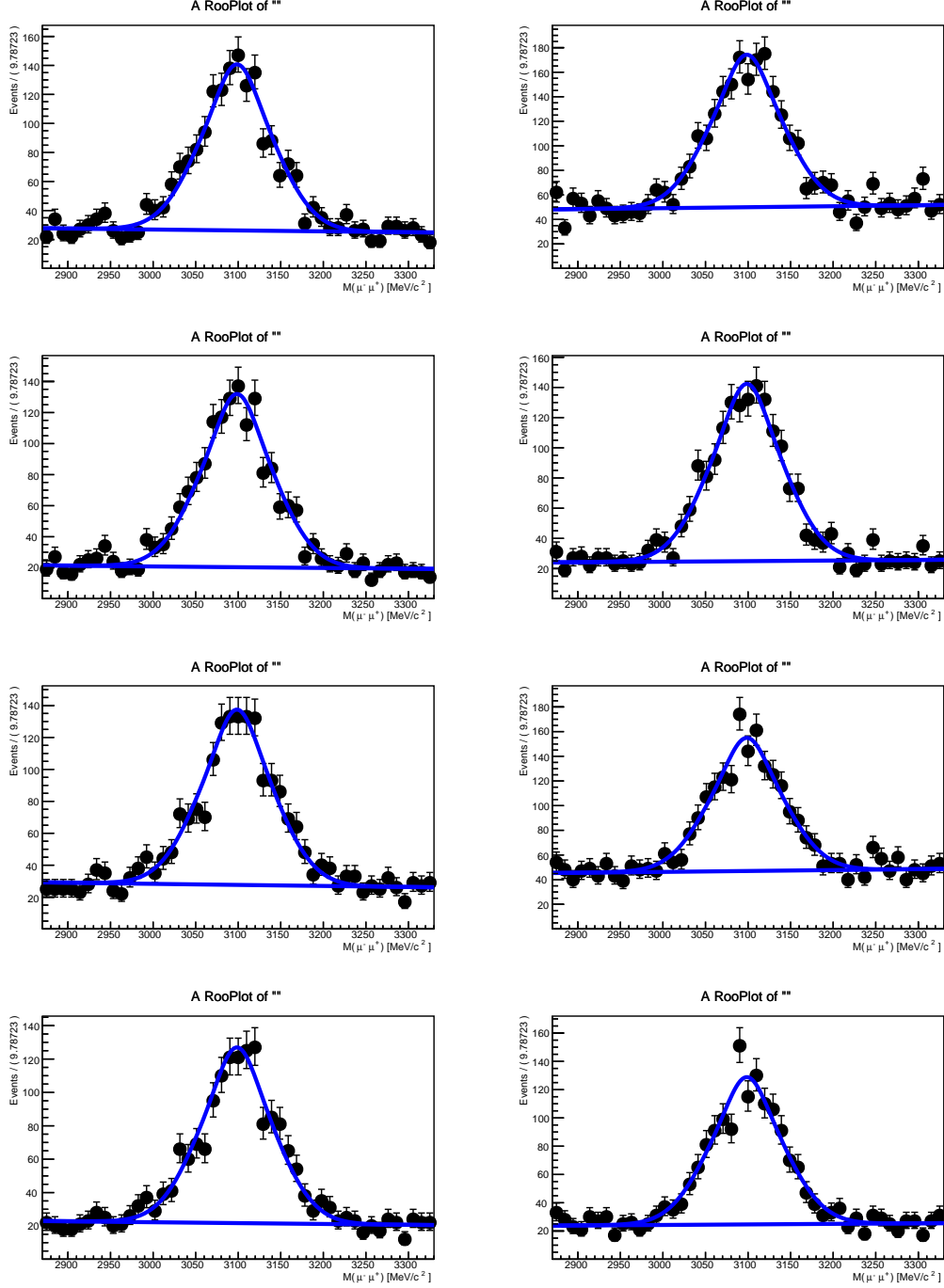


Figure 7: Fit to the invariant mass distribution of J/ψ candidates in the track calibration sample of proton-lead data. The left and right hand side columns correspond to $p\text{Pb}$ and PbP data, respectively. The first and third rows correspond to the "pre-matched" samples for μ^+ and μ^- probe tracks, respectively. The second and forth rows correspond to the "matched" samples for μ^+ and μ^- probe tracks, respectively.

values. The correction factors are $\frac{\epsilon(p\text{Pb, data})}{\epsilon(pp, \text{MC})}$ and $\frac{\epsilon(\text{PbP, data})}{\epsilon(pp, \text{MC})}$. All numbers are determined from the tracking calibration stream and have detector occupancy properly reweighted to match the analysis simulation and data samples.

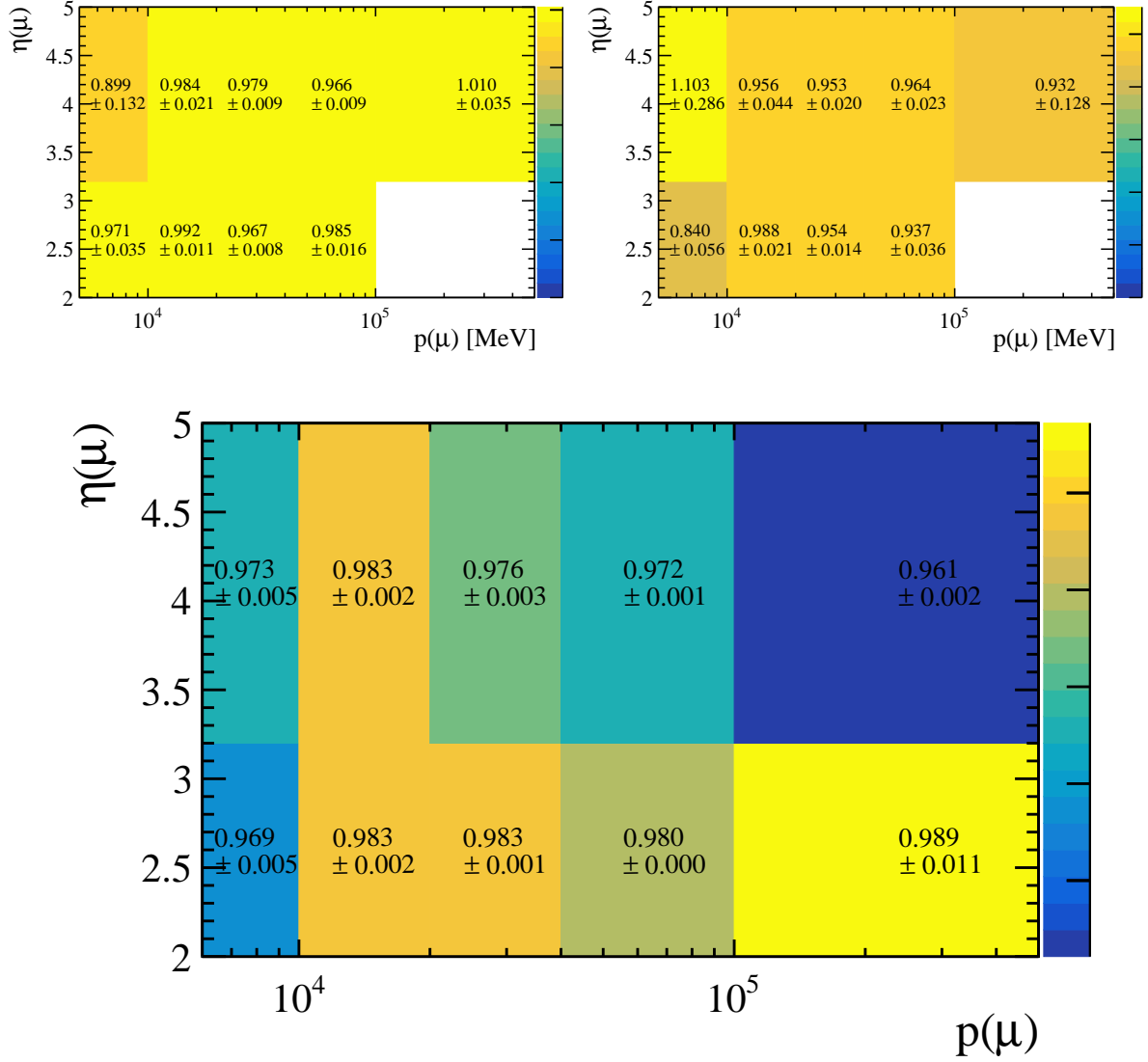


Figure 8: Tracking efficiency in bins of η and p for top left: p Pb data, top right: Pbp, bottom: pp simulation reweighted with the number of SPD hist to match the occupancy of the p Pb simulation samples used to compute the efficiencies in this analysis.

6.3 Selection efficiency

The selection efficiency is defined as

$$\epsilon_{\text{sel}}(p_T, y^*) = \frac{J/\psi \text{ selected in bin } (p_T, y^*)}{J/\psi \text{ in bin } (p_T, y^*) \text{ with both } \mu \text{ reconstructed as long tracks}}. \quad (15)$$

For the selection efficiency computation, particle identification criteria, the global event cut on the number of VELO clusters and the finding of the primary vertex are excluded since their efficiencies are derived from data as described below and in the next section. The main reduction of the efficiency in the selection is caused by the transverse momentum requirements on the daughter tracks. This loss of efficiency is purely of kinematic nature and can be calculated from the simulation samples (with the assumption that J/ψ mesons

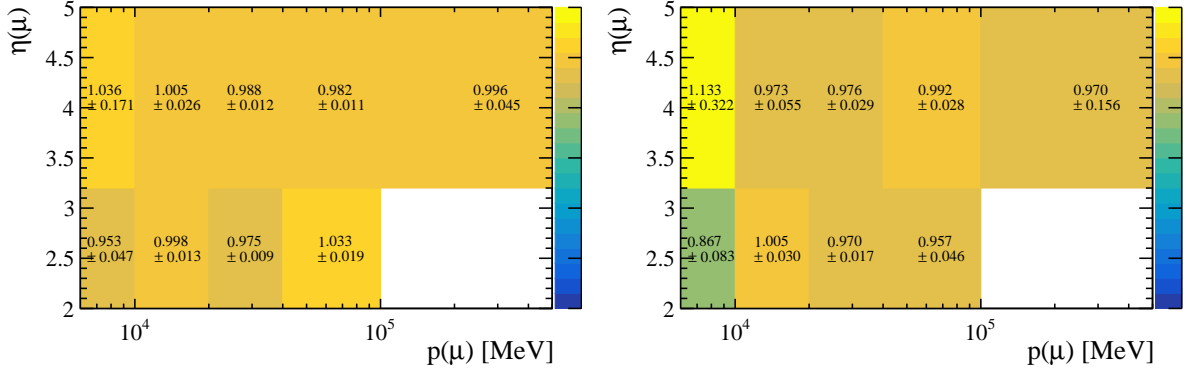


Figure 9: Ratio between data and reweighted pp simulation of per-track tracking efficiency in bins of the track η and p . Left: $p\text{Pb}$, right: $\text{Pb}p$.

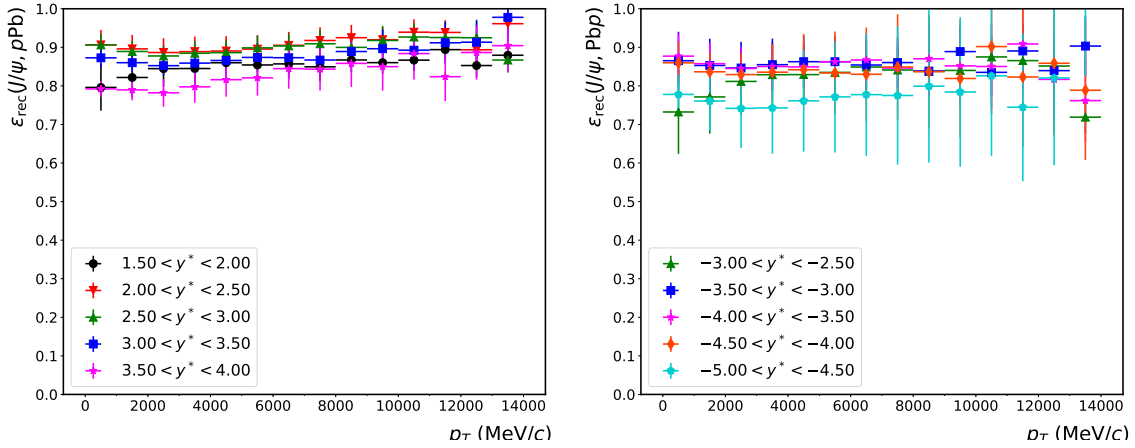


Figure 10: Reconstruction efficiency ϵ_{rec} as a function of p_T in different y^* bins for left: J/ψ in $p\text{Pb}$, right: J/ψ in $\text{Pb}p$.

are not produced polarized). Figure 11 shows the selection efficiencies, with statistical errors only. Tables 22, 23, 24 and 25 give the corresponding numerical values.

The efficiency of the global event cut on the number of VELO hits is computed directly from data, using di-muon candidates triggered by the **NoBias** trigger. For this trigger line, the global event cut is not applied, and the cut efficiency can be computed by counting the number of J/ψ signal candidates with a number of VELO hits greater than 8000. The efficiency is found equal to $99.9 \pm 0.1\%$ for both $p\text{Pb}$ and $\text{Pb}p$. Figure 12 show the distribution of VELO clusters for J/ψ signal candidates (after background subtraction) in the no bias triggered sample, for $p\text{Pb}$ and $\text{Pb}p$. The efficiency of this global event cut is assumed to be the same for candidates coming from b decays, and also to be independent of the charmonium p_T and y^* values. The efficiency of the requirement that the number of reconstructed primary vertex is larger or equal to one is computed from J/ψ pp simulations, and found equal to $99.9 \pm 0.1\%$. It is here also assumed to be identical for $p\text{Pb}$ and $\text{Pb}p$, and for candidates from b decays and not to depend on the kinematics of the signal candidate.

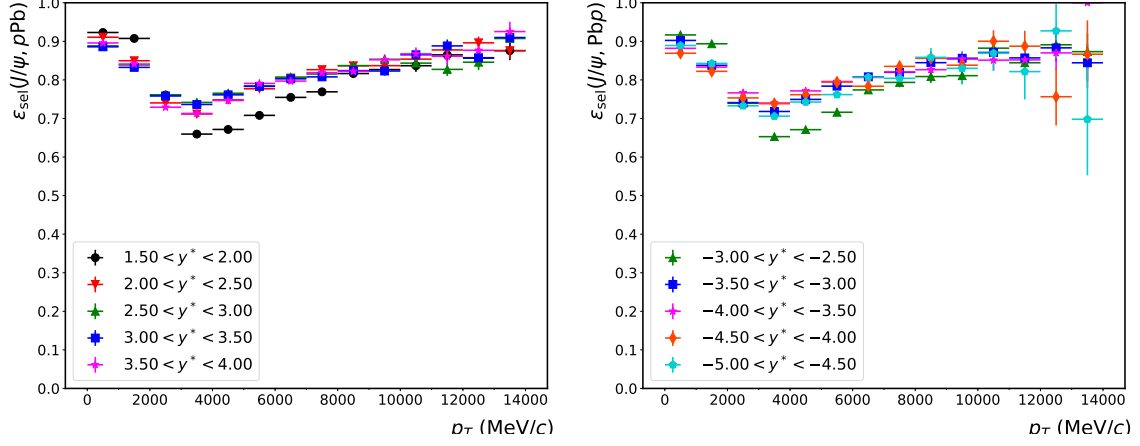


Figure 11: Selection efficiency ϵ_{sel} as a function of p_T in different y^* bins for left: J/ψ in $p\text{Pb}$, right: J/ψ in PbP .

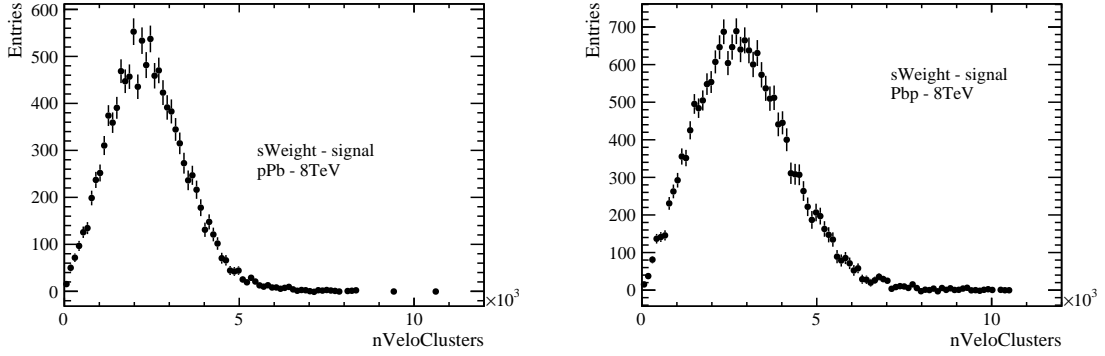


Figure 12: Number of VELO clusters, after background subtraction, for left: J/ψ in $p\text{Pb}$ and right: J/ψ in PbP .

6.4 PID efficiency

The PID efficiency is defined as

$$\epsilon_{\text{PID}}(p_T, y^*) = \frac{J/\psi \text{ satisfying the PID selection in bin } (p_T, y^*)}{J/\psi \text{ selected in bin } (p_T, y^*)}. \quad (16)$$

The PID efficiency for muons is taken from data using calibration tables (PIDCalib tables) obtained from control samples, namely J/ψ candidates with one of the two muon identified with tight criteria and the other one not identified. These calibration tables give the efficiency of the PID selections as a function of the pseudo-rapidity, of the total momentum of the muon tracks and of the track multiplicity of the event estimated from the number of hits in the SPD. They are available for the pp , $p\text{Pb}$ and PbP data taking, however the $p\text{Pb}$ and PbP tables have large statistical uncertainties. In this analysis, the pp tables are used, but re-weighted as a function of the SPD multiplicity to take into account the differences in multiplicities between pp , $p\text{Pb}$ and PbP . The efficiencies obtained this way are more precise and compatible with the efficiencies measured with the calibration samples in $p\text{Pb}$

and Pbp as can be seen in Figs. 13 and 14 which give the efficiencies as a function of the momentum and pseudo-rapidity of the muon of the $lsMu\text{on}$ and of the $\text{ProbNN}(\mu) > 0.5$ requirements.

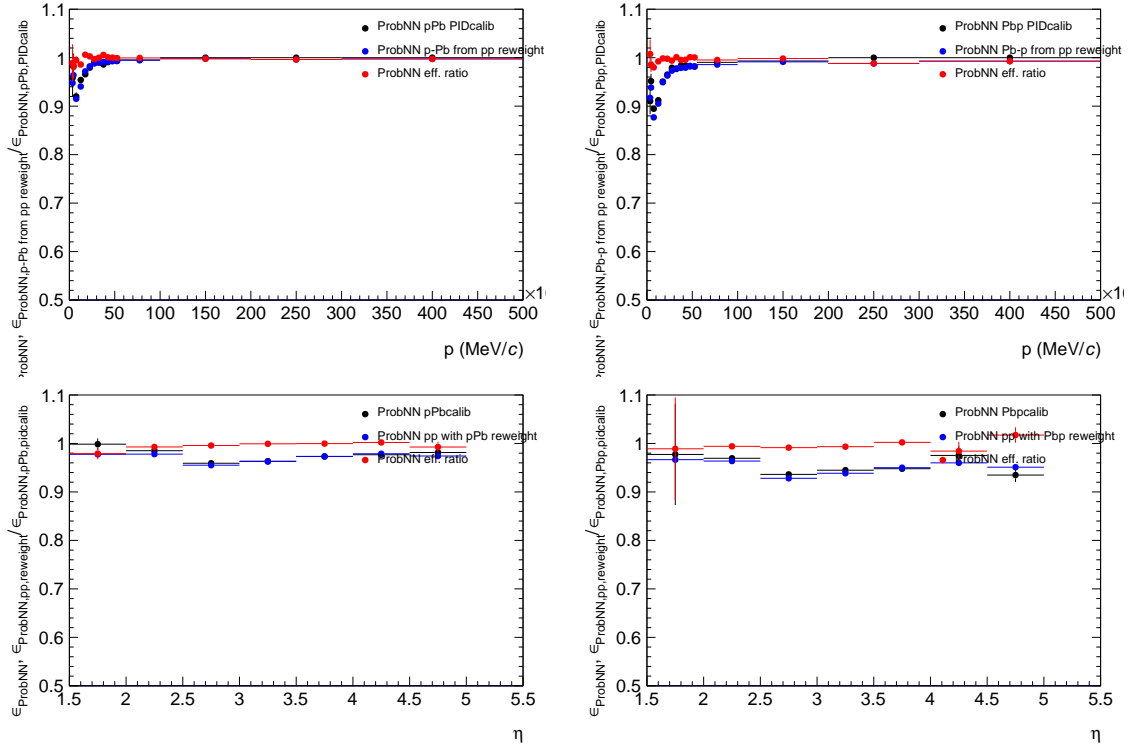


Figure 13: Muon PID efficiency obtained from the pp calibration tables reweighted with the pPb/PbP multiplicity (blue), from the pPb/PbP calibration tables (black) and their ratios (red), for the $\text{ProbNN}(\mu) > 0.5$ selection as a function of momentum top left: pPb , top right PbP , as a function of η bottom left: pPb , bottom right: PbP .

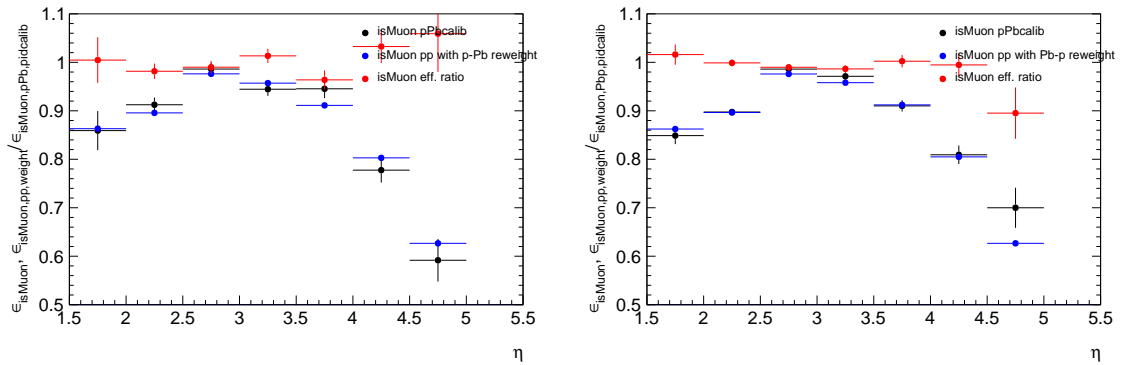


Figure 14: Muon PID efficiency obtained from the pp calibration tables reweighted with the pPb/PbP multiplicity (blue), from the pPb/PbP calibration tables (black) and their ratios (red), for the $isMu\text{on}$ selection as a function of η left: pPb , right PbP .

386 The SPD multiplicity in Pbp events can be larger than the maximum seen in pp
 387 collisions, and exceed the maximum multiplicity of the pp tables. This can be seen in
 388 Fig. 15 where the muon ID efficiency from the pp , pPb and Pbp is shown as a function
 389 of the SPD multiplicity, integrated over p and η . In the bins $1000 < \text{SPD} < 1200$ and
 390 $1200 < \text{SPD} < 1400$, where there is no measurement of the PID efficiency in pp , the pp
 391 efficiencies of the bin $800 < \text{SPD} < 1000$ are used, scaled by the ratio of the efficiencies
 392 obtained in Pbp in these bins.

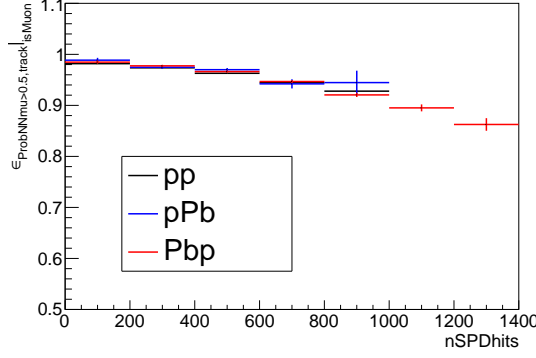


Figure 15: Particle identification efficiency measured in data for black: pp , blue: pPb and red: Pbp for muons, as a function of the SPD multiplicity, integrated over p and η .

393 The efficiencies ϵ_{PID} as a function of the J/ψ kinematic variables are obtained re-
 394 weighting the simulation samples with weights equal to the efficiencies measured in data
 395 for each muon track, as a function of its kinematic variables. These efficiencies are shown
 396 in Fig. 16. The error bars in these figures are the total uncertainties, described in detail
 397 in Sect. 7.6. Tables 26, 27, 28 and 29 give the corresponding numerical values.

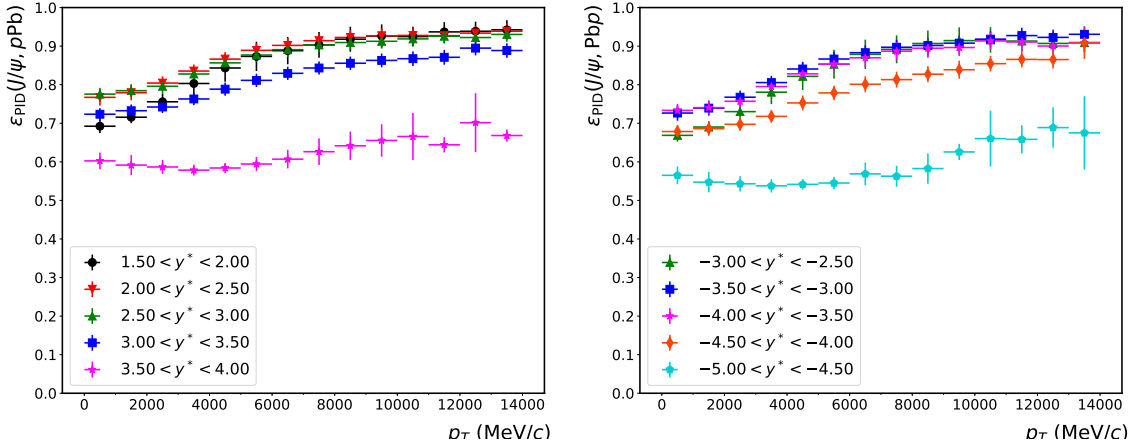


Figure 16: Particle identification efficiency ϵ_{PID} as a function of p_T in different y^* bins for left: J/ψ in pPb , right: J/ψ in Pbp .

6.5 Trigger efficiency

The trigger efficiency is defined as follows

$$\epsilon_{\text{tri}}(p_T, y^*) = \frac{J/\psi \text{ TOS of L0 and HLT1 in bin } (p_T, y^*)}{J/\psi \text{ selected in bin } (p_T, y^*)}, \quad (17)$$

where here the selection includes the PID requirements. The efficiencies are computed with the simulated samples, applying on them the simulation of the PID. Note that since the analysis is done on the TURBO candidates, the efficiency of the HLT2 is included in the reconstruction, PID and selection efficiencies. The trigger efficiency as a function of the candidate p_T in different y^* bins is shown in Fig. 17, where the error bars are the statistical uncertainties of the statistics of the simulation samples. Tables 30, 31, 32 and 33 give the corresponding numerical values.

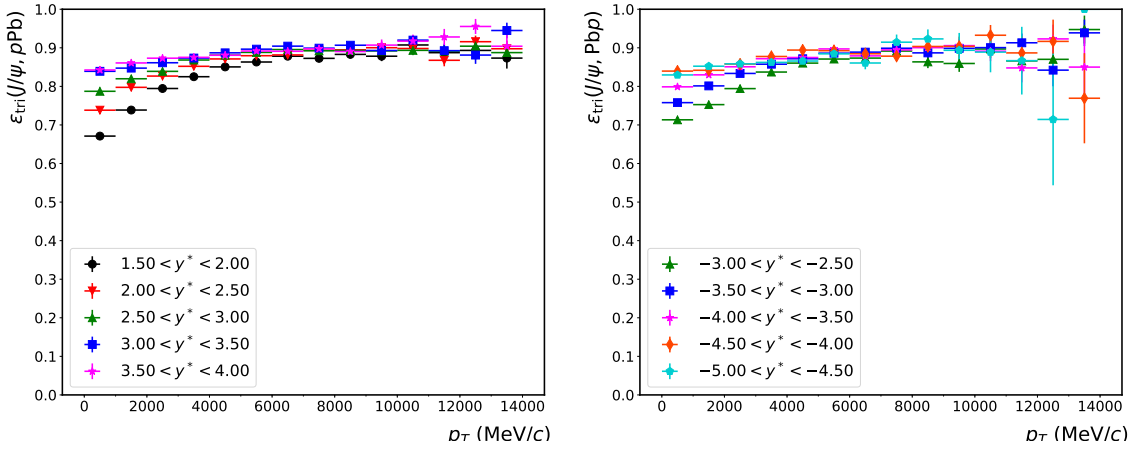


Figure 17: Trigger (L0 and HLT1) efficiency ϵ_{tri} as a function of p_T in different y^* bins for left: J/ψ in pPb, right: J/ψ in PbPb.

6.6 Total efficiencies

The total efficiency, equal to the product all efficiencies mentioned above, is given in Fig. 18. The errors are the statistical errors from the simulation statistics and the systematic uncertainties affecting the efficiencies and detailed in the following section, added quadratically. The numerical results are given in Tables 34, 35, 36 and 37.

7 Systematic uncertainties

The systematic uncertainties affecting the various quantities measured in the analysis are reported in this section. Some uncertainties are correlated between bins. The correlation of these uncertainties with the pp reference cross-section is also detailed. A large systematic uncertainty is due to the unknown polarization of the J/ψ mesons at production. In this analysis, this effect is ignored, assuming they are produced un-polarized. This is justified by the fact that the polarization measured in pp collisions at similar energies is small.

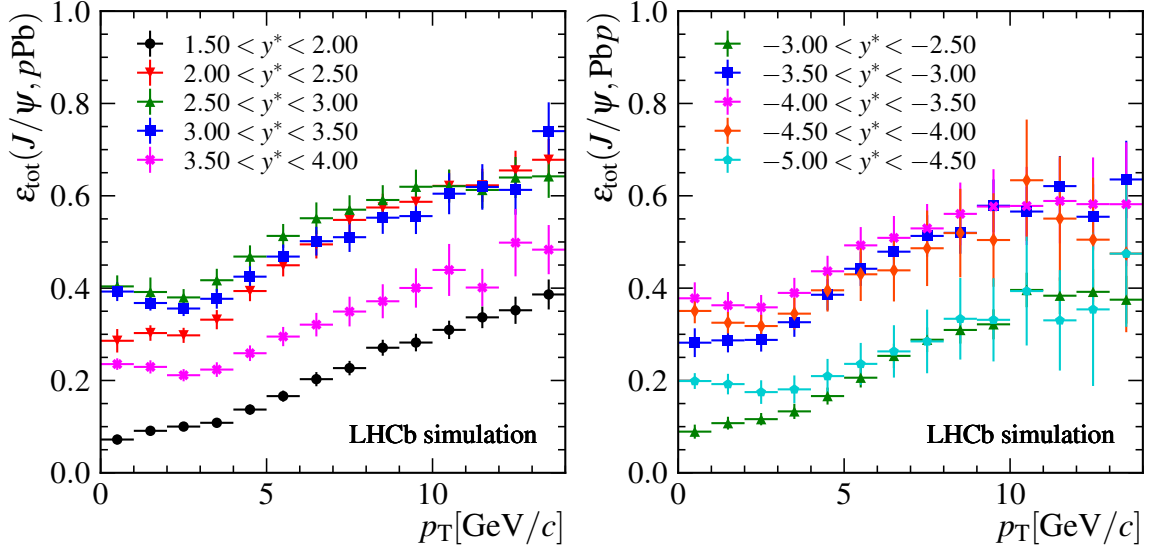


Figure 18: Total efficiency ϵ_{tot} as a function of p_T in different y^* bins for left: J/ψ in $p\text{Pb}$, right: J/ψ in PbPb .

Note that this is not true for J/ψ from b decays which have a large polarization in the decay of the b hadrons, but this polarization is largely diluted when measuring it with respect to the detector axis and has no effect on the efficiencies.

7.1 Monte Carlo statistics

This uncertainty is the statistical error on the individual efficiencies, due to the finite size of the simulation samples. This uncertainty is uncorrelated between bins and measurements. It varies from 0.05% to 10.9% for $p\text{Pb}$ and from 0.1% to 13.3% for PbPb .

7.2 Signal extraction

The choice of the fit model for the mass and t_z distributions affects the number of events. The uncertainty associated with the choice of the signal mass function is estimated using a different function, namely the sum of a Gaussian function and a Crystal Ball function instead of the single Crystal Ball function used in the nominal fit. Figure 19 shows the distribution of the ratios of the number of events obtained for the nominal and alternate fit model. An uncertainty equal to the RMS of the distribution, 1.3% is then used, associated with the mass fit model. This uncertainty is correlated between bins and between $p\text{Pb}$ and PbPb .

7.3 Bin to bin migration

Due to finite resolution on the p_T and y measurements, events can be counted in a wrong bin. However, the resolutions are small compared to the bin widths used for this measurement. Fig. 20 shows the comparison of true and reconstructed values of p_T and

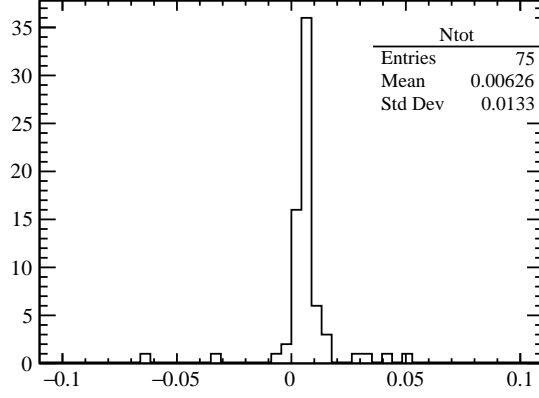


Figure 19: Ratio of number of signal events obtained with the nominal fit (single Crystal Ball function) and the alternate fit (Crystal Ball plus Gaussian functions).

439 y (in two example bins) of the MC candidates and the bin to bin migration effect is
 440 estimated to be less than 1% and, therefore, neglected.

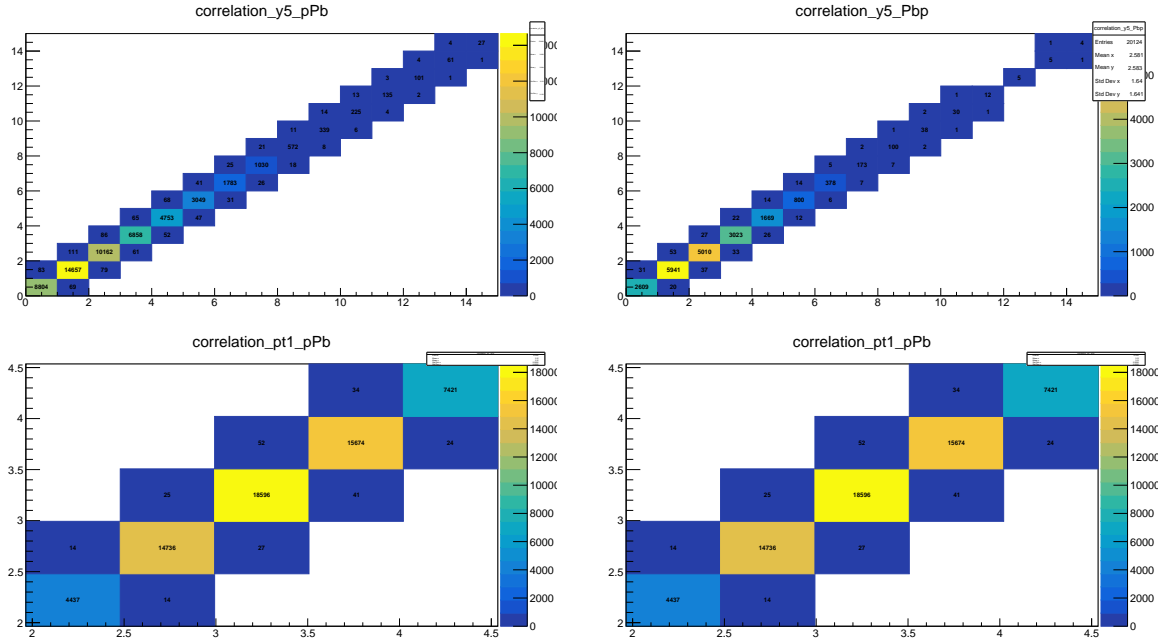


Figure 20: Effect of bin to bin migration in MC. y -axis: generator level values, x -axis: reconstruction level values. Top plots show the bin to bin migration effect for p_T (for the most forward rapidity bin), while bottom plots show the effect on the rapidity bins ($p_T < 1\text{GeV}/c$). Left: $p\text{Pb}$, right: Pbp .

7.4 Tracking efficiency

The tracking efficiency correction tables have uncertainties due to three sources: the statistics of the calibration sample, the signal extraction uncertainty and the offline selection uncertainty. The signal extraction systematic uncertainty for the tracking efficiency, described in Sec. 6.2, largely cancels in the efficiency calculation. However for bins where the signal purity is small especially in the "pre-matched" sample, the signal yield is found to be dependent on the mass window in the fit (essentially because of the background shape). For the high purity bins, the effect is much smaller than the statistical uncertainty. The change of the efficiency in each bin is considered as systematic uncertainty, as shown in Fig. 21.

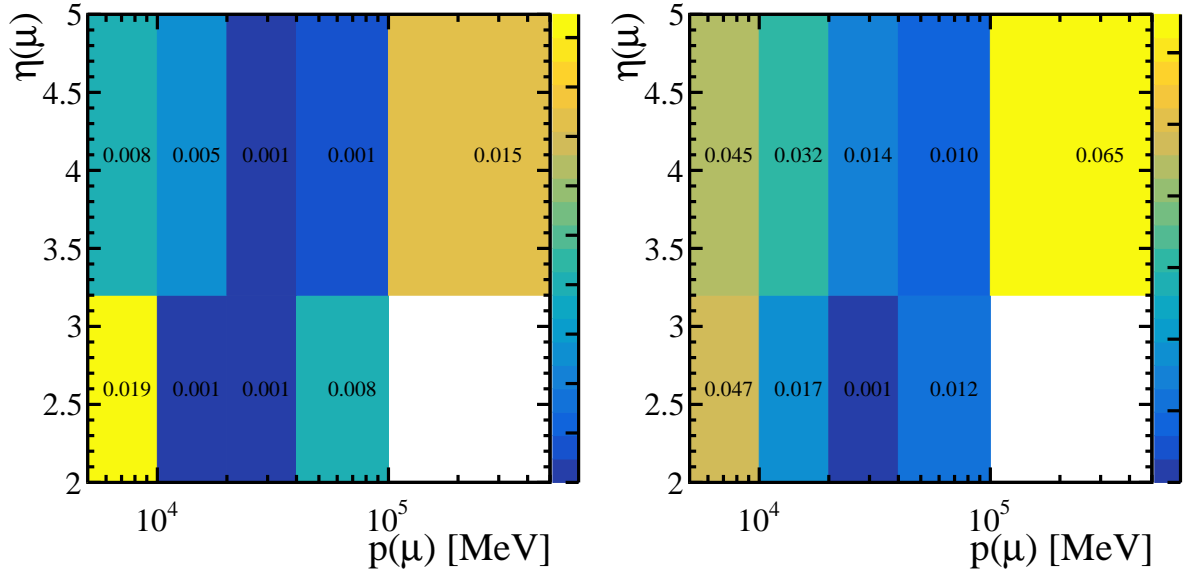


Figure 21: Systematic uncertainty due to signal extraction for the tracking efficiency computation. Left: $p\text{Pb}$, right: $\text{Pb}p$.

The effect of the additional offline selections is checked with the $p\text{Pb}$ sample. The tracking efficiency in both data and simulation are calculated again without these cuts. It is found that for the simulation the efficiency changes by less than 0.1%, while for data the variation of the efficiency is of 1% as shown in Fig. 22, which plots the probe track matching efficiency estimated with offline cuts with respect that estimated without offline cuts, in the $p\text{Pb}$ sample. The change of the efficiency in each bin is considered as a systematic uncertainty per track, correlated in all bins, and is supposed to be common for forward and backward sample. The total uncertainty from these three effects, obtained adding them in quadrature varies from 2.6% to 7.9% for $p\text{Pb}$ and from 5.7% to 26.5% for $\text{Pb}p$.

The long method has an uncertainty of 0.8% per track, as suggested by the tracking group [51]. The tracking uncertainties are correlated between bins.

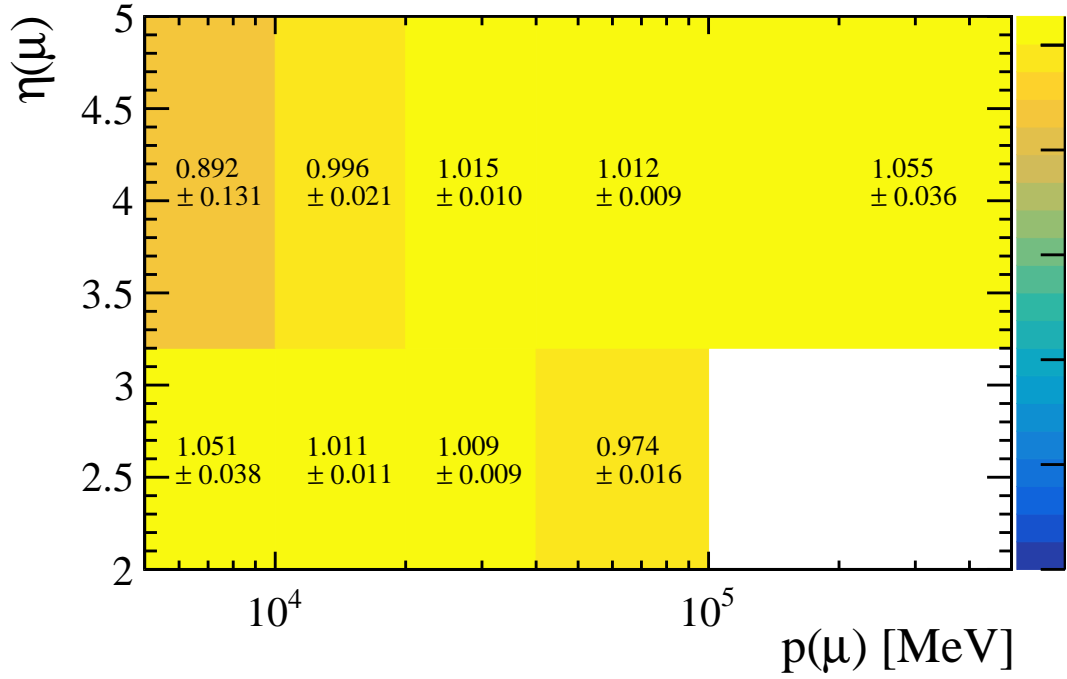


Figure 22: Ratio of probe track matching efficiency with and without additional offline selections in the $p\text{Pb}$ sample.

7.5 Selection efficiency

7.5.1 Global event cut

The large **NoBias** sample gives a reliable way to compute on data the efficiency of the global event cut on the number of VELO clusters. The precision on the efficiency is equal to 0.1% given the large sample collected of **NoBias** triggered events. This uncertainty can be neglected for the final result.

7.5.2 Primary vertex reconstruction efficiency

The primary vertex reconstruction efficiency is taken from pp simulations. Given the larger particle multiplicity in $p\text{Pb}$ collisions with respect to pp collisions, we assume that the PV finding is fully efficient.

7.5.3 Mass resolution effect

Candidates are selected in the mass interval $|M(\mu^+\mu^-) - M(J/\psi)| < 120 \text{ MeV}/c^2$. Differences in the mass resolution between data and MC may bias the selection efficiency determination. To check this effect, the σ parameter of the Crystal Ball function is extracted both in data and in simulation. The mass resolution is found to be larger in data with respect to Monte Carlo simulations of about 10%, as shown in the left plot of Fig. 23.

The selection efficiency has been recomputed by reducing, in each p_T and y^* bin, the mass window by the inverse of the the values in Fig. 23 (left). The ratio of the efficiency

computed with the new mass cut over the nominal cut is depicted in Fig. 23 (right). A small reduction of the efficiency is visible, but the magnitude of the effect is at maximum 0.5%, and therefore ignored in the following. Larger deviations seen at high p_T are due to the lack of statistics in MC data that makes the σ parameter of the fit is not well constrained and therefore we do not consider these deviation as a meaningful systematic estimate.

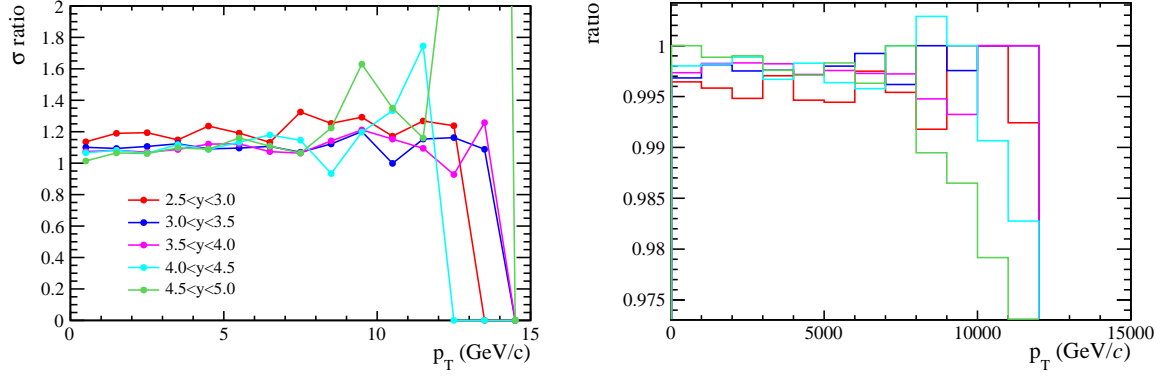


Figure 23: Left) Data over MC ratio of the σ parameter of the Crystal Ball function for the invariant mass fit. Right) Ratio of the selection efficiency obtained with an invariant mass cut reduced for the data/MC mass resolution difference over the nominal efficiency.

7.5.4 Other selection requirements

The efficiency for the selection cut $\text{Track-}\chi^2/\text{ndf} < 3$ is cross checked comparing the distributions of the selection variable between data and simulation. In Monte Carlo, candidates are required to be truth matched, while for data the signal shape is obtained with the `sPlot` technique. In Figure 24 (right) it is possible to see that, although the shape of the distribution is not perfectly reproduced in simulation, the chosen cut is fully efficient (less than 0.1% of candidates fall above the cut).

The track ghost probability distribution is shown in Figure 24 (left). In this case, the cut chosen correspond to the default cut applied at the reconstruction level.

7.6 PID efficiency

The PID efficiency uncertainty has the following sources:

1. The uncertainty induced by the finite statistics of the calibration sample in pp data,
2. The uncertainty due to the binning choice of the correction tables for the muons,
3. The uncertainty due to the usage of `sWeights` to derive the correction tables, equal to 1%.

The uncertainty due to the binning choice is determined by changing the binning schemes for the calibration tables, for p , η and the SPD multiplicity. The PID efficiencies are recomputed with these new tables and the largest deviation between all different cases

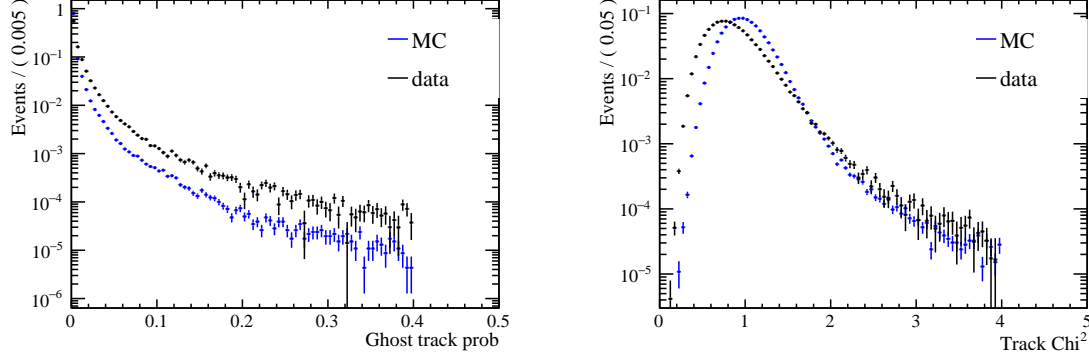


Figure 24: Comparison between $p\text{Pb}$ simulation (blue) and data (black): track ghost probability distribution is shown on the left and the $\text{Track-}\chi^2/ndf$ distribution on the right.

is been chosen as systematic uncertainty. The relative uncertainty due to the choice of calibration table binning varies from 0.2% to 1.4% depending on the analysis bin. The total uncertainty due to the PID, obtained adding in quadrature the different sources, varies from 2% to 11% for $p\text{Pb}$ and from 2.1% to 15.3% for $\text{Pb}p$.

7.7 Trigger efficiency

The central values of the trigger efficiencies are taken from the simulation. They are checked on data using the TISTOS method, for L0 and HLT1 separately. First it is checked that the TISTOS method for L0 gives a good estimate of the L0 trigger efficiency in the simulation. This is shown in Fig. 25 where the ratio $\frac{\epsilon_{\text{TISTOS}}}{\epsilon_{\text{L0}}}$ for L0 as a function of p_{T} is seen consistent with 1.

Then the efficiency is measured in data with the TISTOS method, and compared with the values obtained in the simulation with the same method. Figure 26 shows the efficiencies measured in data, and the ratio with the efficiency in the simulation. In case the ratio between the data and simulation TISTOS efficiencies for L0 is larger than 1σ with statistical uncertainties, the difference between data and simulation is taken as systematic uncertainty. When the difference is smaller than 1σ , then the statistical uncertainty on the ratio is taken as relative systematic uncertainty. For bins with $p_{\text{T}} > 8 \text{ GeV}/c$, for which the statistics in data are too small, the uncertainty is taken equal to 1%, comparing with close bins. The uncertainties determined are between 1.0% and 10.9% depending on the bin, for $p\text{Pb}$. For $\text{Pb}p$, they vary between 1.0% and 7.4%. The ratios of data to simulation TISTOS efficiencies for L0 in the $\text{Pb}p$ case are shown in Fig. 27. For high p_{T} bins, $p_{\text{T}} > 8 \text{ GeV}/c$, an uncertainty of 1% is used.

The same method is applied for the HLT1 trigger, but the statistics are much lower in that case. Figure 28 gives the comparison of the TISTOS method and the direct efficiency measurement in the $p\text{Pb}$ simulation for J/ψ , and Fig. 29 the comparison between data and simulation, for $p\text{Pb}$ and $\text{Pb}p$. An uncertainty of 2% is assigned to the determination of the HLT1 efficiency, which is the mean value of the deviation.

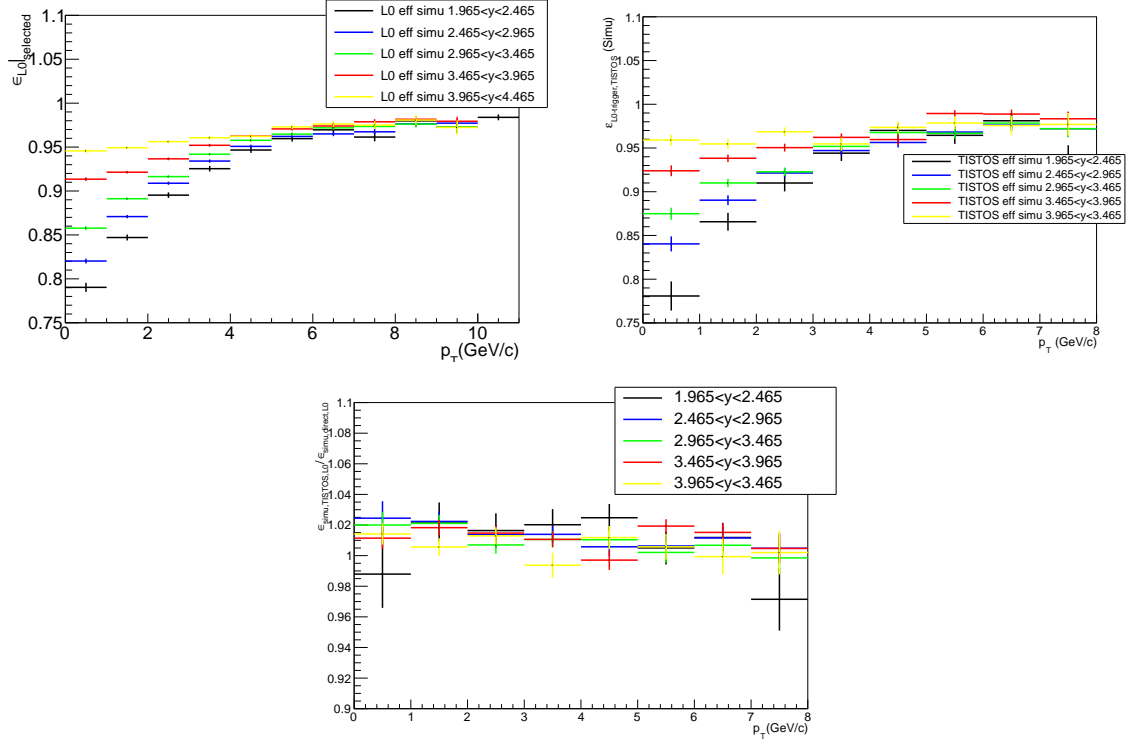


Figure 25: L0 efficiency in the $p\text{Pb}$ simulation, as a function of the J/ψ p_T , in different rapidity bins, top left: measured directly, top right: measured with the TISTOS method, bottom: ratio between the two.

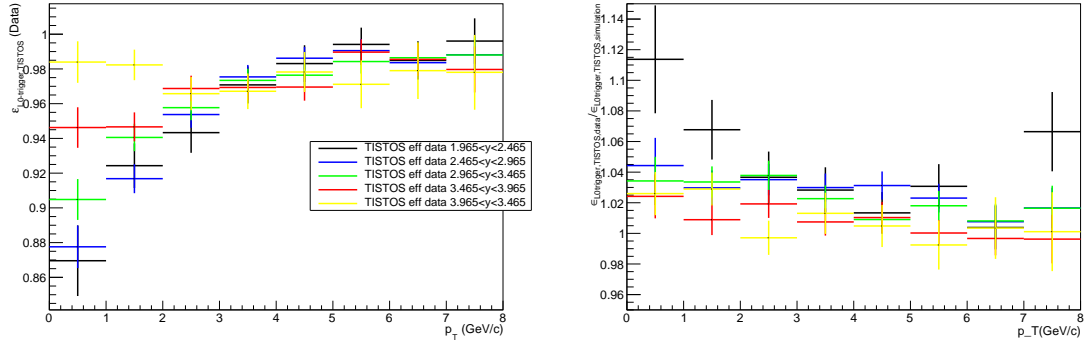


Figure 26: left: L0 efficiency in the $p\text{Pb}$ data, as a function of the J/ψ p_T , in different rapidity bins, right: ratio with the simulation efficiencies.

7.8 Luminosity

The luminosity is determined using the same procedure than for the 2013 $p\text{Pb}$ run [53]. Only van der Meer scans were used for this determination. The relative uncertainties on the $p\text{Pb}$ luminosity is 2.6% and the one on the PbPb luminosity is 2.5%, correlated amongst bins.

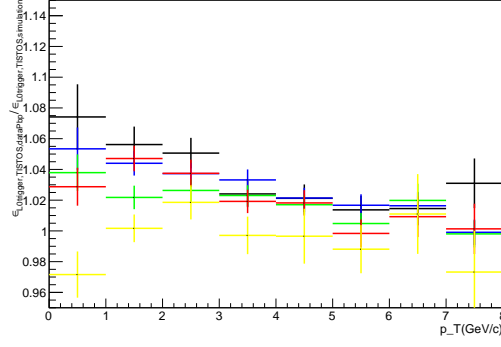


Figure 27: Ratio of L0 efficiency in the Pbp data compared to $p\text{Pb}$ simulation, as a function of the J/ψ p_T , in different rapidity bins, measured with the TISTOS method.

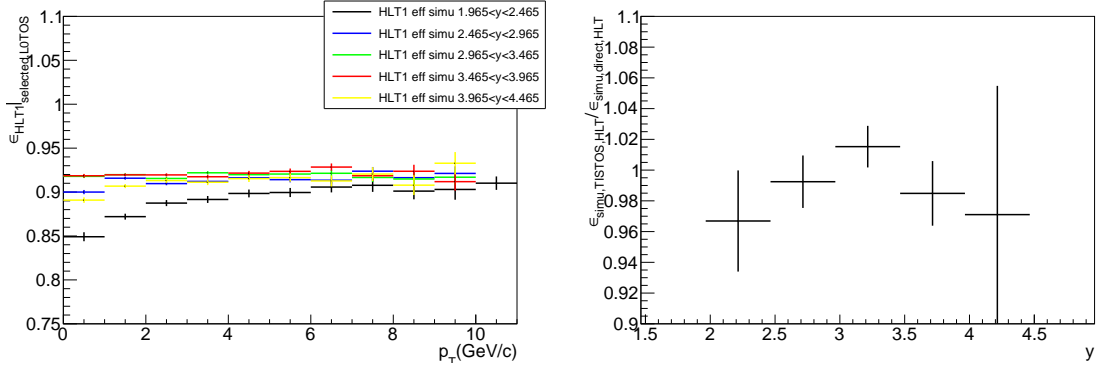


Figure 28: Left: HLT1 efficiency measured directly in the $p\text{Pb}$ simulation, as a function of the J/ψ p_T , in different rapidity bins. Right: ratio of the direct efficiency with the efficiency measured with the TISTOS method, in the $p\text{Pb}$ simulation, as a function of the J/ψ rapidity.

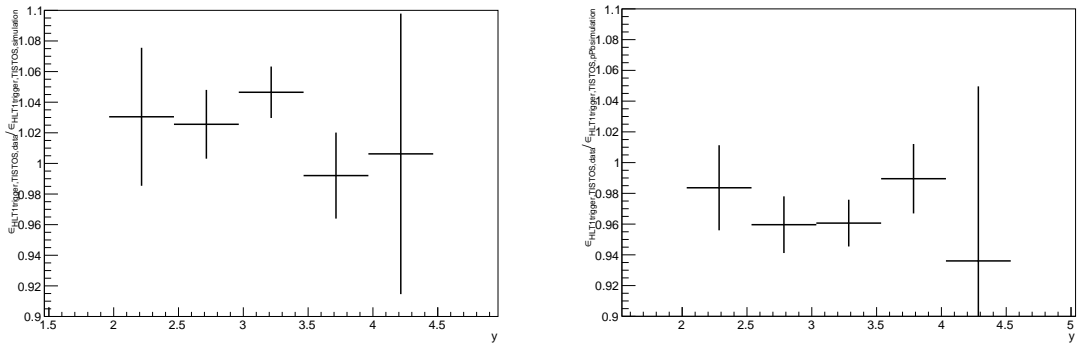


Figure 29: Ratio of HLT1 efficiency in the left: $p\text{Pb}$ and right: Pbp data compared to $p\text{Pb}$ simulation, as a function of the J/ψ rapidity, measured with the TISTOS method.

7.9 Summary

Table 7 summarizes all systematic uncertainties affecting the measurements presented in this note. The correlated systematic uncertainties are assumed to be uncorrelated with the similar ones for pp .

Table 7: Summary of systematic uncertainties.

Source	$p\text{Pb}$	$\text{Pb}p$	Comment
L0	1.0% – 10.9%	1.0% – 7.4%	correlated
HLT	2.0%	2.0%	correlated
Tracking correction table	2.6% – 7.9%	5.7% – 26.5%	correlated
Tracking efficiency method	1.6%	1.6%	correlated
PID	2.0% – 11.0%	2.1% – 15.3%	correlated
Monte Carlo statistics	0.4% – 7.0%	0.6% – 37.0%	uncorrelated
Truth matching	0.1%	0.1%	correlated
Signal extraction	1.3%	1.3%	correlated
$\mathcal{B}(J/\psi \rightarrow \mu^+\mu^-)$	0.05%	0.05%	correlated
Luminosity	2.6%	2.5%	correlated

8 Reference pp cross-sections

The center-of-mass energy of the proton-Lead colliding system in this analysis is $\sqrt{s_{NN}} = 8.16$ TeV. The measurements of the nuclear modification factors require the knowledge of the production cross-sections at the same centre of mass energy in proton-proton collisions. The J/ψ cross-section has been measured in pp collisions at 2.76 TeV [54], 7 TeV [55, 56], 8 TeV [57] and 13 TeV [58]. The J/ψ cross-sections at $\sqrt{s} = 8.16$ TeV are determined using interpolation methods described in Ref. [59] and used for the publication of the J/ψ nuclear modification factor in $p\text{Pb}$ collisions at $\sqrt{s_{NN}} = 5$ TeV [60]. The J/ψ cross-sections are determined using interpolations from measurements at other energies.

8.1 J/ψ cross-section in pp collisions at 8.16 TeV

The J/ψ cross-section is interpolated in all p_T and $y(=y^*)$ bins of the analysis and also as a function of p_T , integrated over y and as a function of y integrated over p_T . Since the 8 TeV point is close to the interpolated energy, 8.16 TeV, the result is dominated by the 8 TeV measurements, so the 2.76 TeV measurement is ignored in this study as it gives no constraint on the result.

In principle, the single differential cross-sections at 8.16 TeV can be integrated from the interpolated double differential cross-section values. However, in order to reduce the uncertainties, single differential interpolations are performed independently. First, the J/ψ cross-section integrated over y or p_T are taken from the published results. When the integrated cross-section values are not available in the published papers, the integration

is done adding all bins, separating correlated or uncorrelated uncertainties. The single differential integration over p_T is made over the range $p_T < 14$ GeV and the integration over y is made in the range $2.5 < y < 4.0$, which is the range common to the p Pb and PbPb measurements of this analysis.

The measurements at 7, 8 and 13 TeV are fitted with an analytic function, and the interpolated results including uncertainties at 8.16 TeV are given by the function. This procedure is performed for each bin independently. In Ref [59], three functions, a linear function $(1 + p_0 \times \sqrt{s})$, a power law function (\sqrt{s}^{p_0}) and an exponential function $(1 - \exp^{-p_0 \times \sqrt{s}})$ are used for the fit. However it is found here that the exponential fit does not work well, especially in the high p_T or y bins. The exponential function probes a saturation of cross-section at higher energies, which may be true for the total cross-section but not necessarily for small or large p_T and for high rapidity bins, for which the increase in the collision energy produces a harder spectrum that favors these regions. This is why, to keep a consistent treatment in all kinematic regions, only the linear and power law functions are considered. The latter is preferred in theory while the former is a first order approximation.

The correlated systematic uncertainties between the measurements at different energies are considered in the following way: for the measurements at 7, 8 and 13 TeV, a common amount is subtracted to the total uncertainty as $\sigma_c = \sqrt{\rho} \times \min(\sigma_7, \sigma_8, \sigma_{13})$ which is supposed to contribute to the desired correlation ρ , and the interpolation is made using the remaining uncertainties that are supposed to be uncorrelated. Then the common correlated uncertainty is added back in quadrature to the interpolated result. The exact correlation coefficient of the systematic uncertainty in fact is very difficult to calculate precisely, while in the default case the correlation among all measurements is assumed to be 50%, following discussions in Ref [58]. The interpolation using only statistical uncertainties was also performed as a cross check, and similar numbers were found for the central values and uncertainties. This is because the interpolated results are largely dominated by the measurements at 8 TeV, which is the closest point in energy.

The difference between the two interpolation functions is used as systematic uncertainty for the method. This uncertainty is much smaller than other systematic uncertainties. In Fig. 30, an example of the interpolation fit is given (the interpolation with the exponential function is also shown for comparison). In Tables 38 and 39, the extrapolated double differential cross-sections are given, while in Table 8 and 9, the results of single differential cross-section extrapolations are listed.

The cross-section at 8.16 TeV is determined for bins in the range $2 < y < 4.5$. A further extrapolation is needed to obtain the cross-sections in the rapidity bins $1.5 < y < 2$ and $4.5 < y < 5$ which are not covered in measurements made in pp collisions, because of the different acceptance. In this case, the interpolation fits use a Gaussian function, a second order polynomial or a 4th order polynomial, all centered at $y = 0$, following the strategy used in Ref [59]. Only statistical uncertainties are considered in the fit, and the systematic uncertainties are added back. The systematic uncertainty of this method is studied in the following way. An alternative fit is performed where every measured values are augmented by their uncertainties. The differences between the new extrapolated results and the one considering only statistical uncertainties are then taken as systematic uncertainties. The average of the integrated value of the fit functions over the rapidity range ($1.5 < y < 2$ or $4.5 < y < 5$), obtained with the three different functions, is taken as the nominal value. Half of the maximum difference between the three fits is taken

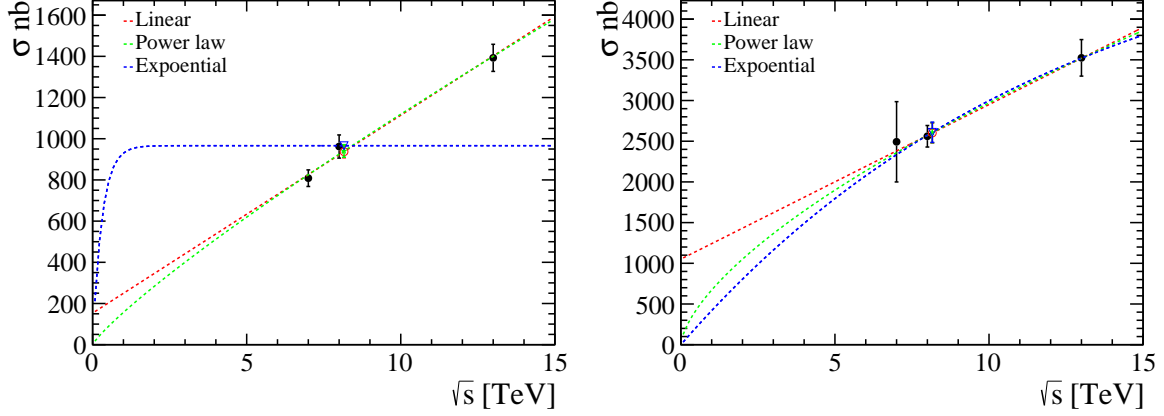


Figure 30: Cross-section interpolation in a (left) p_T bin and (right) y bin as examples. The interpolation is made using only uncorrelated uncertainty. The measurements at each energy and the interpolated results are shown with total uncertainties.

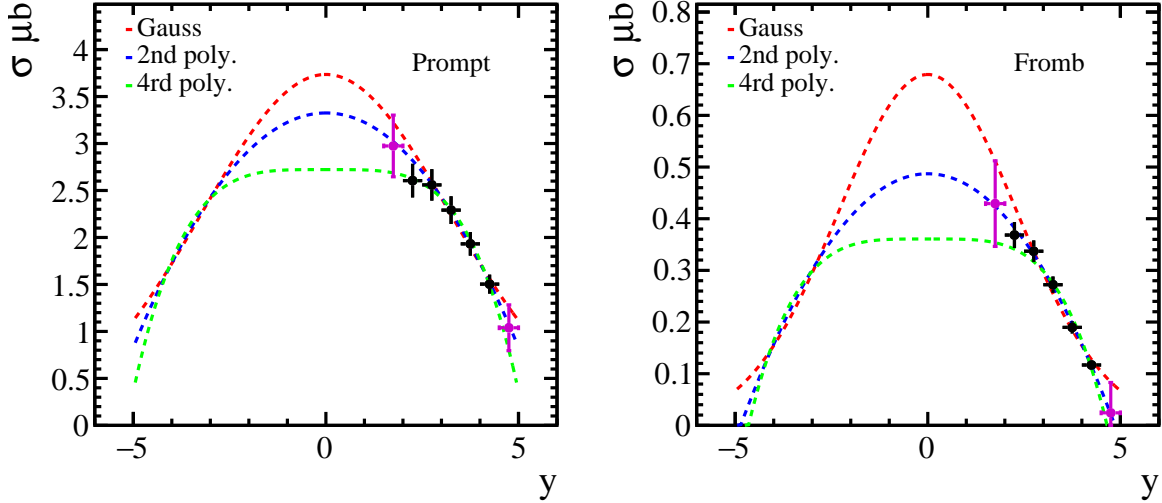


Figure 31: Interpolation fit to determine J/ψ cross-section in bins of $1.5 < y < 2$ and $4.5 < y < 5$ for left: prompt J/ψ and right: J/ψ from- b .

as additional systematic uncertainty. The interpolation fit is shown in Fig. 31, and the results are given in Table 9. It should be noted that the interpolation is only done for rapidity integrated over p_T . As a crosscheck, the extrapolated value at $y = 0$ is compared to the ALICE measurement [61]. The ALICE measurement in the range $p_T > 0 \text{ GeV}/c$ and $|y| < 0.9$ for center-of-mass energy of 7 TeV is $10.6 \pm 1.9 \mu\text{b}$. The extrapolated value, $11.6 \pm 1.8 \mu\text{b}$, obtained with the method described above is in good agreement with expectation.

The interpolated results are expected to be very close to the values measured at 8 TeV. This is confirmed in Fig. 32, where the interpolated results are compared to the 8 TeV measurements.

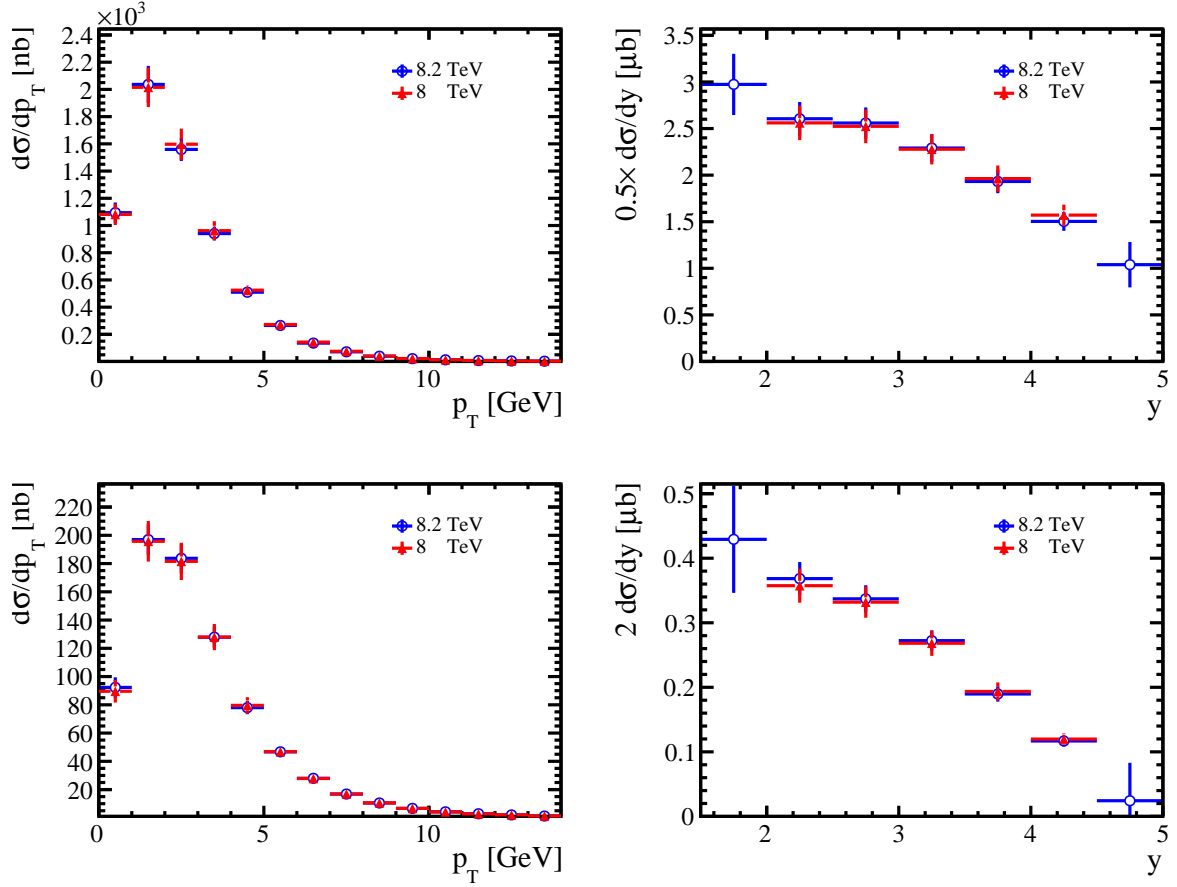


Figure 32: Extrapolated single differential cross-section for J/ψ at 8.16 TeV, as a function of left: p_T and right: rapidity, compared with measurements at 8 TeV. The top two plots are for prompt J/ψ , while the bottom one are for J/ψ from b .

Table 8: Extrapolated cross-section (in nb) at 8.16 TeV in different p_T bins for rapidity integrated over $2.5 < y < 4$. The first uncertainty is statistical, the second is the difference between interpolation functions, and the third is total uncertainty dominated by other LHCb measurements.

Prompt J/ψ	
[0 – 1]	$1094.3 \pm 5.6 \pm 2.3 \pm 74.5$
[1 – 2]	$2036.7 \pm 6.6 \pm 5.5 \pm 136.0$
[2 – 3]	$1559.1 \pm 5.0 \pm 8.8 \pm 84.4$
[3 – 4]	$940.7 \pm 3.2 \pm 3.6 \pm 51.0$
[4 – 5]	$509.9 \pm 2.0 \pm 1.2 \pm 27.7$
[5 – 6]	$265.5 \pm 1.3 \pm 0.4 \pm 14.6$
[6 – 7]	$135.8 \pm 0.9 \pm 0.5 \pm 7.4$
[7 – 8]	$71.7 \pm 0.6 \pm 0.4 \pm 4.0$
[8 – 9]	$39.4 \pm 0.4 \pm 0.4 \pm 2.2$
[9 – 10]	$21.7 \pm 0.3 \pm 0.4 \pm 1.2$
[10 – 11]	$13.0 \pm 0.2 \pm 0.2 \pm 0.8$
[11 – 12]	$7.5 \pm 0.2 \pm 0.2 \pm 0.5$
[12 – 13]	$4.7 \pm 0.1 \pm 0.1 \pm 0.3$
[13 – 14]	$2.9 \pm 0.1 \pm 0.1 \pm 0.2$
J/ψ from- b	
[0 – 1]	$92.3 \pm 1.9 \pm 0.2 \pm 6.9$
[1 – 2]	$197.0 \pm 1.9 \pm 0.2 \pm 10.7$
[2 – 3]	$183.7 \pm 1.5 \pm 0.7 \pm 10.4$
[3 – 4]	$127.8 \pm 1.1 \pm 0.7 \pm 7.3$
[4 – 5]	$78.0 \pm 0.7 \pm 1.1 \pm 4.6$
[5 – 6]	$46.7 \pm 0.5 \pm 0.6 \pm 3.1$
[6 – 7]	$28.0 \pm 0.4 \pm 0.6 \pm 1.8$
[7 – 8]	$16.8 \pm 0.2 \pm 0.4 \pm 1.1$
[8 – 9]	$10.5 \pm 0.2 \pm 0.3 \pm 0.7$
[9 – 10]	$6.7 \pm 0.1 \pm 0.2 \pm 0.5$
[10 – 11]	$4.2 \pm 0.1 \pm 0.2 \pm 0.3$
[11 – 12]	$2.9 \pm 0.1 \pm 0.1 \pm 0.2$
[12 – 13]	$2.0 \pm 0.1 \pm 0.1 \pm 0.2$
[13 – 14]	$1.3 \pm 0.1 \pm 0.1 \pm 0.1$

Table 9: Extrapolated cross-section (in μb) at 8.16 TeV in different y bins for p_{T} integrated over $p_{\text{T}} < 14 \text{ GeV}/c$. The first uncertainty is statistical, the second is the difference between interpolation functions, and the third is total uncertainty dominated by other LHCb measurements.

Prompt J/ψ	
[1.50 – 2.0]	$2.974 \pm 0.009 \pm 0.267 \pm 0.328$
[2.00 – 2.5]	$2.605 \pm 0.021 \pm 0.000 \pm 0.179$
[2.50 – 3.0]	$2.559 \pm 0.008 \pm 0.000 \pm 0.167$
[3.00 – 3.5]	$2.291 \pm 0.005 \pm 0.000 \pm 0.147$
[3.50 – 4.0]	$1.932 \pm 0.005 \pm 0.000 \pm 0.126$
[4.00 – 4.5]	$1.503 \pm 0.005 \pm 0.000 \pm 0.101$
[4.50 – 5.0]	$1.039 \pm 0.007 \pm 0.233 \pm 0.244$
J/ψ from- b	
[1.50 – 2.0]	$0.429 \pm 0.003 \pm 0.079 \pm 0.083$
[2.00 – 2.5]	$0.368 \pm 0.006 \pm 0.000 \pm 0.025$
[2.50 – 3.0]	$0.337 \pm 0.003 \pm 0.000 \pm 0.021$
[3.00 – 3.5]	$0.272 \pm 0.002 \pm 0.000 \pm 0.016$
[3.50 – 4.0]	$0.190 \pm 0.002 \pm 0.000 \pm 0.012$
[4.00 – 4.5]	$0.117 \pm 0.001 \pm 0.000 \pm 0.009$
[4.50 – 5.0]	$0.024 \pm 0.002 \pm 0.059 \pm 0.059$

9 Results

From the number of signal candidates, the efficiencies, and the luminosities ($\mathcal{L}_{p\text{Pb}} = 13.6 \pm 0.3 \text{ nb}^{-1}$ and $\mathcal{L}_{p\text{Pb}} = 20.8 \pm 0.5 \text{ nb}^{-1}$, the absolute cross-sections of J/ψ cross-sections can be computed in the binning scheme defined for the analysis. From them, and from the pp reference cross-sections, nuclear modification factors are extracted. Finally, forward to backward ratios are also measured.

9.1 Absolute J/ψ production cross-sections

The absolute prompt J/ψ production cross-section is shown in Fig. 33, as a function of p_T for different rapidity bins, for $p\text{Pb}$. The numerical results are in Tables 40 and 41. The absolute J/ψ from b production cross-section is shown in Fig. 34, as a function of p_T for different rapidity bins, for $p\text{Pb}$. The numerical results are in Tables 42 and 43.

The absolute prompt J/ψ production cross-section is shown in Fig. 35, as a function of p_T for different rapidity bins, for $\text{Pb}p$. The numerical results are in Tables 44 and 45. The absolute J/ψ from b production cross-section is shown in Fig. 36, as a function of p_T for different rapidity bins, for $\text{Pb}p$. The numerical results are in Tables 46 and 47.

The absolute cross-sections, integrated over p_T in the range $0 < p_T < 14 \text{ GeV}/c$, as a function of y^* are shown in Fig. 37, for prompt J/ψ and J/ψ from b . The cross-sections, integrated over y^* in the analysis bins, as a function of p_T are shown in Fig. 39. The same plots with the cross-section in pp collisions at the same energy, multiplied by 208 (atomic mass number of the Pb atom) are represented in Fig. 38 (integrated over p_T) and in Fig. 40.

9.2 Fraction of J/ψ from b decays

The fraction of J/ψ produced in b decays, or b fraction, $f_b = \frac{N_{\text{from } b}}{N_{\text{from } b} + N_{\text{prompt}}}$ is shown in Fig. 41, as a function of p_T for different rapidity bins, for $p\text{Pb}$ and $\text{Pb}p$ and also for comparison for pp at 8 TeV. The numerical results are in Tables 48, 49, 50 and 51.

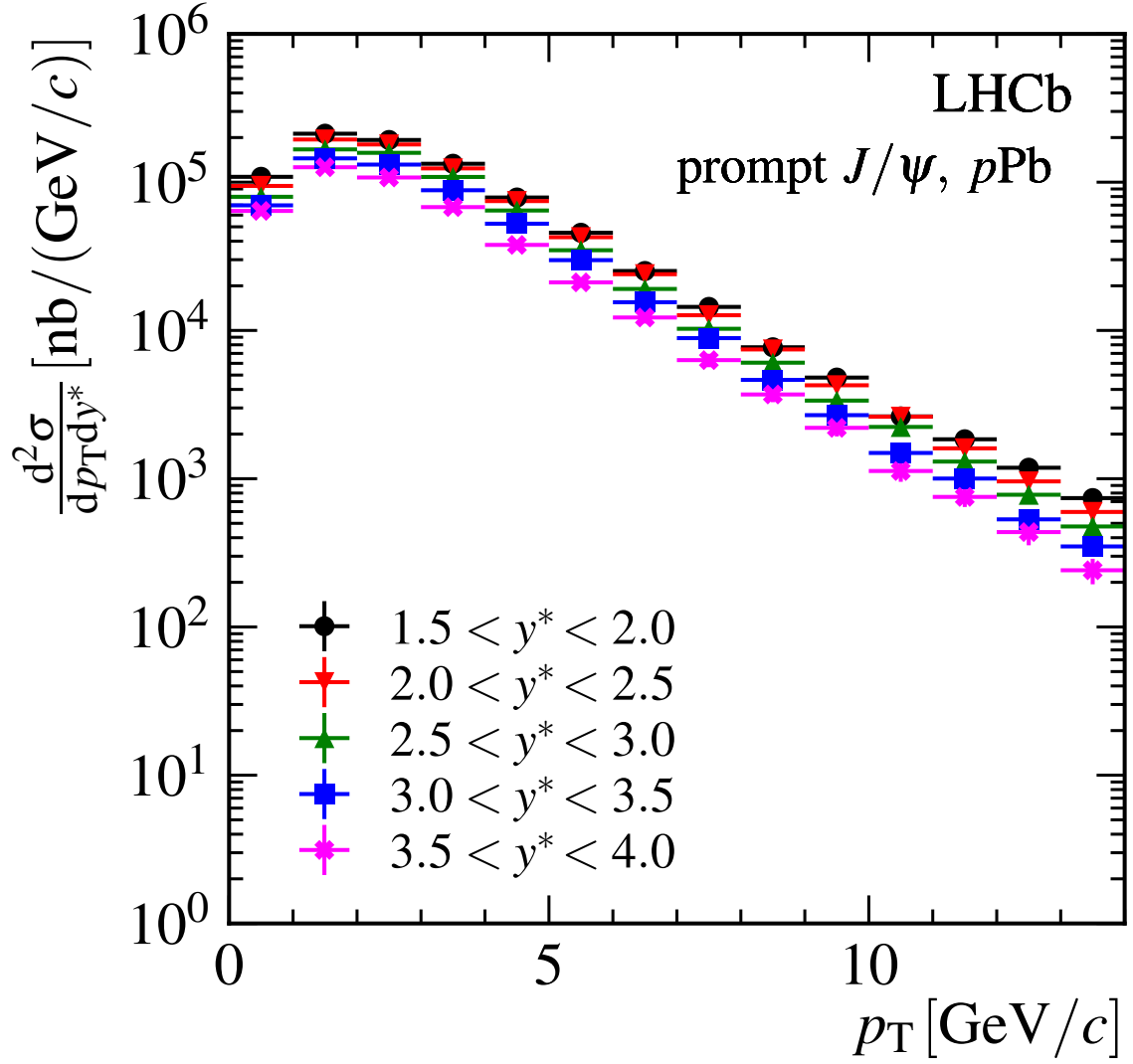


Figure 33: Prompt J/ψ absolute production cross-section in pPb, as a function of p_T for the different rapidity bins. Horizontal error bars are the bin widths, vertical error bars the total uncertainties.

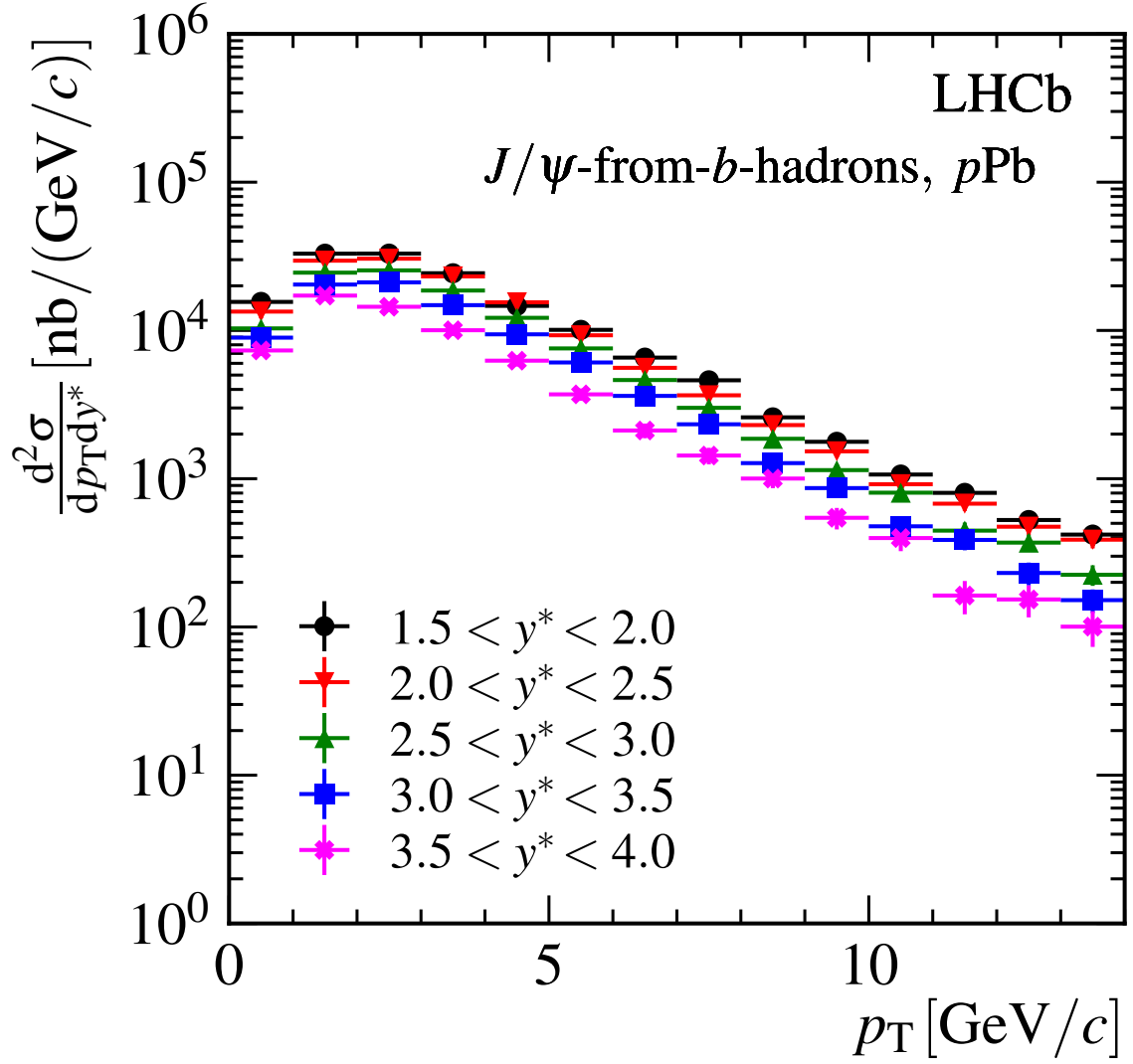


Figure 34: J/ψ from b absolute production cross-section in $p\text{Pb}$, as a function of p_T for the different rapidity bins. Horizontal error bars are the bin widths, vertical error bars the total uncertainties.

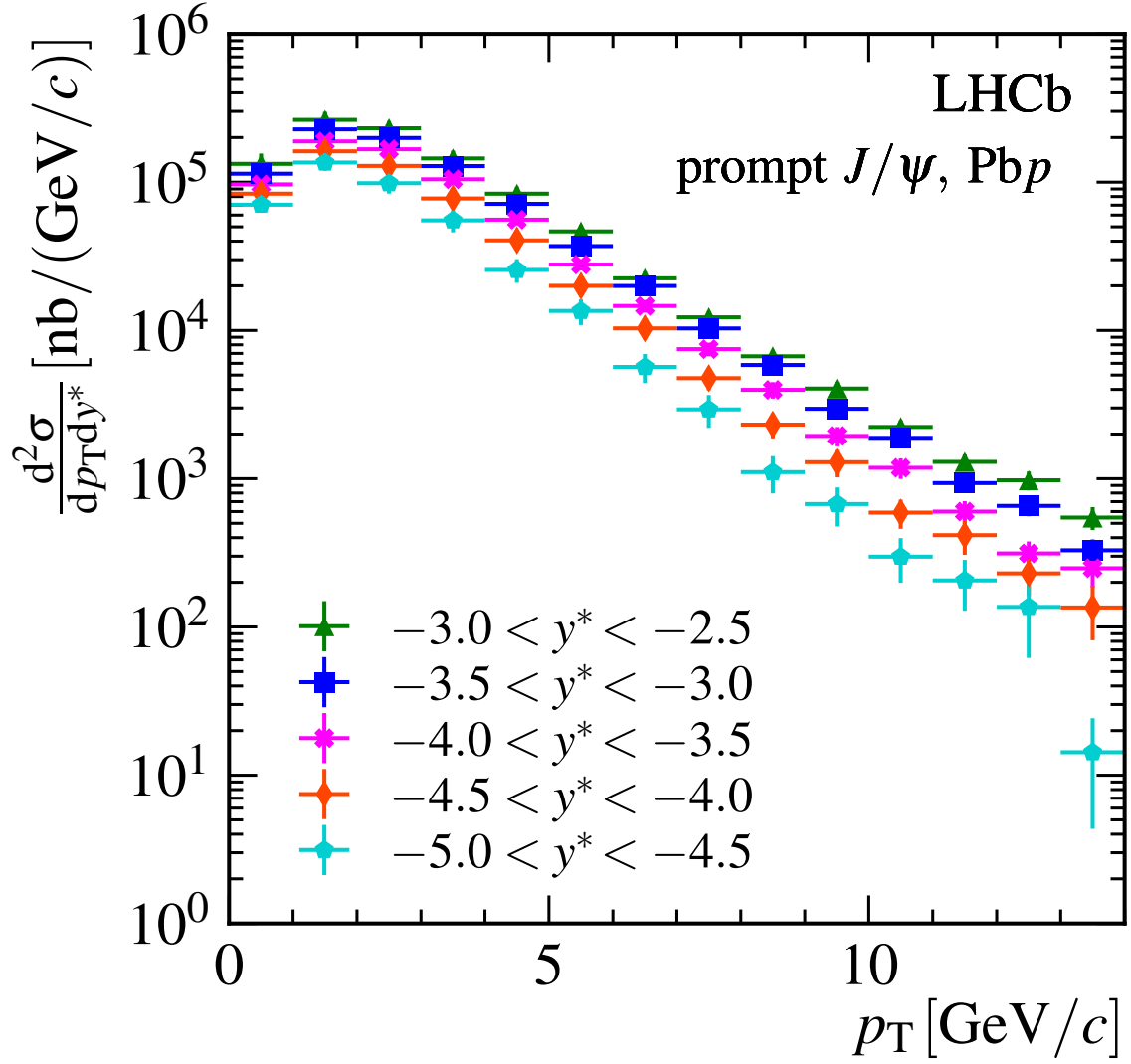


Figure 35: Prompt J/ψ absolute production cross-section in PbP, as a function of p_T for the different rapidity bins. Horizontal error bars are the bin widths, vertical error bars the total uncertainties.

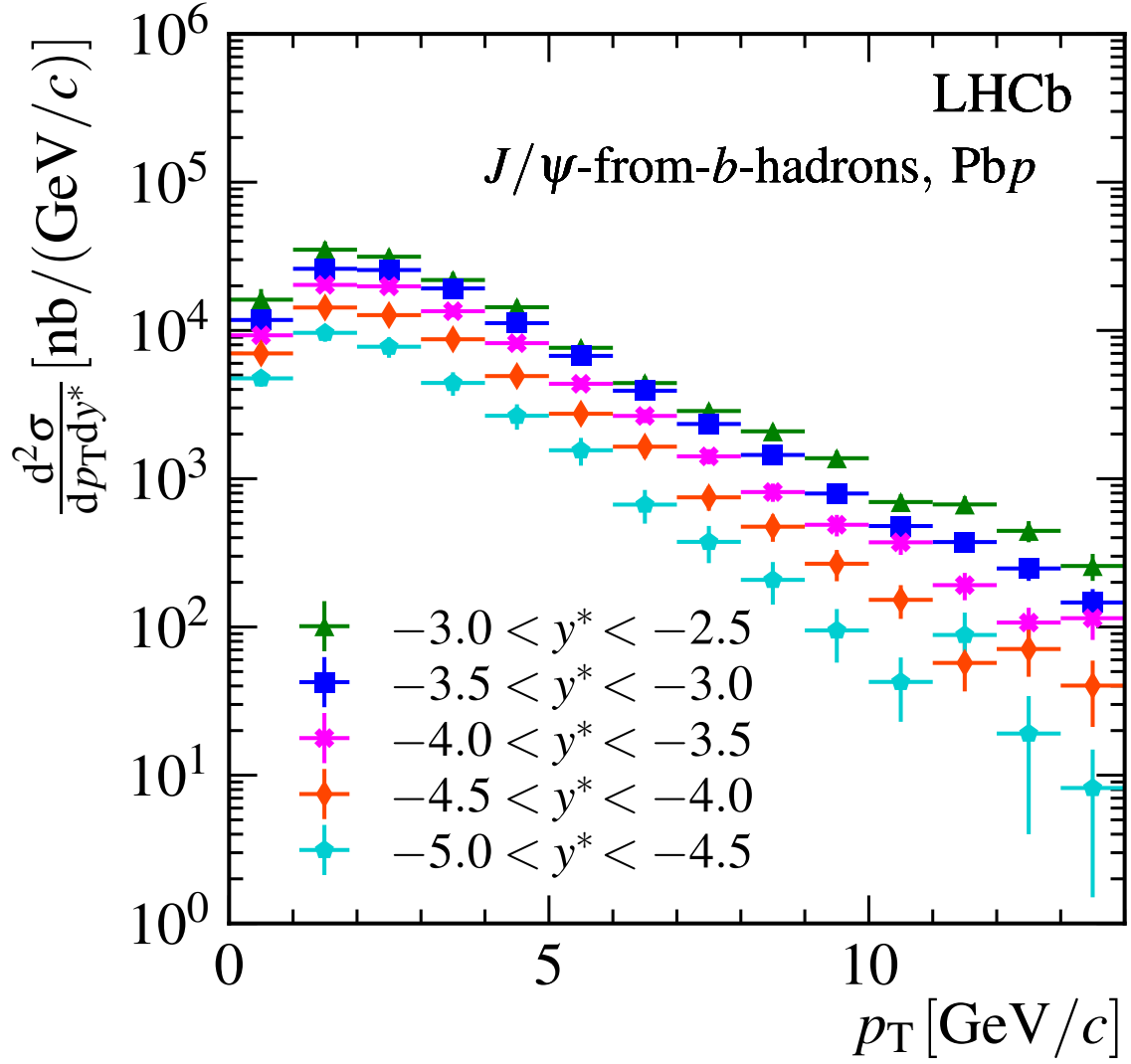


Figure 36: J/ψ from b absolute production cross-section in PbP, as a function of p_T for the different rapidity bins. Horizontal error bars are the bin widths, vertical error bars the total uncertainties.

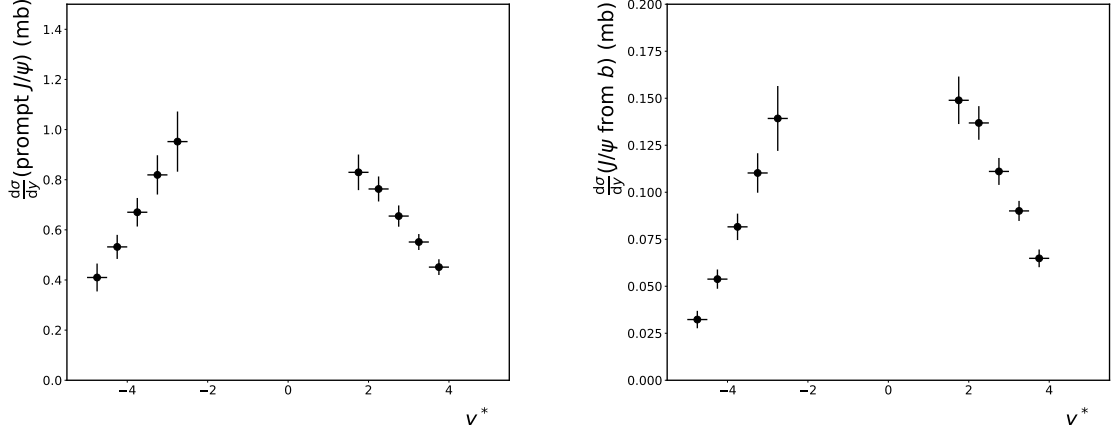


Figure 37: Absolute production cross-section, integrated over p_T in the range $0 < p_T < 14 \text{ GeV}/c$, as a function of y^* for left: prompt J/ψ , right: J/ψ from b . Horizontal error bars are the bin widths, vertical error bars the total uncertainties.

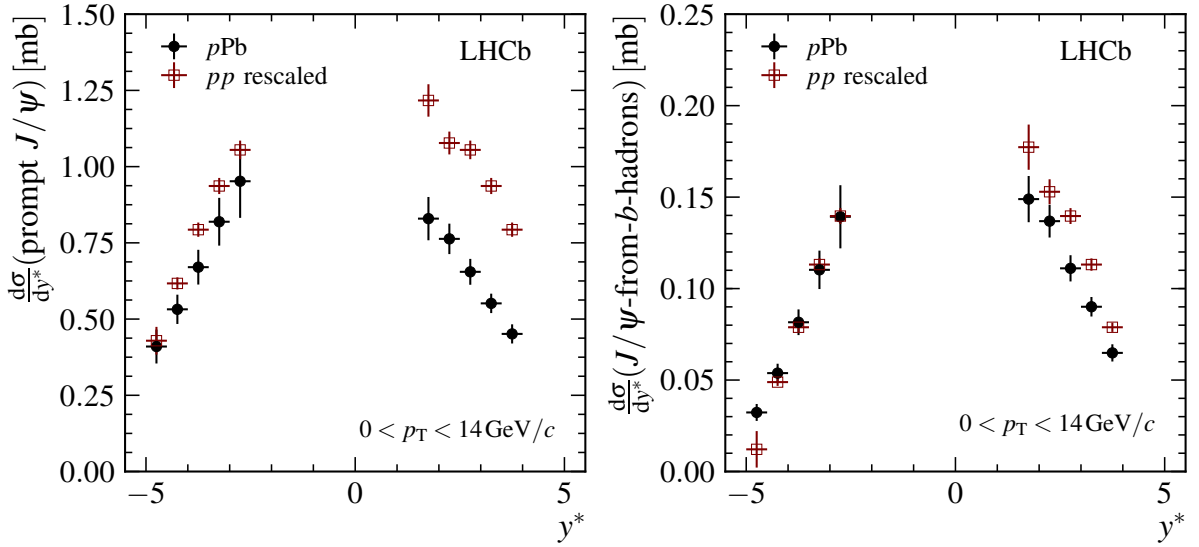


Figure 38: Black: Absolute production cross-section black circles: in $p\text{Pb}$, blue stars: in pp multiplied by 208, integrated over p_T in the range $0 < p_T < 14 \text{ GeV}/c$, as a function of y^* for left: prompt J/ψ , right: J/ψ from b . Horizontal error bars are the bin widths, vertical error bars the total uncertainties.

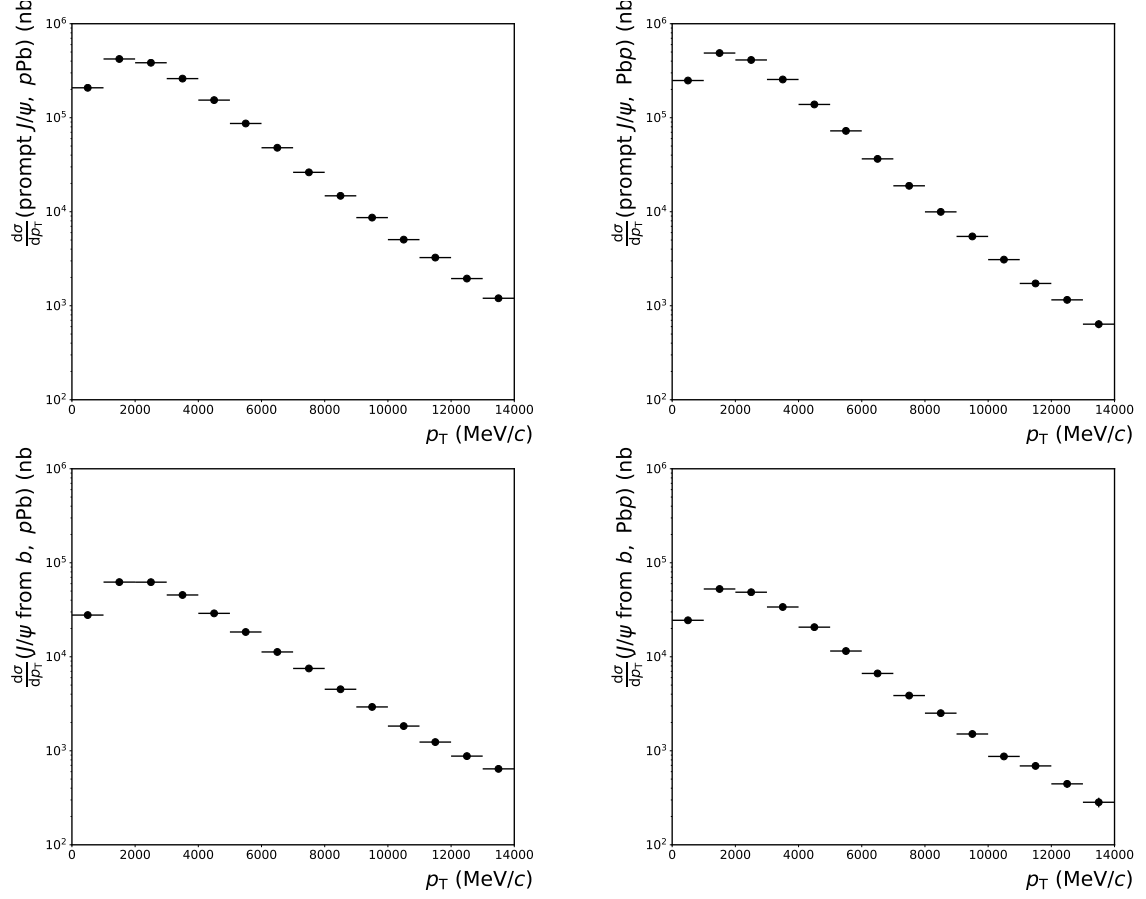


Figure 39: Absolute production cross-section, integrated over y^* in the analysis range, as a function of p_T for top left: prompt J/ψ in $p\text{Pb}$, top right: prompt J/ψ from b in Pbp , bottom left: J/ψ from b in $p\text{Pb}$, bottom right: J/ψ from b in Pbp . Horizontal error bars are the bin widths, vertical error bars the total uncertainties.

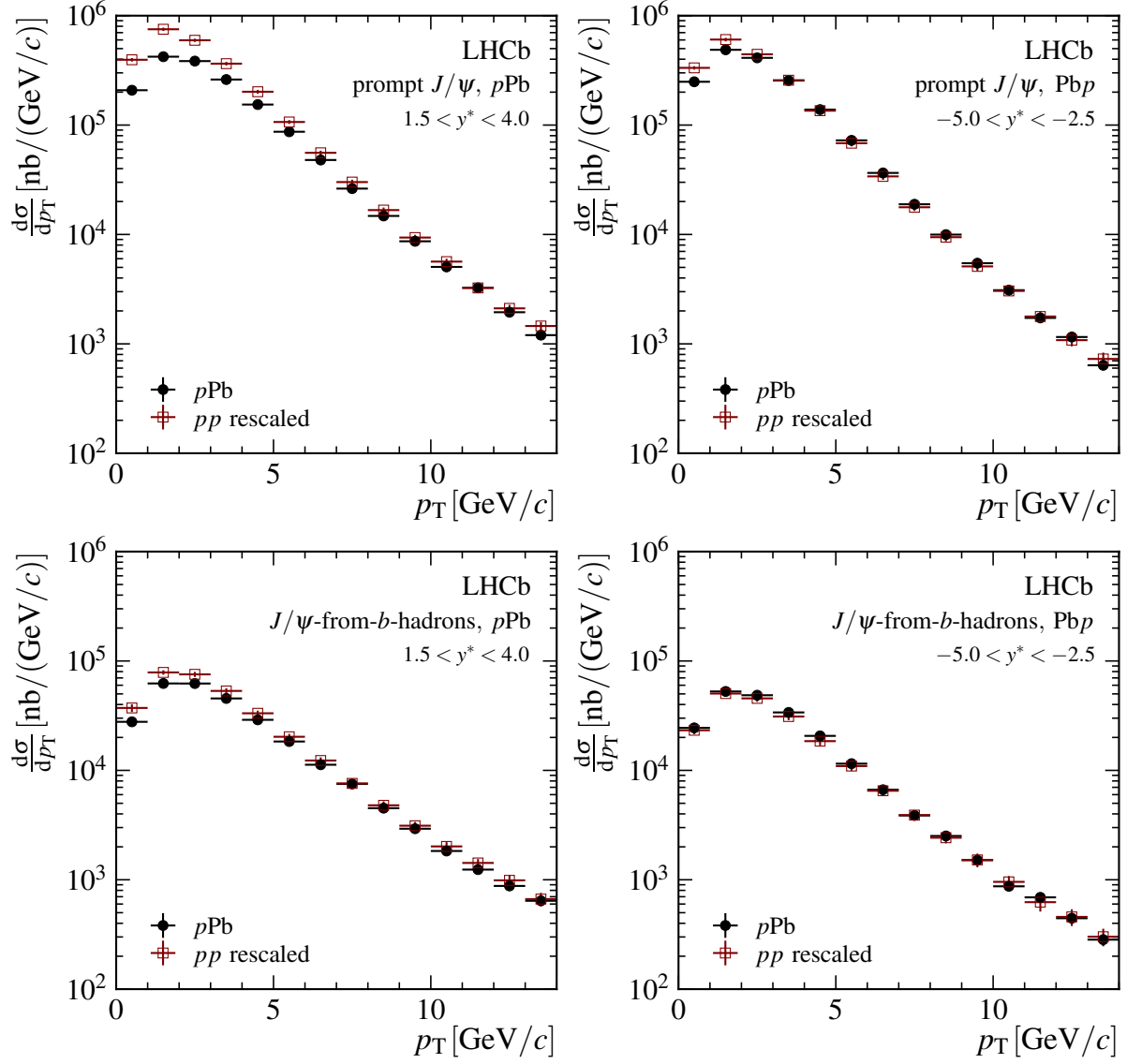


Figure 40: Absolute production cross-section, integrated over y^* in the analysis range, as a function of p_T for top left: prompt J/ψ in pPb , top right: J/ψ from b in pPb , bottom left: prompt J/ψ in PbP , bottom right: J/ψ from b in PbP , black circles: pPb , blue stars: pp multiplied by 208. Horizontal error bars are the bin widths, vertical error bars the total uncertainties.

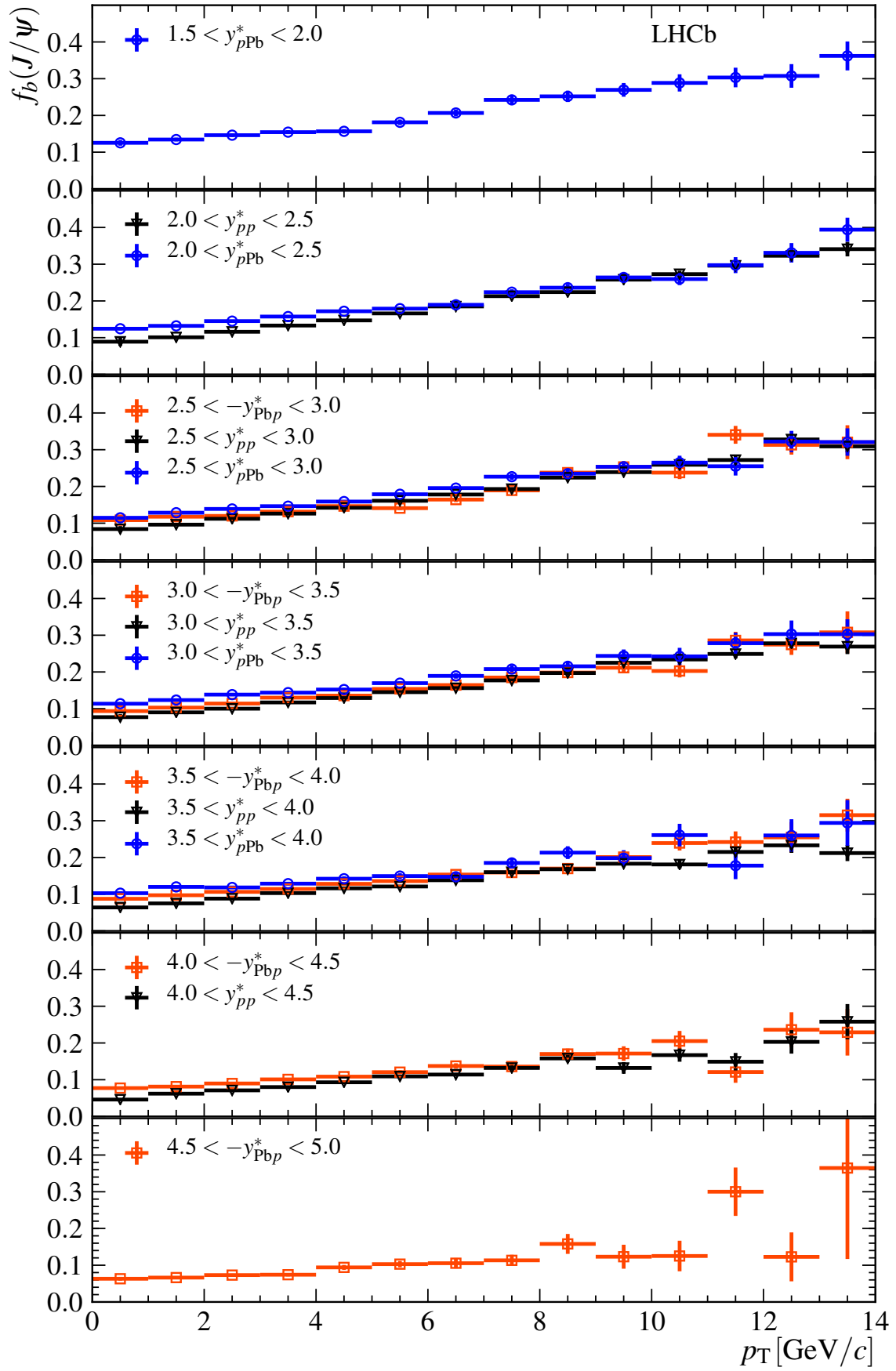


Figure 41: Fraction of J/ψ from b for (blue circles) $p\text{Pb}$, (red squares) $\text{Pb}p$ and (black triangles) pp at 8 TeV, as a function of p_T for the different rapidity bins. Horizontal error bars are the bin widths, vertical error bars the total uncertainties.

9.3 J/ψ nuclear modification factors

The nuclear modification factor, $R_{p\text{Pb}}$ as a function of p_T for the different rapidity bins of the analysis is shown on Fig. 42 for $p\text{Pb}$. The numerical values are given in Tables 52, 53, 54 and 55

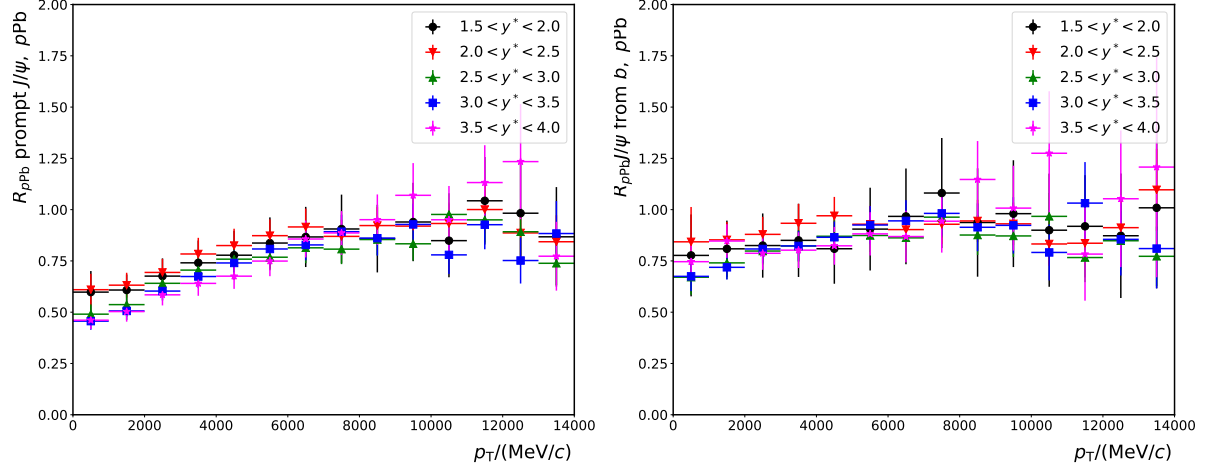


Figure 42: J/ψ nuclear modification factor in $p\text{Pb}$, $R_{p\text{Pb}}$ as a function of p_T for the different rapidity bins. Left: prompt J/ψ , right: J/ψ from b .

The nuclear modification factor, $R_{p\text{Pb}}$ as a function of p_T for the different rapidity bins of the analysis is shown on Fig. 42 for $\text{Pb}p$. The numerical values are given in Tables 56, 57, 58 and 59

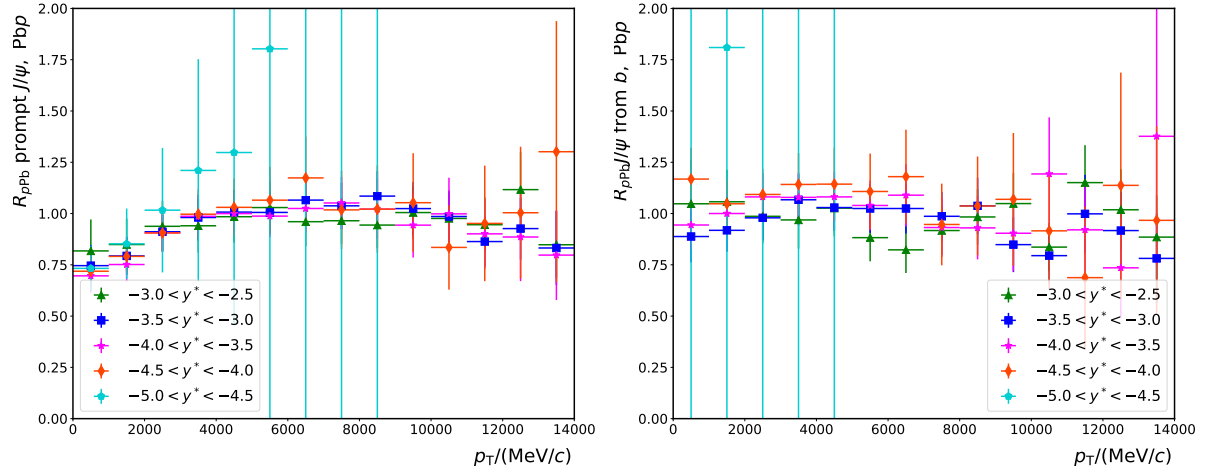


Figure 43: J/ψ nuclear modification factor in $\text{Pb}p$, $R_{p\text{Pb}}$ as a function of p_T for the different rapidity bins. Left: prompt J/ψ , right: J/ψ from b .

The measured values of $R_{p\text{Pb}}$, integrated over p_T in the range $0 < p_T < 14 \text{ GeV}/c$, as a function of y^* are shown in Fig. 44, for prompt J/ψ and J/ψ from b . The prompt J/ψ results are compared with a number of phenomenological calculations, which can be

grouped into three different approaches to quantify nuclear modifications between pp and the $p\text{Pb}$ collision system:

1. Calculations using collinear factorisation as basis to separate the non-perturbative initial state and the hard matrix element calculation. They use nuclear parton distribution functions instead of ordinary proton distribution functions based on fits of world data on eA , pA Drell-Yan and pA hadron production. Hard-matrix elements are available at Leading Order and fixed Next-to-Leading order both for p_T integrated as well as for p_T differential distributions. The uncertainties within this approach are typically large due to missing data constraining the gluon content of the nucleus at the relatively large x values probed in at the LHC². This approach is agnostic about the physics behind the nuclear modification apart from the assumption that collinear factorisation holds.
2. Calculations using the so-called Color-Glass-Condensate (CGC) framework. This approach does not use collinear parton distribution function for the nucleus based on the claim that this factorisation (as well as k_T factorisation, which we do not discuss here) is broken at a phenomenologically relevant level due to the fact that not only 2, but also 3 and 4-point multi-parton correlation functions become important, when the involved scales are close to the saturation scale, *i.e.* when the system is a "dense" gluonic system. These multi-parton correlators correspond to higher twist terms in the usual collinear approach, that are neglected in the latter approach due to their power suppression. The state-of-the-art phenomenological calculations are carried out within a framework that uses this approach only for one of the two projectiles, *i.e.* for a "dense-dilute" collision system, within certain limits simplifying the calculation. Therefore, the calculation is restricted to forward production, where the incoming parton from the proton is treated within collinear or k_T factorisation. The approach is in principle also applicable to forward production in pp collisions and has been also applied there. The nuclear modification arises in this set-up due to the difference in the saturation scale driven by the different geometry or nuclear size. A basic introduction to the basics are given in Ref. [22]. The current calculations are within the approach at leading order.
3. The third approach is based on the phenomenological observation that nuclear modification at a variety of collision energies can be described by the effect of "medium" induced small angle gluon radiation of the $c\bar{c}$ pair probing the nucleus taking properly into account the coherent interference before and after the hard gluon interaction. This process should be a higher order effect within the first two approaches. An introduction to the physical mechanism is given in Ref. [39].

The production mechanism of charmonium in pp collisions, in particular, the role of different NRQCD amplitudes, the usage of the Color Evaporation Model and the color singlet model, are still under debate. Therefore, the theoretical models are only compared to the nuclear modification factor and not to the absolute cross sections in $p\text{Pb}$ collisions. We compare with all three types of calculations for the rapidity dependence. First, a MC generator HELAC-Onia for quarkonium production within the collinear approach [62, 63]

²The situation is much worse as for the proton, since there is no equivalent of HERA data for nuclear-lepton collisions.

is used to quantify nuclear effects. The authors of the model calculations [21] tune the matrix elements to describe pp data, hence reducing the pp production model dependence and the impact of higher order corrections and use as input different parton distribution functions. The large uncertainties are a direct result of the largely data-unconstrained gluonic content of nuclei within collinear parton distribution functions. Two different nPDFs are used for the model-data comparison: nCTEQ15 [14] and EPS09 [12]. The differences in the parton distribution functions arise from different input data, different weights of the data, different lowest input scales. Furthermore, nCTEQ fits directly the data, whereas the EPS09 group fits the ratio of the nuclear and the proton pdfs. Within the large uncertainties the data is described. However, for a full exploitation of the power of the data precision, one would need to disentangle the different parton distribution function parameterisations contributing to the uncertainty band, *i.e.* exploiting the correlation of the different data points at different p_T and y .

The green curve illustrates the modification within the coherent energy loss model [25]. This calculation focuses also on the nuclear modification and hence uses as input parameterisations of world pp /light ion- p collision data for the denominator. The data is also well described within the experimental uncertainties.

The last model [24,64] is a representative of the CGC approach and is only compared at forward rapidity due to the limitation to a "dilute-dense" collision system. The description of the data is good and the theoretical uncertainty is surprisingly small. Also the absolute scales of the cross section were consistent with the data available at $\sqrt{s_{NN}} = 5$ TeV.

The cross-sections, integrated over y^* in the analysis bins, as a function of p_T are shown in Fig. 45.

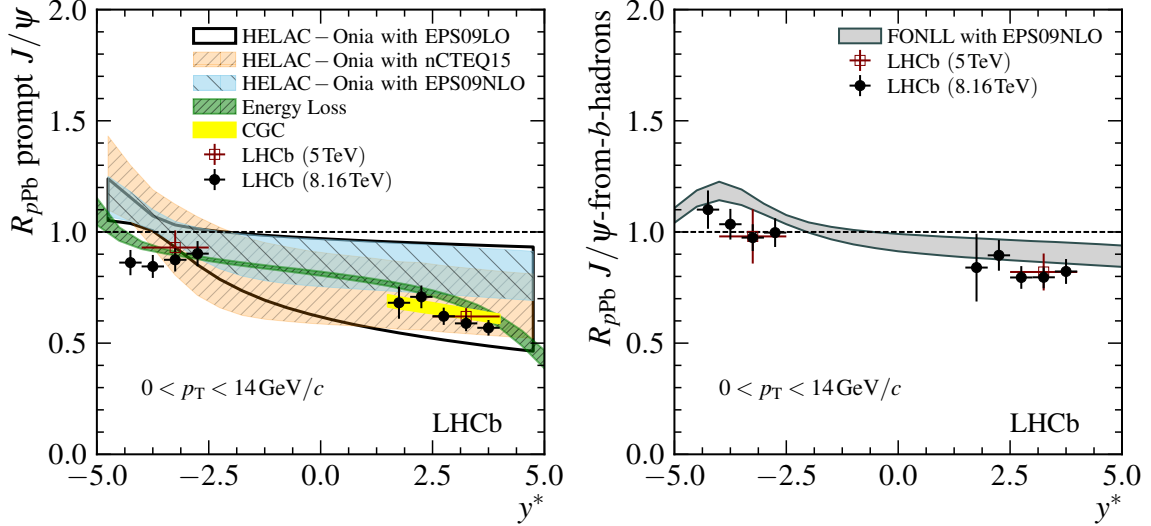


Figure 44: J/ψ nuclear modification factor, R_{pPb} , integrated over p_T in the range $0 < p_T < 14$ GeV/ c , as a function of y^* for left: prompt J/ψ , right: J/ψ from b . Horizontal error bars are the bin widths, vertical error bars the total uncertainties.

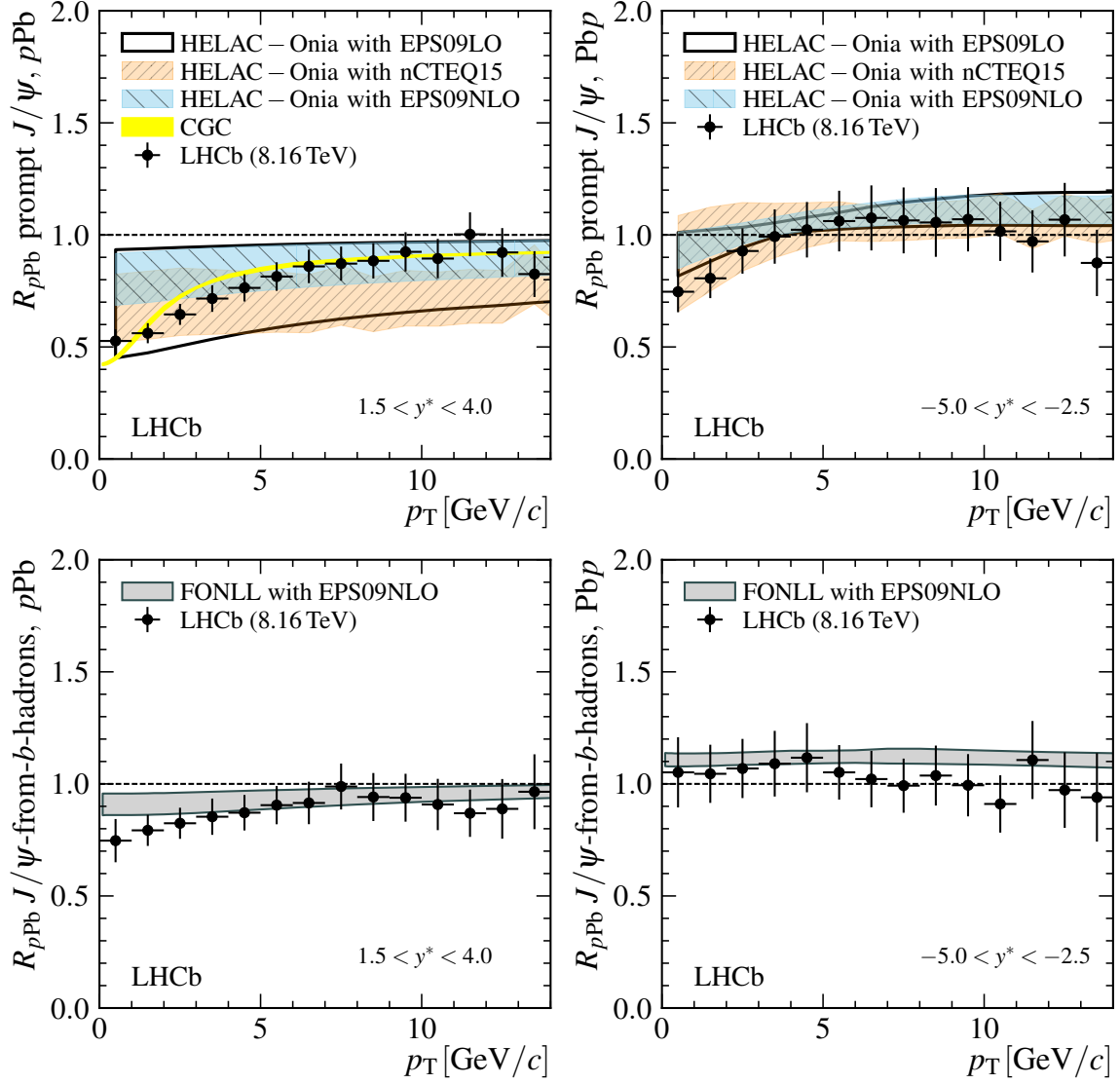


Figure 45: J/ψ nuclear modification factor, R_{pPb} , integrated over y^* in the analysis range, as a function of p_T for top left: prompt J/ψ in pPb , top right: J/ψ from b in pPb , bottom left: prompt J/ψ in $PbPb$, bottom right: J/ψ from b in $PbPb$. Horizontal error bars are the bin widths, vertical error bars the total uncertainties.

9.4 J/ψ forward to backward ratio

The prompt J/ψ and J/ψ from b forward-to-backward ratios, R_{FB} are shown in Fig. 46 in the different rapidity bins of the analysis. The integrated ratios as a function of y^* integrated over p_T , and of p_T integrated over y , are shown in Fig. 47 and 48, respectively.

10 Conclusions

The cross-section for prompt J/ψ and J/ψ from b as a function of p_T and y^* are measured in pPb and $PbPb$ collisions at 8.16 TeV. Fraction of b production, nuclear modification factors

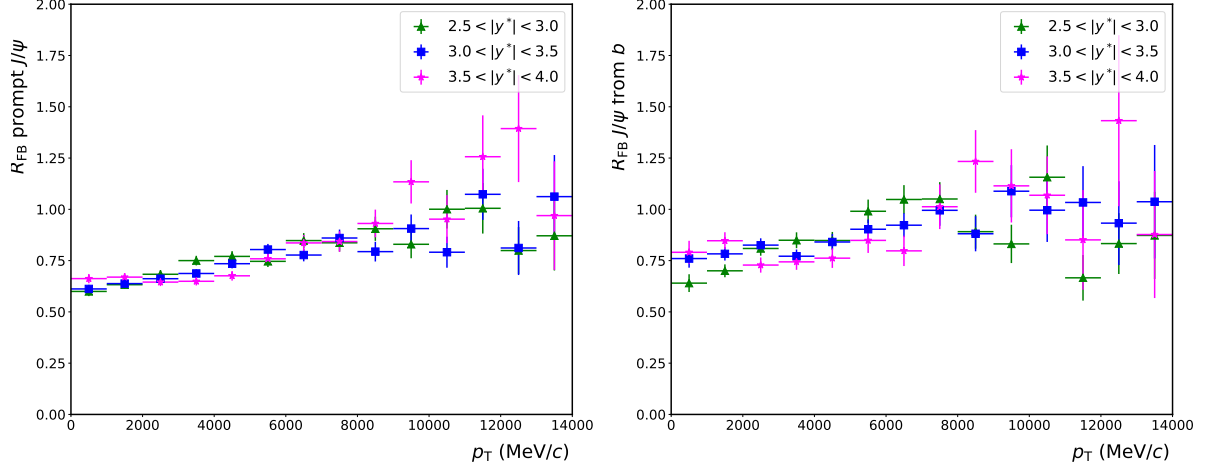


Figure 46: J/ψ forward to backward ratios, R_{FB} as a function of p_T for the different rapidity bins. Left: prompt J/ψ , right: J/ψ from b . Horizontal error bars are the bin widths, vertical error bars the total uncertainties.

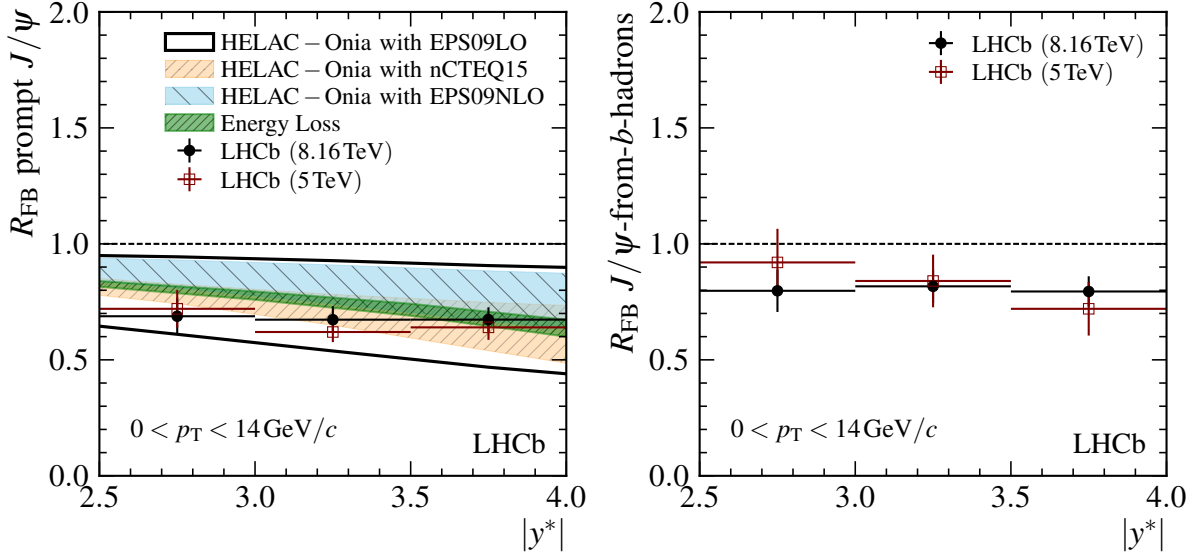


Figure 47: J/ψ forward to backward ratios, R_{FB} as a function of y^* , integrated over p_T . Left: prompt J/ψ , right: J/ψ from b . Horizontal error bars are the bin widths, vertical error bars the total uncertainties.

727 and forward-backward ratios are derived. These quantities are compared to theoretical
728 predictions. The precision of the measurements is significantly improved compared to
729 Run 1 results at 5 TeV.

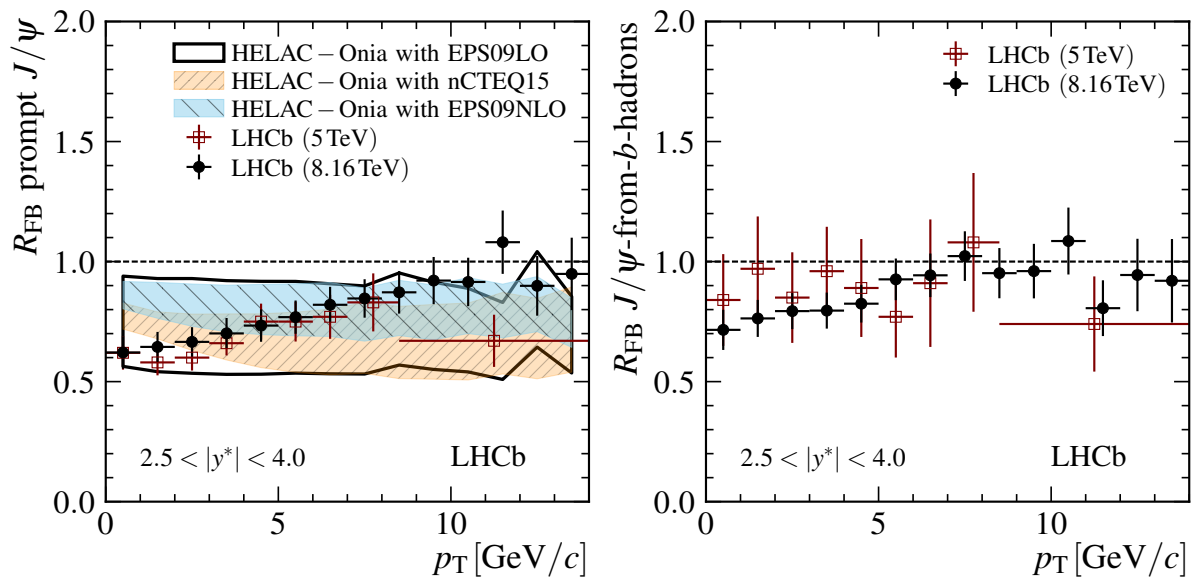


Figure 48: J/ψ forward to backward ratios, R_{FB} as a function of p_T , integrated over the common rapidity range $2.5 < y^* < 4.0$. Left: prompt J/ψ , right: J/ψ from b . Horizontal error bars are the bin widths, vertical error bars the total uncertainties.

Appendices

A Mass and t_z fit results

A.1 Event yields for J/ψ in $p\text{Pb}$

Table 10: Fit results for J/ψ in $p\text{Pb}$, in bins of p_T and y^* . The uncertainties are statistical only.

	p_T bin	y^* bin	N(prompt)	N (from b)	b fraction
0	$< p_T < 1000$	$1.5 < y^* < 2.0$	3166.3 ± 78.7	453.9 ± 29.7	0.125 ± 0.008
0	$< p_T < 1000$	$2.0 < y^* < 2.5$	10908.3 ± 156.1	1549.2 ± 55.7	0.124 ± 0.004
0	$< p_T < 1000$	$2.5 < y^* < 3.0$	13010.3 ± 176.9	1685.1 ± 61.0	0.115 ± 0.004
0	$< p_T < 1000$	$3.0 < y^* < 3.5$	11074.6 ± 155.9	1419.1 ± 54.9	0.114 ± 0.004
0	$< p_T < 1000$	$3.5 < y^* < 4.0$	6091.7 ± 103.7	697.5 ± 38.2	0.103 ± 0.005
1000	$< p_T < 2000$	$1.5 < y^* < 2.0$	7804.9 ± 121.8	1211.5 ± 47.4	0.134 ± 0.005
1000	$< p_T < 2000$	$2.0 < y^* < 2.5$	23748.7 ± 220.8	3616.5 ± 82.3	0.132 ± 0.003
1000	$< p_T < 2000$	$2.5 < y^* < 3.0$	26340.2 ± 235.9	3884.4 ± 86.2	0.129 ± 0.003
1000	$< p_T < 2000$	$3.0 < y^* < 3.5$	21524.4 ± 203.1	3032.4 ± 75.1	0.123 ± 0.003
1000	$< p_T < 2000$	$3.5 < y^* < 4.0$	11693.0 ± 139.3	1593.1 ± 55.9	0.120 ± 0.004
2000	$< p_T < 3000$	$1.5 < y^* < 2.0$	7797.2 ± 114.6	1335.4 ± 47.0	0.146 ± 0.005
2000	$< p_T < 3000$	$2.0 < y^* < 2.5$	21624.6 ± 199.1	3668.8 ± 78.1	0.145 ± 0.003
2000	$< p_T < 3000$	$2.5 < y^* < 3.0$	24231.1 ± 214.8	3904.0 ± 81.7	0.139 ± 0.003
2000	$< p_T < 3000$	$3.0 < y^* < 3.5$	18905.7 ± 181.0	3035.3 ± 72.0	0.138 ± 0.003
2000	$< p_T < 3000$	$3.5 < y^* < 4.0$	9191.5 ± 117.3	1234.4 ± 46.7	0.118 ± 0.004
3000	$< p_T < 4000$	$1.5 < y^* < 2.0$	5829.5 ± 92.8	1065.1 ± 39.4	0.154 ± 0.005
3000	$< p_T < 4000$	$2.0 < y^* < 2.5$	16608.1 ± 164.0	3104.0 ± 68.8	0.157 ± 0.003
3000	$< p_T < 4000$	$2.5 < y^* < 3.0$	18289.3 ± 169.4	3134.2 ± 69.8	0.146 ± 0.003
3000	$< p_T < 4000$	$3.0 < y^* < 3.5$	13443.9 ± 141.5	2256.9 ± 60.0	0.144 ± 0.004
3000	$< p_T < 4000$	$3.5 < y^* < 4.0$	6137.3 ± 83.9	906.9 ± 34.8	0.129 ± 0.005
4000	$< p_T < 5000$	$1.5 < y^* < 2.0$	4365.2 ± 77.2	811.2 ± 34.1	0.157 ± 0.006
4000	$< p_T < 5000$	$2.0 < y^* < 2.5$	11867.4 ± 129.0	2463.6 ± 59.9	0.172 ± 0.004
4000	$< p_T < 5000$	$2.5 < y^* < 3.0$	12196.0 ± 128.2	2303.3 ± 57.7	0.159 ± 0.004
4000	$< p_T < 5000$	$3.0 < y^* < 3.5$	9011.3 ± 109.3	1616.8 ± 49.0	0.152 ± 0.004
4000	$< p_T < 5000$	$3.5 < y^* < 4.0$	3952.9 ± 72.3	654.8 ± 32.3	0.142 ± 0.007
5000	$< p_T < 6000$	$1.5 < y^* < 2.0$	3060.4 ± 62.4	677.7 ± 30.8	0.181 ± 0.008
5000	$< p_T < 6000$	$2.0 < y^* < 2.5$	7729.9 ± 99.0	1685.5 ± 48.2	0.179 ± 0.005
5000	$< p_T < 6000$	$2.5 < y^* < 3.0$	7209.0 ± 95.6	1569.0 ± 46.6	0.179 ± 0.005
5000	$< p_T < 6000$	$3.0 < y^* < 3.5$	5640.8 ± 83.9	1151.3 ± 40.2	0.170 ± 0.005
5000	$< p_T < 6000$	$3.5 < y^* < 4.0$	2517.6 ± 55.3	442.1 ± 25.3	0.149 ± 0.008
6000	$< p_T < 7000$	$1.5 < y^* < 2.0$	2064.3 ± 50.5	537.8 ± 27.0	0.207 ± 0.009
6000	$< p_T < 7000$	$2.0 < y^* < 2.5$	4788.9 ± 76.4	1119.3 ± 39.0	0.189 ± 0.006
6000	$< p_T < 7000$	$2.5 < y^* < 3.0$	4245.9 ± 71.5	1031.8 ± 36.5	0.195 ± 0.006
6000	$< p_T < 7000$	$3.0 < y^* < 3.5$	3144.0 ± 61.7	733.8 ± 31.7	0.189 ± 0.007
6000	$< p_T < 7000$	$3.5 < y^* < 4.0$	1586.1 ± 43.9	274.3 ± 20.9	0.147 ± 0.010
7000	$< p_T < 8000$	$1.5 < y^* < 2.0$	1321.5 ± 40.1	422.7 ± 23.3	0.242 ± 0.012
7000	$< p_T < 8000$	$2.0 < y^* < 2.5$	2804.2 ± 57.3	808.6 ± 32.1	0.224 ± 0.008
7000	$< p_T < 8000$	$2.5 < y^* < 3.0$	2364.3 ± 53.4	692.5 ± 30.3	0.227 ± 0.009
7000	$< p_T < 8000$	$3.0 < y^* < 3.5$	1830.9 ± 46.8	480.3 ± 25.5	0.208 ± 0.010
7000	$< p_T < 8000$	$3.5 < y^* < 4.0$	890.5 ± 33.9	202.3 ± 16.9	0.185 ± 0.014
8000	$< p_T < 9000$	$1.5 < y^* < 2.0$	843.3 ± 31.9	284.0 ± 19.6	0.252 ± 0.015
8000	$< p_T < 9000$	$2.0 < y^* < 2.5$	1729.5 ± 45.1	534.3 ± 26.2	0.236 ± 0.010
8000	$< p_T < 9000$	$2.5 < y^* < 3.0$	1447.5 ± 41.4	444.1 ± 23.8	0.235 ± 0.011
8000	$< p_T < 9000$	$3.0 < y^* < 3.5$	1036.5 ± 35.2	284.6 ± 20.0	0.215 ± 0.013
8000	$< p_T < 9000$	$3.5 < y^* < 4.0$	555.7 ± 25.5	150.5 ± 13.9	0.213 ± 0.017

Table 11: Fit results for J/ψ in pPb, in bins of p_T and y^* . The uncertainties are statistical only.

p_T bin	y^* bin	N(prompt)	N (from b)	b fraction
9000 < p_T < 10000	1.5 < y^* < 2.0	548.5 \pm 25.6	202.4 \pm 16.1	0.270 \pm 0.019
9000 < p_T < 10000	2.0 < y^* < 2.5	1012.5 \pm 34.0	363.0 \pm 20.9	0.264 \pm 0.013
9000 < p_T < 10000	2.5 < y^* < 3.0	842.5 \pm 32.1	286.2 \pm 19.0	0.254 \pm 0.015
9000 < p_T < 10000	3.0 < y^* < 3.5	603.1 \pm 27.0	194.3 \pm 15.7	0.244 \pm 0.018
9000 < p_T < 10000	3.5 < y^* < 4.0	356.6 \pm 20.9	88.2 \pm 10.9	0.198 \pm 0.022
10000 < p_T < 11000	1.5 < y^* < 2.0	329.3 \pm 19.6	133.5 \pm 12.7	0.289 \pm 0.023
10000 < p_T < 11000	2.0 < y^* < 2.5	658.0 \pm 27.4	230.7 \pm 16.8	0.260 \pm 0.016
10000 < p_T < 11000	2.5 < y^* < 3.0	560.8 \pm 25.9	202.0 \pm 16.3	0.265 \pm 0.019
10000 < p_T < 11000	3.0 < y^* < 3.5	364.6 \pm 20.7	116.7 \pm 12.5	0.242 \pm 0.023
10000 < p_T < 11000	3.5 < y^* < 4.0	200.2 \pm 16.2	70.7 \pm 9.1	0.261 \pm 0.031
11000 < p_T < 12000	1.5 < y^* < 2.0	251.1 \pm 16.6	109.3 \pm 11.3	0.303 \pm 0.027
11000 < p_T < 12000	2.0 < y^* < 2.5	403.4 \pm 21.7	170.8 \pm 14.6	0.297 \pm 0.022
11000 < p_T < 12000	2.5 < y^* < 3.0	323.1 \pm 19.5	110.6 \pm 12.6	0.255 \pm 0.025
11000 < p_T < 12000	3.0 < y^* < 3.5	250.9 \pm 17.2	96.7 \pm 11.8	0.278 \pm 0.029
11000 < p_T < 12000	3.5 < y^* < 4.0	122.3 \pm 12.2	26.4 \pm 6.1	0.178 \pm 0.037
12000 < p_T < 13000	1.5 < y^* < 2.0	168.7 \pm 14.0	74.9 \pm 9.4	0.308 \pm 0.032
12000 < p_T < 13000	2.0 < y^* < 2.5	253.9 \pm 17.1	125.6 \pm 12.1	0.331 \pm 0.026
12000 < p_T < 13000	2.5 < y^* < 3.0	201.6 \pm 15.1	95.8 \pm 10.3	0.322 \pm 0.029
12000 < p_T < 13000	3.0 < y^* < 3.5	131.8 \pm 12.7	57.3 \pm 8.5	0.303 \pm 0.037
12000 < p_T < 13000	3.5 < y^* < 4.0	88.0 \pm 9.7	30.9 \pm 5.9	0.260 \pm 0.044
13000 < p_T < 14000	1.5 < y^* < 2.0	115.6 \pm 11.6	65.6 \pm 8.9	0.362 \pm 0.039
13000 < p_T < 14000	2.0 < y^* < 2.5	163.5 \pm 13.6	106.3 \pm 11.0	0.394 \pm 0.033
13000 < p_T < 14000	2.5 < y^* < 3.0	123.6 \pm 11.9	58.4 \pm 8.1	0.321 \pm 0.037
13000 < p_T < 14000	3.0 < y^* < 3.5	104.5 \pm 10.6	45.4 \pm 7.1	0.303 \pm 0.041
13000 < p_T < 14000	3.5 < y^* < 4.0	47.1 \pm 7.5	19.6 \pm 4.8	0.294 \pm 0.062

A.2 Event yields for J/ψ in PbP

Table 12: Fit results for J/ψ in PbP, in bins of p_T and y^* . The uncertainties are statistical only.

	p_T bin	y^* bin	N(prompt)	N (from b)	b fraction
0	$< p_T < 1000$	$2.5 < y^* < 3.0$	7351.7 ± 127.5	892.0 ± 42.8	0.108 ± 0.005
0	$< p_T < 1000$	$3.0 < y^* < 3.5$	19933.7 ± 232.5	2056.7 ± 70.8	0.094 ± 0.003
0	$< p_T < 1000$	$3.5 < y^* < 4.0$	22656.0 ± 275.1	2173.1 ± 78.2	0.088 ± 0.003
0	$< p_T < 1000$	$4.0 < y^* < 4.5$	18188.2 ± 255.2	1521.7 ± 68.5	0.077 ± 0.003
0	$< p_T < 1000$	$4.5 < y^* < 5.0$	8687.8 ± 177.1	585.7 ± 47.8	0.063 ± 0.005
1000	$< p_T < 2000$	$2.5 < y^* < 3.0$	17544.4 ± 191.4	2337.2 ± 65.8	0.118 ± 0.003
1000	$< p_T < 2000$	$3.0 < y^* < 3.5$	40377.1 ± 314.1	4635.0 ± 99.2	0.103 ± 0.002
1000	$< p_T < 2000$	$3.5 < y^* < 4.0$	42385.4 ± 343.5	4565.3 ± 102.0	0.097 ± 0.002
1000	$< p_T < 2000$	$4.0 < y^* < 4.5$	32549.9 ± 310.5	2877.9 ± 84.2	0.081 ± 0.002
1000	$< p_T < 2000$	$4.5 < y^* < 5.0$	16168.9 ± 219.8	1148.3 ± 58.2	0.066 ± 0.003
2000	$< p_T < 3000$	$2.5 < y^* < 3.0$	16641.4 ± 173.1	2264.7 ± 61.4	0.120 ± 0.003
2000	$< p_T < 3000$	$3.0 < y^* < 3.5$	35458.7 ± 277.3	4563.4 ± 91.0	0.114 ± 0.002
2000	$< p_T < 3000$	$3.5 < y^* < 4.0$	37053.2 ± 308.3	4408.6 ± 93.7	0.106 ± 0.002
2000	$< p_T < 3000$	$4.0 < y^* < 4.5$	25380.7 ± 254.2	2501.7 ± 72.5	0.090 ± 0.003
2000	$< p_T < 3000$	$4.5 < y^* < 5.0$	10669.5 ± 165.0	841.9 ± 43.7	0.073 ± 0.004
3000	$< p_T < 4000$	$2.5 < y^* < 3.0$	11935.7 ± 136.7	1806.5 ± 51.6	0.131 ± 0.004
3000	$< p_T < 4000$	$3.0 < y^* < 3.5$	25972.2 ± 220.1	3884.3 ± 79.6	0.130 ± 0.003
3000	$< p_T < 4000$	$3.5 < y^* < 4.0$	25275.2 ± 223.5	3259.3 ± 75.5	0.114 ± 0.003
3000	$< p_T < 4000$	$4.0 < y^* < 4.5$	16602.3 ± 184.5	1863.8 ± 57.6	0.101 ± 0.003
3000	$< p_T < 4000$	$4.5 < y^* < 5.0$	6194.8 ± 112.7	496.1 ± 31.0	0.074 ± 0.005
4000	$< p_T < 5000$	$2.5 < y^* < 3.0$	8617.4 ± 110.8	1478.8 ± 45.9	0.146 ± 0.004
4000	$< p_T < 5000$	$3.0 < y^* < 3.5$	17076.0 ± 159.8	2678.2 ± 62.8	0.136 ± 0.003
4000	$< p_T < 5000$	$3.5 < y^* < 4.0$	15122.4 ± 150.9	2222.2 ± 58.2	0.128 ± 0.003
4000	$< p_T < 5000$	$4.0 < y^* < 4.5$	9931.0 ± 124.4	1207.1 ± 44.6	0.108 ± 0.004
4000	$< p_T < 5000$	$4.5 < y^* < 5.0$	3324.2 ± 78.3	345.3 ± 25.2	0.094 ± 0.007
5000	$< p_T < 6000$	$2.5 < y^* < 3.0$	5948.9 ± 88.2	975.6 ± 37.2	0.141 ± 0.005
5000	$< p_T < 6000$	$3.0 < y^* < 3.5$	10158.4 ± 115.9	1846.1 ± 50.2	0.154 ± 0.004
5000	$< p_T < 6000$	$3.5 < y^* < 4.0$	8498.2 ± 105.6	1334.4 ± 43.6	0.136 ± 0.004
5000	$< p_T < 6000$	$4.0 < y^* < 4.5$	5330.2 ± 86.2	731.2 ± 33.0	0.121 ± 0.005
5000	$< p_T < 6000$	$4.5 < y^* < 5.0$	1981.2 ± 55.0	227.5 ± 19.4	0.103 ± 0.009
6000	$< p_T < 7000$	$2.5 < y^* < 3.0$	3529.7 ± 67.4	693.7 ± 31.0	0.164 ± 0.007
6000	$< p_T < 7000$	$3.0 < y^* < 3.5$	5925.5 ± 85.4	1164.9 ± 39.7	0.164 ± 0.005
6000	$< p_T < 7000$	$3.5 < y^* < 4.0$	4614.9 ± 76.0	836.9 ± 34.1	0.154 ± 0.006
6000	$< p_T < 7000$	$4.0 < y^* < 4.5$	2808.8 ± 60.2	447.2 ± 25.3	0.137 ± 0.007
6000	$< p_T < 7000$	$4.5 < y^* < 5.0$	925.2 ± 39.5	109.1 ± 14.7	0.105 ± 0.014
7000	$< p_T < 8000$	$2.5 < y^* < 3.0$	2192.5 ± 51.4	511.6 ± 26.2	0.189 ± 0.009
7000	$< p_T < 8000$	$3.0 < y^* < 3.5$	3283.1 ± 61.9	744.5 ± 29.9	0.185 ± 0.007
7000	$< p_T < 8000$	$3.5 < y^* < 4.0$	2456.2 ± 54.7	464.6 ± 25.4	0.159 ± 0.008
7000	$< p_T < 8000$	$4.0 < y^* < 4.5$	1437.0 ± 41.0	225.7 ± 17.6	0.136 ± 0.010
7000	$< p_T < 8000$	$4.5 < y^* < 5.0$	517.9 ± 27.4	66.2 ± 9.3	0.113 ± 0.015
8000	$< p_T < 9000$	$2.5 < y^* < 3.0$	1284.7 ± 39.3	400.4 ± 23.1	0.238 ± 0.012
8000	$< p_T < 9000$	$3.0 < y^* < 3.5$	1884.5 ± 46.9	466.2 ± 23.9	0.198 ± 0.009
8000	$< p_T < 9000$	$3.5 < y^* < 4.0$	1382.2 ± 40.4	282.6 ± 18.9	0.170 ± 0.010
8000	$< p_T < 9000$	$4.0 < y^* < 4.5$	745.9 ± 30.1	152.8 ± 14.3	0.170 ± 0.015
8000	$< p_T < 9000$	$4.5 < y^* < 5.0$	229.1 ± 21.0	43.0 ± 7.6	0.158 ± 0.027

Table 13: Fit results for J/ψ in PbPb, in bins of p_T and y^* . The uncertainties are statistical only.

p_T bin	y^* bin	N(prompt)	N (from b)	b fraction
9000 < p_T < 10000	2.5 < y^* < 3.0	808.8 ± 30.8	274.1 ± 18.1	0.253 ± 0.015
9000 < p_T < 10000	3.0 < y^* < 3.5	1062.4 ± 35.8	284.9 ± 19.2	0.211 ± 0.013
9000 < p_T < 10000	3.5 < y^* < 4.0	694.9 ± 28.2	174.9 ± 14.6	0.201 ± 0.015
9000 < p_T < 10000	4.0 < y^* < 4.5	404.1 ± 22.5	83.5 ± 10.4	0.171 ± 0.020
9000 < p_T < 10000	4.5 < y^* < 5.0	138.7 ± 15.2	19.5 ± 5.5	0.123 ± 0.033
10000 < p_T < 11000	2.5 < y^* < 3.0	548.6 ± 25.4	170.9 ± 14.2	0.238 ± 0.018
10000 < p_T < 11000	3.0 < y^* < 3.5	662.0 ± 28.9	168.3 ± 15.6	0.203 ± 0.018
10000 < p_T < 11000	3.5 < y^* < 4.0	424.4 ± 22.4	133.5 ± 12.7	0.239 ± 0.020
10000 < p_T < 11000	4.0 < y^* < 4.5	232.1 ± 17.6	59.9 ± 8.8	0.205 ± 0.028
10000 < p_T < 11000	4.5 < y^* < 5.0	72.7 ± 10.4	10.4 ± 3.6	0.125 ± 0.042
11000 < p_T < 12000	2.5 < y^* < 3.0	308.8 ± 19.1	159.5 ± 13.6	0.341 ± 0.024
11000 < p_T < 12000	3.0 < y^* < 3.5	359.7 ± 20.7	144.0 ± 13.6	0.286 ± 0.023
11000 < p_T < 12000	3.5 < y^* < 4.0	219.0 ± 16.8	69.9 ± 9.5	0.242 ± 0.029
11000 < p_T < 12000	4.0 < y^* < 4.5	142.0 ± 13.3	19.5 ± 5.1	0.121 ± 0.029
11000 < p_T < 12000	4.5 < y^* < 5.0	42.2 ± 7.5	18.1 ± 4.5	0.300 ± 0.066
12000 < p_T < 13000	2.5 < y^* < 3.0	237.2 ± 16.1	108.2 ± 10.7	0.313 ± 0.027
12000 < p_T < 13000	3.0 < y^* < 3.5	225.4 ± 16.1	85.3 ± 10.0	0.275 ± 0.028
12000 < p_T < 13000	3.5 < y^* < 4.0	113.0 ± 11.7	38.6 ± 7.3	0.255 ± 0.041
12000 < p_T < 13000	4.0 < y^* < 4.5	71.9 ± 8.7	22.2 ± 5.0	0.236 ± 0.048
12000 < p_T < 13000	4.5 < y^* < 5.0	30.0 ± 8.4	4.2 ± 2.7	0.123 ± 0.067
13000 < p_T < 14000	2.5 < y^* < 3.0	127.2 ± 13.5	59.9 ± 9.1	0.320 ± 0.046
13000 < p_T < 14000	3.0 < y^* < 3.5	129.6 ± 15.9	57.6 ± 10.8	0.308 ± 0.057
13000 < p_T < 14000	3.5 < y^* < 4.0	89.8 ± 10.1	41.3 ± 6.9	0.315 ± 0.045
13000 < p_T < 14000	4.0 < y^* < 4.5	39.9 ± 6.9	11.8 ± 3.7	0.229 ± 0.063
13000 < p_T < 14000	4.5 < y^* < 5.0	4.2 ± 2.6	2.4 ± 1.8	0.365 ± 0.248

B Efficiencies numerical results

B.1 Acceptance efficiencies

B.1.1 Acceptance efficiencies for J/ψ in $p\text{Pb}$

Table 14: Acceptance efficiency for J/ψ in $p\text{Pb}$.

p_{T} bin	y^* bin	ϵ_{acc}
0 < p_{T} < 1000	1.5 < y^* < 2.0	0.212 ± 0.001
0 < p_{T} < 1000	2.0 < y^* < 2.5	0.615 ± 0.002
0 < p_{T} < 1000	2.5 < y^* < 3.0	0.826 ± 0.001
0 < p_{T} < 1000	3.0 < y^* < 3.5	0.841 ± 0.001
0 < p_{T} < 1000	3.5 < y^* < 4.0	0.657 ± 0.002
1000 < p_{T} < 2000	1.5 < y^* < 2.0	0.232 ± 0.001
1000 < p_{T} < 2000	2.0 < y^* < 2.5	0.643 ± 0.001
1000 < p_{T} < 2000	2.5 < y^* < 3.0	0.820 ± 0.001
1000 < p_{T} < 2000	3.0 < y^* < 3.5	0.832 ± 0.001
1000 < p_{T} < 2000	3.5 < y^* < 4.0	0.682 ± 0.001
2000 < p_{T} < 3000	1.5 < y^* < 2.0	0.261 ± 0.001
2000 < p_{T} < 3000	2.0 < y^* < 2.5	0.686 ± 0.001
2000 < p_{T} < 3000	2.5 < y^* < 3.0	0.856 ± 0.001
2000 < p_{T} < 3000	3.0 < y^* < 3.5	0.866 ± 0.001
2000 < p_{T} < 3000	3.5 < y^* < 4.0	0.727 ± 0.001
3000 < p_{T} < 4000	1.5 < y^* < 2.0	0.295 ± 0.001
3000 < p_{T} < 4000	2.0 < y^* < 2.5	0.741 ± 0.001
3000 < p_{T} < 4000	2.5 < y^* < 3.0	0.889 ± 0.001
3000 < p_{T} < 4000	3.0 < y^* < 3.5	0.899 ± 0.001
3000 < p_{T} < 4000	3.5 < y^* < 4.0	0.781 ± 0.001
4000 < p_{T} < 5000	1.5 < y^* < 2.0	0.332 ± 0.001
4000 < p_{T} < 5000	2.0 < y^* < 2.5	0.787 ± 0.001
4000 < p_{T} < 5000	2.5 < y^* < 3.0	0.919 ± 0.001
4000 < p_{T} < 5000	3.0 < y^* < 3.5	0.926 ± 0.001
4000 < p_{T} < 5000	3.5 < y^* < 4.0	0.831 ± 0.002
5000 < p_{T} < 6000	1.5 < y^* < 2.0	0.366 ± 0.002
5000 < p_{T} < 6000	2.0 < y^* < 2.5	0.830 ± 0.002
5000 < p_{T} < 6000	2.5 < y^* < 3.0	0.939 ± 0.001
5000 < p_{T} < 6000	3.0 < y^* < 3.5	0.946 ± 0.001
5000 < p_{T} < 6000	3.5 < y^* < 4.0	0.862 ± 0.002
6000 < p_{T} < 7000	1.5 < y^* < 2.0	0.404 ± 0.003
6000 < p_{T} < 7000	2.0 < y^* < 2.5	0.858 ± 0.002
6000 < p_{T} < 7000	2.5 < y^* < 3.0	0.952 ± 0.002
6000 < p_{T} < 7000	3.0 < y^* < 3.5	0.959 ± 0.002
6000 < p_{T} < 7000	3.5 < y^* < 4.0	0.886 ± 0.003
7000 < p_{T} < 8000	1.5 < y^* < 2.0	0.443 ± 0.005
7000 < p_{T} < 8000	2.0 < y^* < 2.5	0.889 ± 0.003
7000 < p_{T} < 8000	2.5 < y^* < 3.0	0.959 ± 0.002
7000 < p_{T} < 8000	3.0 < y^* < 3.5	0.966 ± 0.002
7000 < p_{T} < 8000	3.5 < y^* < 4.0	0.905 ± 0.004
8000 < p_{T} < 9000	1.5 < y^* < 2.0	0.474 ± 0.006
8000 < p_{T} < 9000	2.0 < y^* < 2.5	0.904 ± 0.004
8000 < p_{T} < 9000	2.5 < y^* < 3.0	0.971 ± 0.002
8000 < p_{T} < 9000	3.0 < y^* < 3.5	0.977 ± 0.002
8000 < p_{T} < 9000	3.5 < y^* < 4.0	0.926 ± 0.005
9000 < p_{T} < 10000	1.5 < y^* < 2.0	0.490 ± 0.008
9000 < p_{T} < 10000	2.0 < y^* < 2.5	0.919 ± 0.005

Table 15: Acceptance efficiency for J/ψ in $p\text{Pb}$.

p_{T} bin	y^* bin	ϵ_{acc}
9000 < p_{T} < 10000	$2.5 < y^* < 3.0$	0.977 ± 0.003
9000 < p_{T} < 10000	$3.0 < y^* < 3.5$	0.983 ± 0.003
9000 < p_{T} < 10000	$3.5 < y^* < 4.0$	0.934 ± 0.007
10000 < p_{T} < 11000	$1.5 < y^* < 2.0$	0.511 ± 0.011
10000 < p_{T} < 11000	$2.0 < y^* < 2.5$	0.935 ± 0.006
10000 < p_{T} < 11000	$2.5 < y^* < 3.0$	0.972 ± 0.004
10000 < p_{T} < 11000	$3.0 < y^* < 3.5$	0.986 ± 0.004
10000 < p_{T} < 11000	$3.5 < y^* < 4.0$	0.943 ± 0.009
11000 < p_{T} < 12000	$1.5 < y^* < 2.0$	0.526 ± 0.014
11000 < p_{T} < 12000	$2.0 < y^* < 2.5$	0.944 ± 0.007
11000 < p_{T} < 12000	$2.5 < y^* < 3.0$	0.975 ± 0.005
11000 < p_{T} < 12000	$3.0 < y^* < 3.5$	0.988 ± 0.004
11000 < p_{T} < 12000	$3.5 < y^* < 4.0$	0.951 ± 0.011
12000 < p_{T} < 13000	$1.5 < y^* < 2.0$	0.578 ± 0.018
12000 < p_{T} < 13000	$2.0 < y^* < 2.5$	0.961 ± 0.007
12000 < p_{T} < 13000	$2.5 < y^* < 3.0$	0.985 ± 0.006
12000 < p_{T} < 13000	$3.0 < y^* < 3.5$	0.997 ± 0.003
12000 < p_{T} < 13000	$3.5 < y^* < 4.0$	0.962 ± 0.013
13000 < p_{T} < 14000	$1.5 < y^* < 2.0$	0.612 ± 0.022
13000 < p_{T} < 14000	$2.0 < y^* < 2.5$	0.961 ± 0.009
13000 < p_{T} < 14000	$2.5 < y^* < 3.0$	0.993 ± 0.005
13000 < p_{T} < 14000	$3.0 < y^* < 3.5$	0.996 ± 0.004
13000 < p_{T} < 14000	$3.5 < y^* < 4.0$	0.961 ± 0.017

Table 16: Acceptance efficiency for J/ψ in PbP.

p_T bin	y^* bin	ϵ_{acc}
0 < p_T < 1000	-3.0 < y^* < -2.5	0.280 ± 0.001
0 < p_T < 1000	-3.5 < y^* < -3.0	0.659 ± 0.001
0 < p_T < 1000	-4.0 < y^* < -3.5	0.838 ± 0.001
0 < p_T < 1000	-4.5 < y^* < -4.0	0.828 ± 0.001
0 < p_T < 1000	-5.0 < y^* < -4.5	0.616 ± 0.002
1000 < p_T < 2000	-3.0 < y^* < -2.5	0.302 ± 0.001
1000 < p_T < 2000	-3.5 < y^* < -3.0	0.681 ± 0.001
1000 < p_T < 2000	-4.0 < y^* < -3.5	0.831 ± 0.001
1000 < p_T < 2000	-4.5 < y^* < -4.0	0.823 ± 0.001
1000 < p_T < 2000	-5.0 < y^* < -4.5	0.646 ± 0.001
2000 < p_T < 3000	-3.0 < y^* < -2.5	0.335 ± 0.001
2000 < p_T < 3000	-3.5 < y^* < -3.0	0.722 ± 0.001
2000 < p_T < 3000	-4.0 < y^* < -3.5	0.863 ± 0.001
2000 < p_T < 3000	-4.5 < y^* < -4.0	0.855 ± 0.001
2000 < p_T < 3000	-5.0 < y^* < -4.5	0.693 ± 0.001
3000 < p_T < 4000	-3.0 < y^* < -2.5	0.378 ± 0.001
3000 < p_T < 4000	-3.5 < y^* < -3.0	0.773 ± 0.001
3000 < p_T < 4000	-4.0 < y^* < -3.5	0.898 ± 0.001
3000 < p_T < 4000	-4.5 < y^* < -4.0	0.892 ± 0.001
3000 < p_T < 4000	-5.0 < y^* < -4.5	0.747 ± 0.001
4000 < p_T < 5000	-3.0 < y^* < -2.5	0.425 ± 0.002
4000 < p_T < 5000	-3.5 < y^* < -3.0	0.818 ± 0.001
4000 < p_T < 5000	-4.0 < y^* < -3.5	0.924 ± 0.001
4000 < p_T < 5000	-4.5 < y^* < -4.0	0.921 ± 0.001
4000 < p_T < 5000	-5.0 < y^* < -4.5	0.794 ± 0.002
5000 < p_T < 6000	-3.0 < y^* < -2.5	0.466 ± 0.002
5000 < p_T < 6000	-3.5 < y^* < -3.0	0.855 ± 0.002
5000 < p_T < 6000	-4.0 < y^* < -3.5	0.942 ± 0.001
5000 < p_T < 6000	-4.5 < y^* < -4.0	0.939 ± 0.001
5000 < p_T < 6000	-5.0 < y^* < -4.5	0.837 ± 0.002
6000 < p_T < 7000	-3.0 < y^* < -2.5	0.505 ± 0.003
6000 < p_T < 7000	-3.5 < y^* < -3.0	0.889 ± 0.002
6000 < p_T < 7000	-4.0 < y^* < -3.5	0.957 ± 0.002
6000 < p_T < 7000	-4.5 < y^* < -4.0	0.956 ± 0.002
6000 < p_T < 7000	-5.0 < y^* < -4.5	0.861 ± 0.003
7000 < p_T < 8000	-3.0 < y^* < -2.5	0.546 ± 0.005
7000 < p_T < 8000	-3.5 < y^* < -3.0	0.907 ± 0.003
7000 < p_T < 8000	-4.0 < y^* < -3.5	0.965 ± 0.002
7000 < p_T < 8000	-4.5 < y^* < -4.0	0.965 ± 0.002
7000 < p_T < 8000	-5.0 < y^* < -4.5	0.891 ± 0.004
8000 < p_T < 9000	-3.0 < y^* < -2.5	0.586 ± 0.006
8000 < p_T < 9000	-3.5 < y^* < -3.0	0.922 ± 0.004
8000 < p_T < 9000	-4.0 < y^* < -3.5	0.973 ± 0.002
8000 < p_T < 9000	-4.5 < y^* < -4.0	0.975 ± 0.003
8000 < p_T < 9000	-5.0 < y^* < -4.5	0.909 ± 0.006

Table 17: Acceptance efficiency for J/ψ in PbP.

p_T bin	y^* bin	ϵ_{acc}
9000 < p_T < 10000	$-3.0 < y^* < -2.5$	0.604 ± 0.008
9000 < p_T < 10000	$-3.5 < y^* < -3.0$	0.936 ± 0.004
9000 < p_T < 10000	$-4.0 < y^* < -3.5$	0.981 ± 0.003
9000 < p_T < 10000	$-4.5 < y^* < -4.0$	0.974 ± 0.004
9000 < p_T < 10000	$-5.0 < y^* < -4.5$	0.915 ± 0.008
10000 < p_T < 11000	$-3.0 < y^* < -2.5$	0.627 ± 0.011
10000 < p_T < 11000	$-3.5 < y^* < -3.0$	0.946 ± 0.005
10000 < p_T < 11000	$-4.0 < y^* < -3.5$	0.986 ± 0.003
10000 < p_T < 11000	$-4.5 < y^* < -4.0$	0.984 ± 0.004
10000 < p_T < 11000	$-5.0 < y^* < -4.5$	0.938 ± 0.010
11000 < p_T < 12000	$-3.0 < y^* < -2.5$	0.667 ± 0.013
11000 < p_T < 12000	$-3.5 < y^* < -3.0$	0.966 ± 0.006
11000 < p_T < 12000	$-4.0 < y^* < -3.5$	0.990 ± 0.003
11000 < p_T < 12000	$-4.5 < y^* < -4.0$	0.987 ± 0.005
11000 < p_T < 12000	$-5.0 < y^* < -4.5$	0.951 ± 0.011
12000 < p_T < 13000	$-3.0 < y^* < -2.5$	0.658 ± 0.017
12000 < p_T < 13000	$-3.5 < y^* < -3.0$	0.967 ± 0.007
12000 < p_T < 13000	$-4.0 < y^* < -3.5$	0.990 ± 0.004
12000 < p_T < 13000	$-4.5 < y^* < -4.0$	0.985 ± 0.007
12000 < p_T < 13000	$-5.0 < y^* < -4.5$	0.950 ± 0.015
13000 < p_T < 14000	$-3.0 < y^* < -2.5$	0.697 ± 0.020
13000 < p_T < 14000	$-3.5 < y^* < -3.0$	0.958 ± 0.010
13000 < p_T < 14000	$-4.0 < y^* < -3.5$	0.993 ± 0.005
13000 < p_T < 14000	$-4.5 < y^* < -4.0$	1.000 ± 0.000
13000 < p_T < 14000	$-5.0 < y^* < -4.5$	0.959 ± 0.018

B.2 Reconstruction efficiencies

B.2.1 Reconstruction efficiencies for J/ψ in $p\text{Pb}$

Table 18: Reconstruction efficiency for J/ψ in $p\text{Pb}$.

p_{T} bin	y^* bin	ϵ_{rec}
$0 < p_{\text{T}} < 1000$	$1.5 < y^* < 2.0$	0.796 ± 0.060
$0 < p_{\text{T}} < 1000$	$2.0 < y^* < 2.5$	0.906 ± 0.039
$0 < p_{\text{T}} < 1000$	$2.5 < y^* < 3.0$	0.906 ± 0.029
$0 < p_{\text{T}} < 1000$	$3.0 < y^* < 3.5$	0.873 ± 0.024
$0 < p_{\text{T}} < 1000$	$3.5 < y^* < 4.0$	0.792 ± 0.020
$1000 < p_{\text{T}} < 2000$	$1.5 < y^* < 2.0$	0.822 ± 0.052
$1000 < p_{\text{T}} < 2000$	$2.0 < y^* < 2.5$	0.896 ± 0.036
$1000 < p_{\text{T}} < 2000$	$2.5 < y^* < 3.0$	0.889 ± 0.027
$1000 < p_{\text{T}} < 2000$	$3.0 < y^* < 3.5$	0.860 ± 0.023
$1000 < p_{\text{T}} < 2000$	$3.5 < y^* < 4.0$	0.790 ± 0.027
$2000 < p_{\text{T}} < 3000$	$1.5 < y^* < 2.0$	0.845 ± 0.047
$2000 < p_{\text{T}} < 3000$	$2.0 < y^* < 2.5$	0.887 ± 0.037
$2000 < p_{\text{T}} < 3000$	$2.5 < y^* < 3.0$	0.878 ± 0.028
$2000 < p_{\text{T}} < 3000$	$3.0 < y^* < 3.5$	0.852 ± 0.025
$2000 < p_{\text{T}} < 3000$	$3.5 < y^* < 4.0$	0.782 ± 0.036
$3000 < p_{\text{T}} < 4000$	$1.5 < y^* < 2.0$	0.845 ± 0.047
$3000 < p_{\text{T}} < 4000$	$2.0 < y^* < 2.5$	0.889 ± 0.039
$3000 < p_{\text{T}} < 4000$	$2.5 < y^* < 3.0$	0.885 ± 0.031
$3000 < p_{\text{T}} < 4000$	$3.0 < y^* < 3.5$	0.859 ± 0.030
$3000 < p_{\text{T}} < 4000$	$3.5 < y^* < 4.0$	0.798 ± 0.041
$4000 < p_{\text{T}} < 5000$	$1.5 < y^* < 2.0$	0.860 ± 0.047
$4000 < p_{\text{T}} < 5000$	$2.0 < y^* < 2.5$	0.890 ± 0.039
$4000 < p_{\text{T}} < 5000$	$2.5 < y^* < 3.0$	0.886 ± 0.032
$4000 < p_{\text{T}} < 5000$	$3.0 < y^* < 3.5$	0.866 ± 0.034
$4000 < p_{\text{T}} < 5000$	$3.5 < y^* < 4.0$	0.816 ± 0.044
$5000 < p_{\text{T}} < 6000$	$1.5 < y^* < 2.0$	0.854 ± 0.041
$5000 < p_{\text{T}} < 6000$	$2.0 < y^* < 2.5$	0.896 ± 0.036
$5000 < p_{\text{T}} < 6000$	$2.5 < y^* < 3.0$	0.899 ± 0.032
$5000 < p_{\text{T}} < 6000$	$3.0 < y^* < 3.5$	0.874 ± 0.037
$5000 < p_{\text{T}} < 6000$	$3.5 < y^* < 4.0$	0.821 ± 0.046
$6000 < p_{\text{T}} < 7000$	$1.5 < y^* < 2.0$	0.857 ± 0.038
$6000 < p_{\text{T}} < 7000$	$2.0 < y^* < 2.5$	0.905 ± 0.035
$6000 < p_{\text{T}} < 7000$	$2.5 < y^* < 3.0$	0.904 ± 0.031
$6000 < p_{\text{T}} < 7000$	$3.0 < y^* < 3.5$	0.873 ± 0.040
$6000 < p_{\text{T}} < 7000$	$3.5 < y^* < 4.0$	0.845 ± 0.052
$7000 < p_{\text{T}} < 8000$	$1.5 < y^* < 2.0$	0.849 ± 0.037
$7000 < p_{\text{T}} < 8000$	$2.0 < y^* < 2.5$	0.918 ± 0.034
$7000 < p_{\text{T}} < 8000$	$2.5 < y^* < 3.0$	0.909 ± 0.035
$7000 < p_{\text{T}} < 8000$	$3.0 < y^* < 3.5$	0.867 ± 0.044
$7000 < p_{\text{T}} < 8000$	$3.5 < y^* < 4.0$	0.843 ± 0.055
$8000 < p_{\text{T}} < 9000$	$1.5 < y^* < 2.0$	0.867 ± 0.032
$8000 < p_{\text{T}} < 9000$	$2.0 < y^* < 2.5$	0.925 ± 0.033
$8000 < p_{\text{T}} < 9000$	$2.5 < y^* < 3.0$	0.900 ± 0.035
$8000 < p_{\text{T}} < 9000$	$3.0 < y^* < 3.5$	0.889 ± 0.044
$8000 < p_{\text{T}} < 9000$	$3.5 < y^* < 4.0$	0.858 ± 0.061
$9000 < p_{\text{T}} < 10000$	$1.5 < y^* < 2.0$	0.860 ± 0.029
$9000 < p_{\text{T}} < 10000$	$2.0 < y^* < 2.5$	0.920 ± 0.032

Table 19: Reconstruction efficiency for J/ψ in $p\text{Pb}$.

p_{T} bin	y^* bin	ϵ_{rec}
9000 < p_{T} < 10000	2.5 < y^* < 3.0	0.918 ± 0.038
9000 < p_{T} < 10000	3.0 < y^* < 3.5	0.896 ± 0.049
9000 < p_{T} < 10000	3.5 < y^* < 4.0	0.850 ± 0.062
10000 < p_{T} < 11000	1.5 < y^* < 2.0	0.867 ± 0.028
10000 < p_{T} < 11000	2.0 < y^* < 2.5	0.939 ± 0.034
10000 < p_{T} < 11000	2.5 < y^* < 3.0	0.927 ± 0.035
10000 < p_{T} < 11000	3.0 < y^* < 3.5	0.893 ± 0.051
10000 < p_{T} < 11000	3.5 < y^* < 4.0	0.884 ± 0.067
11000 < p_{T} < 12000	1.5 < y^* < 2.0	0.894 ± 0.030
11000 < p_{T} < 12000	2.0 < y^* < 2.5	0.939 ± 0.032
11000 < p_{T} < 12000	2.5 < y^* < 3.0	0.925 ± 0.039
11000 < p_{T} < 12000	3.0 < y^* < 3.5	0.912 ± 0.055
11000 < p_{T} < 12000	3.5 < y^* < 4.0	0.824 ± 0.063
12000 < p_{T} < 13000	1.5 < y^* < 2.0	0.853 ± 0.030
12000 < p_{T} < 13000	2.0 < y^* < 2.5	0.894 ± 0.030
12000 < p_{T} < 13000	2.5 < y^* < 3.0	0.925 ± 0.042
12000 < p_{T} < 13000	3.0 < y^* < 3.5	0.913 ± 0.058
12000 < p_{T} < 13000	3.5 < y^* < 4.0	0.887 ± 0.070
13000 < p_{T} < 14000	1.5 < y^* < 2.0	0.879 ± 0.027
13000 < p_{T} < 14000	2.0 < y^* < 2.5	0.961 ± 0.036
13000 < p_{T} < 14000	2.5 < y^* < 3.0	0.867 ± 0.032
13000 < p_{T} < 14000	3.0 < y^* < 3.5	0.978 ± 0.062
13000 < p_{T} < 14000	3.5 < y^* < 4.0	0.904 ± 0.069

Table 20: Reconstruction efficiency for J/ψ in PbP.

	p_T bin	y^* bin	ϵ_{acc}
0	$< p_T < 1000$	$-3.0 < y^* < -2.5$	0.732 ± 0.109
0	$< p_T < 1000$	$-3.5 < y^* < -3.0$	0.865 ± 0.075
0	$< p_T < 1000$	$-4.0 < y^* < -3.5$	0.877 ± 0.059
0	$< p_T < 1000$	$-4.5 < y^* < -4.0$	0.860 ± 0.054
0	$< p_T < 1000$	$-5.0 < y^* < -4.5$	0.778 ± 0.052
1000	$< p_T < 2000$	$-3.0 < y^* < -2.5$	0.771 ± 0.095
1000	$< p_T < 2000$	$-3.5 < y^* < -3.0$	0.853 ± 0.069
1000	$< p_T < 2000$	$-4.0 < y^* < -3.5$	0.858 ± 0.055
1000	$< p_T < 2000$	$-4.5 < y^* < -4.0$	0.837 ± 0.050
1000	$< p_T < 2000$	$-5.0 < y^* < -4.5$	0.761 ± 0.077
2000	$< p_T < 3000$	$-3.0 < y^* < -2.5$	0.812 ± 0.086
2000	$< p_T < 3000$	$-3.5 < y^* < -3.0$	0.846 ± 0.068
2000	$< p_T < 3000$	$-4.0 < y^* < -3.5$	0.845 ± 0.055
2000	$< p_T < 3000$	$-4.5 < y^* < -4.0$	0.829 ± 0.055
2000	$< p_T < 3000$	$-5.0 < y^* < -4.5$	0.742 ± 0.103
3000	$< p_T < 4000$	$-3.0 < y^* < -2.5$	0.829 ± 0.083
3000	$< p_T < 4000$	$-3.5 < y^* < -3.0$	0.855 ± 0.068
3000	$< p_T < 4000$	$-4.0 < y^* < -3.5$	0.850 ± 0.056
3000	$< p_T < 4000$	$-4.5 < y^* < -4.0$	0.836 ± 0.073
3000	$< p_T < 4000$	$-5.0 < y^* < -4.5$	0.743 ± 0.119
4000	$< p_T < 5000$	$-3.0 < y^* < -2.5$	0.829 ± 0.080
4000	$< p_T < 5000$	$-3.5 < y^* < -3.0$	0.863 ± 0.068
4000	$< p_T < 5000$	$-4.0 < y^* < -3.5$	0.849 ± 0.057
4000	$< p_T < 5000$	$-4.5 < y^* < -4.0$	0.842 ± 0.093
4000	$< p_T < 5000$	$-5.0 < y^* < -4.5$	0.761 ± 0.132
5000	$< p_T < 6000$	$-3.0 < y^* < -2.5$	0.835 ± 0.073
5000	$< p_T < 6000$	$-3.5 < y^* < -3.0$	0.863 ± 0.065
5000	$< p_T < 6000$	$-4.0 < y^* < -3.5$	0.863 ± 0.061
5000	$< p_T < 6000$	$-4.5 < y^* < -4.0$	0.834 ± 0.107
5000	$< p_T < 6000$	$-5.0 < y^* < -4.5$	0.771 ± 0.144
6000	$< p_T < 7000$	$-3.0 < y^* < -2.5$	0.849 ± 0.068
6000	$< p_T < 7000$	$-3.5 < y^* < -3.0$	0.854 ± 0.064
6000	$< p_T < 7000$	$-4.0 < y^* < -3.5$	0.867 ± 0.069
6000	$< p_T < 7000$	$-4.5 < y^* < -4.0$	0.830 ± 0.121
6000	$< p_T < 7000$	$-5.0 < y^* < -4.5$	0.777 ± 0.159
7000	$< p_T < 8000$	$-3.0 < y^* < -2.5$	0.841 ± 0.061
7000	$< p_T < 8000$	$-3.5 < y^* < -3.0$	0.860 ± 0.065
7000	$< p_T < 8000$	$-4.0 < y^* < -3.5$	0.846 ± 0.075
7000	$< p_T < 8000$	$-4.5 < y^* < -4.0$	0.849 ± 0.137
7000	$< p_T < 8000$	$-5.0 < y^* < -4.5$	0.775 ± 0.179
8000	$< p_T < 9000$	$-3.0 < y^* < -2.5$	0.838 ± 0.061
8000	$< p_T < 9000$	$-3.5 < y^* < -3.0$	0.838 ± 0.062
8000	$< p_T < 9000$	$-4.0 < y^* < -3.5$	0.870 ± 0.096
8000	$< p_T < 9000$	$-4.5 < y^* < -4.0$	0.837 ± 0.147
8000	$< p_T < 9000$	$-5.0 < y^* < -4.5$	0.799 ± 0.198

Table 21: Reconstruction efficiency for J/ψ in PbP.

p_T bin	y^* bin	ϵ_{rec}
9000 < p_T < 10000	$-3.0 < y^* < -2.5$	0.840 ± 0.056
9000 < p_T < 10000	$-3.5 < y^* < -3.0$	0.889 ± 0.063
9000 < p_T < 10000	$-4.0 < y^* < -3.5$	0.852 ± 0.105
9000 < p_T < 10000	$-4.5 < y^* < -4.0$	0.819 ± 0.153
9000 < p_T < 10000	$-5.0 < y^* < -4.5$	0.784 ± 0.194
10000 < p_T < 11000	$-3.0 < y^* < -2.5$	0.875 ± 0.053
10000 < p_T < 11000	$-3.5 < y^* < -3.0$	0.835 ± 0.061
10000 < p_T < 11000	$-4.0 < y^* < -3.5$	0.850 ± 0.109
10000 < p_T < 11000	$-4.5 < y^* < -4.0$	0.902 ± 0.175
10000 < p_T < 11000	$-5.0 < y^* < -4.5$	0.826 ± 0.207
11000 < p_T < 12000	$-3.0 < y^* < -2.5$	0.866 ± 0.050
11000 < p_T < 12000	$-3.5 < y^* < -3.0$	0.891 ± 0.071
11000 < p_T < 12000	$-4.0 < y^* < -3.5$	0.909 ± 0.115
11000 < p_T < 12000	$-4.5 < y^* < -4.0$	0.823 ± 0.181
11000 < p_T < 12000	$-5.0 < y^* < -4.5$	0.745 ± 0.192
12000 < p_T < 13000	$-3.0 < y^* < -2.5$	0.852 ± 0.062
12000 < p_T < 13000	$-3.5 < y^* < -3.0$	0.840 ± 0.064
12000 < p_T < 13000	$-4.0 < y^* < -3.5$	0.817 ± 0.114
12000 < p_T < 13000	$-4.5 < y^* < -4.0$	0.859 ± 0.186
12000 < p_T < 13000	$-5.0 < y^* < -4.5$	0.820 ± 0.226
13000 < p_T < 14000	$-3.0 < y^* < -2.5$	0.719 ± 0.042
13000 < p_T < 14000	$-3.5 < y^* < -3.0$	0.903 ± 0.078
13000 < p_T < 14000	$-4.0 < y^* < -3.5$	0.762 ± 0.108
13000 < p_T < 14000	$-4.5 < y^* < -4.0$	0.789 ± 0.181
13000 < p_T < 14000	$-5.0 < y^* < -4.5$	1.056 ± 0.230

741 B.3 Selection efficiencies

742 B.3.1 Selection efficiencies for J/ψ in $p\text{Pb}$

Table 22: Selection efficiency for J/ψ in $p\text{Pb}$.

p_{T} bin	y^* bin	ϵ_{sel}
0 < p_{T} < 1000	1.5 < y^* < 2.0	0.923 ± 0.003
0 < p_{T} < 1000	2.0 < y^* < 2.5	0.911 ± 0.002
0 < p_{T} < 1000	2.5 < y^* < 3.0	0.888 ± 0.002
0 < p_{T} < 1000	3.0 < y^* < 3.5	0.886 ± 0.002
0 < p_{T} < 1000	3.5 < y^* < 4.0	0.896 ± 0.002
1000 < p_{T} < 2000	1.5 < y^* < 2.0	0.908 ± 0.002
1000 < p_{T} < 2000	2.0 < y^* < 2.5	0.850 ± 0.002
1000 < p_{T} < 2000	2.5 < y^* < 3.0	0.839 ± 0.002
1000 < p_{T} < 2000	3.0 < y^* < 3.5	0.832 ± 0.002
1000 < p_{T} < 2000	3.5 < y^* < 4.0	0.841 ± 0.002
2000 < p_{T} < 3000	1.5 < y^* < 2.0	0.761 ± 0.003
2000 < p_{T} < 3000	2.0 < y^* < 2.5	0.740 ± 0.002
2000 < p_{T} < 3000	2.5 < y^* < 3.0	0.761 ± 0.002
2000 < p_{T} < 3000	3.0 < y^* < 3.5	0.758 ± 0.002
2000 < p_{T} < 3000	3.5 < y^* < 4.0	0.729 ± 0.003
3000 < p_{T} < 4000	1.5 < y^* < 2.0	0.660 ± 0.004
3000 < p_{T} < 4000	2.0 < y^* < 2.5	0.712 ± 0.003
3000 < p_{T} < 4000	2.5 < y^* < 3.0	0.742 ± 0.002
3000 < p_{T} < 4000	3.0 < y^* < 3.5	0.736 ± 0.003
3000 < p_{T} < 4000	3.5 < y^* < 4.0	0.713 ± 0.003
4000 < p_{T} < 5000	1.5 < y^* < 2.0	0.672 ± 0.005
4000 < p_{T} < 5000	2.0 < y^* < 2.5	0.748 ± 0.003
4000 < p_{T} < 5000	2.5 < y^* < 3.0	0.765 ± 0.003
4000 < p_{T} < 5000	3.0 < y^* < 3.5	0.761 ± 0.003
4000 < p_{T} < 5000	3.5 < y^* < 4.0	0.747 ± 0.004
5000 < p_{T} < 6000	1.5 < y^* < 2.0	0.708 ± 0.006
5000 < p_{T} < 6000	2.0 < y^* < 2.5	0.777 ± 0.004
5000 < p_{T} < 6000	2.5 < y^* < 3.0	0.785 ± 0.004
5000 < p_{T} < 6000	3.0 < y^* < 3.5	0.783 ± 0.004
5000 < p_{T} < 6000	3.5 < y^* < 4.0	0.791 ± 0.005
6000 < p_{T} < 7000	1.5 < y^* < 2.0	0.755 ± 0.007
6000 < p_{T} < 7000	2.0 < y^* < 2.5	0.805 ± 0.005
6000 < p_{T} < 7000	2.5 < y^* < 3.0	0.807 ± 0.005
6000 < p_{T} < 7000	3.0 < y^* < 3.5	0.803 ± 0.005
6000 < p_{T} < 7000	3.5 < y^* < 4.0	0.797 ± 0.006
7000 < p_{T} < 8000	1.5 < y^* < 2.0	0.769 ± 0.009
7000 < p_{T} < 8000	2.0 < y^* < 2.5	0.826 ± 0.006
7000 < p_{T} < 8000	2.5 < y^* < 3.0	0.815 ± 0.006
7000 < p_{T} < 8000	3.0 < y^* < 3.5	0.808 ± 0.007
7000 < p_{T} < 8000	3.5 < y^* < 4.0	0.818 ± 0.008
8000 < p_{T} < 9000	1.5 < y^* < 2.0	0.817 ± 0.011
8000 < p_{T} < 9000	2.0 < y^* < 2.5	0.837 ± 0.008
8000 < p_{T} < 9000	2.5 < y^* < 3.0	0.837 ± 0.008
8000 < p_{T} < 9000	3.0 < y^* < 3.5	0.824 ± 0.009
8000 < p_{T} < 9000	3.5 < y^* < 4.0	0.822 ± 0.011
9000 < p_{T} < 10000	1.5 < y^* < 2.0	0.827 ± 0.013
9000 < p_{T} < 10000	2.0 < y^* < 2.5	0.837 ± 0.010

Table 23: Selection efficiency for J/ψ in $p\text{Pb}$.

p_{T} bin	y^* bin	ϵ_{sel}
9000 < p_{T} < 10000	2.5 < y^* < 3.0	0.853 ± 0.010
9000 < p_{T} < 10000	3.0 < y^* < 3.5	0.823 ± 0.012
9000 < p_{T} < 10000	3.5 < y^* < 4.0	0.852 ± 0.014
10000 < p_{T} < 11000	1.5 < y^* < 2.0	0.837 ± 0.016
10000 < p_{T} < 11000	2.0 < y^* < 2.5	0.854 ± 0.012
10000 < p_{T} < 11000	2.5 < y^* < 3.0	0.844 ± 0.013
10000 < p_{T} < 11000	3.0 < y^* < 3.5	0.865 ± 0.014
10000 < p_{T} < 11000	3.5 < y^* < 4.0	0.867 ± 0.017
11000 < p_{T} < 12000	1.5 < y^* < 2.0	0.865 ± 0.018
11000 < p_{T} < 12000	2.0 < y^* < 2.5	0.878 ± 0.014
11000 < p_{T} < 12000	2.5 < y^* < 3.0	0.827 ± 0.017
11000 < p_{T} < 12000	3.0 < y^* < 3.5	0.888 ± 0.017
11000 < p_{T} < 12000	3.5 < y^* < 4.0	0.861 ± 0.022
12000 < p_{T} < 13000	1.5 < y^* < 2.0	0.856 ± 0.024
12000 < p_{T} < 13000	2.0 < y^* < 2.5	0.896 ± 0.016
12000 < p_{T} < 13000	2.5 < y^* < 3.0	0.846 ± 0.020
12000 < p_{T} < 13000	3.0 < y^* < 3.5	0.858 ± 0.022
12000 < p_{T} < 13000	3.5 < y^* < 4.0	0.877 ± 0.025
13000 < p_{T} < 14000	1.5 < y^* < 2.0	0.876 ± 0.025
13000 < p_{T} < 14000	2.0 < y^* < 2.5	0.876 ± 0.021
13000 < p_{T} < 14000	2.5 < y^* < 3.0	0.907 ± 0.021
13000 < p_{T} < 14000	3.0 < y^* < 3.5	0.910 ± 0.024
13000 < p_{T} < 14000	3.5 < y^* < 4.0	0.925 ± 0.025

Table 24: Selection efficiency for J/ψ in PbP.

p_T bin	y^* bin	ϵ_{sel}
0 < p_T < 1000	-3.0 < y^* < -2.5	0.917 ± 0.004
0 < p_T < 1000	-3.5 < y^* < -3.0	0.902 ± 0.003
0 < p_T < 1000	-4.0 < y^* < -3.5	0.882 ± 0.003
0 < p_T < 1000	-4.5 < y^* < -4.0	0.869 ± 0.003
0 < p_T < 1000	-5.0 < y^* < -4.5	0.889 ± 0.004
1000 < p_T < 2000	-3.0 < y^* < -2.5	0.894 ± 0.003
1000 < p_T < 2000	-3.5 < y^* < -3.0	0.838 ± 0.002
1000 < p_T < 2000	-4.0 < y^* < -3.5	0.833 ± 0.002
1000 < p_T < 2000	-4.5 < y^* < -4.0	0.822 ± 0.002
1000 < p_T < 2000	-5.0 < y^* < -4.5	0.843 ± 0.003
2000 < p_T < 3000	-3.0 < y^* < -2.5	0.741 ± 0.004
2000 < p_T < 3000	-3.5 < y^* < -3.0	0.740 ± 0.003
2000 < p_T < 3000	-4.0 < y^* < -3.5	0.766 ± 0.002
2000 < p_T < 3000	-4.5 < y^* < -4.0	0.753 ± 0.003
2000 < p_T < 3000	-5.0 < y^* < -4.5	0.733 ± 0.004
3000 < p_T < 4000	-3.0 < y^* < -2.5	0.653 ± 0.004
3000 < p_T < 4000	-3.5 < y^* < -3.0	0.718 ± 0.003
3000 < p_T < 4000	-4.0 < y^* < -3.5	0.740 ± 0.003
3000 < p_T < 4000	-4.5 < y^* < -4.0	0.738 ± 0.003
3000 < p_T < 4000	-5.0 < y^* < -4.5	0.706 ± 0.005
4000 < p_T < 5000	-3.0 < y^* < -2.5	0.671 ± 0.006
4000 < p_T < 5000	-3.5 < y^* < -3.0	0.749 ± 0.004
4000 < p_T < 5000	-4.0 < y^* < -3.5	0.771 ± 0.004
4000 < p_T < 5000	-4.5 < y^* < -4.0	0.762 ± 0.005
4000 < p_T < 5000	-5.0 < y^* < -4.5	0.743 ± 0.006
5000 < p_T < 6000	-3.0 < y^* < -2.5	0.716 ± 0.008
5000 < p_T < 6000	-3.5 < y^* < -3.0	0.784 ± 0.005
5000 < p_T < 6000	-4.0 < y^* < -3.5	0.796 ± 0.006
5000 < p_T < 6000	-4.5 < y^* < -4.0	0.794 ± 0.006
5000 < p_T < 6000	-5.0 < y^* < -4.5	0.762 ± 0.009
6000 < p_T < 7000	-3.0 < y^* < -2.5	0.774 ± 0.010
6000 < p_T < 7000	-3.5 < y^* < -3.0	0.808 ± 0.007
6000 < p_T < 7000	-4.0 < y^* < -3.5	0.806 ± 0.008
6000 < p_T < 7000	-4.5 < y^* < -4.0	0.784 ± 0.010
6000 < p_T < 7000	-5.0 < y^* < -4.5	0.807 ± 0.013
7000 < p_T < 8000	-3.0 < y^* < -2.5	0.794 ± 0.013
7000 < p_T < 8000	-3.5 < y^* < -3.0	0.820 ± 0.010
7000 < p_T < 8000	-4.0 < y^* < -3.5	0.821 ± 0.011
7000 < p_T < 8000	-4.5 < y^* < -4.0	0.835 ± 0.013
7000 < p_T < 8000	-5.0 < y^* < -4.5	0.804 ± 0.020
8000 < p_T < 9000	-3.0 < y^* < -2.5	0.809 ± 0.017
8000 < p_T < 9000	-3.5 < y^* < -3.0	0.845 ± 0.013
8000 < p_T < 9000	-4.0 < y^* < -3.5	0.826 ± 0.015
8000 < p_T < 9000	-4.5 < y^* < -4.0	0.856 ± 0.018
8000 < p_T < 9000	-5.0 < y^* < -4.5	0.859 ± 0.024

Table 25: Selection efficiency for J/ψ in PbP.

p_T bin	y^* bin	ϵ_{sel}
9000 < p_T < 10000	$-3.0 < y^* < -2.5$	0.811 ± 0.022
9000 < p_T < 10000	$-3.5 < y^* < -3.0$	0.856 ± 0.017
9000 < p_T < 10000	$-4.0 < y^* < -3.5$	0.854 ± 0.020
9000 < p_T < 10000	$-4.5 < y^* < -4.0$	0.838 ± 0.027
9000 < p_T < 10000	$-5.0 < y^* < -4.5$	0.830 ± 0.041
10000 < p_T < 11000	$-3.0 < y^* < -2.5$	0.882 ± 0.023
10000 < p_T < 11000	$-3.5 < y^* < -3.0$	0.871 ± 0.022
10000 < p_T < 11000	$-4.0 < y^* < -3.5$	0.851 ± 0.027
10000 < p_T < 11000	$-4.5 < y^* < -4.0$	0.900 ± 0.029
10000 < p_T < 11000	$-5.0 < y^* < -4.5$	0.869 ± 0.046
11000 < p_T < 12000	$-3.0 < y^* < -2.5$	0.844 ± 0.030
11000 < p_T < 12000	$-3.5 < y^* < -3.0$	0.857 ± 0.028
11000 < p_T < 12000	$-4.0 < y^* < -3.5$	0.852 ± 0.034
11000 < p_T < 12000	$-4.5 < y^* < -4.0$	0.887 ± 0.040
11000 < p_T < 12000	$-5.0 < y^* < -4.5$	0.822 ± 0.072
12000 < p_T < 13000	$-3.0 < y^* < -2.5$	0.891 ± 0.033
12000 < p_T < 13000	$-3.5 < y^* < -3.0$	0.883 ± 0.035
12000 < p_T < 13000	$-4.0 < y^* < -3.5$	0.870 ± 0.043
12000 < p_T < 13000	$-4.5 < y^* < -4.0$	0.756 ± 0.075
12000 < p_T < 13000	$-5.0 < y^* < -4.5$	0.927 ± 0.070
13000 < p_T < 14000	$-3.0 < y^* < -2.5$	0.873 ± 0.048
13000 < p_T < 14000	$-3.5 < y^* < -3.0$	0.844 ± 0.048
13000 < p_T < 14000	$-4.0 < y^* < -3.5$	1.000 ± 0.000
13000 < p_T < 14000	$-4.5 < y^* < -4.0$	0.867 ± 0.088
13000 < p_T < 14000	$-5.0 < y^* < -4.5$	0.698 ± 0.145

B.4 PID efficiencies

B.4.1 PID efficiencies for J/ψ in $p\text{Pb}$

Table 26: PID efficiency for J/ψ in $p\text{Pb}$.

p_{T} bin	y^* bin	ϵ_{PID}
0 < p_{T} < 1000	1.5 < y^* < 2.0	0.692 ± 0.018
0 < p_{T} < 1000	2.0 < y^* < 2.5	0.767 ± 0.021
0 < p_{T} < 1000	2.5 < y^* < 3.0	0.776 ± 0.016
0 < p_{T} < 1000	3.0 < y^* < 3.5	0.723 ± 0.016
0 < p_{T} < 1000	3.5 < y^* < 4.0	0.603 ± 0.022
1000 < p_{T} < 2000	1.5 < y^* < 2.0	0.716 ± 0.015
1000 < p_{T} < 2000	2.0 < y^* < 2.5	0.779 ± 0.020
1000 < p_{T} < 2000	2.5 < y^* < 3.0	0.785 ± 0.017
1000 < p_{T} < 2000	3.0 < y^* < 3.5	0.733 ± 0.016
1000 < p_{T} < 2000	3.5 < y^* < 4.0	0.592 ± 0.026
2000 < p_{T} < 3000	1.5 < y^* < 2.0	0.756 ± 0.022
2000 < p_{T} < 3000	2.0 < y^* < 2.5	0.804 ± 0.017
2000 < p_{T} < 3000	2.5 < y^* < 3.0	0.796 ± 0.018
2000 < p_{T} < 3000	3.0 < y^* < 3.5	0.742 ± 0.015
2000 < p_{T} < 3000	3.5 < y^* < 4.0	0.587 ± 0.018
3000 < p_{T} < 4000	1.5 < y^* < 2.0	0.803 ± 0.030
3000 < p_{T} < 4000	2.0 < y^* < 2.5	0.835 ± 0.017
3000 < p_{T} < 4000	2.5 < y^* < 3.0	0.828 ± 0.017
3000 < p_{T} < 4000	3.0 < y^* < 3.5	0.763 ± 0.016
3000 < p_{T} < 4000	3.5 < y^* < 4.0	0.578 ± 0.014
4000 < p_{T} < 5000	1.5 < y^* < 2.0	0.843 ± 0.036
4000 < p_{T} < 5000	2.0 < y^* < 2.5	0.866 ± 0.018
4000 < p_{T} < 5000	2.5 < y^* < 3.0	0.857 ± 0.018
4000 < p_{T} < 5000	3.0 < y^* < 3.5	0.788 ± 0.017
4000 < p_{T} < 5000	3.5 < y^* < 4.0	0.584 ± 0.013
5000 < p_{T} < 6000	1.5 < y^* < 2.0	0.873 ± 0.038
5000 < p_{T} < 6000	2.0 < y^* < 2.5	0.889 ± 0.018
5000 < p_{T} < 6000	2.5 < y^* < 3.0	0.877 ± 0.019
5000 < p_{T} < 6000	3.0 < y^* < 3.5	0.811 ± 0.017
5000 < p_{T} < 6000	3.5 < y^* < 4.0	0.594 ± 0.018
6000 < p_{T} < 7000	1.5 < y^* < 2.0	0.888 ± 0.035
6000 < p_{T} < 7000	2.0 < y^* < 2.5	0.902 ± 0.019
6000 < p_{T} < 7000	2.5 < y^* < 3.0	0.891 ± 0.019
6000 < p_{T} < 7000	3.0 < y^* < 3.5	0.829 ± 0.017
6000 < p_{T} < 7000	3.5 < y^* < 4.0	0.607 ± 0.024
7000 < p_{T} < 8000	1.5 < y^* < 2.0	0.903 ± 0.033
7000 < p_{T} < 8000	2.0 < y^* < 2.5	0.914 ± 0.019
7000 < p_{T} < 8000	2.5 < y^* < 3.0	0.903 ± 0.019
7000 < p_{T} < 8000	3.0 < y^* < 3.5	0.843 ± 0.017
7000 < p_{T} < 8000	3.5 < y^* < 4.0	0.626 ± 0.035
8000 < p_{T} < 9000	1.5 < y^* < 2.0	0.918 ± 0.032
8000 < p_{T} < 9000	2.0 < y^* < 2.5	0.923 ± 0.019
8000 < p_{T} < 9000	2.5 < y^* < 3.0	0.909 ± 0.019
8000 < p_{T} < 9000	3.0 < y^* < 3.5	0.856 ± 0.017
8000 < p_{T} < 9000	3.5 < y^* < 4.0	0.642 ± 0.037
9000 < p_{T} < 10000	1.5 < y^* < 2.0	0.926 ± 0.030
9000 < p_{T} < 10000	2.0 < y^* < 2.5	0.927 ± 0.019

Table 27: PID efficiency for J/ψ in $p\text{Pb}$.

p_{T} bin	y^* bin	ϵ_{PID}
9000 < p_{T} < 10000	2.5 < y^* < 3.0	0.913 ± 0.019
9000 < p_{T} < 10000	3.0 < y^* < 3.5	0.863 ± 0.018
9000 < p_{T} < 10000	3.5 < y^* < 4.0	0.655 ± 0.042
10000 < p_{T} < 11000	1.5 < y^* < 2.0	0.925 ± 0.026
10000 < p_{T} < 11000	2.0 < y^* < 2.5	0.928 ± 0.019
10000 < p_{T} < 11000	2.5 < y^* < 3.0	0.919 ± 0.019
10000 < p_{T} < 11000	3.0 < y^* < 3.5	0.867 ± 0.019
10000 < p_{T} < 11000	3.5 < y^* < 4.0	0.666 ± 0.061
11000 < p_{T} < 12000	1.5 < y^* < 2.0	0.937 ± 0.025
11000 < p_{T} < 12000	2.0 < y^* < 2.5	0.927 ± 0.019
11000 < p_{T} < 12000	2.5 < y^* < 3.0	0.926 ± 0.019
11000 < p_{T} < 12000	3.0 < y^* < 3.5	0.871 ± 0.019
11000 < p_{T} < 12000	3.5 < y^* < 4.0	0.644 ± 0.020
12000 < p_{T} < 13000	1.5 < y^* < 2.0	0.939 ± 0.025
12000 < p_{T} < 13000	2.0 < y^* < 2.5	0.934 ± 0.019
12000 < p_{T} < 13000	2.5 < y^* < 3.0	0.922 ± 0.019
12000 < p_{T} < 13000	3.0 < y^* < 3.5	0.895 ± 0.019
12000 < p_{T} < 13000	3.5 < y^* < 4.0	0.702 ± 0.076
13000 < p_{T} < 14000	1.5 < y^* < 2.0	0.942 ± 0.025
13000 < p_{T} < 14000	2.0 < y^* < 2.5	0.939 ± 0.019
13000 < p_{T} < 14000	2.5 < y^* < 3.0	0.930 ± 0.019
13000 < p_{T} < 14000	3.0 < y^* < 3.5	0.889 ± 0.019
13000 < p_{T} < 14000	3.5 < y^* < 4.0	0.668 ± 0.016

Table 28: PID efficiency for J/ψ in Pb p .

p_T bin	y^* bin	ϵ_{PID}
0 < p_T < 1000	-3.0 < y^* < -2.5	0.669 ± 0.016
0 < p_T < 1000	-3.5 < y^* < -3.0	0.727 ± 0.020
0 < p_T < 1000	-4.0 < y^* < -3.5	0.733 ± 0.017
0 < p_T < 1000	-4.5 < y^* < -4.0	0.679 ± 0.017
0 < p_T < 1000	-5.0 < y^* < -4.5	0.565 ± 0.023
1000 < p_T < 2000	-3.0 < y^* < -2.5	0.690 ± 0.015
1000 < p_T < 2000	-3.5 < y^* < -3.0	0.739 ± 0.020
1000 < p_T < 2000	-4.0 < y^* < -3.5	0.741 ± 0.017
1000 < p_T < 2000	-4.5 < y^* < -4.0	0.686 ± 0.018
1000 < p_T < 2000	-5.0 < y^* < -4.5	0.547 ± 0.027
2000 < p_T < 3000	-3.0 < y^* < -2.5	0.730 ± 0.024
2000 < p_T < 3000	-3.5 < y^* < -3.0	0.768 ± 0.017
2000 < p_T < 3000	-4.0 < y^* < -3.5	0.757 ± 0.018
2000 < p_T < 3000	-4.5 < y^* < -4.0	0.697 ± 0.017
2000 < p_T < 3000	-5.0 < y^* < -4.5	0.543 ± 0.020
3000 < p_T < 4000	-3.0 < y^* < -2.5	0.781 ± 0.031
3000 < p_T < 4000	-3.5 < y^* < -3.0	0.806 ± 0.018
3000 < p_T < 4000	-4.0 < y^* < -3.5	0.795 ± 0.018
3000 < p_T < 4000	-4.5 < y^* < -4.0	0.718 ± 0.016
3000 < p_T < 4000	-5.0 < y^* < -4.5	0.538 ± 0.017
4000 < p_T < 5000	-3.0 < y^* < -2.5	0.822 ± 0.035
4000 < p_T < 5000	-3.5 < y^* < -3.0	0.841 ± 0.019
4000 < p_T < 5000	-4.0 < y^* < -3.5	0.828 ± 0.019
4000 < p_T < 5000	-4.5 < y^* < -4.0	0.753 ± 0.019
4000 < p_T < 5000	-5.0 < y^* < -4.5	0.542 ± 0.014
5000 < p_T < 6000	-3.0 < y^* < -2.5	0.853 ± 0.037
5000 < p_T < 6000	-3.5 < y^* < -3.0	0.867 ± 0.019
5000 < p_T < 6000	-4.0 < y^* < -3.5	0.853 ± 0.022
5000 < p_T < 6000	-4.5 < y^* < -4.0	0.779 ± 0.019
5000 < p_T < 6000	-5.0 < y^* < -4.5	0.545 ± 0.016
6000 < p_T < 7000	-3.0 < y^* < -2.5	0.879 ± 0.038
6000 < p_T < 7000	-3.5 < y^* < -3.0	0.883 ± 0.019
6000 < p_T < 7000	-4.0 < y^* < -3.5	0.870 ± 0.023
6000 < p_T < 7000	-4.5 < y^* < -4.0	0.801 ± 0.021
6000 < p_T < 7000	-5.0 < y^* < -4.5	0.569 ± 0.029
7000 < p_T < 8000	-3.0 < y^* < -2.5	0.892 ± 0.036
7000 < p_T < 8000	-3.5 < y^* < -3.0	0.897 ± 0.020
7000 < p_T < 8000	-4.0 < y^* < -3.5	0.887 ± 0.023
7000 < p_T < 8000	-4.5 < y^* < -4.0	0.813 ± 0.021
7000 < p_T < 8000	-5.0 < y^* < -4.5	0.563 ± 0.027
8000 < p_T < 9000	-3.0 < y^* < -2.5	0.907 ± 0.034
8000 < p_T < 9000	-3.5 < y^* < -3.0	0.902 ± 0.020
8000 < p_T < 9000	-4.0 < y^* < -3.5	0.895 ± 0.025
8000 < p_T < 9000	-4.5 < y^* < -4.0	0.827 ± 0.021
8000 < p_T < 9000	-5.0 < y^* < -4.5	0.583 ± 0.039

Table 29: PID efficiency for J/ψ in Pbp.

p_T bin	y^* bin	ϵ_{PID}
9000 < p_T < 10000	$-3.0 < y^* < -2.5$	0.914 ± 0.034
9000 < p_T < 10000	$-3.5 < y^* < -3.0$	0.908 ± 0.020
9000 < p_T < 10000	$-4.0 < y^* < -3.5$	0.896 ± 0.022
9000 < p_T < 10000	$-4.5 < y^* < -4.0$	0.839 ± 0.023
9000 < p_T < 10000	$-5.0 < y^* < -4.5$	0.626 ± 0.021
10000 < p_T < 11000	$-3.0 < y^* < -2.5$	0.916 ± 0.033
10000 < p_T < 11000	$-3.5 < y^* < -3.0$	0.918 ± 0.020
10000 < p_T < 11000	$-4.0 < y^* < -3.5$	0.913 ± 0.022
10000 < p_T < 11000	$-4.5 < y^* < -4.0$	0.855 ± 0.020
10000 < p_T < 11000	$-5.0 < y^* < -4.5$	0.660 ± 0.072
11000 < p_T < 12000	$-3.0 < y^* < -2.5$	0.913 ± 0.027
11000 < p_T < 12000	$-3.5 < y^* < -3.0$	0.927 ± 0.020
11000 < p_T < 12000	$-4.0 < y^* < -3.5$	0.911 ± 0.025
11000 < p_T < 12000	$-4.5 < y^* < -4.0$	0.866 ± 0.021
11000 < p_T < 12000	$-5.0 < y^* < -4.5$	0.658 ± 0.036
12000 < p_T < 13000	$-3.0 < y^* < -2.5$	0.907 ± 0.029
12000 < p_T < 13000	$-3.5 < y^* < -3.0$	0.923 ± 0.020
12000 < p_T < 13000	$-4.0 < y^* < -3.5$	0.900 ± 0.021
12000 < p_T < 13000	$-4.5 < y^* < -4.0$	0.865 ± 0.023
12000 < p_T < 13000	$-5.0 < y^* < -4.5$	0.689 ± 0.052
13000 < p_T < 14000	$-3.0 < y^* < -2.5$	0.909 ± 0.025
13000 < p_T < 14000	$-3.5 < y^* < -3.0$	0.931 ± 0.021
13000 < p_T < 14000	$-4.0 < y^* < -3.5$	0.909 ± 0.023
13000 < p_T < 14000	$-4.5 < y^* < -4.0$	0.908 ± 0.041
13000 < p_T < 14000	$-5.0 < y^* < -4.5$	0.675 ± 0.095

747 B.5 Trigger efficiencies

748 B.5.1 Trigger efficiencies for J/ψ in $p\text{Pb}$

Table 30: Trigger efficiency for J/ψ in $p\text{Pb}$.

p_{T} bin	y^* bin	ϵ_{tri}
$0 < p_{\text{T}} < 1000$	$1.5 < y^* < 2.0$	0.671 ± 0.006
$0 < p_{\text{T}} < 1000$	$2.0 < y^* < 2.5$	0.738 ± 0.003
$0 < p_{\text{T}} < 1000$	$2.5 < y^* < 3.0$	0.787 ± 0.003
$0 < p_{\text{T}} < 1000$	$3.0 < y^* < 3.5$	0.839 ± 0.003
$0 < p_{\text{T}} < 1000$	$3.5 < y^* < 4.0$	0.842 ± 0.004
$1000 < p_{\text{T}} < 2000$	$1.5 < y^* < 2.0$	0.739 ± 0.004
$1000 < p_{\text{T}} < 2000$	$2.0 < y^* < 2.5$	0.798 ± 0.002
$1000 < p_{\text{T}} < 2000$	$2.5 < y^* < 3.0$	0.820 ± 0.002
$1000 < p_{\text{T}} < 2000$	$3.0 < y^* < 3.5$	0.847 ± 0.002
$1000 < p_{\text{T}} < 2000$	$3.5 < y^* < 4.0$	0.861 ± 0.003
$2000 < p_{\text{T}} < 3000$	$1.5 < y^* < 2.0$	0.795 ± 0.004
$2000 < p_{\text{T}} < 3000$	$2.0 < y^* < 2.5$	0.827 ± 0.002
$2000 < p_{\text{T}} < 3000$	$2.5 < y^* < 3.0$	0.839 ± 0.002
$2000 < p_{\text{T}} < 3000$	$3.0 < y^* < 3.5$	0.861 ± 0.002
$2000 < p_{\text{T}} < 3000$	$3.5 < y^* < 4.0$	0.873 ± 0.003
$3000 < p_{\text{T}} < 4000$	$1.5 < y^* < 2.0$	0.825 ± 0.005
$3000 < p_{\text{T}} < 4000$	$2.0 < y^* < 2.5$	0.852 ± 0.003
$3000 < p_{\text{T}} < 4000$	$2.5 < y^* < 3.0$	0.868 ± 0.002
$3000 < p_{\text{T}} < 4000$	$3.0 < y^* < 3.5$	0.873 ± 0.003
$3000 < p_{\text{T}} < 4000$	$3.5 < y^* < 4.0$	0.875 ± 0.004
$4000 < p_{\text{T}} < 5000$	$1.5 < y^* < 2.0$	0.850 ± 0.005
$4000 < p_{\text{T}} < 5000$	$2.0 < y^* < 2.5$	0.871 ± 0.003
$4000 < p_{\text{T}} < 5000$	$2.5 < y^* < 3.0$	0.881 ± 0.003
$4000 < p_{\text{T}} < 5000$	$3.0 < y^* < 3.5$	0.887 ± 0.003
$4000 < p_{\text{T}} < 5000$	$3.5 < y^* < 4.0$	0.881 ± 0.004
$5000 < p_{\text{T}} < 6000$	$1.5 < y^* < 2.0$	0.863 ± 0.006
$5000 < p_{\text{T}} < 6000$	$2.0 < y^* < 2.5$	0.880 ± 0.004
$5000 < p_{\text{T}} < 6000$	$2.5 < y^* < 3.0$	0.888 ± 0.003
$5000 < p_{\text{T}} < 6000$	$3.0 < y^* < 3.5$	0.897 ± 0.004
$5000 < p_{\text{T}} < 6000$	$3.5 < y^* < 4.0$	0.892 ± 0.005
$6000 < p_{\text{T}} < 7000$	$1.5 < y^* < 2.0$	0.878 ± 0.007
$6000 < p_{\text{T}} < 7000$	$2.0 < y^* < 2.5$	0.882 ± 0.004
$6000 < p_{\text{T}} < 7000$	$2.5 < y^* < 3.0$	0.896 ± 0.004
$6000 < p_{\text{T}} < 7000$	$3.0 < y^* < 3.5$	0.904 ± 0.005
$6000 < p_{\text{T}} < 7000$	$3.5 < y^* < 4.0$	0.891 ± 0.007
$7000 < p_{\text{T}} < 8000$	$1.5 < y^* < 2.0$	0.873 ± 0.008
$7000 < p_{\text{T}} < 8000$	$2.0 < y^* < 2.5$	0.894 ± 0.005
$7000 < p_{\text{T}} < 8000$	$2.5 < y^* < 3.0$	0.892 ± 0.006
$7000 < p_{\text{T}} < 8000$	$3.0 < y^* < 3.5$	0.899 ± 0.006
$7000 < p_{\text{T}} < 8000$	$3.5 < y^* < 4.0$	0.897 ± 0.009
$8000 < p_{\text{T}} < 9000$	$1.5 < y^* < 2.0$	0.883 ± 0.010
$8000 < p_{\text{T}} < 9000$	$2.0 < y^* < 2.5$	0.895 ± 0.007
$8000 < p_{\text{T}} < 9000$	$2.5 < y^* < 3.0$	0.893 ± 0.007
$8000 < p_{\text{T}} < 9000$	$3.0 < y^* < 3.5$	0.907 ± 0.008
$8000 < p_{\text{T}} < 9000$	$3.5 < y^* < 4.0$	0.890 ± 0.012
$9000 < p_{\text{T}} < 10000$	$1.5 < y^* < 2.0$	0.878 ± 0.013
$9000 < p_{\text{T}} < 10000$	$2.0 < y^* < 2.5$	0.900 ± 0.009

Table 31: Trigger efficiency for J/ψ in $p\text{Pb}$.

p_{T} bin	y^* bin	ϵ_{tri}
9000 < p_{T} < 10000	2.5 < y^* < 3.0	0.892 ± 0.010
9000 < p_{T} < 10000	3.0 < y^* < 3.5	0.893 ± 0.011
9000 < p_{T} < 10000	3.5 < y^* < 4.0	0.907 ± 0.015
10000 < p_{T} < 11000	1.5 < y^* < 2.0	0.907 ± 0.014
10000 < p_{T} < 11000	2.0 < y^* < 2.5	0.898 ± 0.011
10000 < p_{T} < 11000	2.5 < y^* < 3.0	0.893 ± 0.012
10000 < p_{T} < 11000	3.0 < y^* < 3.5	0.920 ± 0.013
10000 < p_{T} < 11000	3.5 < y^* < 4.0	0.917 ± 0.017
11000 < p_{T} < 12000	1.5 < y^* < 2.0	0.887 ± 0.018
11000 < p_{T} < 12000	2.0 < y^* < 2.5	0.868 ± 0.016
11000 < p_{T} < 12000	2.5 < y^* < 3.0	0.891 ± 0.016
11000 < p_{T} < 12000	3.0 < y^* < 3.5	0.893 ± 0.018
11000 < p_{T} < 12000	3.5 < y^* < 4.0	0.928 ± 0.021
12000 < p_{T} < 13000	1.5 < y^* < 2.0	0.893 ± 0.023
12000 < p_{T} < 13000	2.0 < y^* < 2.5	0.916 ± 0.016
12000 < p_{T} < 13000	2.5 < y^* < 3.0	0.904 ± 0.018
12000 < p_{T} < 13000	3.0 < y^* < 3.5	0.881 ± 0.023
12000 < p_{T} < 13000	3.5 < y^* < 4.0	0.955 ± 0.020
13000 < p_{T} < 14000	1.5 < y^* < 2.0	0.873 ± 0.027
13000 < p_{T} < 14000	2.0 < y^* < 2.5	0.898 ± 0.021
13000 < p_{T} < 14000	2.5 < y^* < 3.0	0.888 ± 0.024
13000 < p_{T} < 14000	3.0 < y^* < 3.5	0.945 ± 0.020
13000 < p_{T} < 14000	3.5 < y^* < 4.0	0.904 ± 0.034

Table 32: Trigger efficiency for J/ψ in PbP.

	p_T bin	y^* bin	ϵ_{tri}
0	$< p_T < 1000$	$-3.0 < y^* < -2.5$	0.713 ± 0.007
0	$< p_T < 1000$	$-3.5 < y^* < -3.0$	0.758 ± 0.005
0	$< p_T < 1000$	$-4.0 < y^* < -3.5$	0.799 ± 0.004
0	$< p_T < 1000$	$-4.5 < y^* < -4.0$	0.840 ± 0.004
0	$< p_T < 1000$	$-5.0 < y^* < -4.5$	0.830 ± 0.007
1000	$< p_T < 2000$	$-3.0 < y^* < -2.5$	0.753 ± 0.004
1000	$< p_T < 2000$	$-3.5 < y^* < -3.0$	0.801 ± 0.003
1000	$< p_T < 2000$	$-4.0 < y^* < -3.5$	0.830 ± 0.003
1000	$< p_T < 2000$	$-4.5 < y^* < -4.0$	0.842 ± 0.003
1000	$< p_T < 2000$	$-5.0 < y^* < -4.5$	0.852 ± 0.004
2000	$< p_T < 3000$	$-3.0 < y^* < -2.5$	0.794 ± 0.004
2000	$< p_T < 3000$	$-3.5 < y^* < -3.0$	0.834 ± 0.003
2000	$< p_T < 3000$	$-4.0 < y^* < -3.5$	0.851 ± 0.002
2000	$< p_T < 3000$	$-4.5 < y^* < -4.0$	0.858 ± 0.003
2000	$< p_T < 3000$	$-5.0 < y^* < -4.5$	0.858 ± 0.005
3000	$< p_T < 4000$	$-3.0 < y^* < -2.5$	0.837 ± 0.005
3000	$< p_T < 4000$	$-3.5 < y^* < -3.0$	0.858 ± 0.003
3000	$< p_T < 4000$	$-4.0 < y^* < -3.5$	0.872 ± 0.003
3000	$< p_T < 4000$	$-4.5 < y^* < -4.0$	0.878 ± 0.003
3000	$< p_T < 4000$	$-5.0 < y^* < -4.5$	0.862 ± 0.006
4000	$< p_T < 5000$	$-3.0 < y^* < -2.5$	0.860 ± 0.006
4000	$< p_T < 5000$	$-3.5 < y^* < -3.0$	0.872 ± 0.004
4000	$< p_T < 5000$	$-4.0 < y^* < -3.5$	0.875 ± 0.004
4000	$< p_T < 5000$	$-4.5 < y^* < -4.0$	0.894 ± 0.004
4000	$< p_T < 5000$	$-5.0 < y^* < -4.5$	0.866 ± 0.008
5000	$< p_T < 6000$	$-3.0 < y^* < -2.5$	0.871 ± 0.007
5000	$< p_T < 6000$	$-3.5 < y^* < -3.0$	0.886 ± 0.005
5000	$< p_T < 6000$	$-4.0 < y^* < -3.5$	0.897 ± 0.005
5000	$< p_T < 6000$	$-4.5 < y^* < -4.0$	0.893 ± 0.006
5000	$< p_T < 6000$	$-5.0 < y^* < -4.5$	0.884 ± 0.010
6000	$< p_T < 7000$	$-3.0 < y^* < -2.5$	0.873 ± 0.009
6000	$< p_T < 7000$	$-3.5 < y^* < -3.0$	0.889 ± 0.007
6000	$< p_T < 7000$	$-4.0 < y^* < -3.5$	0.879 ± 0.007
6000	$< p_T < 7000$	$-4.5 < y^* < -4.0$	0.885 ± 0.009
6000	$< p_T < 7000$	$-5.0 < y^* < -4.5$	0.861 ± 0.016
7000	$< p_T < 8000$	$-3.0 < y^* < -2.5$	0.892 ± 0.011
7000	$< p_T < 8000$	$-3.5 < y^* < -3.0$	0.899 ± 0.009
7000	$< p_T < 8000$	$-4.0 < y^* < -3.5$	0.895 ± 0.010
7000	$< p_T < 8000$	$-4.5 < y^* < -4.0$	0.878 ± 0.013
7000	$< p_T < 8000$	$-5.0 < y^* < -4.5$	0.915 ± 0.020
8000	$< p_T < 9000$	$-3.0 < y^* < -2.5$	0.864 ± 0.016
8000	$< p_T < 9000$	$-3.5 < y^* < -3.0$	0.887 ± 0.013
8000	$< p_T < 9000$	$-4.0 < y^* < -3.5$	0.900 ± 0.013
8000	$< p_T < 9000$	$-4.5 < y^* < -4.0$	0.903 ± 0.017
8000	$< p_T < 9000$	$-5.0 < y^* < -4.5$	0.923 ± 0.025

Table 33: Trigger efficiency for J/ψ in PbP.

p_T bin	y^* bin	ϵ_{tri}
9000 < p_T < 10000	$-3.0 < y^* < -2.5$	0.859 ± 0.022
9000 < p_T < 10000	$-3.5 < y^* < -3.0$	0.899 ± 0.016
9000 < p_T < 10000	$-4.0 < y^* < -3.5$	0.906 ± 0.018
9000 < p_T < 10000	$-4.5 < y^* < -4.0$	0.904 ± 0.025
9000 < p_T < 10000	$-5.0 < y^* < -4.5$	0.894 ± 0.045
10000 < p_T < 11000	$-3.0 < y^* < -2.5$	0.897 ± 0.024
10000 < p_T < 11000	$-3.5 < y^* < -3.0$	0.900 ± 0.021
10000 < p_T < 11000	$-4.0 < y^* < -3.5$	0.891 ± 0.026
10000 < p_T < 11000	$-4.5 < y^* < -4.0$	0.933 ± 0.027
10000 < p_T < 11000	$-5.0 < y^* < -4.5$	0.889 ± 0.052
11000 < p_T < 12000	$-3.0 < y^* < -2.5$	0.866 ± 0.032
11000 < p_T < 12000	$-3.5 < y^* < -3.0$	0.913 ± 0.024
11000 < p_T < 12000	$-4.0 < y^* < -3.5$	0.848 ± 0.037
11000 < p_T < 12000	$-4.5 < y^* < -4.0$	0.887 ± 0.044
11000 < p_T < 12000	$-5.0 < y^* < -4.5$	0.867 ± 0.088
12000 < p_T < 13000	$-3.0 < y^* < -2.5$	0.870 ± 0.038
12000 < p_T < 13000	$-3.5 < y^* < -3.0$	0.842 ± 0.042
12000 < p_T < 13000	$-4.0 < y^* < -3.5$	0.923 ± 0.037
12000 < p_T < 13000	$-4.5 < y^* < -4.0$	0.917 ± 0.056
12000 < p_T < 13000	$-5.0 < y^* < -4.5$	0.714 ± 0.171
13000 < p_T < 14000	$-3.0 < y^* < -2.5$	0.947 ± 0.036
13000 < p_T < 14000	$-3.5 < y^* < -3.0$	0.939 ± 0.034
13000 < p_T < 14000	$-4.0 < y^* < -3.5$	0.850 ± 0.080
13000 < p_T < 14000	$-4.5 < y^* < -4.0$	0.769 ± 0.117
13000 < p_T < 14000	$-5.0 < y^* < -4.5$	1.000 ± 0.000

B.5.3 Total efficiencies for J/ψ in $p\text{Pb}$

Table 34: Total efficiency for J/ψ in $p\text{Pb}$, with total, correlated and uncorrelated uncertainties.

	p_T bin	y^* bin	ϵ_{tot}
0	$< p_T < 1000$	$1.5 < y^* < 2.0$	0.072 ± 0.010 (0.010, 0.001)
0	$< p_T < 1000$	$2.0 < y^* < 2.5$	0.286 ± 0.025 (0.025, 0.002)
0	$< p_T < 1000$	$2.5 < y^* < 3.0$	0.404 ± 0.024 (0.024, 0.002)
0	$< p_T < 1000$	$3.0 < y^* < 3.5$	0.393 ± 0.021 (0.020, 0.002)
0	$< p_T < 1000$	$3.5 < y^* < 4.0$	0.235 ± 0.013 (0.012, 0.002)
1000	$< p_T < 2000$	$1.5 < y^* < 2.0$	0.091 ± 0.007 (0.007, 0.001)
1000	$< p_T < 2000$	$2.0 < y^* < 2.5$	0.303 ± 0.017 (0.017, 0.001)
1000	$< p_T < 2000$	$2.5 < y^* < 3.0$	0.392 ± 0.031 (0.031, 0.002)
1000	$< p_T < 2000$	$3.0 < y^* < 3.5$	0.368 ± 0.016 (0.016, 0.002)
1000	$< p_T < 2000$	$3.5 < y^* < 4.0$	0.229 ± 0.014 (0.014, 0.001)
2000	$< p_T < 3000$	$1.5 < y^* < 2.0$	0.100 ± 0.007 (0.007, 0.001)
2000	$< p_T < 3000$	$2.0 < y^* < 2.5$	0.298 ± 0.016 (0.016, 0.002)
2000	$< p_T < 3000$	$2.5 < y^* < 3.0$	0.380 ± 0.018 (0.018, 0.002)
2000	$< p_T < 3000$	$3.0 < y^* < 3.5$	0.356 ± 0.016 (0.016, 0.002)
2000	$< p_T < 3000$	$3.5 < y^* < 4.0$	0.211 ± 0.013 (0.013, 0.001)
3000	$< p_T < 4000$	$1.5 < y^* < 2.0$	0.108 ± 0.009 (0.009, 0.001)
3000	$< p_T < 4000$	$2.0 < y^* < 2.5$	0.332 ± 0.021 (0.021, 0.002)
3000	$< p_T < 4000$	$2.5 < y^* < 3.0$	0.417 ± 0.025 (0.025, 0.002)
3000	$< p_T < 4000$	$3.0 < y^* < 3.5$	0.377 ± 0.021 (0.021, 0.002)
3000	$< p_T < 4000$	$3.5 < y^* < 4.0$	0.224 ± 0.016 (0.016, 0.002)
4000	$< p_T < 5000$	$1.5 < y^* < 2.0$	0.137 ± 0.011 (0.011, 0.002)
4000	$< p_T < 5000$	$2.0 < y^* < 2.5$	0.394 ± 0.022 (0.022, 0.003)
4000	$< p_T < 5000$	$2.5 < y^* < 3.0$	0.468 ± 0.024 (0.024, 0.003)
4000	$< p_T < 5000$	$3.0 < y^* < 3.5$	0.425 ± 0.022 (0.022, 0.003)
4000	$< p_T < 5000$	$3.5 < y^* < 4.0$	0.259 ± 0.017 (0.017, 0.003)
5000	$< p_T < 6000$	$1.5 < y^* < 2.0$	0.166 ± 0.012 (0.012, 0.003)
5000	$< p_T < 6000$	$2.0 < y^* < 2.5$	0.450 ± 0.024 (0.024, 0.004)
5000	$< p_T < 6000$	$2.5 < y^* < 3.0$	0.513 ± 0.026 (0.026, 0.004)
5000	$< p_T < 6000$	$3.0 < y^* < 3.5$	0.468 ± 0.026 (0.026, 0.004)
5000	$< p_T < 6000$	$3.5 < y^* < 4.0$	0.295 ± 0.021 (0.021, 0.003)
6000	$< p_T < 7000$	$1.5 < y^* < 2.0$	0.203 ± 0.015 (0.015, 0.004)
6000	$< p_T < 7000$	$2.0 < y^* < 2.5$	0.495 ± 0.031 (0.030, 0.005)
6000	$< p_T < 7000$	$2.5 < y^* < 3.0$	0.551 ± 0.034 (0.034, 0.006)
6000	$< p_T < 7000$	$3.0 < y^* < 3.5$	0.502 ± 0.031 (0.031, 0.006)
6000	$< p_T < 7000$	$3.5 < y^* < 4.0$	0.321 ± 0.025 (0.025, 0.005)
7000	$< p_T < 8000$	$1.5 < y^* < 2.0$	0.227 ± 0.016 (0.015, 0.005)
7000	$< p_T < 8000$	$2.0 < y^* < 2.5$	0.548 ± 0.029 (0.028, 0.007)
7000	$< p_T < 8000$	$2.5 < y^* < 3.0$	0.570 ± 0.031 (0.030, 0.007)
7000	$< p_T < 8000$	$3.0 < y^* < 3.5$	0.510 ± 0.032 (0.031, 0.008)
7000	$< p_T < 8000$	$3.5 < y^* < 4.0$	0.349 ± 0.032 (0.031, 0.007)
8000	$< p_T < 9000$	$1.5 < y^* < 2.0$	0.271 ± 0.017 (0.016, 0.007)
8000	$< p_T < 9000$	$2.0 < y^* < 2.5$	0.575 ± 0.030 (0.028, 0.009)
8000	$< p_T < 9000$	$2.5 < y^* < 3.0$	0.591 ± 0.032 (0.031, 0.010)
8000	$< p_T < 9000$	$3.0 < y^* < 3.5$	0.553 ± 0.035 (0.033, 0.010)
8000	$< p_T < 9000$	$3.5 < y^* < 4.0$	0.372 ± 0.037 (0.036, 0.010)
9000	$< p_T < 10000$	$1.5 < y^* < 2.0$	0.282 ± 0.019 (0.017, 0.010)
9000	$< p_T < 10000$	$2.0 < y^* < 2.5$	0.587 ± 0.031 (0.029, 0.012)

Table 35: Total efficiency for J/ψ in $p\text{Pb}$, with total, correlated and uncorrelated uncertainties.

p_T bin	y^* bin	ϵ_{tot}
9000 < p_T < 10000	2.5 < y^* < 3.0	0.620 ± 0.037 (0.035, 0.013)
9000 < p_T < 10000	3.0 < y^* < 3.5	0.556 ± 0.039 (0.036, 0.014)
9000 < p_T < 10000	3.5 < y^* < 4.0	0.400 ± 0.043 (0.041, 0.013)
10000 < p_T < 11000	1.5 < y^* < 2.0	0.310 ± 0.020 (0.016, 0.012)
10000 < p_T < 11000	2.0 < y^* < 2.5	0.622 ± 0.034 (0.031, 0.015)
10000 < p_T < 11000	2.5 < y^* < 3.0	0.621 ± 0.036 (0.032, 0.017)
10000 < p_T < 11000	3.0 < y^* < 3.5	0.605 ± 0.044 (0.041, 0.018)
10000 < p_T < 11000	3.5 < y^* < 4.0	0.439 ± 0.056 (0.054, 0.017)
11000 < p_T < 12000	1.5 < y^* < 2.0	0.337 ± 0.023 (0.017, 0.016)
11000 < p_T < 12000	2.0 < y^* < 2.5	0.623 ± 0.036 (0.030, 0.020)
11000 < p_T < 12000	2.5 < y^* < 3.0	0.613 ± 0.040 (0.033, 0.022)
11000 < p_T < 12000	3.0 < y^* < 3.5	0.619 ± 0.049 (0.043, 0.024)
11000 < p_T < 12000	3.5 < y^* < 4.0	0.401 ± 0.040 (0.035, 0.020)
12000 < p_T < 13000	1.5 < y^* < 2.0	0.352 ± 0.029 (0.020, 0.021)
12000 < p_T < 13000	2.0 < y^* < 2.5	0.655 ± 0.043 (0.036, 0.023)
12000 < p_T < 13000	2.5 < y^* < 3.0	0.640 ± 0.045 (0.036, 0.026)
12000 < p_T < 13000	3.0 < y^* < 3.5	0.613 ± 0.054 (0.045, 0.030)
12000 < p_T < 13000	3.5 < y^* < 4.0	0.499 ± 0.073 (0.069, 0.025)
13000 < p_T < 14000	1.5 < y^* < 2.0	0.386 ± 0.032 (0.019, 0.026)
13000 < p_T < 14000	2.0 < y^* < 2.5	0.678 ± 0.045 (0.034, 0.029)
13000 < p_T < 14000	2.5 < y^* < 3.0	0.642 ± 0.047 (0.032, 0.034)
13000 < p_T < 14000	3.0 < y^* < 3.5	0.740 ± 0.062 (0.054, 0.032)
13000 < p_T < 14000	3.5 < y^* < 4.0	0.483 ± 0.053 (0.041, 0.034)

Table 36: Total efficiency for J/ψ in PbP, with total, correlated and uncorrelated uncertainties.

p_T bin	y^* bin	ϵ_{tot}
0 < p_T < 1000	-3.0 < y^* < -2.5	0.089 ± 0.015 (0.015, 0.002)
0 < p_T < 1000	-3.5 < y^* < -3.0	0.282 ± 0.031 (0.031, 0.003)
0 < p_T < 1000	-4.0 < y^* < -3.5	0.378 ± 0.035 (0.034, 0.003)
0 < p_T < 1000	-4.5 < y^* < -4.0	0.351 ± 0.027 (0.027, 0.003)
0 < p_T < 1000	-5.0 < y^* < -4.5	0.199 ± 0.017 (0.017, 0.003)
1000 < p_T < 2000	-3.0 < y^* < -2.5	0.108 ± 0.014 (0.014, 0.001)
1000 < p_T < 2000	-3.5 < y^* < -3.0	0.287 ± 0.026 (0.026, 0.002)
1000 < p_T < 2000	-4.0 < y^* < -3.5	0.363 ± 0.029 (0.029, 0.002)
1000 < p_T < 2000	-4.5 < y^* < -4.0	0.325 ± 0.023 (0.023, 0.002)
1000 < p_T < 2000	-5.0 < y^* < -4.5	0.192 ± 0.022 (0.022, 0.002)
2000 < p_T < 3000	-3.0 < y^* < -2.5	0.116 ± 0.013 (0.013, 0.001)
2000 < p_T < 3000	-3.5 < y^* < -3.0	0.288 ± 0.025 (0.025, 0.002)
2000 < p_T < 3000	-4.0 < y^* < -3.5	0.358 ± 0.027 (0.027, 0.002)
2000 < p_T < 3000	-4.5 < y^* < -4.0	0.318 ± 0.024 (0.024, 0.002)
2000 < p_T < 3000	-5.0 < y^* < -4.5	0.175 ± 0.026 (0.026, 0.002)
3000 < p_T < 4000	-3.0 < y^* < -2.5	0.133 ± 0.016 (0.016, 0.002)
3000 < p_T < 4000	-3.5 < y^* < -3.0	0.326 ± 0.032 (0.032, 0.002)
3000 < p_T < 4000	-4.0 < y^* < -3.5	0.390 ± 0.033 (0.032, 0.003)
3000 < p_T < 4000	-4.5 < y^* < -4.0	0.345 ± 0.034 (0.034, 0.003)
3000 < p_T < 4000	-5.0 < y^* < -4.5	0.181 ± 0.030 (0.030, 0.002)
4000 < p_T < 5000	-3.0 < y^* < -2.5	0.166 ± 0.018 (0.018, 0.002)
4000 < p_T < 5000	-3.5 < y^* < -3.0	0.386 ± 0.034 (0.033, 0.004)
4000 < p_T < 5000	-4.0 < y^* < -3.5	0.437 ± 0.034 (0.033, 0.004)
4000 < p_T < 5000	-4.5 < y^* < -4.0	0.395 ± 0.046 (0.046, 0.004)
4000 < p_T < 5000	-5.0 < y^* < -4.5	0.209 ± 0.037 (0.037, 0.004)
5000 < p_T < 6000	-3.0 < y^* < -2.5	0.206 ± 0.021 (0.021, 0.004)
5000 < p_T < 6000	-3.5 < y^* < -3.0	0.442 ± 0.037 (0.037, 0.005)
5000 < p_T < 6000	-4.0 < y^* < -3.5	0.493 ± 0.040 (0.039, 0.006)
5000 < p_T < 6000	-4.5 < y^* < -4.0	0.430 ± 0.058 (0.058, 0.006)
5000 < p_T < 6000	-5.0 < y^* < -4.5	0.236 ± 0.045 (0.045, 0.006)
6000 < p_T < 7000	-3.0 < y^* < -2.5	0.253 ± 0.026 (0.026, 0.006)
6000 < p_T < 7000	-3.5 < y^* < -3.0	0.479 ± 0.041 (0.041, 0.008)
6000 < p_T < 7000	-4.0 < y^* < -3.5	0.509 ± 0.047 (0.047, 0.009)
6000 < p_T < 7000	-4.5 < y^* < -4.0	0.439 ± 0.067 (0.067, 0.010)
6000 < p_T < 7000	-5.0 < y^* < -4.5	0.263 ± 0.057 (0.056, 0.009)
7000 < p_T < 8000	-3.0 < y^* < -2.5	0.288 ± 0.027 (0.025, 0.008)
7000 < p_T < 8000	-3.5 < y^* < -3.0	0.513 ± 0.045 (0.043, 0.011)
7000 < p_T < 8000	-4.0 < y^* < -3.5	0.529 ± 0.053 (0.051, 0.013)
7000 < p_T < 8000	-4.5 < y^* < -4.0	0.486 ± 0.082 (0.080, 0.015)
7000 < p_T < 8000	-5.0 < y^* < -4.5	0.285 ± 0.069 (0.068, 0.013)
8000 < p_T < 9000	-3.0 < y^* < -2.5	0.309 ± 0.029 (0.027, 0.012)
8000 < p_T < 9000	-3.5 < y^* < -3.0	0.520 ± 0.045 (0.042, 0.016)
8000 < p_T < 9000	-4.0 < y^* < -3.5	0.561 ± 0.068 (0.065, 0.018)
8000 < p_T < 9000	-4.5 < y^* < -4.0	0.519 ± 0.096 (0.093, 0.022)
8000 < p_T < 9000	-5.0 < y^* < -4.5	0.334 ± 0.088 (0.086, 0.019)

Table 37: Total efficiency for J/ψ in PbP, with total, correlated and uncorrelated uncertainties.

p_T bin	y^* bin	ϵ_{tot}
9000 < p_T < 10000	$-3.0 < y^* < -2.5$	0.322 ± 0.033 (0.028, 0.017)
9000 < p_T < 10000	$-3.5 < y^* < -3.0$	0.578 ± 0.057 (0.053, 0.021)
9000 < p_T < 10000	$-4.0 < y^* < -3.5$	0.577 ± 0.081 (0.077, 0.025)
9000 < p_T < 10000	$-4.5 < y^* < -4.0$	0.504 ± 0.101 (0.096, 0.031)
9000 < p_T < 10000	$-5.0 < y^* < -4.5$	0.331 ± 0.090 (0.083, 0.034)
10000 < p_T < 11000	$-3.0 < y^* < -2.5$	0.396 ± 0.037 (0.030, 0.022)
10000 < p_T < 11000	$-3.5 < y^* < -3.0$	0.566 ± 0.054 (0.046, 0.029)
10000 < p_T < 11000	$-4.0 < y^* < -3.5$	0.578 ± 0.085 (0.077, 0.035)
10000 < p_T < 11000	$-4.5 < y^* < -4.0$	0.634 ± 0.131 (0.125, 0.040)
10000 < p_T < 11000	$-5.0 < y^* < -4.5$	0.394 ± 0.118 (0.108, 0.046)
11000 < p_T < 12000	$-3.0 < y^* < -2.5$	0.384 ± 0.040 (0.027, 0.029)
11000 < p_T < 12000	$-3.5 < y^* < -3.0$	0.621 ± 0.065 (0.054, 0.036)
11000 < p_T < 12000	$-4.0 < y^* < -3.5$	0.589 ± 0.092 (0.078, 0.048)
11000 < p_T < 12000	$-4.5 < y^* < -4.0$	0.551 ± 0.135 (0.123, 0.056)
11000 < p_T < 12000	$-5.0 < y^* < -4.5$	0.330 ± 0.109 (0.087, 0.065)
12000 < p_T < 13000	$-3.0 < y^* < -2.5$	0.392 ± 0.049 (0.034, 0.035)
12000 < p_T < 13000	$-3.5 < y^* < -3.0$	0.555 ± 0.070 (0.047, 0.053)
12000 < p_T < 13000	$-4.0 < y^* < -3.5$	0.582 ± 0.101 (0.085, 0.055)
12000 < p_T < 13000	$-4.5 < y^* < -4.0$	0.505 ± 0.134 (0.111, 0.076)
12000 < p_T < 13000	$-5.0 < y^* < -4.5$	0.354 ± 0.166 (0.102, 0.131)
13000 < p_T < 14000	$-3.0 < y^* < -2.5$	0.375 ± 0.052 (0.027, 0.044)
13000 < p_T < 14000	$-3.5 < y^* < -3.0$	0.635 ± 0.084 (0.060, 0.059)
13000 < p_T < 14000	$-4.0 < y^* < -3.5$	0.582 ± 0.134 (0.086, 0.103)
13000 < p_T < 14000	$-4.5 < y^* < -4.0$	0.475 ± 0.170 (0.112, 0.129)
13000 < p_T < 14000	$-5.0 < y^* < -4.5$	0.475 ± 0.159 (0.124, 0.099)

752 C pp cross-section extrapolation numerical results

753 C.1 $\frac{d^2\sigma}{dp_T dy}$ for prompt J/ψ in pp at 8.2 TeV

Table 38: Extrapolated cross-section (in nb) at 8.2 TeV in different p_T and y bins for prompt J/ψ . The first uncertainty is statistical and the second is the total systematic uncertainty.

y bin	[1.5 – 2.0]	[2 – 2.5]	[2.5 – 3]	[3 – 3.5]	[3.5 – 4]	[4 – 4.5]	[4.5 – 5]
[0 – 1]	$873.7 \pm 8.2 \pm 77.0$	$743.9 \pm 25.2 \pm 57.6$	$781.3 \pm 8.4 \pm 54.7$	$734.9 \pm 5.4 \pm 49.9$	$667.3 \pm 4.7 \pm 45.2$	$559.4 \pm 4.7 \pm 39.0$	$462.4 \pm 7.1 \pm 54.4$
[1 – 2]	$1678.0 \pm 9.3 \pm 152.0$	$1476.6 \pm 19.6 \pm 104.0$	$1489.5 \pm 8.9 \pm 99.9$	$1375.0 \pm 6.4 \pm 91.9$	$1204.8 \pm 6.4 \pm 82.3$	$981.0 \pm 6.6 \pm 67.1$	$765.3 \pm 9.2 \pm 124.0$
[2 – 3]	$1369.6 \pm 7.4 \pm 139.6$	$1244.7 \pm 13.6 \pm 87.8$	$1183.6 \pm 7.2 \pm 67.9$	$1047.7 \pm 5.1 \pm 54.4$	$884.3 \pm 4.4 \pm 47.0$	$683.4 \pm 4.9 \pm 41.2$	$465.4 \pm 6.7 \pm 120.0$
[3 – 4]	$863.9 \pm 4.7 \pm 98.9$	$759.6 \pm 8.0 \pm 54.1$	$739.3 \pm 4.4 \pm 42.2$	$629.3 \pm 3.4 \pm 33.0$	$509.6 \pm 3.0 \pm 27.1$	$374.5 \pm 3.2 \pm 23.4$	$219.5 \pm 4.2 \pm 90.9$
[4 – 5]	$487.1 \pm 3.0 \pm 61.7$	$434.5 \pm 4.9 \pm 32.7$	$408.2 \pm 2.8 \pm 23.3$	$340.8 \pm 2.1 \pm 18.0$	$268.6 \pm 2.0 \pm 14.4$	$189.0 \pm 2.2 \pm 11.8$	$94.8 \pm 2.8 \pm 58.6$
[5 – 6]	$261.7 \pm 1.9 \pm 32.9$	$234.2 \pm 2.4 \pm 15.4$	$217.5 \pm 1.8 \pm 12.3$	$177.2 \pm 1.5 \pm 9.5$	$135.4 \pm 1.2 \pm 7.7$	$90.2 \pm 1.4 \pm 5.6$	$36.1 \pm 1.7 \pm 37.4$
[6 – 7]	$139.6 \pm 1.3 \pm 20.4$	$125.7 \pm 1.7 \pm 8.4$	$112.5 \pm 1.2 \pm 6.5$	$90.0 \pm 1.0 \pm 4.9$	$68.6 \pm 0.8 \pm 3.7$	$42.3 \pm 0.8 \pm 2.8$	$13.0 \pm 1.0 \pm 20.1$
[7 – 8]	$76.5 \pm 0.8 \pm 12.7$	$70.0 \pm 1.2 \pm 4.6$	$61.1 \pm 0.7 \pm 3.7$	$47.8 \pm 0.6 \pm 2.6$	$34.2 \pm 0.5 \pm 2.0$	$22.5 \pm 0.6 \pm 1.5$	$4.9 \pm 0.7 \pm 11.3$
[8 – 9]	$43.1 \pm 0.6 \pm 7.5$	$38.8 \pm 0.8 \pm 2.7$	$34.1 \pm 0.6 \pm 1.9$	$25.9 \pm 0.5 \pm 1.5$	$18.7 \pm 0.4 \pm 1.1$	$10.9 \pm 0.4 \pm 0.8$	$1.2 \pm 0.5 \pm 6.7$
[9 – 10]	$24.6 \pm 0.4 \pm 4.5$	$22.3 \pm 0.5 \pm 1.5$	$19.4 \pm 0.4 \pm 1.1$	$13.9 \pm 0.4 \pm 0.8$	$9.9 \pm 0.3 \pm 0.7$	$5.9 \pm 0.2 \pm 0.5$	$0.0 \pm 0.3 \pm 4.0$
[10 – 11]	$14.9 \pm 0.3 \pm 2.8$	$13.5 \pm 0.4 \pm 1.0$	$11.0 \pm 0.3 \pm 0.7$	$9.2 \pm 0.2 \pm 0.6$	$5.7 \pm 0.2 \pm 0.4$	$3.4 \pm 0.2 \pm 0.3$	$0.0 \pm 0.2 \pm 2.5$
[11 – 12]	$8.5 \pm 0.2 \pm 1.5$	$7.7 \pm 0.2 \pm 0.6$	$6.6 \pm 0.2 \pm 0.4$	$5.2 \pm 0.2 \pm 0.3$	$3.2 \pm 0.1 \pm 0.2$	$2.1 \pm 0.2 \pm 0.2$	$0.0 \pm 0.2 \pm 1.6$
[12 – 13]	$5.8 \pm 0.2 \pm 1.3$	$5.2 \pm 0.2 \pm 0.4$	$4.2 \pm 0.1 \pm 0.3$	$3.4 \pm 0.1 \pm 0.2$	$1.7 \pm 0.1 \pm 0.2$	$1.1 \pm 0.1 \pm 0.1$	$0.0 \pm 0.1 \pm 1.1$
[13 – 14]	$4.1 \pm 0.1 \pm 1.0$	$3.4 \pm 0.2 \pm 0.3$	$3.1 \pm 0.1 \pm 0.2$	$1.9 \pm 0.1 \pm 0.2$	$1.5 \pm 0.1 \pm 0.1$	$0.5 \pm 0.1 \pm 0.1$	$0.0 \pm 0.1 \pm 0.8$

C.2 $\frac{d^2\sigma}{dp_T dy}$ for J/ψ from b in pp at 8.2 TeV

Table 39: Extrapolated cross-section (in nb) at 8.2 TeV in different p_T and y bins for J/ψ from- b . The first uncertainty is statistical and the second is the total systematic uncertainty.

y bin	[1.5 – 2.0]	[2 – 2.5]	[2.5 – 3]	[3 – 3.5]	[3.5 – 4]	[4 – 4.5]	[4.5 – 5]
[0 – 1]	$96.4 \pm 3.1 \pm 19.2$	$76.4 \pm 8.6 \pm 10.2$	$74.0 \pm 3.0 \pm 7.0$	$63.7 \pm 1.7 \pm 4.7$	$47.2 \pm 1.2 \pm 3.2$	$28.8 \pm 1.3 \pm 2.3$	$9.9 \pm 1.9 \pm 12.1$
[1 – 2]	$195.8 \pm 2.8 \pm 27.8$	$166.6 \pm 4.4 \pm 12.2$	$159.3 \pm 2.7 \pm 9.1$	$136.4 \pm 2.0 \pm 7.7$	$97.5 \pm 1.7 \pm 5.4$	$65.5 \pm 1.7 \pm 4.5$	$25.6 \pm 2.2 \pm 26.1$
[2 – 3]	$192.2 \pm 2.3 \pm 32.7$	$166.6 \pm 3.5 \pm 11.4$	$153.1 \pm 2.2 \pm 8.4$	$125.5 \pm 1.5 \pm 7.5$	$88.2 \pm 1.3 \pm 5.6$	$55.8 \pm 1.2 \pm 4.0$	$14.9 \pm 1.6 \pm 26.3$
[3 – 4]	$137.5 \pm 1.6 \pm 25.5$	$119.2 \pm 2.7 \pm 8.0$	$108.6 \pm 1.4 \pm 6.6$	$86.5 \pm 1.3 \pm 4.6$	$60.1 \pm 0.9 \pm 3.9$	$36.7 \pm 0.7 \pm 2.8$	$6.7 \pm 1.0 \pm 19.2$
[4 – 5]	$87.0 \pm 1.0 \pm 16.4$	$76.7 \pm 1.7 \pm 4.8$	$67.2 \pm 0.8 \pm 4.1$	$52.3 \pm 0.7 \pm 2.9$	$36.5 \pm 0.6 \pm 2.5$	$20.7 \pm 0.6 \pm 1.8$	$1.2 \pm 0.8 \pm 13.8$
[5 – 6]	$53.6 \pm 0.8 \pm 10.9$	$48.0 \pm 1.1 \pm 3.1$	$41.6 \pm 0.7 \pm 2.6$	$31.6 \pm 0.6 \pm 2.1$	$20.2 \pm 0.4 \pm 1.4$	$11.9 \pm 0.4 \pm 0.9$	$0.0 \pm 0.6 \pm 8.9$
[6 – 7]	$32.6 \pm 0.6 \pm 7.2$	$29.8 \pm 0.6 \pm 2.0$	$25.8 \pm 0.7 \pm 1.7$	$18.4 \pm 0.4 \pm 1.2$	$11.7 \pm 0.3 \pm 1.0$	$6.7 \pm 0.3 \pm 0.6$	$0.0 \pm 0.4 \pm 5.5$
[7 – 8]	$20.5 \pm 0.4 \pm 4.7$	$18.9 \pm 0.5 \pm 1.3$	$15.0 \pm 0.3 \pm 1.0$	$11.4 \pm 0.3 \pm 0.7$	$7.3 \pm 0.2 \pm 0.6$	$3.8 \pm 0.2 \pm 0.3$	$0.0 \pm 0.2 \pm 3.5$
[8 – 9]	$13.3 \pm 0.3 \pm 3.5$	$11.7 \pm 0.4 \pm 0.8$	$10.2 \pm 0.3 \pm 0.7$	$6.7 \pm 0.2 \pm 0.5$	$4.2 \pm 0.2 \pm 0.3$	$2.2 \pm 0.1 \pm 0.2$	$0.0 \pm 0.2 \pm 2.2$
[9 – 10]	$8.7 \pm 0.2 \pm 2.1$	$7.9 \pm 0.3 \pm 0.5$	$6.3 \pm 0.2 \pm 0.4$	$4.5 \pm 0.2 \pm 0.4$	$2.6 \pm 0.1 \pm 0.3$	$1.2 \pm 0.1 \pm 0.2$	$0.0 \pm 0.2 \pm 1.8$
[10 – 11]	$5.7 \pm 0.2 \pm 1.6$	$5.3 \pm 0.2 \pm 0.4$	$4.0 \pm 0.1 \pm 0.3$	$2.9 \pm 0.1 \pm 0.3$	$1.5 \pm 0.1 \pm 0.2$	$0.8 \pm 0.1 \pm 0.1$	$0.0 \pm 0.1 \pm 1.0$
[11 – 12]	$4.2 \pm 0.1 \pm 1.1$	$3.9 \pm 0.1 \pm 0.2$	$2.8 \pm 0.1 \pm 0.2$	$1.8 \pm 0.1 \pm 0.2$	$1.0 \pm 0.1 \pm 0.1$	$0.4 \pm 0.1 \pm 0.1$	$0.0 \pm 0.1 \pm 1.0$
[12 – 13]	$2.9 \pm 0.1 \pm 0.9$	$2.5 \pm 0.1 \pm 0.2$	$2.1 \pm 0.1 \pm 0.2$	$1.3 \pm 0.1 \pm 0.1$	$0.7 \pm 0.1 \pm 0.1$	$0.3 \pm 0.0 \pm 0.1$	$0.0 \pm 0.1 \pm 0.6$
[13 – 14]	$2.0 \pm 0.1 \pm 0.7$	$1.7 \pm 0.1 \pm 0.2$	$1.4 \pm 0.1 \pm 0.1$	$0.9 \pm 0.1 \pm 0.1$	$0.4 \pm 0.1 \pm 0.1$	$0.2 \pm 0.0 \pm 0.0$	$0.0 \pm 0.0 \pm 0.4$

D Cross-section numerical results

D.1 $\frac{d^2\sigma}{dp_T dy}$ for prompt J/ψ in $p\text{Pb}$

Table 40: Prompt J/ψ absolute production cross-section in $p\text{Pb}$, as a function of p_T for the different rapidity bins. The quoted uncertainties are the total uncertainties, and the breakdown into statistical uncertainties, and correlated and uncorrelated uncertainties.

p_T bin	y^* bin	σ (nb)	stat.	corr.	uncorr.
$0 < p_T < 1$	$1.5 < y^* < 2.0$	$108\,657 \pm 15\,997$			$2\,699$
$0 < p_T < 1$	$2.0 < y^* < 2.5$	$94\,344 \pm 8\,947$			$1\,350$
$0 < p_T < 1$	$2.5 < y^* < 3.0$	$79\,697 \pm 5\,377$			$1\,083$
$0 < p_T < 1$	$3.0 < y^* < 3.5$	$69\,771 \pm 4\,317$			982
$0 < p_T < 1$	$3.5 < y^* < 4.0$	$63\,988 \pm 4\,053$			$1\,089$
$1 < p_T < 2$	$1.5 < y^* < 2.0$	$212\,248 \pm 18\,102$			$3\,311$
$1 < p_T < 2$	$2.0 < y^* < 2.5$	$194\,043 \pm 12\,331$			$1\,803$
$1 < p_T < 2$	$2.5 < y^* < 3.0$	$166\,362 \pm 14\,334$			$1\,489$
$1 < p_T < 2$	$3.0 < y^* < 3.5$	$144\,752 \pm 7\,883$			$1\,366$
$1 < p_T < 2$	$3.5 < y^* < 4.0$	$126\,072 \pm 8\,819$			$1\,501$
$2 < p_T < 3$	$1.5 < y^* < 2.0$	$192\,561 \pm 14\,760$			$2\,829$
$2 < p_T < 3$	$2.0 < y^* < 2.5$	$179\,636 \pm 11\,334$			$1\,653$
$2 < p_T < 3$	$2.5 < y^* < 3.0$	$157\,764 \pm 8\,942$			$1\,398$
$2 < p_T < 3$	$3.0 < y^* < 3.5$	$131\,411 \pm 7\,287$			$1\,258$
$2 < p_T < 3$	$3.5 < y^* < 4.0$	$107\,542 \pm 7\,573$			$1\,372$
$3 < p_T < 4$	$1.5 < y^* < 2.0$	$133\,095 \pm 12\,195$			$2\,117$
$3 < p_T < 4$	$2.0 < y^* < 2.5$	$123\,846 \pm 8\,676$			$1\,222$
$3 < p_T < 4$	$2.5 < y^* < 3.0$	$108\,452 \pm 7\,279$			$1\,004$
$3 < p_T < 4$	$3.0 < y^* < 3.5$	$88\,219 \pm 5\,719$			928
$3 < p_T < 4$	$3.5 < y^* < 4.0$	$67\,887 \pm 5\,282$			928
$4 < p_T < 5$	$1.5 < y^* < 2.0$	$78\,814 \pm 6\,740$			$1\,393$
$4 < p_T < 5$	$2.0 < y^* < 2.5$	$74\,553 \pm 4\,778$			810
$4 < p_T < 5$	$2.5 < y^* < 3.0$	$64\,407 \pm 3\,903$			676
$4 < p_T < 5$	$3.0 < y^* < 3.5$	$52\,461 \pm 3\,247$			636
$4 < p_T < 5$	$3.5 < y^* < 4.0$	$37\,748 \pm 2\,794$			690
$5 < p_T < 6$	$1.5 < y^* < 2.0$	$45\,570 \pm 3\,669$			929
$5 < p_T < 6$	$2.0 < y^* < 2.5$	$42\,533 \pm 2\,668$			544
$5 < p_T < 6$	$2.5 < y^* < 3.0$	$34\,749 \pm 2\,082$			460
$5 < p_T < 6$	$3.0 < y^* < 3.5$	$29\,789 \pm 1\,935$			442
$5 < p_T < 6$	$3.5 < y^* < 4.0$	$21\,101 \pm 1\,681$			463
$6 < p_T < 7$	$1.5 < y^* < 2.0$	$25\,171 \pm 2\,135$			615
$6 < p_T < 7$	$2.0 < y^* < 2.5$	$23\,940 \pm 1\,681$			382
$6 < p_T < 7$	$2.5 < y^* < 3.0$	$19\,046 \pm 1\,351$			320
$6 < p_T < 7$	$3.0 < y^* < 3.5$	$15\,500 \pm 1\,109$			304
$6 < p_T < 7$	$3.5 < y^* < 4.0$	$12\,225 \pm 1\,090$			338
$7 < p_T < 8$	$1.5 < y^* < 2.0$	$14\,411 \pm 1\,165$			437
$7 < p_T < 8$	$2.0 < y^* < 2.5$	$12\,662 \pm 803$			258

Table 41: Prompt J/ψ absolute production cross-section in $p\text{Pb}$, as a function of p_{T} for the different rapidity bins. The quoted uncertainties are the total uncertainties, and the breakdown into statistical uncertainties, and correlated and uncorrelated uncertainties.

p_{T} bin	y^* bin	σ (nb)	stat.	corr.	uncorr.	
$7 < p_{\text{T}} < 8$	$3.0 < y^* < 3.5$	$8\,873 \pm 655$			227	600
$7 < p_{\text{T}} < 8$	$3.5 < y^* < 4.0$	$6\,305 \pm 656$			240	597
$8 < p_{\text{T}} < 9$	$1.5 < y^* < 2.0$	$7\,699 \pm 615$			291	501
$8 < p_{\text{T}} < 9$	$2.0 < y^* < 2.5$	$7\,443 \pm 486$			194	429
$8 < p_{\text{T}} < 9$	$2.5 < y^* < 3.0$	$6\,059 \pm 413$			173	360
$8 < p_{\text{T}} < 9$	$3.0 < y^* < 3.5$	$4\,639 \pm 361$			157	312
$8 < p_{\text{T}} < 9$	$3.5 < y^* < 4.0$	$3\,699 \pm 418$			169	370
$9 < p_{\text{T}} < 10$	$1.5 < y^* < 2.0$	$4\,808 \pm 419$			224	315
$9 < p_{\text{T}} < 10$	$2.0 < y^* < 2.5$	$4\,266 \pm 296$			143	244
$9 < p_{\text{T}} < 10$	$2.5 < y^* < 3.0$	$3\,363 \pm 258$			128	213
$9 < p_{\text{T}} < 10$	$3.0 < y^* < 3.5$	$2\,682 \pm 236$			120	191
$9 < p_{\text{T}} < 10$	$3.5 < y^* < 4.0$	$2\,203 \pm 275$			129	232
$10 < p_{\text{T}} < 11$	$1.5 < y^* < 2.0$	$2\,630 \pm 242$			156	154
$10 < p_{\text{T}} < 11$	$2.0 < y^* < 2.5$	$2\,618 \pm 196$			109	150
$10 < p_{\text{T}} < 11$	$2.5 < y^* < 3.0$	$2\,234 \pm 178$			103	132
$10 < p_{\text{T}} < 11$	$3.0 < y^* < 3.5$	$1\,491 \pm 145$			84	109
$10 < p_{\text{T}} < 11$	$3.5 < y^* < 4.0$	$1\,127 \pm 174$			91	141
$11 < p_{\text{T}} < 12$	$1.5 < y^* < 2.0$	$1\,844 \pm 185$			121	108
$11 < p_{\text{T}} < 12$	$2.0 < y^* < 2.5$	$1\,602 \pm 134$			86	90
$11 < p_{\text{T}} < 12$	$2.5 < y^* < 3.0$	$1\,304 \pm 121$			78	80
$11 < p_{\text{T}} < 12$	$3.0 < y^* < 3.5$	$1\,002 \pm 109$			68	76
$11 < p_{\text{T}} < 12$	$3.5 < y^* < 4.0$	753 ± 109			75	69
$12 < p_{\text{T}} < 13$	$1.5 < y^* < 2.0$	$1\,185 \pm 143$			98	76
$12 < p_{\text{T}} < 13$	$2.0 < y^* < 2.5$	958 ± 94			64	59
$12 < p_{\text{T}} < 13$	$2.5 < y^* < 3.0$	779 ± 82			58	49
$12 < p_{\text{T}} < 13$	$3.0 < y^* < 3.5$	531 ± 71			51	41
$12 < p_{\text{T}} < 13$	$3.5 < y^* < 4.0$	436 ± 80			47	61
$13 < p_{\text{T}} < 14$	$1.5 < y^* < 2.0$	739 ± 99			74	42
$13 < p_{\text{T}} < 14$	$2.0 < y^* < 2.5$	596 ± 65			49	34
$13 < p_{\text{T}} < 14$	$2.5 < y^* < 3.0$	476 ± 59			45	27
$13 < p_{\text{T}} < 14$	$3.0 < y^* < 3.5$	349 ± 47			35	27
$13 < p_{\text{T}} < 14$	$3.5 < y^* < 4.0$	241 ± 47			38	21

D.2 $\frac{d^2\sigma}{dp_T dy}$ for J/ψ from b in $p\text{Pb}$

Table 42: J/ψ from b absolute production cross-section in $p\text{Pb}$, as a function of p_T for the different rapidity bins. The quoted uncertainties are the total uncertainties, and the breakdown into statistical uncertainties, and correlated and uncorrelated uncertainties.

p_T bin	y^* bin	σ (nb)	stat.	corr.	uncorr.
$0 < p_T < 1$	$1.5 < y^* < 2.0$	$15\,578 \pm 2\,480$			1 020 2 248 238
$0 < p_T < 1$	$2.0 < y^* < 2.5$	$13\,398 \pm 1\,345$			481 1 252 96
$0 < p_T < 1$	$2.5 < y^* < 3.0$	$10\,322 \pm 777$			373 679 59
$0 < p_T < 1$	$3.0 < y^* < 3.5$	$8\,940 \pm 640$			346 536 51
$0 < p_T < 1$	$3.5 < y^* < 4.0$	$7\,326 \pm 600$			401 443 57
$1 < p_T < 2$	$1.5 < y^* < 2.0$	$32\,946 \pm 3\,048$			1 289 2 744 317
$1 < p_T < 2$	$2.0 < y^* < 2.5$	$29\,549 \pm 1\,975$			672 1 851 145
$1 < p_T < 2$	$2.5 < y^* < 3.0$	$24\,533 \pm 2\,171$			544 2 099 105
$1 < p_T < 2$	$3.0 < y^* < 3.5$	$20\,392 \pm 1\,204$			505 1 089 91
$1 < p_T < 2$	$3.5 < y^* < 4.0$	$17\,176 \pm 1\,328$			602 1 179 100
$2 < p_T < 3$	$1.5 < y^* < 2.0$	$32\,980 \pm 2\,739$			1 160 2 459 324
$2 < p_T < 3$	$2.0 < y^* < 2.5$	$30\,476 \pm 2\,010$			648 1 895 167
$2 < p_T < 3$	$2.5 < y^* < 3.0$	$25\,418 \pm 1\,519$			532 1 417 123
$2 < p_T < 3$	$3.0 < y^* < 3.5$	$21\,098 \pm 1\,256$			500 1 147 108
$2 < p_T < 3$	$3.5 < y^* < 4.0$	$14\,442 \pm 1\,139$			546 995 101
$3 < p_T < 4$	$1.5 < y^* < 2.0$	$24\,317 \pm 2\,371$			900 2 176 280
$3 < p_T < 4$	$2.0 < y^* < 2.5$	$23\,146 \pm 1\,685$			512 1 599 143
$3 < p_T < 4$	$2.5 < y^* < 3.0$	$18\,585 \pm 1\,303$			414 1 231 101
$3 < p_T < 4$	$3.0 < y^* < 3.5$	$14\,809 \pm 1\,026$			393 943 88
$3 < p_T < 4$	$3.5 < y^* < 4.0$	$10\,031 \pm 859$			385 763 84
$4 < p_T < 5$	$1.5 < y^* < 2.0$	$14\,646 \pm 1\,371$			615 1 210 190
$4 < p_T < 5$	$2.0 < y^* < 2.5$	$15\,476 \pm 1\,047$			376 971 109
$4 < p_T < 5$	$2.5 < y^* < 3.0$	$12\,163 \pm 787$			304 721 78
$4 < p_T < 5$	$3.0 < y^* < 3.5$	$9\,412 \pm 638$			285 567 66
$4 < p_T < 5$	$3.5 < y^* < 4.0$	$6\,253 \pm 544$			308 444 60
$5 < p_T < 6$	$1.5 < y^* < 2.0$	$10\,091 \pm 909$			458 770 153
$5 < p_T < 6$	$2.0 < y^* < 2.5$	$9\,274 \pm 628$			265 564 78
$5 < p_T < 6$	$2.5 < y^* < 3.0$	$7\,562 \pm 495$			224 437 60
$5 < p_T < 6$	$3.0 < y^* < 3.5$	$6\,080 \pm 439$			212 380 53
$5 < p_T < 6$	$3.5 < y^* < 4.0$	$3\,705 \pm 354$			211 280 43
$6 < p_T < 7$	$1.5 < y^* < 2.0$	$6\,558 \pm 626$			329 519 116
$6 < p_T < 7$	$2.0 < y^* < 2.5$	$5\,595 \pm 429$			194 378 58
$6 < p_T < 7$	$2.5 < y^* < 3.0$	$4\,628 \pm 358$			163 315 46
$6 < p_T < 7$	$3.0 < y^* < 3.5$	$3\,617 \pm 294$			156 245 40
$6 < p_T < 7$	$3.5 < y^* < 4.0$	$2\,114 \pm 240$			161 176 32
$7 < p_T < 8$	$1.5 < y^* < 2.0$	$4\,609 \pm 428$			253 329 104
$7 < p_T < 8$	$2.0 < y^* < 2.5$	$3\,651 \pm 262$			144 214 46

Table 43: J/ψ from b absolute production cross-section in $p\text{Pb}$, as a function of p_T for the different rapidity bins. The quoted uncertainties are the total uncertainties, and the breakdown into statistical uncertainties, and correlated and uncorrelated uncertainties.

p_T bin	y^* bin	σ (nb)	stat.	corr.	uncorr.		
$7 < p_T < 8$	$2.5 < y^* < 3.0$	$3\,005 \pm 229$			131	183	39
$7 < p_T < 8$	$3.0 < y^* < 3.5$	$2\,327 \pm 203$			123	157	34
$7 < p_T < 8$	$3.5 < y^* < 4.0$	$1\,432 \pm 183$			120	135	28
$8 < p_T < 9$	$1.5 < y^* < 2.0$	$2\,593 \pm 255$			178	168	69
$8 < p_T < 9$	$2.0 < y^* < 2.5$	$2\,299 \pm 177$			112	132	36
$8 < p_T < 9$	$2.5 < y^* < 3.0$	$1\,859 \pm 152$			99	110	31
$8 < p_T < 9$	$3.0 < y^* < 3.5$	$1\,273 \pm 126$			89	85	24
$8 < p_T < 9$	$3.5 < y^* < 4.0$	$1\,002 \pm 139$			92	100	26
$9 < p_T < 10$	$1.5 < y^* < 2.0$	$1\,774 \pm 192$			140	116	60
$9 < p_T < 10$	$2.0 < y^* < 2.5$	$1\,529 \pm 127$			87	87	30
$9 < p_T < 10$	$2.5 < y^* < 3.0$	$1\,142 \pm 107$			75	72	23
$9 < p_T < 10$	$3.0 < y^* < 3.5$	864 ± 95			69	61	21
$9 < p_T < 10$	$3.5 < y^* < 4.0$	544 ± 90			67	57	17
$10 < p_T < 11$	$1.5 < y^* < 2.0$	$1\,066 \pm 126$			101	62	42
$10 < p_T < 11$	$2.0 < y^* < 2.5$	917 ± 88			66	52	22
$10 < p_T < 11$	$2.5 < y^* < 3.0$	804 ± 83			64	47	21
$10 < p_T < 11$	$3.0 < y^* < 3.5$	477 ± 63			51	35	14
$10 < p_T < 11$	$3.5 < y^* < 4.0$	397 ± 73			51	50	15
$11 < p_T < 12$	$1.5 < y^* < 2.0$	802 ± 102			82	47	38
$11 < p_T < 12$	$2.0 < y^* < 2.5$	678 ± 72			57	38	21
$11 < p_T < 12$	$2.5 < y^* < 3.0$	446 ± 60			50	27	15
$11 < p_T < 12$	$3.0 < y^* < 3.5$	386 ± 57			47	29	14
$11 < p_T < 12$	$3.5 < y^* < 4.0$	162 ± 41			37	15	8
$12 < p_T < 13$	$1.5 < y^* < 2.0$	526 ± 80			65	33	32
$12 < p_T < 13$	$2.0 < y^* < 2.5$	474 ± 57			45	29	16
$12 < p_T < 13$	$2.5 < y^* < 3.0$	370 ± 48			39	23	15
$12 < p_T < 13$	$3.0 < y^* < 3.5$	231 ± 40			34	18	11
$12 < p_T < 13$	$3.5 < y^* < 4.0$	153 ± 37			29	21	7
$13 < p_T < 14$	$1.5 < y^* < 2.0$	419 ± 67			56	24	28
$13 < p_T < 14$	$2.0 < y^* < 2.5$	387 ± 48			39	22	16
$13 < p_T < 14$	$2.5 < y^* < 3.0$	224 ± 35			31	13	11
$13 < p_T < 14$	$3.0 < y^* < 3.5$	151 ± 27			23	11	6
$13 < p_T < 14$	$3.5 < y^* < 4.0$	100 ± 27			24	9	7

D.3 $\frac{d^2\sigma}{dp_T dy}$ for prompt J/ψ in PbP

Table 44: Prompt J/ψ absolute production cross-section in PbP, as a function of p_T for the different rapidity bins. The quoted uncertainties are the total uncertainties, and the breakdown into statistical uncertainties, and correlated and uncorrelated uncertainties.

p_T bin	y^* bin	σ (nb)	stat.	corr.	uncorr.
$0 < p_T < 1$	$-3.0 < y^* < -2.5$	$132\,894 \pm 23\,083$		2 304	22 837 2 450
$0 < p_T < 1$	$-3.5 < y^* < -3.0$	$114\,027 \pm 13\,080$		1 329	12 958 1 180
$0 < p_T < 1$	$-4.0 < y^* < -3.5$	$96\,631 \pm 9\,326$		1 173	9 211 862
$0 < p_T < 1$	$-4.5 < y^* < -4.0$	$83\,634 \pm 6\,917$		1 173	6 770 799
$0 < p_T < 1$	$-5.0 < y^* < -4.5$	$70\,463 \pm 6\,562$		1 436	6 323 1 005
$1 < p_T < 2$	$-3.0 < y^* < -2.5$	$262\,999 \pm 34\,840$		2 869	34 609 2 788
$1 < p_T < 2$	$-3.5 < y^* < -3.0$	$226\,925 \pm 21\,642$		1 765	21 522 1 448
$1 < p_T < 2$	$-4.0 < y^* < -3.5$	$188\,313 \pm 15\,943$		1 526	15 833 1 084
$1 < p_T < 2$	$-4.5 < y^* < -4.0$	$161\,424 \pm 12\,452$		1 540	12 312 1 049
$1 < p_T < 2$	$-5.0 < y^* < -4.5$	$135\,661 \pm 16\,272$		1 844	16 119 1 248
$2 < p_T < 3$	$-3.0 < y^* < -2.5$	$230\,851 \pm 27\,367$		2 400	27 159 2 355
$2 < p_T < 3$	$-3.5 < y^* < -3.0$	$198\,584 \pm 18\,402$		1 553	18 293 1 256
$2 < p_T < 3$	$-4.0 < y^* < -3.5$	$166\,681 \pm 13\,402$		1 386	13 296 964
$2 < p_T < 3$	$-4.5 < y^* < -4.0$	$128\,711 \pm 10\,559$		1 288	10 445 855
$2 < p_T < 3$	$-5.0 < y^* < -4.5$	$98\,394 \pm 14\,741$		1 521	14 628 1 004
$3 < p_T < 4$	$-3.0 < y^* < -2.5$	$144\,596 \pm 18\,402$		1 656	18 251 1 670
$3 < p_T < 4$	$-3.5 < y^* < -3.0$	$128\,374 \pm 13\,018$		1 088	12 939 933
$3 < p_T < 4$	$-4.0 < y^* < -3.5$	$104\,574 \pm 9\,289$		924	9 215 717
$3 < p_T < 4$	$-4.5 < y^* < -4.0$	$77\,643 \pm 8\,068$		863	7 999 607
$3 < p_T < 4$	$-5.0 < y^* < -4.5$	$55\,252 \pm 9\,397$		1 004	9 315 715
$4 < p_T < 5$	$-3.0 < y^* < -2.5$	$83\,591 \pm 9\,609$		1 074	9 476 1 179
$4 < p_T < 5$	$-3.5 < y^* < -3.0$	$71\,385 \pm 6\,590$		667	6 523 649
$4 < p_T < 5$	$-4.0 < y^* < -3.5$	$55\,851 \pm 4\,620$		557	4 558 504
$4 < p_T < 5$	$-4.5 < y^* < -4.0$	$40\,500 \pm 4\,888$		507	4 844 409
$4 < p_T < 5$	$-5.0 < y^* < -4.5$	$25\,584 \pm 4\,648$		602	4 588 436
$5 < p_T < 6$	$-3.0 < y^* < -2.5$	$46\,558 \pm 5\,016$		690	4 898 836
$5 < p_T < 6$	$-3.5 < y^* < -3.0$	$37\,056 \pm 3\,316$		422	3 259 439
$5 < p_T < 6$	$-4.0 < y^* < -3.5$	$27\,810 \pm 2\,398$		345	2 350 331
$5 < p_T < 6$	$-4.5 < y^* < -4.0$	$19\,985 \pm 2\,768$		323	2 734 289
$5 < p_T < 6$	$-5.0 < y^* < -4.5$	$13\,538 \pm 2\,661$		376	2 615 317
$6 < p_T < 7$	$-3.0 < y^* < -2.5$	$22\,469 \pm 2\,466$		429	2 376 504
$6 < p_T < 7$	$-3.5 < y^* < -3.0$	$19\,946 \pm 1\,832$		287	1 781 319
$6 < p_T < 7$	$-4.0 < y^* < -3.5$	$14\,620 \pm 1\,443$		240	1 400 255
$6 < p_T < 7$	$-4.5 < y^* < -4.0$	$10\,326 \pm 1\,629$		221	1 597 231
$6 < p_T < 7$	$-5.0 < y^* < -4.5$	$5\,671 \pm 1\,256$		242	1 216 201

Table 45: Prompt J/ψ absolute production cross-section in PbP, as a function of p_T for the different rapidity bins. The quoted uncertainties are the total uncertainties, and the breakdown into statistical uncertainties, and correlated and uncorrelated uncertainties.

p_T bin	y^* bin	σ (nb)	stat.	corr.	uncorr.		
$7 < p_T < 8$	$-3.5 < y^* < -3.0$	$10\,316 \pm 968$			194	921	224
$7 < p_T < 8$	$-4.0 < y^* < -3.5$	$7\,480 \pm 794$			166	755	181
$7 < p_T < 8$	$-4.5 < y^* < -4.0$	$4\,763 \pm 824$			135	799	146
$7 < p_T < 8$	$-5.0 < y^* < -4.5$	$2\,933 \pm 732$			155	702	137
$8 < p_T < 9$	$-3.0 < y^* < -2.5$	$6\,693 \pm 695$			205	608	267
$8 < p_T < 9$	$-3.5 < y^* < -3.0$	$5\,845 \pm 555$			145	504	179
$8 < p_T < 9$	$-4.0 < y^* < -3.5$	$3\,973 \pm 507$			116	477	126
$8 < p_T < 9$	$-4.5 < y^* < -4.0$	$2\,316 \pm 442$			93	421	96
$8 < p_T < 9$	$-5.0 < y^* < -4.5$	$1\,107 \pm 311$			101	287	64
$9 < p_T < 10$	$-3.0 < y^* < -2.5$	$4\,054 \pm 453$			154	367	214
$9 < p_T < 10$	$-3.5 < y^* < -3.0$	$2\,960 \pm 320$			99	283	110
$9 < p_T < 10$	$-4.0 < y^* < -3.5$	$1\,942 \pm 288$			78	264	84
$9 < p_T < 10$	$-4.5 < y^* < -4.0$	$1\,292 \pm 271$			71	249	79
$9 < p_T < 10$	$-5.0 < y^* < -4.5$	674 ± 198			74	170	70
$10 < p_T < 11$	$-3.0 < y^* < -2.5$	$2\,233 \pm 243$			103	179	126
$10 < p_T < 11$	$-3.5 < y^* < -3.0$	$1\,886 \pm 205$			82	161	95
$10 < p_T < 11$	$-4.0 < y^* < -3.5$	$1\,183 \pm 187$			62	161	72
$10 < p_T < 11$	$-4.5 < y^* < -4.0$	590 ± 131			44	117	37
$10 < p_T < 11$	$-5.0 < y^* < -4.5$	297 ± 99			42	82	35
$11 < p_T < 12$	$-3.0 < y^* < -2.5$	$1\,297 \pm 160$			80	98	97
$11 < p_T < 12$	$-3.5 < y^* < -3.0$	933 ± 114			53	85	54
$11 < p_T < 12$	$-4.0 < y^* < -3.5$	599 ± 105			46	81	49
$11 < p_T < 12$	$-4.5 < y^* < -4.0$	415 ± 109			38	93	42
$11 < p_T < 12$	$-5.0 < y^* < -4.5$	205 ± 77			36	54	40
$12 < p_T < 13$	$-3.0 < y^* < -2.5$	975 ± 141			66	89	87
$12 < p_T < 13$	$-3.5 < y^* < -3.0$	655 ± 97			46	58	62
$12 < p_T < 13$	$-4.0 < y^* < -3.5$	313 ± 64			32	46	29
$12 < p_T < 13$	$-4.5 < y^* < -4.0$	229 ± 67			27	50	34
$12 < p_T < 13$	$-5.0 < y^* < -4.5$	136 ± 74			38	39	50
$13 < p_T < 14$	$-3.0 < y^* < -2.5$	546 ± 96			57	41	64
$13 < p_T < 14$	$-3.5 < y^* < -3.0$	328 ± 60			40	32	30
$13 < p_T < 14$	$-4.0 < y^* < -3.5$	248 ± 64			27	37	43
$13 < p_T < 14$	$-4.5 < y^* < -4.0$	135 ± 54			23	32	36
$13 < p_T < 14$	$-5.0 < y^* < -4.5$	14 ± 9			8	3	2

D.4 $\frac{d^2\sigma}{dp_T dy}$ for J/ψ from b in Pb p

Table 46: J/ψ from b absolute production cross-section in Pb p , as a function of p_T for the different rapidity bins. The quoted uncertainties are the total uncertainties, and the breakdown into statistical uncertainties, and correlated and uncorrelated uncertainties.

p_T bin	y^* bin	σ (nb)	stat.	corr.	uncorr.
$0 < p_T < 1$	$-3.0 < y^* < -2.5$	$16\,124 \pm 2\,892$		773	2\,770 297
$0 < p_T < 1$	$-3.5 < y^* < -3.0$	$11\,764 \pm 1\,402$		404	1\,337 121
$0 < p_T < 1$	$-4.0 < y^* < -3.5$	$9\,268 \pm 948$		333	883 82
$0 < p_T < 1$	$-4.5 < y^* < -4.0$	$6\,997 \pm 651$		315	566 66
$0 < p_T < 1$	$-5.0 < y^* < -4.5$	$4\,750 \pm 580$		387	426 67
$1 < p_T < 2$	$-3.0 < y^* < -2.5$	$35\,035 \pm 4\,729$		986	4\,610 371
$1 < p_T < 2$	$-3.5 < y^* < -3.0$	$26\,049 \pm 2\,538$		557	2\,470 166
$1 < p_T < 2$	$-4.0 < y^* < -3.5$	$20\,283 \pm 1\,768$		453	1\,705 116
$1 < p_T < 2$	$-4.5 < y^* < -4.0$	$14\,272 \pm 1\,169$		417	1\,088 92
$1 < p_T < 2$	$-5.0 < y^* < -4.5$	$9\,634 \pm 1\,247$		488	1\,144 88
$2 < p_T < 3$	$-3.0 < y^* < -2.5$	$31\,415 \pm 3\,806$		851	3\,696 320
$2 < p_T < 3$	$-3.5 < y^* < -3.0$	$25\,556 \pm 2\,414$		509	2\,354 161
$2 < p_T < 3$	$-4.0 < y^* < -3.5$	$19\,831 \pm 1\,641$		421	1\,581 114
$2 < p_T < 3$	$-4.5 < y^* < -4.0$	$12\,686 \pm 1\,096$		367	1\,029 84
$2 < p_T < 3$	$-5.0 < y^* < -4.5$	$7\,763 \pm 1\,225$		402	1\,154 79
$3 < p_T < 4$	$-3.0 < y^* < -2.5$	$21\,884 \pm 2\,843$		625	2\,762 252
$3 < p_T < 4$	$-3.5 < y^* < -3.0$	$19\,199 \pm 1\,979$		393	1\,935 139
$3 < p_T < 4$	$-4.0 < y^* < -3.5$	$13\,485 \pm 1\,232$		312	1\,188 92
$3 < p_T < 4$	$-4.5 < y^* < -4.0$	$8\,716 \pm 940$		269	897 68
$3 < p_T < 4$	$-5.0 < y^* < -4.5$	$4\,424 \pm 797$		276	746 57
$4 < p_T < 5$	$-3.0 < y^* < -2.5$	$14\,344 \pm 1\,698$		444	1\,626 202
$4 < p_T < 5$	$-3.5 < y^* < -3.0$	$11\,196 \pm 1\,061$		262	1\,023 101
$4 < p_T < 5$	$-4.0 < y^* < -3.5$	$8\,207 \pm 707$		215	669 74
$4 < p_T < 5$	$-4.5 < y^* < -4.0$	$4\,922 \pm 618$		181	588 49
$4 < p_T < 5$	$-5.0 < y^* < -4.5$	$2\,657 \pm 516$		194	476 45
$5 < p_T < 6$	$-3.0 < y^* < -2.5$	$7\,635 \pm 865$		290	803 137
$5 < p_T < 6$	$-3.5 < y^* < -3.0$	$6\,734 \pm 625$		183	592 79
$5 < p_T < 6$	$-4.0 < y^* < -3.5$	$4\,366 \pm 399$		142	369 51
$5 < p_T < 6$	$-4.5 < y^* < -4.0$	$2\,741 \pm 396$		123	375 39
$5 < p_T < 6$	$-5.0 < y^* < -4.5$	$1\,554 \pm 330$		132	300 36
$6 < p_T < 7$	$-3.0 < y^* < -2.5$	$4\,416 \pm 516$		197	467 99
$6 < p_T < 7$	$-3.5 < y^* < -3.0$	$3\,921 \pm 380$		133	350 62
$6 < p_T < 7$	$-4.0 < y^* < -3.5$	$2\,651 \pm 279$		108	253 46
$6 < p_T < 7$	$-4.5 < y^* < -4.0$	$1\,644 \pm 273$		93	254 36
$6 < p_T < 7$	$-5.0 < y^* < -4.5$	668 ± 170		89	143 23

Table 47: J/ψ from b absolute production cross-section in Pbp , as a function of p_T for the different rapidity bins. The quoted uncertainties are the total uncertainties, and the breakdown into statistical uncertainties, and correlated and uncorrelated uncertainties.

p_T bin	y^* bin	σ (nb)	stat.	corr.	uncorr.
$7 < p_T < 8$	$-3.5 < y^* < -3.0$	2339 ± 234			93 209 50
$7 < p_T < 8$	$-4.0 < y^* < -3.5$	1414 ± 165			77 142 34
$7 < p_T < 8$	$-4.5 < y^* < -4.0$	748 ± 140			58 125 22
$7 < p_T < 8$	$-5.0 < y^* < -4.5$	374 ± 105			52 89 17
$8 < p_T < 9$	$-3.0 < y^* < -2.5$	2086 ± 239			120 189 83
$8 < p_T < 9$	$-3.5 < y^* < -3.0$	1445 ± 151			74 124 44
$8 < p_T < 9$	$-4.0 < y^* < -3.5$	812 ± 114			54 97 25
$8 < p_T < 9$	$-4.5 < y^* < -4.0$	474 ± 99			44 86 19
$8 < p_T < 9$	$-5.0 < y^* < -4.5$	207 ± 66			36 53 12
$9 < p_T < 10$	$-3.0 < y^* < -2.5$	1374 ± 170			90 124 72
$9 < p_T < 10$	$-3.5 < y^* < -3.0$	794 ± 97			53 76 29
$9 < p_T < 10$	$-4.0 < y^* < -3.5$	488 ± 80			40 66 21
$9 < p_T < 10$	$-4.5 < y^* < -4.0$	266 ± 63			33 51 16
$9 < p_T < 10$	$-5.0 < y^* < -4.5$	94 ± 37			26 23 9
$10 < p_T < 11$	$-3.0 < y^* < -2.5$	695 ± 89			57 56 39
$10 < p_T < 11$	$-3.5 < y^* < -3.0$	479 ± 65			44 41 24
$10 < p_T < 11$	$-4.0 < y^* < -3.5$	372 ± 65			35 50 22
$10 < p_T < 11$	$-4.5 < y^* < -4.0$	152 ± 39			22 30 9
$10 < p_T < 11$	$-5.0 < y^* < -4.5$	42 ± 19			14 11 5
$11 < p_T < 12$	$-3.0 < y^* < -2.5$	670 ± 91			57 50 50
$11 < p_T < 12$	$-3.5 < y^* < -3.0$	373 ± 53			35 34 21
$11 < p_T < 12$	$-4.0 < y^* < -3.5$	191 ± 40			26 25 15
$11 < p_T < 12$	$-4.5 < y^* < -4.0$	57 ± 20			14 12 5
$11 < p_T < 12$	$-5.0 < y^* < -4.5$	88 ± 36			22 23 17
$12 < p_T < 13$	$-3.0 < y^* < -2.5$	444 ± 72			44 41 39
$12 < p_T < 13$	$-3.5 < y^* < -3.0$	247 ± 43			29 22 23
$12 < p_T < 13$	$-4.0 < y^* < -3.5$	107 ± 27			20 15 10
$12 < p_T < 13$	$-4.5 < y^* < -4.0$	70 ± 24			16 15 10
$12 < p_T < 13$	$-5.0 < y^* < -4.5$	19 ± 15			12 5 7
$13 < p_T < 14$	$-3.0 < y^* < -2.5$	257 ± 53			39 19 30
$13 < p_T < 14$	$-3.5 < y^* < -3.0$	146 ± 33			27 14 13
$13 < p_T < 14$	$-4.0 < y^* < -3.5$	114 ± 32			19 17 20
$13 < p_T < 14$	$-4.5 < y^* < -4.0$	40 ± 19			12 9 10
$13 < p_T < 14$	$-5.0 < y^* < -4.5$	8 ± 6			6 2 1

D.5 J/ψ b fraction

Table 48: f_b of J/ψ in $p\text{Pb}$, in bins of p_T and y^* . The uncertainty is the total one.

p_T bin	y^* bin	f_b
$0 < p_T < 1$	$1.5 < y^* < 2.0$	0.13 ± 0.01
$0 < p_T < 1$	$2.0 < y^* < 2.5$	0.12 ± 0.00
$0 < p_T < 1$	$2.5 < y^* < 3.0$	0.11 ± 0.00
$0 < p_T < 1$	$3.0 < y^* < 3.5$	0.11 ± 0.00
$0 < p_T < 1$	$3.5 < y^* < 4.0$	0.10 ± 0.01
$1 < p_T < 2$	$1.5 < y^* < 2.0$	0.13 ± 0.01
$1 < p_T < 2$	$2.0 < y^* < 2.5$	0.13 ± 0.00
$1 < p_T < 2$	$2.5 < y^* < 3.0$	0.13 ± 0.00
$1 < p_T < 2$	$3.0 < y^* < 3.5$	0.12 ± 0.00
$1 < p_T < 2$	$3.5 < y^* < 4.0$	0.12 ± 0.00
$2 < p_T < 3$	$1.5 < y^* < 2.0$	0.15 ± 0.00
$2 < p_T < 3$	$2.0 < y^* < 2.5$	0.15 ± 0.00
$2 < p_T < 3$	$2.5 < y^* < 3.0$	0.14 ± 0.00
$2 < p_T < 3$	$3.0 < y^* < 3.5$	0.14 ± 0.00
$2 < p_T < 3$	$3.5 < y^* < 4.0$	0.12 ± 0.00
$3 < p_T < 4$	$1.5 < y^* < 2.0$	0.15 ± 0.01
$3 < p_T < 4$	$2.0 < y^* < 2.5$	0.16 ± 0.00
$3 < p_T < 4$	$2.5 < y^* < 3.0$	0.15 ± 0.00
$3 < p_T < 4$	$3.0 < y^* < 3.5$	0.14 ± 0.00
$3 < p_T < 4$	$3.5 < y^* < 4.0$	0.13 ± 0.00
$4 < p_T < 5$	$1.5 < y^* < 2.0$	0.16 ± 0.01
$4 < p_T < 5$	$2.0 < y^* < 2.5$	0.17 ± 0.00
$4 < p_T < 5$	$2.5 < y^* < 3.0$	0.16 ± 0.00
$4 < p_T < 5$	$3.0 < y^* < 3.5$	0.15 ± 0.00
$4 < p_T < 5$	$3.5 < y^* < 4.0$	0.14 ± 0.01
$5 < p_T < 6$	$1.5 < y^* < 2.0$	0.18 ± 0.01
$5 < p_T < 6$	$2.0 < y^* < 2.5$	0.18 ± 0.00
$5 < p_T < 6$	$2.5 < y^* < 3.0$	0.18 ± 0.00
$5 < p_T < 6$	$3.0 < y^* < 3.5$	0.17 ± 0.01
$5 < p_T < 6$	$3.5 < y^* < 4.0$	0.15 ± 0.01
$6 < p_T < 7$	$1.5 < y^* < 2.0$	0.21 ± 0.01
$6 < p_T < 7$	$2.0 < y^* < 2.5$	0.19 ± 0.01
$6 < p_T < 7$	$2.5 < y^* < 3.0$	0.20 ± 0.01
$6 < p_T < 7$	$3.0 < y^* < 3.5$	0.19 ± 0.01
$6 < p_T < 7$	$3.5 < y^* < 4.0$	0.15 ± 0.01
$7 < p_T < 8$	$1.5 < y^* < 2.0$	0.24 ± 0.01
$7 < p_T < 8$	$2.0 < y^* < 2.5$	0.22 ± 0.01

Table 49: f_b of J/ψ in pPb, in bins of p_T and y^* . The uncertainty is the total one.

p_T bin	y^* bin	f_b
$7 < p_T < 8$	$3.0 < y^* < 3.5$	0.21 ± 0.01
$7 < p_T < 8$	$3.5 < y^* < 4.0$	0.19 ± 0.01
$8 < p_T < 9$	$1.5 < y^* < 2.0$	0.25 ± 0.02
$8 < p_T < 9$	$2.0 < y^* < 2.5$	0.24 ± 0.01
$8 < p_T < 9$	$2.5 < y^* < 3.0$	0.23 ± 0.01
$8 < p_T < 9$	$3.0 < y^* < 3.5$	0.22 ± 0.01
$8 < p_T < 9$	$3.5 < y^* < 4.0$	0.21 ± 0.02
$9 < p_T < 10$	$1.5 < y^* < 2.0$	0.27 ± 0.02
$9 < p_T < 10$	$2.0 < y^* < 2.5$	0.26 ± 0.01
$9 < p_T < 10$	$2.5 < y^* < 3.0$	0.25 ± 0.01
$9 < p_T < 10$	$3.0 < y^* < 3.5$	0.24 ± 0.02
$9 < p_T < 10$	$3.5 < y^* < 4.0$	0.20 ± 0.02
$10 < p_T < 11$	$1.5 < y^* < 2.0$	0.29 ± 0.02
$10 < p_T < 11$	$2.0 < y^* < 2.5$	0.26 ± 0.02
$10 < p_T < 11$	$2.5 < y^* < 3.0$	0.26 ± 0.02
$10 < p_T < 11$	$3.0 < y^* < 3.5$	0.24 ± 0.02
$10 < p_T < 11$	$3.5 < y^* < 4.0$	0.26 ± 0.03
$11 < p_T < 12$	$1.5 < y^* < 2.0$	0.30 ± 0.03
$11 < p_T < 12$	$2.0 < y^* < 2.5$	0.30 ± 0.02
$11 < p_T < 12$	$2.5 < y^* < 3.0$	0.25 ± 0.03
$11 < p_T < 12$	$3.0 < y^* < 3.5$	0.28 ± 0.03
$11 < p_T < 12$	$3.5 < y^* < 4.0$	0.18 ± 0.04
$12 < p_T < 13$	$1.5 < y^* < 2.0$	0.31 ± 0.03
$12 < p_T < 13$	$2.0 < y^* < 2.5$	0.33 ± 0.03
$12 < p_T < 13$	$2.5 < y^* < 3.0$	0.32 ± 0.03
$12 < p_T < 13$	$3.0 < y^* < 3.5$	0.30 ± 0.04
$12 < p_T < 13$	$3.5 < y^* < 4.0$	0.26 ± 0.04
$13 < p_T < 14$	$1.5 < y^* < 2.0$	0.36 ± 0.04
$13 < p_T < 14$	$2.0 < y^* < 2.5$	0.39 ± 0.03
$13 < p_T < 14$	$2.5 < y^* < 3.0$	0.32 ± 0.04
$13 < p_T < 14$	$3.0 < y^* < 3.5$	0.30 ± 0.04
$13 < p_T < 14$	$3.5 < y^* < 4.0$	0.29 ± 0.06

Table 50: f_b of J/ψ in Pb p , in bins of p_T and y^* . The uncertainty is the total one.

p_T bin	y^* bin	f_b
$0 < p_T < 1$	$-3.0 < y^* < -2.5$	0.11 ± 0.00
$0 < p_T < 1$	$-3.5 < y^* < -3.0$	0.09 ± 0.00
$0 < p_T < 1$	$-4.0 < y^* < -3.5$	0.09 ± 0.00
$0 < p_T < 1$	$-4.5 < y^* < -4.0$	0.08 ± 0.00
$0 < p_T < 1$	$-5.0 < y^* < -4.5$	0.06 ± 0.01
$1 < p_T < 2$	$-3.0 < y^* < -2.5$	0.12 ± 0.00
$1 < p_T < 2$	$-3.5 < y^* < -3.0$	0.10 ± 0.00
$1 < p_T < 2$	$-4.0 < y^* < -3.5$	0.10 ± 0.00
$1 < p_T < 2$	$-4.5 < y^* < -4.0$	0.08 ± 0.00
$1 < p_T < 2$	$-5.0 < y^* < -4.5$	0.07 ± 0.00
$2 < p_T < 3$	$-3.0 < y^* < -2.5$	0.12 ± 0.00
$2 < p_T < 3$	$-3.5 < y^* < -3.0$	0.11 ± 0.00
$2 < p_T < 3$	$-4.0 < y^* < -3.5$	0.11 ± 0.00
$2 < p_T < 3$	$-4.5 < y^* < -4.0$	0.09 ± 0.00
$2 < p_T < 3$	$-5.0 < y^* < -4.5$	0.07 ± 0.00
$3 < p_T < 4$	$-3.0 < y^* < -2.5$	0.13 ± 0.00
$3 < p_T < 4$	$-3.5 < y^* < -3.0$	0.13 ± 0.00
$3 < p_T < 4$	$-4.0 < y^* < -3.5$	0.11 ± 0.00
$3 < p_T < 4$	$-4.5 < y^* < -4.0$	0.10 ± 0.00
$3 < p_T < 4$	$-5.0 < y^* < -4.5$	0.07 ± 0.00
$4 < p_T < 5$	$-3.0 < y^* < -2.5$	0.15 ± 0.00
$4 < p_T < 5$	$-3.5 < y^* < -3.0$	0.14 ± 0.00
$4 < p_T < 5$	$-4.0 < y^* < -3.5$	0.13 ± 0.00
$4 < p_T < 5$	$-4.5 < y^* < -4.0$	0.11 ± 0.00
$4 < p_T < 5$	$-5.0 < y^* < -4.5$	0.09 ± 0.01
$5 < p_T < 6$	$-3.0 < y^* < -2.5$	0.14 ± 0.01
$5 < p_T < 6$	$-3.5 < y^* < -3.0$	0.15 ± 0.00
$5 < p_T < 6$	$-4.0 < y^* < -3.5$	0.14 ± 0.00
$5 < p_T < 6$	$-4.5 < y^* < -4.0$	0.12 ± 0.01
$5 < p_T < 6$	$-5.0 < y^* < -4.5$	0.10 ± 0.01
$6 < p_T < 7$	$-3.0 < y^* < -2.5$	0.16 ± 0.01
$6 < p_T < 7$	$-3.5 < y^* < -3.0$	0.16 ± 0.01
$6 < p_T < 7$	$-4.0 < y^* < -3.5$	0.15 ± 0.01
$6 < p_T < 7$	$-4.5 < y^* < -4.0$	0.14 ± 0.01
$6 < p_T < 7$	$-5.0 < y^* < -4.5$	0.11 ± 0.01

Table 51: f_b of J/ψ in Pb p , in bins of p_T and y^* . The uncertainty is the total one.

p_T bin	y^* bin	f_b
$7 < p_T < 8$	$-3.5 < y^* < -3.0$	0.18 ± 0.01
$7 < p_T < 8$	$-4.0 < y^* < -3.5$	0.16 ± 0.01
$7 < p_T < 8$	$-4.5 < y^* < -4.0$	0.14 ± 0.01
$7 < p_T < 8$	$-5.0 < y^* < -4.5$	0.11 ± 0.02
$8 < p_T < 9$	$-3.0 < y^* < -2.5$	0.24 ± 0.01
$8 < p_T < 9$	$-3.5 < y^* < -3.0$	0.20 ± 0.01
$8 < p_T < 9$	$-4.0 < y^* < -3.5$	0.17 ± 0.01
$8 < p_T < 9$	$-4.5 < y^* < -4.0$	0.17 ± 0.01
$8 < p_T < 9$	$-5.0 < y^* < -4.5$	0.16 ± 0.03
$9 < p_T < 10$	$-3.0 < y^* < -2.5$	0.25 ± 0.01
$9 < p_T < 10$	$-3.5 < y^* < -3.0$	0.21 ± 0.01
$9 < p_T < 10$	$-4.0 < y^* < -3.5$	0.20 ± 0.02
$9 < p_T < 10$	$-4.5 < y^* < -4.0$	0.17 ± 0.02
$9 < p_T < 10$	$-5.0 < y^* < -4.5$	0.12 ± 0.03
$10 < p_T < 11$	$-3.0 < y^* < -2.5$	0.24 ± 0.02
$10 < p_T < 11$	$-3.5 < y^* < -3.0$	0.20 ± 0.02
$10 < p_T < 11$	$-4.0 < y^* < -3.5$	0.24 ± 0.02
$10 < p_T < 11$	$-4.5 < y^* < -4.0$	0.21 ± 0.03
$10 < p_T < 11$	$-5.0 < y^* < -4.5$	0.13 ± 0.04
$11 < p_T < 12$	$-3.0 < y^* < -2.5$	0.34 ± 0.02
$11 < p_T < 12$	$-3.5 < y^* < -3.0$	0.29 ± 0.02
$11 < p_T < 12$	$-4.0 < y^* < -3.5$	0.24 ± 0.03
$11 < p_T < 12$	$-4.5 < y^* < -4.0$	0.12 ± 0.03
$11 < p_T < 12$	$-5.0 < y^* < -4.5$	0.30 ± 0.07
$12 < p_T < 13$	$-3.0 < y^* < -2.5$	0.31 ± 0.03
$12 < p_T < 13$	$-3.5 < y^* < -3.0$	0.27 ± 0.03
$12 < p_T < 13$	$-4.0 < y^* < -3.5$	0.25 ± 0.04
$12 < p_T < 13$	$-4.5 < y^* < -4.0$	0.24 ± 0.05
$12 < p_T < 13$	$-5.0 < y^* < -4.5$	0.12 ± 0.07
$13 < p_T < 14$	$-3.0 < y^* < -2.5$	0.32 ± 0.05
$13 < p_T < 14$	$-3.5 < y^* < -3.0$	0.31 ± 0.06
$13 < p_T < 14$	$-4.0 < y^* < -3.5$	0.32 ± 0.04
$13 < p_T < 14$	$-4.5 < y^* < -4.0$	0.23 ± 0.06
$13 < p_T < 14$	$-5.0 < y^* < -4.5$	0.36 ± 0.25

761 **E Nuclear modification factor numerical results**

762 **E.1 $R_{p\text{Pb}}$ for prompt J/ψ in $p\text{Pb}$**

Table 52: Prompt J/ψ nuclear modification factor, $R_{p\text{Pb}}$ in $p\text{Pb}$, as a function of p_{T} for the different rapidity bins.

	p_{T} bin	y^* bin	$R_{p\text{Pb}}$
0	$< p_{\text{T}} < 1000$	$1.5 < y^* < 2.0$	0.598 ± 0.103
0	$< p_{\text{T}} < 1000$	$2.0 < y^* < 2.5$	0.610 ± 0.077
0	$< p_{\text{T}} < 1000$	$2.5 < y^* < 3.0$	0.490 ± 0.048
0	$< p_{\text{T}} < 1000$	$3.0 < y^* < 3.5$	0.456 ± 0.042
0	$< p_{\text{T}} < 1000$	$3.5 < y^* < 4.0$	0.461 ± 0.043
1000	$< p_{\text{T}} < 2000$	$1.5 < y^* < 2.0$	0.608 ± 0.076
1000	$< p_{\text{T}} < 2000$	$2.0 < y^* < 2.5$	0.632 ± 0.061
1000	$< p_{\text{T}} < 2000$	$2.5 < y^* < 3.0$	0.537 ± 0.059
1000	$< p_{\text{T}} < 2000$	$3.0 < y^* < 3.5$	0.506 ± 0.044
1000	$< p_{\text{T}} < 2000$	$3.5 < y^* < 4.0$	0.503 ± 0.049
2000	$< p_{\text{T}} < 3000$	$1.5 < y^* < 2.0$	0.676 ± 0.086
2000	$< p_{\text{T}} < 3000$	$2.0 < y^* < 2.5$	0.694 ± 0.066
2000	$< p_{\text{T}} < 3000$	$2.5 < y^* < 3.0$	0.641 ± 0.052
2000	$< p_{\text{T}} < 3000$	$3.0 < y^* < 3.5$	0.603 ± 0.046
2000	$< p_{\text{T}} < 3000$	$3.5 < y^* < 4.0$	0.585 ± 0.052
3000	$< p_{\text{T}} < 4000$	$1.5 < y^* < 2.0$	0.741 ± 0.109
3000	$< p_{\text{T}} < 4000$	$2.0 < y^* < 2.5$	0.784 ± 0.079
3000	$< p_{\text{T}} < 4000$	$2.5 < y^* < 3.0$	0.705 ± 0.062
3000	$< p_{\text{T}} < 4000$	$3.0 < y^* < 3.5$	0.674 ± 0.056
3000	$< p_{\text{T}} < 4000$	$3.5 < y^* < 4.0$	0.640 ± 0.060
4000	$< p_{\text{T}} < 5000$	$1.5 < y^* < 2.0$	0.778 ± 0.119
4000	$< p_{\text{T}} < 5000$	$2.0 < y^* < 2.5$	0.825 ± 0.082
4000	$< p_{\text{T}} < 5000$	$2.5 < y^* < 3.0$	0.759 ± 0.063
4000	$< p_{\text{T}} < 5000$	$3.0 < y^* < 3.5$	0.740 ± 0.060
4000	$< p_{\text{T}} < 5000$	$3.5 < y^* < 4.0$	0.676 ± 0.062
5000	$< p_{\text{T}} < 6000$	$1.5 < y^* < 2.0$	0.837 ± 0.125
5000	$< p_{\text{T}} < 6000$	$2.0 < y^* < 2.5$	0.873 ± 0.080
5000	$< p_{\text{T}} < 6000$	$2.5 < y^* < 3.0$	0.768 ± 0.064
5000	$< p_{\text{T}} < 6000$	$3.0 < y^* < 3.5$	0.808 ± 0.068
5000	$< p_{\text{T}} < 6000$	$3.5 < y^* < 4.0$	0.749 ± 0.074
6000	$< p_{\text{T}} < 7000$	$1.5 < y^* < 2.0$	0.867 ± 0.147
6000	$< p_{\text{T}} < 7000$	$2.0 < y^* < 2.5$	0.916 ± 0.090
6000	$< p_{\text{T}} < 7000$	$2.5 < y^* < 3.0$	0.814 ± 0.075
6000	$< p_{\text{T}} < 7000$	$3.0 < y^* < 3.5$	0.828 ± 0.075
6000	$< p_{\text{T}} < 7000$	$3.5 < y^* < 4.0$	0.857 ± 0.090
7000	$< p_{\text{T}} < 8000$	$1.5 < y^* < 2.0$	0.906 ± 0.168
7000	$< p_{\text{T}} < 8000$	$2.0 < y^* < 2.5$	0.870 ± 0.081
7000	$< p_{\text{T}} < 8000$	$2.5 < y^* < 3.0$	0.807 ± 0.073
7000	$< p_{\text{T}} < 8000$	$3.0 < y^* < 3.5$	0.893 ± 0.083
7000	$< p_{\text{T}} < 8000$	$3.5 < y^* < 4.0$	0.886 ± 0.107
8000	$< p_{\text{T}} < 9000$	$1.5 < y^* < 2.0$	0.859 ± 0.165
8000	$< p_{\text{T}} < 9000$	$2.0 < y^* < 2.5$	0.922 ± 0.090
8000	$< p_{\text{T}} < 9000$	$2.5 < y^* < 3.0$	0.854 ± 0.077
8000	$< p_{\text{T}} < 9000$	$3.0 < y^* < 3.5$	0.861 ± 0.085
8000	$< p_{\text{T}} < 9000$	$3.5 < y^* < 4.0$	0.951 ± 0.123
9000	$< p_{\text{T}} < 10000$	$1.5 < y^* < 2.0$	0.940 ± 0.191
9000	$< p_{\text{T}} < 10000$	$2.0 < y^* < 2.5$	0.920 ± 0.091
9000	$< p_{\text{T}} < 10000$	$2.5 < y^* < 3.0$	0.833 ± 0.081
9000	$< p_{\text{T}} < 10000$	$3.0 < y^* < 3.5$	0.928 ± 0.101
9000	$< p_{\text{T}} < 10000$	$3.5 < y^* < 4.0$	1.070 ± 0.157
10000	$< p_{\text{T}} < 11000$	$1.5 < y^* < 2.0$	0.849 ± 0.179
10000	$< p_{\text{T}} < 11000$	$2.0 < y^* < 2.5$	0.932 ± 0.102

Table 53: Prompt J/ψ nuclear modification factor, $R_{p\text{Pb}}$ in $p\text{Pb}$, as a function of p_{T} for the different rapidity bins..

p_{T} bin	y^* bin	$R_{p\text{Pb}}$
$10000 < p_{\text{T}} < 11000$	$3.0 < y^* < 3.5$	0.779 ± 0.093
$10000 < p_{\text{T}} < 11000$	$3.5 < y^* < 4.0$	0.951 ± 0.165
$11000 < p_{\text{T}} < 12000$	$1.5 < y^* < 2.0$	1.043 ± 0.213
$11000 < p_{\text{T}} < 12000$	$2.0 < y^* < 2.5$	1.000 ± 0.118
$11000 < p_{\text{T}} < 12000$	$2.5 < y^* < 3.0$	0.950 ± 0.110
$11000 < p_{\text{T}} < 12000$	$3.0 < y^* < 3.5$	0.927 ± 0.120
$11000 < p_{\text{T}} < 12000$	$3.5 < y^* < 4.0$	1.132 ± 0.182
$12000 < p_{\text{T}} < 13000$	$1.5 < y^* < 2.0$	0.983 ± 0.253
$12000 < p_{\text{T}} < 13000$	$2.0 < y^* < 2.5$	0.886 ± 0.116
$12000 < p_{\text{T}} < 13000$	$2.5 < y^* < 3.0$	0.892 ± 0.116
$12000 < p_{\text{T}} < 13000$	$3.0 < y^* < 3.5$	0.752 ± 0.112
$12000 < p_{\text{T}} < 13000$	$3.5 < y^* < 4.0$	1.234 ± 0.281
$13000 < p_{\text{T}} < 14000$	$1.5 < y^* < 2.0$	0.868 ± 0.242
$13000 < p_{\text{T}} < 14000$	$2.0 < y^* < 2.5$	0.843 ± 0.129
$13000 < p_{\text{T}} < 14000$	$2.5 < y^* < 3.0$	0.738 ± 0.106
$13000 < p_{\text{T}} < 14000$	$3.0 < y^* < 3.5$	0.884 ± 0.158
$13000 < p_{\text{T}} < 14000$	$3.5 < y^* < 4.0$	0.773 ± 0.168

E.2 $R_{p\text{Pb}}$ for J/ψ from b in $p\text{Pb}$

Table 54: J/ψ from b nuclear modification factor, $R_{p\text{Pb}}$ in $p\text{Pb}$, as a function of p_{T} for the different rapidity bins.

	p_{T} bin	y^* bin	$R_{p\text{Pb}}$
0	$< p_{\text{T}} < 1000$	$1.5 < y^* < 2.0$	0.777 ± 0.200
0	$< p_{\text{T}} < 1000$	$2.0 < y^* < 2.5$	0.843 ± 0.170
0	$< p_{\text{T}} < 1000$	$2.5 < y^* < 3.0$	0.671 ± 0.086
0	$< p_{\text{T}} < 1000$	$3.0 < y^* < 3.5$	0.675 ± 0.072
0	$< p_{\text{T}} < 1000$	$3.5 < y^* < 4.0$	0.746 ± 0.082
1000	$< p_{\text{T}} < 2000$	$1.5 < y^* < 2.0$	0.809 ± 0.138
1000	$< p_{\text{T}} < 2000$	$2.0 < y^* < 2.5$	0.853 ± 0.088
1000	$< p_{\text{T}} < 2000$	$2.5 < y^* < 3.0$	0.740 ± 0.079
1000	$< p_{\text{T}} < 2000$	$3.0 < y^* < 3.5$	0.719 ± 0.060
1000	$< p_{\text{T}} < 2000$	$3.5 < y^* < 4.0$	0.847 ± 0.082
2000	$< p_{\text{T}} < 3000$	$1.5 < y^* < 2.0$	0.825 ± 0.156
2000	$< p_{\text{T}} < 3000$	$2.0 < y^* < 2.5$	0.879 ± 0.086
2000	$< p_{\text{T}} < 3000$	$2.5 < y^* < 3.0$	0.798 ± 0.066
2000	$< p_{\text{T}} < 3000$	$3.0 < y^* < 3.5$	0.808 ± 0.069
2000	$< p_{\text{T}} < 3000$	$3.5 < y^* < 4.0$	0.787 ± 0.081
3000	$< p_{\text{T}} < 4000$	$1.5 < y^* < 2.0$	0.850 ± 0.178
3000	$< p_{\text{T}} < 4000$	$2.0 < y^* < 2.5$	0.934 ± 0.095
3000	$< p_{\text{T}} < 4000$	$2.5 < y^* < 3.0$	0.823 ± 0.077
3000	$< p_{\text{T}} < 4000$	$3.0 < y^* < 3.5$	0.823 ± 0.073
3000	$< p_{\text{T}} < 4000$	$3.5 < y^* < 4.0$	0.802 ± 0.087
4000	$< p_{\text{T}} < 5000$	$1.5 < y^* < 2.0$	0.809 ± 0.171
4000	$< p_{\text{T}} < 5000$	$2.0 < y^* < 2.5$	0.970 ± 0.092
4000	$< p_{\text{T}} < 5000$	$2.5 < y^* < 3.0$	0.870 ± 0.078
4000	$< p_{\text{T}} < 5000$	$3.0 < y^* < 3.5$	0.865 ± 0.077
4000	$< p_{\text{T}} < 5000$	$3.5 < y^* < 4.0$	0.824 ± 0.092
5000	$< p_{\text{T}} < 6000$	$1.5 < y^* < 2.0$	0.905 ± 0.202
5000	$< p_{\text{T}} < 6000$	$2.0 < y^* < 2.5$	0.929 ± 0.090
5000	$< p_{\text{T}} < 6000$	$2.5 < y^* < 3.0$	0.874 ± 0.081
5000	$< p_{\text{T}} < 6000$	$3.0 < y^* < 3.5$	0.925 ± 0.092
5000	$< p_{\text{T}} < 6000$	$3.5 < y^* < 4.0$	0.882 ± 0.106
6000	$< p_{\text{T}} < 7000$	$1.5 < y^* < 2.0$	0.967 ± 0.233
6000	$< p_{\text{T}} < 7000$	$2.0 < y^* < 2.5$	0.903 ± 0.094
6000	$< p_{\text{T}} < 7000$	$2.5 < y^* < 3.0$	0.862 ± 0.091
6000	$< p_{\text{T}} < 7000$	$3.0 < y^* < 3.5$	0.945 ± 0.101
6000	$< p_{\text{T}} < 7000$	$3.5 < y^* < 4.0$	0.869 ± 0.126
7000	$< p_{\text{T}} < 8000$	$1.5 < y^* < 2.0$	1.081 ± 0.268
7000	$< p_{\text{T}} < 8000$	$2.0 < y^* < 2.5$	0.929 ± 0.096
7000	$< p_{\text{T}} < 8000$	$2.5 < y^* < 3.0$	0.963 ± 0.099
7000	$< p_{\text{T}} < 8000$	$3.0 < y^* < 3.5$	0.982 ± 0.108
7000	$< p_{\text{T}} < 8000$	$3.5 < y^* < 4.0$	0.944 ± 0.153
8000	$< p_{\text{T}} < 9000$	$1.5 < y^* < 2.0$	0.937 ± 0.264
8000	$< p_{\text{T}} < 9000$	$2.0 < y^* < 2.5$	0.945 ± 0.103
8000	$< p_{\text{T}} < 9000$	$2.5 < y^* < 3.0$	0.876 ± 0.097
8000	$< p_{\text{T}} < 9000$	$3.0 < y^* < 3.5$	0.914 ± 0.117
8000	$< p_{\text{T}} < 9000$	$3.5 < y^* < 4.0$	1.147 ± 0.187
9000	$< p_{\text{T}} < 10000$	$1.5 < y^* < 2.0$	0.980 ± 0.260
9000	$< p_{\text{T}} < 10000$	$2.0 < y^* < 2.5$	0.931 ± 0.104
9000	$< p_{\text{T}} < 10000$	$2.5 < y^* < 3.0$	0.872 ± 0.103
9000	$< p_{\text{T}} < 10000$	$3.0 < y^* < 3.5$	0.923 ± 0.137
9000	$< p_{\text{T}} < 10000$	$3.5 < y^* < 4.0$	1.007 ± 0.207
10000	$< p_{\text{T}} < 11000$	$1.5 < y^* < 2.0$	0.900 ± 0.276
10000	$< p_{\text{T}} < 11000$	$2.0 < y^* < 2.5$	0.833 ± 0.106

Table 55: J/ψ from b nuclear modification factor, $R_{p\text{Pb}}$ in $p\text{Pb}$, as a function of p_{T} for the different rapidity bins.

p_{T} bin	y^* bin	$R_{p\text{Pb}}$
$10000 < p_{\text{T}} < 11000$	$2.5 < y^* < 3.0$	0.967 ± 0.114
$10000 < p_{\text{T}} < 11000$	$3.0 < y^* < 3.5$	0.791 ± 0.136
$10000 < p_{\text{T}} < 11000$	$3.5 < y^* < 4.0$	1.275 ± 0.302
$11000 < p_{\text{T}} < 12000$	$1.5 < y^* < 2.0$	0.919 ± 0.249
$11000 < p_{\text{T}} < 12000$	$2.0 < y^* < 2.5$	0.836 ± 0.102
$11000 < p_{\text{T}} < 12000$	$2.5 < y^* < 3.0$	0.766 ± 0.120
$11000 < p_{\text{T}} < 12000$	$3.0 < y^* < 3.5$	1.032 ± 0.200
$11000 < p_{\text{T}} < 12000$	$3.5 < y^* < 4.0$	0.783 ± 0.227
$12000 < p_{\text{T}} < 13000$	$1.5 < y^* < 2.0$	0.873 ± 0.304
$12000 < p_{\text{T}} < 13000$	$2.0 < y^* < 2.5$	0.912 ± 0.137
$12000 < p_{\text{T}} < 13000$	$2.5 < y^* < 3.0$	0.848 ± 0.144
$12000 < p_{\text{T}} < 13000$	$3.0 < y^* < 3.5$	0.855 ± 0.176
$12000 < p_{\text{T}} < 13000$	$3.5 < y^* < 4.0$	1.053 ± 0.333
$13000 < p_{\text{T}} < 14000$	$1.5 < y^* < 2.0$	1.009 ± 0.392
$13000 < p_{\text{T}} < 14000$	$2.0 < y^* < 2.5$	1.097 ± 0.200
$13000 < p_{\text{T}} < 14000$	$2.5 < y^* < 3.0$	0.772 ± 0.145
$13000 < p_{\text{T}} < 14000$	$3.0 < y^* < 3.5$	0.810 ± 0.194
$13000 < p_{\text{T}} < 14000$	$3.5 < y^* < 4.0$	1.208 ± 0.537

E.3 $R_{p\text{Pb}}$ for prompt J/ψ in PbP

Table 56: Prompt J/ψ nuclear modification factor, $R_{p\text{Pb}}$ in PbP, as a function of p_T for the different rapidity bins.

p_T bin	y^* bin	$R_{p\text{Pb}}$
0 < p_T < 1000	2.5 < y^* < 3.0	0.818 \pm 0.153
0 < p_T < 1000	3.0 < y^* < 3.5	0.746 \pm 0.100
0 < p_T < 1000	3.5 < y^* < 4.0	0.696 \pm 0.082
0 < p_T < 1000	4.0 < y^* < 4.5	0.719 \pm 0.078
0 < p_T < 1000	4.5 < y^* < 5.0	0.733 \pm 0.111
1000 < p_T < 2000	2.5 < y^* < 3.0	0.849 \pm 0.126
1000 < p_T < 2000	3.0 < y^* < 3.5	0.793 \pm 0.092
1000 < p_T < 2000	3.5 < y^* < 4.0	0.751 \pm 0.082
1000 < p_T < 2000	4.0 < y^* < 4.5	0.791 \pm 0.082
1000 < p_T < 2000	4.5 < y^* < 5.0	0.852 \pm 0.172
2000 < p_T < 3000	2.5 < y^* < 3.0	0.938 \pm 0.124
2000 < p_T < 3000	3.0 < y^* < 3.5	0.911 \pm 0.097
2000 < p_T < 3000	3.5 < y^* < 4.0	0.906 \pm 0.087
2000 < p_T < 3000	4.0 < y^* < 4.5	0.905 \pm 0.092
2000 < p_T < 3000	4.5 < y^* < 5.0	1.016 \pm 0.303
3000 < p_T < 4000	2.5 < y^* < 3.0	0.940 \pm 0.131
3000 < p_T < 4000	3.0 < y^* < 3.5	0.981 \pm 0.112
3000 < p_T < 4000	3.5 < y^* < 4.0	0.987 \pm 0.102
3000 < p_T < 4000	4.0 < y^* < 4.5	0.997 \pm 0.121
3000 < p_T < 4000	4.5 < y^* < 5.0	1.210 \pm 0.542
4000 < p_T < 5000	2.5 < y^* < 3.0	0.985 \pm 0.127
4000 < p_T < 5000	3.0 < y^* < 3.5	1.007 \pm 0.107
4000 < p_T < 5000	3.5 < y^* < 4.0	1.000 \pm 0.099
4000 < p_T < 5000	4.0 < y^* < 4.5	1.030 \pm 0.141
4000 < p_T < 5000	4.5 < y^* < 5.0	1.298 \pm 0.837
5000 < p_T < 6000	2.5 < y^* < 3.0	1.029 \pm 0.126
5000 < p_T < 6000	3.0 < y^* < 3.5	1.005 \pm 0.105
5000 < p_T < 6000	3.5 < y^* < 4.0	0.987 \pm 0.102
5000 < p_T < 6000	4.0 < y^* < 4.5	1.065 \pm 0.163
5000 < p_T < 6000	4.5 < y^* < 5.0	1.803 \pm 1.903
6000 < p_T < 7000	2.5 < y^* < 3.0	0.960 \pm 0.120
6000 < p_T < 7000	3.0 < y^* < 3.5	1.065 \pm 0.114
6000 < p_T < 7000	3.5 < y^* < 4.0	1.025 \pm 0.116
6000 < p_T < 7000	4.0 < y^* < 4.5	1.174 \pm 0.202
6000 < p_T < 7000	4.5 < y^* < 5.0	2.098 \pm 3.280
7000 < p_T < 8000	2.5 < y^* < 3.0	0.965 \pm 0.113
7000 < p_T < 8000	3.0 < y^* < 3.5	1.038 \pm 0.113
7000 < p_T < 8000	3.5 < y^* < 4.0	1.052 \pm 0.128
7000 < p_T < 8000	4.0 < y^* < 4.5	1.018 \pm 0.191
7000 < p_T < 8000	4.5 < y^* < 5.0	2.879 \pm 6.690
8000 < p_T < 9000	2.5 < y^* < 3.0	0.944 \pm 0.113
8000 < p_T < 9000	3.0 < y^* < 3.5	1.085 \pm 0.123
8000 < p_T < 9000	3.5 < y^* < 4.0	1.022 \pm 0.145
8000 < p_T < 9000	4.0 < y^* < 4.5	1.022 \pm 0.213
8000 < p_T < 9000	4.5 < y^* < 5.0	4.435 \pm 24.864
9000 < p_T < 10000	2.5 < y^* < 3.0	1.005 \pm 0.128
9000 < p_T < 10000	3.0 < y^* < 3.5	1.024 \pm 0.129
9000 < p_T < 10000	3.5 < y^* < 4.0	0.943 \pm 0.158
9000 < p_T < 10000	4.0 < y^* < 4.5	1.053 \pm 0.241
9000 < p_T < 10000	4.5 < y^* < 5.0	-3.244 \pm 0.000

Table 57: Prompt J/ψ nuclear modification factor, $R_{p\text{Pb}}$ in $\text{Pb}p$, as a function of p_{T} for the different rapidity bins..

p_{T} bin	y^* bin	$R_{p\text{Pb}}$
$10000 < p_{\text{T}} < 11000$	$3.0 < y^* < 3.5$	0.986 ± 0.127
$10000 < p_{\text{T}} < 11000$	$3.5 < y^* < 4.0$	0.998 ± 0.176
$10000 < p_{\text{T}} < 11000$	$4.0 < y^* < 4.5$	0.835 ± 0.206
$10000 < p_{\text{T}} < 11000$	$4.5 < y^* < 5.0$	-1.432 ± 0.000
$11000 < p_{\text{T}} < 12000$	$2.5 < y^* < 3.0$	0.945 ± 0.133
$11000 < p_{\text{T}} < 12000$	$3.0 < y^* < 3.5$	0.863 ± 0.122
$11000 < p_{\text{T}} < 12000$	$3.5 < y^* < 4.0$	0.901 ± 0.171
$11000 < p_{\text{T}} < 12000$	$4.0 < y^* < 4.5$	0.952 ± 0.282
$11000 < p_{\text{T}} < 12000$	$4.5 < y^* < 5.0$	-0.990 ± 0.000
$12000 < p_{\text{T}} < 13000$	$2.5 < y^* < 3.0$	1.117 ± 0.183
$12000 < p_{\text{T}} < 13000$	$3.0 < y^* < 3.5$	0.927 ± 0.150
$12000 < p_{\text{T}} < 13000$	$3.5 < y^* < 4.0$	0.886 ± 0.215
$12000 < p_{\text{T}} < 13000$	$4.0 < y^* < 4.5$	1.004 ± 0.322
$12000 < p_{\text{T}} < 13000$	$4.5 < y^* < 5.0$	-0.656 ± 0.000
$13000 < p_{\text{T}} < 14000$	$2.5 < y^* < 3.0$	0.848 ± 0.161
$13000 < p_{\text{T}} < 14000$	$3.0 < y^* < 3.5$	0.832 ± 0.181
$13000 < p_{\text{T}} < 14000$	$3.5 < y^* < 4.0$	0.797 ± 0.219
$13000 < p_{\text{T}} < 14000$	$4.0 < y^* < 4.5$	1.301 ± 0.637
$13000 < p_{\text{T}} < 14000$	$4.5 < y^* < 5.0$	-0.069 ± 0.000

E.4 $R_{p\text{Pb}}$ for J/ψ from b in $\text{Pb}p$

Table 58: J/ψ from b nuclear modification factor, $R_{p\text{Pb}}$ in $\text{Pb}p$, as a function of p_{T} for the different rapidity bins.

	p_{T} bin	y^* bin	$R_{p\text{Pb}}$	
0	$< p_{\text{T}} < 1000$	$2.5 < y^* < 3.0$	$1.048 \pm$	0.217
0	$< p_{\text{T}} < 1000$	$3.0 < y^* < 3.5$	$0.888 \pm$	0.127
0	$< p_{\text{T}} < 1000$	$3.5 < y^* < 4.0$	$0.944 \pm$	0.118
0	$< p_{\text{T}} < 1000$	$4.0 < y^* < 4.5$	$1.168 \pm$	0.153
0	$< p_{\text{T}} < 1000$	$4.5 < y^* < 5.0$	$2.307 \pm$	2.868
1000	$< p_{\text{T}} < 2000$	$2.5 < y^* < 3.0$	$1.057 \pm$	0.156
1000	$< p_{\text{T}} < 2000$	$3.0 < y^* < 3.5$	$0.918 \pm$	0.104
1000	$< p_{\text{T}} < 2000$	$3.5 < y^* < 4.0$	$1.000 \pm$	0.105
1000	$< p_{\text{T}} < 2000$	$4.0 < y^* < 4.5$	$1.048 \pm$	0.115
1000	$< p_{\text{T}} < 2000$	$4.5 < y^* < 5.0$	$1.809 \pm$	1.866
2000	$< p_{\text{T}} < 3000$	$2.5 < y^* < 3.0$	$0.987 \pm$	0.132
2000	$< p_{\text{T}} < 3000$	$3.0 < y^* < 3.5$	$0.979 \pm$	0.110
2000	$< p_{\text{T}} < 3000$	$3.5 < y^* < 4.0$	$1.081 \pm$	0.114
2000	$< p_{\text{T}} < 3000$	$4.0 < y^* < 4.5$	$1.093 \pm$	0.125
2000	$< p_{\text{T}} < 3000$	$4.5 < y^* < 5.0$	$2.505 \pm$	4.448
3000	$< p_{\text{T}} < 4000$	$2.5 < y^* < 3.0$	$0.969 \pm$	0.140
3000	$< p_{\text{T}} < 4000$	$3.0 < y^* < 3.5$	$1.067 \pm$	0.125
3000	$< p_{\text{T}} < 4000$	$3.5 < y^* < 4.0$	$1.079 \pm$	0.122
3000	$< p_{\text{T}} < 4000$	$4.0 < y^* < 4.5$	$1.142 \pm$	0.152
3000	$< p_{\text{T}} < 4000$	$4.5 < y^* < 5.0$	$3.175 \pm$	9.129
4000	$< p_{\text{T}} < 5000$	$2.5 < y^* < 3.0$	$1.026 \pm$	0.137
4000	$< p_{\text{T}} < 5000$	$3.0 < y^* < 3.5$	$1.029 \pm$	0.114
4000	$< p_{\text{T}} < 5000$	$3.5 < y^* < 4.0$	$1.081 \pm$	0.120
4000	$< p_{\text{T}} < 5000$	$4.0 < y^* < 4.5$	$1.143 \pm$	0.178
4000	$< p_{\text{T}} < 5000$	$4.5 < y^* < 5.0$	$10.646 \pm$	122.657
5000	$< p_{\text{T}} < 6000$	$2.5 < y^* < 3.0$	$0.882 \pm$	0.115
5000	$< p_{\text{T}} < 6000$	$3.0 < y^* < 3.5$	$1.025 \pm$	0.119
5000	$< p_{\text{T}} < 6000$	$3.5 < y^* < 4.0$	$1.039 \pm$	0.121
5000	$< p_{\text{T}} < 6000$	$4.0 < y^* < 4.5$	$1.108 \pm$	0.185
5000	$< p_{\text{T}} < 6000$	$4.5 < y^* < 5.0$	$-7.474 \pm$	0.000
6000	$< p_{\text{T}} < 7000$	$2.5 < y^* < 3.0$	$0.823 \pm$	0.113
6000	$< p_{\text{T}} < 7000$	$3.0 < y^* < 3.5$	$1.025 \pm$	0.122
6000	$< p_{\text{T}} < 7000$	$3.5 < y^* < 4.0$	$1.090 \pm$	0.151
6000	$< p_{\text{T}} < 7000$	$4.0 < y^* < 4.5$	$1.180 \pm$	0.229
6000	$< p_{\text{T}} < 7000$	$4.5 < y^* < 5.0$	$-3.215 \pm$	0.000
7000	$< p_{\text{T}} < 8000$	$2.5 < y^* < 3.0$	$0.917 \pm$	0.119
7000	$< p_{\text{T}} < 8000$	$3.0 < y^* < 3.5$	$0.987 \pm$	0.119
7000	$< p_{\text{T}} < 8000$	$3.5 < y^* < 4.0$	$0.932 \pm$	0.143
7000	$< p_{\text{T}} < 8000$	$4.0 < y^* < 4.5$	$0.947 \pm$	0.199
7000	$< p_{\text{T}} < 8000$	$4.5 < y^* < 5.0$	$-1.802 \pm$	0.000
8000	$< p_{\text{T}} < 9000$	$2.5 < y^* < 3.0$	$0.983 \pm$	0.135
8000	$< p_{\text{T}} < 9000$	$3.0 < y^* < 3.5$	$1.038 \pm$	0.137
8000	$< p_{\text{T}} < 9000$	$3.5 < y^* < 4.0$	$0.930 \pm$	0.154
8000	$< p_{\text{T}} < 9000$	$4.0 < y^* < 4.5$	$1.037 \pm$	0.241
8000	$< p_{\text{T}} < 9000$	$4.5 < y^* < 5.0$	$-0.999 \pm$	0.000
9000	$< p_{\text{T}} < 10000$	$2.5 < y^* < 3.0$	$1.049 \pm$	0.150
9000	$< p_{\text{T}} < 10000$	$3.0 < y^* < 3.5$	$0.848 \pm$	0.134
9000	$< p_{\text{T}} < 10000$	$3.5 < y^* < 4.0$	$0.904 \pm$	0.186
9000	$< p_{\text{T}} < 10000$	$4.0 < y^* < 4.5$	$1.069 \pm$	0.323
9000	$< p_{\text{T}} < 10000$	$4.5 < y^* < 5.0$	$-0.456 \pm$	0.000

Table 59: J/ψ from b nuclear modification factor, $R_{p\text{Pb}}$ in $\text{Pb}p$, as a function of p_{T} for the different rapidity bins.

p_{T} bin	y^* bin	$R_{p\text{Pb}}$
$10000 < p_{\text{T}} < 11000$	$3.0 < y^* < 3.5$	0.795 ± 0.139
$10000 < p_{\text{T}} < 11000$	$3.5 < y^* < 4.0$	1.193 ± 0.276
$10000 < p_{\text{T}} < 11000$	$4.0 < y^* < 4.5$	0.916 ± 0.285
$10000 < p_{\text{T}} < 11000$	$4.5 < y^* < 5.0$	-0.205 ± 0.000
$11000 < p_{\text{T}} < 12000$	$2.5 < y^* < 3.0$	1.151 ± 0.182
$11000 < p_{\text{T}} < 12000$	$3.0 < y^* < 3.5$	0.998 ± 0.190
$11000 < p_{\text{T}} < 12000$	$3.5 < y^* < 4.0$	0.920 ± 0.232
$11000 < p_{\text{T}} < 12000$	$4.0 < y^* < 4.5$	0.687 ± 0.346
$11000 < p_{\text{T}} < 12000$	$4.5 < y^* < 5.0$	-0.425 ± 0.000
$12000 < p_{\text{T}} < 13000$	$2.5 < y^* < 3.0$	1.018 ± 0.198
$12000 < p_{\text{T}} < 13000$	$3.0 < y^* < 3.5$	0.917 ± 0.189
$12000 < p_{\text{T}} < 13000$	$3.5 < y^* < 4.0$	0.735 ± 0.241
$12000 < p_{\text{T}} < 13000$	$4.0 < y^* < 4.5$	1.137 ± 0.550
$12000 < p_{\text{T}} < 13000$	$4.5 < y^* < 5.0$	-0.092 ± 0.000
$13000 < p_{\text{T}} < 14000$	$2.5 < y^* < 3.0$	0.885 ± 0.204
$13000 < p_{\text{T}} < 14000$	$3.0 < y^* < 3.5$	0.781 ± 0.219
$13000 < p_{\text{T}} < 14000$	$3.5 < y^* < 4.0$	1.377 ± 0.626
$13000 < p_{\text{T}} < 14000$	$4.0 < y^* < 4.5$	0.967 ± 0.458
$13000 < p_{\text{T}} < 14000$	$4.5 < y^* < 5.0$	-0.039 ± 0.000

F Forward to backward ratios numerical results

F.1 R_{FB} for prompt J/ψ

Table 60: Prompt J/ψ forward to backward ratio, R_{FB} , as a function of p_{T} for the different rapidity bins.

p_{T} bin	y^* bin	R_{FB}
0 < p_{T} < 1000	2.5 < y^* < 3.0	0.600 ± 0.023
0 < p_{T} < 1000	3.0 < y^* < 3.5	0.612 ± 0.020
0 < p_{T} < 1000	3.5 < y^* < 4.0	0.662 ± 0.023
1000 < p_{T} < 2000	2.5 < y^* < 3.0	0.633 ± 0.019
1000 < p_{T} < 2000	3.0 < y^* < 3.5	0.638 ± 0.018
1000 < p_{T} < 2000	3.5 < y^* < 4.0	0.669 ± 0.020
2000 < p_{T} < 3000	2.5 < y^* < 3.0	0.683 ± 0.021
2000 < p_{T} < 3000	3.0 < y^* < 3.5	0.662 ± 0.019
2000 < p_{T} < 3000	3.5 < y^* < 4.0	0.645 ± 0.019
3000 < p_{T} < 4000	2.5 < y^* < 3.0	0.750 ± 0.023
3000 < p_{T} < 4000	3.0 < y^* < 3.5	0.687 ± 0.020
3000 < p_{T} < 4000	3.5 < y^* < 4.0	0.649 ± 0.020
4000 < p_{T} < 5000	2.5 < y^* < 3.0	0.771 ± 0.026
4000 < p_{T} < 5000	3.0 < y^* < 3.5	0.735 ± 0.023
4000 < p_{T} < 5000	3.5 < y^* < 4.0	0.676 ± 0.023
5000 < p_{T} < 6000	2.5 < y^* < 3.0	0.746 ± 0.028
5000 < p_{T} < 6000	3.0 < y^* < 3.5	0.804 ± 0.027
5000 < p_{T} < 6000	3.5 < y^* < 4.0	0.759 ± 0.029
6000 < p_{T} < 7000	2.5 < y^* < 3.0	0.848 ± 0.036
6000 < p_{T} < 7000	3.0 < y^* < 3.5	0.777 ± 0.031
6000 < p_{T} < 7000	3.5 < y^* < 4.0	0.836 ± 0.039
7000 < p_{T} < 8000	2.5 < y^* < 3.0	0.837 ± 0.043
7000 < p_{T} < 8000	3.0 < y^* < 3.5	0.860 ± 0.041
7000 < p_{T} < 8000	3.5 < y^* < 4.0	0.843 ± 0.050
8000 < p_{T} < 9000	2.5 < y^* < 3.0	0.905 ± 0.059
8000 < p_{T} < 9000	3.0 < y^* < 3.5	0.794 ± 0.048
8000 < p_{T} < 9000	3.5 < y^* < 4.0	0.931 ± 0.068
9000 < p_{T} < 10000	2.5 < y^* < 3.0	0.830 ± 0.068
9000 < p_{T} < 10000	3.0 < y^* < 3.5	0.906 ± 0.069
9000 < p_{T} < 10000	3.5 < y^* < 4.0	1.134 ± 0.106

Table 61: Prompt J/ψ forward to backward ratio, R_{FB} , as a function of p_{T} for the different rapidity bins.

p_{T} bin	y^* bin	$R_{p\text{Pb}}$
$10000 < p_{\text{T}} < 11000$	$3.0 < y^* < 3.5$	0.791 ± 0.076
$10000 < p_{\text{T}} < 11000$	$3.5 < y^* < 4.0$	0.952 ± 0.117
$11000 < p_{\text{T}} < 12000$	$2.5 < y^* < 3.0$	1.005 ± 0.123
$11000 < p_{\text{T}} < 12000$	$3.0 < y^* < 3.5$	1.073 ± 0.125
$11000 < p_{\text{T}} < 12000$	$3.5 < y^* < 4.0$	1.257 ± 0.202
$12000 < p_{\text{T}} < 13000$	$2.5 < y^* < 3.0$	0.799 ± 0.114
$12000 < p_{\text{T}} < 13000$	$3.0 < y^* < 3.5$	0.811 ± 0.132
$12000 < p_{\text{T}} < 13000$	$3.5 < y^* < 4.0$	1.394 ± 0.261
$13000 < p_{\text{T}} < 14000$	$2.5 < y^* < 3.0$	0.871 ± 0.169
$13000 < p_{\text{T}} < 14000$	$3.0 < y^* < 3.5$	1.062 ± 0.203
$13000 < p_{\text{T}} < 14000$	$3.5 < y^* < 4.0$	0.969 ± 0.265
$14000 < p_{\text{T}} < 15000$	$2.5 < y^* < 3.0$	1.113 ± 0.188
$14000 < p_{\text{T}} < 15000$	$3.0 < y^* < 3.5$	0.843 ± 0.198
$14000 < p_{\text{T}} < 15000$	$3.5 < y^* < 4.0$	1.631 ± 0.533

F.2 R_{FB} for J/ψ from b

Table 62: J/ψ from b forward to backward ratio, R_{FB} , as a function of p_{T} for the different rapidity bins.

p_{T} bin	y^* bin	R_{FB}
$0 < p_{\text{T}} < 1000$	$2.5 < y^* < 3.0$	0.640 ± 0.043
$0 < p_{\text{T}} < 1000$	$3.0 < y^* < 3.5$	0.760 ± 0.044
$0 < p_{\text{T}} < 1000$	$3.5 < y^* < 4.0$	0.791 ± 0.056
$1000 < p_{\text{T}} < 2000$	$2.5 < y^* < 3.0$	0.700 ± 0.031
$1000 < p_{\text{T}} < 2000$	$3.0 < y^* < 3.5$	0.783 ± 0.033
$1000 < p_{\text{T}} < 2000$	$3.5 < y^* < 4.0$	0.847 ± 0.041
$2000 < p_{\text{T}} < 3000$	$2.5 < y^* < 3.0$	0.809 ± 0.035
$2000 < p_{\text{T}} < 3000$	$3.0 < y^* < 3.5$	0.826 ± 0.033
$2000 < p_{\text{T}} < 3000$	$3.5 < y^* < 4.0$	0.728 ± 0.037
$3000 < p_{\text{T}} < 4000$	$2.5 < y^* < 3.0$	0.849 ± 0.039
$3000 < p_{\text{T}} < 4000$	$3.0 < y^* < 3.5$	0.771 ± 0.033
$3000 < p_{\text{T}} < 4000$	$3.5 < y^* < 4.0$	0.744 ± 0.039
$4000 < p_{\text{T}} < 5000$	$2.5 < y^* < 3.0$	0.848 ± 0.042
$4000 < p_{\text{T}} < 5000$	$3.0 < y^* < 3.5$	0.841 ± 0.039
$4000 < p_{\text{T}} < 5000$	$3.5 < y^* < 4.0$	0.762 ± 0.047
$5000 < p_{\text{T}} < 6000$	$2.5 < y^* < 3.0$	0.991 ± 0.057
$5000 < p_{\text{T}} < 6000$	$3.0 < y^* < 3.5$	0.903 ± 0.048
$5000 < p_{\text{T}} < 6000$	$3.5 < y^* < 4.0$	0.849 ± 0.061
$6000 < p_{\text{T}} < 7000$	$2.5 < y^* < 3.0$	1.048 ± 0.070
$6000 < p_{\text{T}} < 7000$	$3.0 < y^* < 3.5$	0.923 ± 0.058
$6000 < p_{\text{T}} < 7000$	$3.5 < y^* < 4.0$	0.797 ± 0.074
$7000 < p_{\text{T}} < 8000$	$2.5 < y^* < 3.0$	1.050 ± 0.082
$7000 < p_{\text{T}} < 8000$	$3.0 < y^* < 3.5$	0.995 ± 0.075
$7000 < p_{\text{T}} < 8000$	$3.5 < y^* < 4.0$	1.013 ± 0.109
$8000 < p_{\text{T}} < 9000$	$2.5 < y^* < 3.0$	0.891 ± 0.083
$8000 < p_{\text{T}} < 9000$	$3.0 < y^* < 3.5$	0.881 ± 0.086
$8000 < p_{\text{T}} < 9000$	$3.5 < y^* < 4.0$	1.233 ± 0.153
$9000 < p_{\text{T}} < 10000$	$2.5 < y^* < 3.0$	0.831 ± 0.093
$9000 < p_{\text{T}} < 10000$	$3.0 < y^* < 3.5$	1.088 ± 0.127
$9000 < p_{\text{T}} < 10000$	$3.5 < y^* < 4.0$	1.114 ± 0.179

Table 63: J/ψ from b forward to backward ratio, R_{FB} , as a function of p_{T} for the different rapidity bins.

p_{T} bin	y^* bin	$R_{p\text{Pb}}$
$10000 < p_{\text{T}} < 11000$	$2.5 < y^* < 3.0$	1.157 ± 0.155
$10000 < p_{\text{T}} < 11000$	$3.0 < y^* < 3.5$	0.996 ± 0.155
$10000 < p_{\text{T}} < 11000$	$3.5 < y^* < 4.0$	1.069 ± 0.190
$11000 < p_{\text{T}} < 12000$	$2.5 < y^* < 3.0$	0.666 ± 0.111
$11000 < p_{\text{T}} < 12000$	$3.0 < y^* < 3.5$	1.034 ± 0.177
$11000 < p_{\text{T}} < 12000$	$3.5 < y^* < 4.0$	0.851 ± 0.243
$12000 < p_{\text{T}} < 13000$	$2.5 < y^* < 3.0$	0.833 ± 0.148
$12000 < p_{\text{T}} < 13000$	$3.0 < y^* < 3.5$	0.933 ± 0.204
$12000 < p_{\text{T}} < 13000$	$3.5 < y^* < 4.0$	1.432 ± 0.417
$13000 < p_{\text{T}} < 14000$	$2.5 < y^* < 3.0$	0.873 ± 0.212
$13000 < p_{\text{T}} < 14000$	$3.0 < y^* < 3.5$	1.037 ± 0.277
$13000 < p_{\text{T}} < 14000$	$3.5 < y^* < 4.0$	0.877 ± 0.310
$14000 < p_{\text{T}} < 15000$	$2.5 < y^* < 3.0$	1.003 ± 0.192
$14000 < p_{\text{T}} < 15000$	$3.0 < y^* < 3.5$	1.036 ± 0.292
$14000 < p_{\text{T}} < 15000$	$3.5 < y^* < 4.0$	1.969 ± 0.931

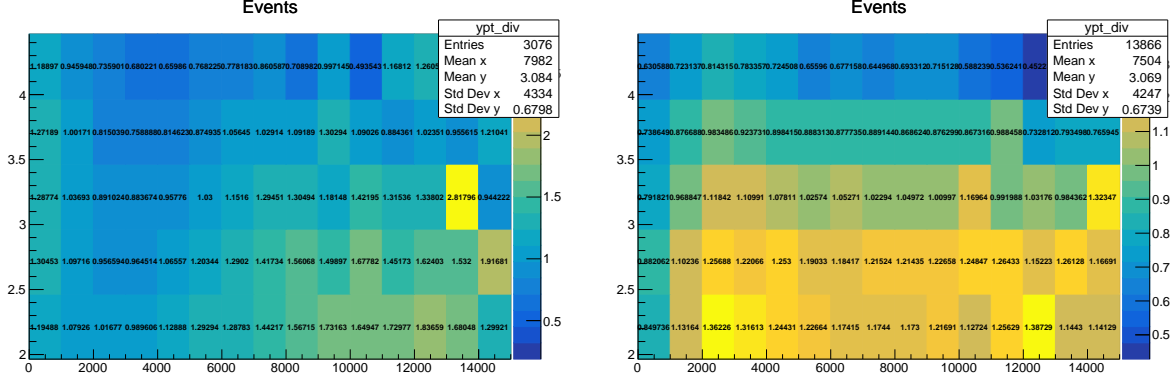


Figure 49: Left: $PbPb$ ratio $Data/simulation$, y-axis rapidity, x-axis transverse momentum. Right pPb ratio $Data/simulation$.

F.3 Simulation data comparisons of kinematic distribution in phase space

The distribution of candidates after all selections is compared between simulation and data in Fig.49. In data, the candidates are extracted with the *sPlot* technique. The comparison is done by comparison of the normalised 2-dimensional distributions in p_T - y space in the bins of the analysis. The $PbPb$ simulation is quite well reproducing the data, whereas in pPb has quite strong deviations. They are presumably coming mainly from the strong suppression of the prompt component, which is not present in the simulation based on pp Pythia events for what concerns the J/ψ . However, given the large granularity of the analysis compared to the observed tendencies, we don't consider an additional uncertainty due to this.

References

- [1] T. Matsui and H. Satz, *J/ψ Suppression by Quark-Gluon Plasma Formation*, Phys. Lett. **B178** (1986) 416.
- [2] A. Mocsy, P. Petreczky, and M. Strickland, *Quarkonia in the Quark Gluon Plasma*, Int. J. Mod. Phys. **A28** (2013) 1340012, [arXiv:1302.2180](#).
- [3] A. Andronic *et al.*, *Heavy-flavour and quarkonium production in the LHC era: from protonproton to heavy-ion collisions*, Eur. Phys. J. **C76** (2016) 07, [arXiv:1506.03981](#).
- [4] ALICE collaboration, B. Abelev *et al.*, *J/ψ suppression at forward rapidity in Pb–Pb collisions at $\sqrt{s_{NN}}=2.76$ TeV*, Phys. Rev. Lett. **109** (2012) 072301, [arXiv:1202.1383](#).
- [5] ALICE collaboration, B. Abelev *et al.*, *Centrality, rapidity and transverse momentum dependence of J/ψ suppression in Pb-Pb collisions at $\sqrt{s_{NN}}=2.76$ TeV*, Phys. Lett. **B734** (2014) 314, [arXiv:1311.0214](#).
- [6] ALICE collaboration, J. Adam *et al.*, *Inclusive, prompt and non-prompt J/ψ production at mid-rapidity in Pb-Pb collisions at $\sqrt{s_{NN}} = 2.76$ TeV*, JHEP **07** (2015) 051, [arXiv:1504.07151](#).
- [7] ALICE collaboration, J. Adam *et al.*, *Differential studies of inclusive J/ψ and ψ(2S) production at forward rapidity in Pb-Pb collisions at $\sqrt{s_{NN}}=2.76$ TeV*, JHEP **05** (2016) 179, [arXiv:1506.08804](#).
- [8] ALICE collaboration, J. Adam *et al.*, *J/ψ suppression at forward rapidity in Pb-Pb collisions at $\sqrt{s_{NN}} = 5.02$ TeV*, Phys. Lett. **B766** (2017) 212, [arXiv:1606.08197](#).
- [9] R. L. Thews, M. Schroedter, and J. Rafelski, *Enhanced J/ψ production in deconfined quark matter*, Phys. Rev. **C63** (2001) 054905, [arXiv:hep-ph/0007323](#).
- [10] P. Braun-Munzinger and J. Stachel, *(Non)thermal aspects of charmonium production and a new look at J/ψ suppression*, Phys. Lett. **B490** (2000) 196, [arXiv:nucl-th/0007059](#).
- [11] M. Hirai, S. Kumano, and T.-H. Nagai, *Determination of nuclear parton distribution functions and their uncertainties in next-to-leading order*, Phys. Rev. **C76** (2007) 065207, [arXiv:0709.3038](#).
- [12] K. J. Eskola, H. Paukkunen, and C. A. Salgado, *EPS09: A New Generation of NLO and LO Nuclear Parton Distribution Functions*, JHEP **04** (2009) 065, [arXiv:0902.4154](#).
- [13] D. de Florian, R. Sassot, P. Zurita, and M. Stratmann, *Global Analysis of Nuclear Parton Distributions*, Phys. Rev. **D85** (2012) 074028, [arXiv:1112.6324](#).
- [14] K. Kovarik *et al.*, *nCTEQ15 - Global analysis of nuclear parton distributions with uncertainties in the CTEQ framework*, Phys. Rev. **D93** (2016) 085037, [arXiv:1509.00792](#).

- [15] K. J. Eskola, P. Paakkinen, H. Paukkunen, and C. A. Salgado, *EPPS16: Nuclear parton distributions with LHC data*, [arXiv:1612.05741](#).
- [16] F. Gelis, E. Iancu, J. Jalilian-Marian, and R. Venugopalan, *The Color Glass Condensate*, *Ann. Rev. Nucl. Part. Sci.* **60** (2010) 463, [arXiv:1002.0333](#).
- [17] H. Fujii, F. Gelis, and R. Venugopalan, *Quark pair production in high energy pA collisions: General features*, *Nucl. Phys.* **A780** (2006) 146, [arXiv:hep-ph/0603099](#).
- [18] R. Vogt, *Shadowing and absorption effects on J/ψ production in dA collisions*, *Phys. Rev.* **C71** (2005) 054902, [arXiv:hep-ph/0411378](#).
- [19] E. G. Ferreira, F. Fleuret, J. P. Lansberg, and A. Rakotozafindrabe, *Cold nuclear matter effects on J/ψ production: Intrinsic and extrinsic transverse momentum effects*, *Phys. Lett.* **B680** (2009) 50, [arXiv:0809.4684](#).
- [20] R. Vogt, *Cold Nuclear Matter Effects on J/ψ and Υ Production at the LHC*, *Phys. Rev.* **C81** (2010) 044903, [arXiv:1003.3497](#).
- [21] J.-P. Lansberg and H.-S. Shao, *Towards an automated tool to evaluate the impact of the nuclear modification of the gluon density on quarkonium, D and B meson production in protonnucleus collisions*, *Eur. Phys. J.* **C77** (2017), no. 1 1, [arXiv:1610.05382](#).
- [22] H. Fujii and K. Watanabe, *Heavy quark pair production in high energy pA collisions: Quarkonium*, *Nucl. Phys.* **A915** (2013) 1, [arXiv:1304.2221](#).
- [23] Y.-Q. Ma, R. Venugopalan, and H.-F. Zhang, *J/ψ production and suppression in high energy proton-nucleus collisions*, *Phys. Rev.* **D92** (2015) 071901, [arXiv:1503.07772](#).
- [24] B. Duclou, T. Lappi, and H. Mntysaari, *Forward J/ψ production in proton-nucleus collisions at high energy*, *Phys. Rev.* **D91** (2015), no. 11 114005, [arXiv:1503.02789](#).
- [25] F. Arleo and S. Peigne, *Heavy-quarkonium suppression in p-A collisions from parton energy loss in cold QCD matter*, *JHEP* **03** (2013) 122, [arXiv:1212.0434](#).
- [26] ALICE, B. Abelev *et al.*, *J/ψ production and nuclear effects in p-Pb collisions at $\sqrt{s_{NN}} = 5.02$ TeV*, *JHEP* **02** (2014) 073, [arXiv:1308.6726](#).
- [27] ALICE collaboration, J. Adam *et al.*, *Rapidity and transverse-momentum dependence of the inclusive J/ψ nuclear modification factor in p-Pb collisions at $\sqrt{s_{NN}} = 5.02$ TeV*, *JHEP* **06** (2015) 055, [arXiv:1503.07179](#).
- [28] ALICE collaboration, J. Adam *et al.*, *Centrality dependence of inclusive J/ψ production in p-Pb collisions at $\sqrt{s_{NN}}=5.02$ TeV*, *JHEP* **11** (2015) 127, [arXiv:1506.08808](#).
- [29] LHCb collaboration, R. Aaij *et al.*, *Study of J/ψ production and cold nuclear matter effects in pPb collisions at $\sqrt{s_{NN}} = 5$ TeV*, *JHEP* **02** (2014) 072, [arXiv:1308.6729](#).
- [30] ATLAS collaboration, G. Aad *et al.*, *Measurement of differential J/ψ production cross sections and forward-backward ratios in p + Pb collisions with the ATLAS detector*, *Phys. Rev.* **C92** (2015), no. 3 034904, [arXiv:1505.08141](#).

- [31] CMS collaboration, A. M. Sirunyan *et al.*, *Measurement of prompt and non prompt J/ψ production in pp and pPb collisions at $\sqrt{s_{NN}} = 5.02$ TeV*, [arXiv:1702.01462](#).
- [32] P. Bozek and W. Broniowski, *Correlations from hydrodynamic flow in p-Pb collisions*, Phys. Lett. **B718** (2013) 1557, [arXiv:1211.0845](#).
- [33] H. Mntysaari, P. Tribedy, B. Schenke, C. Shen, in preparation.
- [34] S. Schlichting and P. Tribedy, *Collectivity in small collision systems : an initial state perspective*, [arXiv:1611.00329](#).
- [35] ALICE collaboration, B. B. Abelev *et al.*, *Suppression of $\psi(2S)$ production in p-Pb collisions at $\sqrt{s_{NN}} = 5.02$ TeV*, JHEP **12** (2014) 073, [arXiv:1405.3796](#).
- [36] ALICE collaboration, J. Adam *et al.*, *Centrality dependence of $\psi(2S)$ suppression in p-Pb collisions at $\sqrt{s_{NN}} = 5.02$ TeV*, JHEP **06** (2016) 050, [arXiv:1603.02816](#).
- [37] LHCb collaboration, R. Aaij *et al.*, *Observation of the decay $B_c^+ \rightarrow \psi(2S)\pi^+$* , Phys. Rev. **D87** (2013) 071103(R), [arXiv:1303.1737](#).
- [38] X. Du and R. Rapp, *Sequential Regeneration of Charmonia in Heavy-Ion Collisions*, Nucl. Phys. **A943** (2015) 147, [arXiv:1504.00670](#).
- [39] F. Arleo and S. Peign, *Disentangling Shadowing from Coherent Energy Loss using the Drell-Yan Process*, Phys. Rev. **D95** (2017), no. 1 011502, [arXiv:1512.01794](#).
- [40] E. Todesco and J. Wenninger, *Large hadron collider momentum calibration and accuracy*, CERN-ACC-2017-0007.
- [41] Particle Data Group, C. Patrignani *et al.*, *Review of particle physics*, Chin. Phys. **C40** (2016) 100001.
- [42] Geant4 collaboration, S. Agostinelli *et al.*, *Geant4: A simulation toolkit*, Nucl. Instrum. Meth. **A506** (2003) 250.
- [43] Geant4 collaboration, J. Allison *et al.*, *Geant4 developments and applications*, IEEE Trans. Nucl. Sci. **53** (2006) 270.
- [44] I. Belyaev *et al.*, *Handling of the generation of primary events in Gauss, the LHCb simulation framework*, J. Phys. Conf. Ser. **331** (2011) 032047.
- [45] T. Pierog *et al.*, *EPOS LHC: Test of collective hadronization with data measured at the CERN Large Hadron Collider*, Phys. Rev. **C92** (2015), no. 3 034906, [arXiv:1306.0121](#).
- [46] D. J. Lange, *The EvtGen particle decay simulation package*, Nucl. Instrum. Meth. **A462** (2001) 152.
- [47] P. Golonka and Z. Was, *PHOTOS Monte Carlo: A precision tool for QED corrections in Z and W decays*, Eur. Phys. J. **C45** (2006) 97, [arXiv:hep-ph/0506026](#).
- [48] T. Sjöstrand, S. Mrenna, and P. Skands, *A brief introduction to PYTHIA 8.1*, Comput. Phys. Commun. **178** (2008) 852, [arXiv:0710.3820](#).

- [49] T. Head *et al.*, *Measurement of J/ψ production cross-section in pp collisions at $\sqrt{s} = 13$ TeV*, LHCb-ANA-2015-004.
- [50] J. Lefrancois, *Crystal ball fits*, [link](#).
- [51] <https://twiki.cern.ch/twiki/bin/view/LHCb/LHCbTrackingEfficiencies>.
- [52] LHCb collaboration, R. Aaij *et al.*, *LHCb detector performance*, Int. J. Mod. Phys. **A30** (2015) 1530022, [arXiv:1412.6352](#).
- [53] LHCb collaboration, R. Aaij *et al.*, *Precision luminosity measurements at LHCb*, JINST **9** (2014) P12005, [arXiv:1410.0149](#).
- [54] LHCb collaboration, R. Aaij *et al.*, *Measurement of J/ψ production in pp collisions at $\sqrt{s} = 2.76$ TeV*, JHEP **02** (2013) 041, [arXiv:1212.1045](#).
- [55] LHCb collaboration, R. Aaij *et al.*, *Measurement of J/ψ production in pp collisions at $\sqrt{s} = 7$ TeV*, Eur. Phys. J. **C71** (2011) 1645, [arXiv:1103.0423](#).
- [56] LHCb collaboration, R. Aaij *et al.*, *Measurement of J/ψ polarization in pp collisions at $\sqrt{s} = 7$ TeV*, Eur. Phys. J. **C73** (2013) 2631, [arXiv:1307.6379](#).
- [57] LHCb collaboration, R. Aaij *et al.*, *Production of J/ψ and Υ mesons in pp collisions at $\sqrt{s} = 8$ TeV*, JHEP **06** (2013) 064, [arXiv:1304.6977](#).
- [58] LHCb collaboration, R. Aaij *et al.*, *Measurement of forward J/ψ production cross-sections in pp collisions at $\sqrt{s} = 13$ TeV*, JHEP **10** (2015) 172, [arXiv:1509.00771](#).
- [59] ALICE and LHCb collaborations, *Reference pp cross-sections for J/ψ studies in proton-lead collisions at $\sqrt{s_{NN}} = 5.02$ TeV and comparisons between ALICE and LHCb results*, Dec, 2013. LHCb-CONF-2013-013, ALICE-PUBLIC-2013-002.
- [60] LHCb collaboration, R. Aaij *et al.*, *Study of $\psi(2S)$ production cross-sections and cold nuclear matter effects in pPb collisions at $\sqrt{s_{NN}} = 5$ TeV*, JHEP **03** (2016) 133, [arXiv:1601.07878](#).
- [61] ALICE collaboration, B. Abelev *et al.*, *Measurement of prompt J/ψ and beauty hadron production cross sections at mid-rapidity in pp collisions at $\sqrt{s} = 7$ TeV*, JHEP **11** (2012) 065, [arXiv:1205.5880](#).
- [62] H.-S. Shao, *HELAC-Onia: An automatic matrix element generator for heavy quarkonium physics*, Comput. Phys. Commun. **184** (2013) 2562, [arXiv:1212.5293](#).
- [63] H.-S. Shao, *HELAC-Onia 2.0: an upgraded matrix-element and event generator for heavy quarkonium physics*, Comput. Phys. Commun. **198** (2016) 238, [arXiv:1507.03435](#).
- [64] B. Duclou, T. Lappi, and H. Mntysaari, *Forward J/ψ production at high energy: centrality dependence and mean transverse momentum*, Phys. Rev. **D94** (2016), no. 7 074031, [arXiv:1605.05680](#).